Library

VOLUME 38 SECOND SERIES NUMBER 2

THE PHYSICAL REVIEW

A JOURNAL OF EXPERIMENTAL AND THEORETICAL PHYSICS

CONDUCTED BY

THE AMERICAN PHYSICAL SOCIETY

BOARD OF EDITORS

Managing Editor, JOHN T. TATE, University of Minnesota, Minneapolis
Assistant Editor, J. W. BUCHTA, University of Minnesota, Minneapolis
E. U. CONDON, C. J. DAVISSON, F. K. RICHTMYER, K. F. HERZFELD, A. W. HULL, F. W. LOOMIS, A. J. DEMPSTER, DAVID M. DENNISON, J. C. SLATER

JULY 15, 1931

Resolving Power Attainable in X-Ray Spectroscopy by Photographic Methods — SAMUEL K. ALLISON 203
500 Kilovolt Cathode Rays — R. E. VOLLRATH 212
X-Ray Absorption Coefficients of Mercury Vapor in the Region of its *L*-Absorption Discontinuities — FRED M. UBER 217
Many-Electron Selection Rules — S. GOUDSMIT AND L. GROPPER 225
Quantum Theory of the Equation of State — J. C. SLATER 237
Quantum Theory and Electron Pair Bond — W. HEITLER 243
Note on the Calculation of Zero Order Eigenfunctions — NEWTON M. GRAY AND LAWRENCE A. WILLS 248
Calculation of Interaction Between Atoms with *s*-Electrons — N. ROSEN 255
Low Velocity Inelastic Collisions — CLARENCE ZENER 277
Probability Law Governing Ionisation by Electron Impact in Mercury Vapor — CURTIS R. HAUPT 282
On the Temperature of Cathode in Vacuum Arc — R. TANBERG AND W. E. BERKEY 296
Wave-Length Standards in the Spectra of Carbon and Tin in the Schumann Region — R. V. ZUMSTEIN AND D. S. MARSTON 305
Some Remarks on the Theory of the Photoelectric Effect — J. FRENKEL 309
Photoelectric Properties of Thin Unbacked Gold Films — RALPH P. WINCH 321
Note on the Structure of the Groups XO_3 — J. C. SLATER 325
Effect of Temperature upon the Ultraviolet Band Spectrum of Ozone and the Structure of this Spectrum — OLIVER R. WULF AND EUGENE H. MELVIN 330
Concerning the Reflection Power of Metals in Thin Layers for the Infrared — R. BOWLING BARNES AND M. CZERNY 338
Stereophotographic Models of Electron Motion in Stark Effect — R. W. WOOD 346
Crystal Structure of Arsenic Triiodide, AsI_3 — DOROTHY HEYWORTH 351
Magnetic Moment of the Palladium Atom — A. N. GUTHRIE AND M. J. COPLEY 360
Surface Energy of Liquids — HENRY MARGENAU 365
Letters to the Editor — 372

The Rotational Analysis of the First Positive Nitrogen (N_1) Bands, *S. Meiring Naude*—372; Forced Predissociation in Nitrogen, *Joseph Kaplan*—373; Removal of Continuous Background from Raman Spectrum of Carbon Tetrachloride, *M. E. High and M. L. Pool*—374; Calculation of Effective Nuclear Magnetic Moments from Hyperfine Structure, *S. W. Nile*—375; A More Fundamental Thermodynamics, *Gilbert N. Lewis*—376; Oscillations in Discharge Tubes, *W. L. Brown and H. McN. Cowan*—376; Photoelectric and Metastable Atom Emission of Electrons from Surfaces, *Carl Kenty*—377.

PUBLISHED BY THE AMERICAN PHYSICAL SOCIETY
EDITORIAL OFFICE: MINNEAPOLIS, MINN.

THE AMERICAN PHYSICAL SOCIETY

OFFICERS OF THE SOCIETY

President:	W. F. G. Swann	Bartol Research Foundation, Philadelphia, Pa.
Vice-President:	Paul D. Foote	The Gulf Companies, Pittsburgh, Pa.
Secretary:	W. L. Severinghaus	Columbia University, New York City
Treasurer:	G. B. Pegram	Columbia University, New York City
Editor:	John T. Tate	University of Minnesota, Minneapolis, Minn.
Local Secretary for the Pacific Coast:	L. B. Loeb	University of California, Berkeley, Calif.

THE PHYSICAL REVIEW

Published by the American Physical Society. Executive office: University of Minnesota, Minneapolis, Minn. Two volumes annually, twelve issues per volume.

First series. From July 1, 1893, to January 1, 1913, the Review was conducted by Edward L. Nicholas, Ernest Merritt and Frederick Bedell, with the financial support of Cornell University. The first four volumes were issued annually; subsequent volumes, semi-annually; thirty-five volumes in all.

Second series. On January 1, 1913, the Review was transferred to the American Physical Society as announced on the first page of the new series which was then begun. Since then it has been conducted by a Board of Editors elected by the Society. Semi-annual volumes begin in January and July. Since July 1, 1929, the Review has been issued twice a month.

Contributors are referred to page 2 of the advertisements for further information.

Annual subscription, throughout the Postal Union, $12.00 in advance.

General index, 1893-1920, $4.00, in advance.

Back Volumes, $9.00 per volume; Back Numbers, $1.50 per copy for issues prior to July 1, 1929 (Vols. 1-33), $.75 per copy for issues subsequent thereto. Postage is free if remittance accompanies order; otherwise postage is extra. No bound volumes can be supplied. The Review offers to purchase a limited number of First Series, Vol. 1, No. 1 (at $2.00 each); Second Series, Vol. 7, No. 1, January 1916; Vol. 7, No. 2, February 1916; Vol. 7, No. 4, April 1916; and Vol. 7, No. 5, May 1916 (at $2.00 each).

Advertisements. Rates will be supplied by the Editor on request. Copy for each number must be received at Minneapolis two weeks prior to the dates of issue; old copy is used until new copy is received. Send electrotypes direct to the printers, George Banta Publishing Co., Menasha, Wis.

Discount of ten per cent is allowed to members of the American Physical Society on purchase of back numbers.

Changes of Address and Complaints of failure to receive the Review, in the case of members of the Physical Society, should be addressed to the Treasurer; in the case of other subscribers, to the Editor. New copies can be sent free in response to complaint of non-delivery only if notice of non-delivery is received within three months of date of issue.

Editorial Correspondence should be addressed to the Physical Review, University of Minnesota, Minneapolis, Minn.

Entered at the post office at Menasha, Wis., as second class matter.
Acceptance for mailing at special rate of postage provided for in section 1103, Act of October 3, 1917, authorized September 6, 1926.

Second Series *July 15, 1931* *Vol. 38, No. 2*

THE
PHYSICAL REVIEW

THE RESOLVING POWER ATTAINABLE IN X-RAY SPECTROSCOPY BY PHOTOGRAPHIC METHODS

SAMUEL K. ALLISON
UNIVERSITY OF CHICAGO

(Received June 1, 1931)

ABSTRACT

If w_c, the (half) range of glancing angle over which a crystal will reflect monochromatic x-rays, has been determined by the double spectrometer method, it is possible to calculate what resolving power is attainable from this crystal by photographic methods. Equations are set up giving the resolving power in terms of a, the slit width, and R, the distance from slit to photographic plate. Some results are: (1) No appreciable increase in resolving power is attainable by making $a/2R < \frac{1}{4}w_c$. (2) If $a/2R > 3w_c$, the resolving power does not involve w_c. (3) The resolving power attainable in the first order is $1/2^{1/2}$ of that attainable in a double spectrometer with crystals of equal perfection. Equations are also derived by which observed line widths in photographic spectrometers may be corrected for slit and crystal diffraction pattern effects. The results are applied to recent experimental results with photographic spectrometers and it is shown that the width of Mo$K\alpha_1$ observed photographically is considerably greater than the values obtained by the double spectrometer.

INTRODUCTION

THE recently increasing use of the double crystal x-ray spectrometer has led to comparisons of its resolving power with that attainable in photographic x-ray spectroscopy.[1,2] A pair of crystals which are as nearly identical as possible (being two previously contiguous sides of a split crystal) can be investigated in parallel positions of the double spectrometer, and the angular width of glancing angle over which monochromatic radiation is reflected can be found. With this information it should be possible to calculate the resolving power attainable from one of the crystals if used in a photographic spectrometer of known slit width and slit-to-plate distance. Such a calculation will be reported in this paper, and extended to the consideration of measurement of line breadths by photographic methods.

THE WIDTH OF THE DIFFRACTION PATTERN FROM A SINGLE CRYSTAL

Let us at first represent the diffraction pattern from a single crystal in the general form

$$I_\xi = F(\xi) \tag{1}$$

[1] Bergen Davis, Phys. Rev. **35,** 209 (1930).
[2] Valasek, Phys. Rev. **36,** 1523 (1930).

In this expression I_ξ is the intensity reflected from a crystal at a glancing angle whose deviation from a reference angle θ is ξ, divided by the intensity reflected when ξ is 0. In the Darwin-Ewald theory [3,4] this reference angle is

$$\theta = \theta_0 + \delta \sec \theta_0 \operatorname{cosec} \theta_0 \tag{2}$$

where

$$\sin \theta_0 = n\lambda/2d \tag{3}$$

and is in the center of the diffraction pattern. Here δ is the deviation of the index of refraction from unity, and n, λ, and d have their usual significance as in the Bragg equation. The function $F(\xi)$ is expressed as follows

$$F(\xi) = \left\{ \frac{\overline{\Delta\theta}}{2\xi - (4\xi^2 - \overline{\Delta\theta}^2)^{1/2}} \right\}^2 \text{for } \xi < -\tfrac{1}{2}\overline{\Delta\theta}; \tag{4}$$

$$F(\xi) = 1 \text{ for } -\tfrac{1}{2}\overline{\Delta\theta} < \xi < \tfrac{1}{2}\overline{\Delta\theta}; \tag{5}$$

and

$$F(\xi) = \left\{ \frac{\overline{\Delta\theta}}{2\xi + (4\xi^2 - \overline{\Delta\theta}^2)^{1/2}} \right\}^2 \text{for } \xi > \tfrac{1}{2}\overline{\Delta\theta}. \tag{6}$$

The expression for $\Delta\theta$ is

$$\Delta\theta = (4F\delta \operatorname{cosec} 2\theta)/Z \tag{7}$$

where F is the structure factor and Z the number of electrons in the unit cell.[5] The best experimental evidence for the nature of the function $F(\xi)$ comes from the shape of the rocking curves obtained in the parallel positions of the double crystal spectrometer. Such curves do not give $F(\xi)$ directly, but give a curve which may be represented as follows[6]

$$I_B = \int_{-\infty}^{\infty} F(\xi)F(\xi - \xi_B)d\xi. \tag{8}$$

In this equation I_B is the intensity reflected from crystal B when B is at a position whose angular deviation from the center of the rocking curve is ξ_B, divided by the intensity reflected when $\xi_B = 0$.

Since the work of Mark and Ehrenberg[7] it has been customary to evaluate the integral (7) on the assumption that $F(\xi)$ has the form

$$F(\xi) = e^{-(\log 2/w_c^2)\xi^2} \tag{9}$$

and not that predicted by the Darwin-Ewald theory as in Eqs. (4), (5), (6). It is seen that Eq. (9) represents a Gaussian error curve of half-width at half maximum w_c. If we assume that Eq. (9) gives the correct form of $F(\xi)$, we can carry out the integration of Eq. (8) with the result

[3] Darwin, Phil. Mag. **27,** 325 and 675 (1914).

[4] Ewald, Phys. Zeits. **26,** 29 (1925).

[5] Allison and Williams, Phys. Rev. **35,** 1476 (1930).

[6] Schwarzschild, Phys. Rev. **32,** 162 (1928), Eq. (8) of this paper is Eq. (31) of Schwarzschild's paper with slightly different notation.

[7] Ehrenberg and Mark, Zeits. f. Physik **42,** 807 (1927).

$$I_B = w_c\left(\frac{\pi}{2\log 2}\right)^{1/2} e^{-(\log 2/2w_c^2)\xi_B^2} \tag{10}$$

Thus the rocking curve on crystal B is also a Gaussian error curve, and if w is the half-width at half maximum of the observed curve, Eq. (10), the relation between w and w_c is

$$w = w_c(2)^{1/2}. \tag{11}$$

If, however, the diffraction pattern curves from a single crystal actually have the theoretical shape as predicted in Eqs. (4), (5), (6), the rocking curve of crystal B should not be of the Gaussian error curve shape, and the correct factor for finding the half width at half maximum of a single crystal diffraction pattern from that of the observed rocking curve is not $2^{1/2}$ as in Eq. (11).

The author has solved Eq. (8) for I_B, assuming F is of the Darwin-Ewald form, by graphical methods, thus obtaining the rocking curve predicted by the theory for parallel positions of the double spectrometer. The resulting curve differs markedly from the Gaussian error curve shape, and the half width at half maximum is approximately given by

$$w = 0.60\Delta\theta \tag{12}$$

where $\Delta\theta$ is defined by Eq. (7). The half width at half maximum of the theoretical single crystal curve (Eqs. (4), (5), (6)) is

$$w_c = 0.531\Delta\theta \tag{13}$$

hence on this basis the observed width on the double spectrometer and the diffraction pattern width are related by

$$w = 1.13w_c. \tag{14}$$

At the time of writing this paper, it is uncertain whether the diffraction pattern width for a single crystal should be calculated from the observed parallel position rocking curve widths by Eq. (14) or by Eq. (11). The experimental rocking curves are very closely of the Gaussian error curve form, and hence favor Eq. (11), although no detailed study of the shape in a single case has been carried out. We shall therefore use Eq. (11), as has been the general practice previously, with the provision that later developments may favor some other factor, as in Eq. (14).

The Resolving Power of the Photographic Spectrometer

Fig. 1 represents the essentials of a type of high resolving power photographic spectrometer which has been designed by Professor Siegbahn at the Univesity of Upsala and used there and at the University of Minnesota by J. Valasek.[2] Others have also used photographic apparatus of this type.[8] In the figure, x-rays from the target T fall upon the crystal, and a narrow band

[8] Duane, Phys. Rev. **37**, 1017 (1931), also unpublished work by J. A. Bearden in this laboratory.

of the reflected rays is selected by the slit of width a. This bundle of x-rays falls on the photographic plate which is put at a distance R.

Let us assume the radiation to be monochromatic, of wave-length λ. The dotted line intersecting the photographic plate at O passes through the geometrical center of the slit aperture and makes a glancing angle θ with the crystal, where θ is the angle calculated from Eq. (2). We will select a point P at a

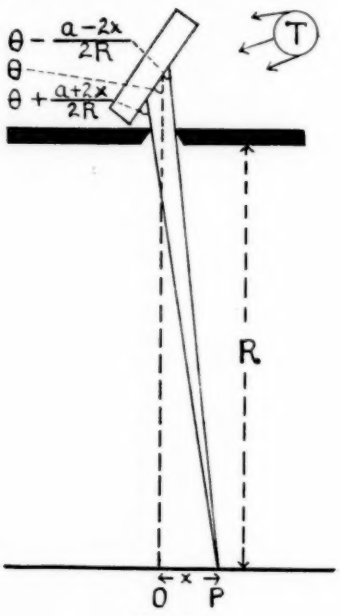

Fig. 1.

distance x from O and calculate the intensity at this point. From the geometry of Fig. 1 it results that radiation can reach P which has been reflected from the crystal over a range of glancing angle from $\theta-(a-2x)/2R$ to $\theta+(a+2x)/2R$. Assuming a single crystal diffraction curve of the form of Eq. (9), we have then

$$I_P = \int_{-(a-2x)/2R}^{(a+2x)/2R} e^{-(\log 2/w_c^2)\xi^2} d\xi. \tag{15}$$

Curves for various angular slit widths $(a/2R)$ obtained by graphical integration of this function are shown in Fig. 2. The abscissae of these curves are angular deviations from O, Fig. 1, and the ordinates are intensities. Several interesting conclusions may be reached from Fig. 2. Let us consider the curve for $a/2R=1/4w_c$. Here the angular half width at half maximum of the impression on the photographic plate is simply w_c, which is the angular half width at half maximum of the crystal diffraction pattern, and the slit width does not contribute to the observed width at all. We may then state that the narrowness of the impression on the photographic plate, or in other words the resolving power of the instrument, is not increased by reducing the half angular width of the slit below approximately one-four of the half width at

half maximum of the crystal used. In any given spectrometer this gives a lower limit to the slit width beyond which nothing is gained by narrowing the slit.[9]

In the other direction, at $a/2R=3w_c$, the half width of the impression on the photographic plate is just what one would expect from the slit dimensions and distance alone, namely, $a/2R$, and the diffraction pattern from the crystal plays no appreciable part.

In order to set up an expression for the resolving power, we must now decide at what angular separation two curves for slightly differing wavelengths would be resolved. The author wishes to make the suggestion here

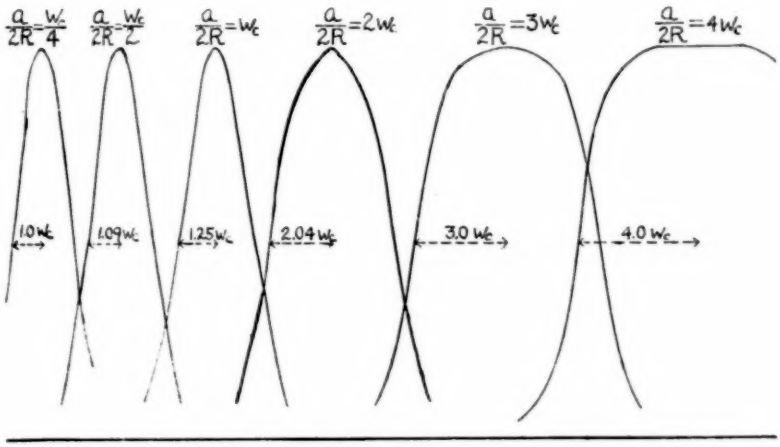

Fig. 2.

that two curves of the type of Fig. 2 shall be said to be resolved if the separation of their maxima is twice their half width at half maximum. In the case of the curves of Fig. 2 which do not greatly deviate from the Gaussian error curve shape, two such curves at the limit of resolution would have a dip between them of approximately 93 percent of the intensity at either maximum. This, of course, is an arbitrary definition of resolution, but is neither more or less so than the classical definition applying to the resolving power of gratings in the optical region. Now differentiating the Bragg equation to get the angular dispersion, we obtain

$$\frac{\lambda}{d\lambda}=\frac{\tan\theta}{2w}. \tag{16}$$

The highest resolving power attainable is obtained if $a/2R\leqq 1/4w_c$; here $w=w_e$ and we get

$$\frac{\lambda}{d\lambda}=\frac{\tan\theta}{2w_e}. \tag{17}$$

[9] If the single crystal diffraction pattern is not of the Gaussian error curve shape, but of the theoretical Darwin-Ewald form, this lower limit is reached somewhere between $a/2R=\frac{1}{4}w_e$ and $a/2R=w_e$, and considerably nearer the higher value than the lower.

If $a/2R \geqq 3w_e$ we have $w = a/2R$ and

$$\frac{\lambda}{d\lambda} = \frac{R \tan \theta}{a}. \tag{18}$$

Comparison with the Maximum Resolving Power Attainable in the Double Spectrometer

If the vertical divergence of the beam of x-rays in the double spectrometer is sufficiently great, it may cause a diminution of resolving power. The calculation of the shape of the rocking curve which combines this geometrical effect with the diffraction pattern widths of the crystals is considerably more difficult than in the photographic case previously considered. One can, however, calculate the two effects separately and estimate the extent to which geometrical effects lower the resolution. The calculation has been carried out, and it is quite possible, using calcite crystals in the (1, 1) position, to limit the vertical divergence to the point where geometrical effects do not enter appreciably, and yet to have sufficient intensity in the beam for measurement.[10] In the (2, 2) position this is much less easily possible due to the much lower value of w_e in the second order. However, the maximum resolving power is attainable only by eliminating geometric effects and we will assume this has been done. If the instrument were operating with a perfectly monochromatic beam of x-rays the half width at half maximum in any position (n_A, n_B) would be given by

$$w = (w_A^2 + w_B^2)^{1/2} \tag{19}$$

where w_A and w_B are the values of w_e corresponding to the orders of reflection n_A and n_B. According to the assumption in the second section of this paper the rocking curve would be of Gaussian error curve shape. We have postulated that two such curves are resolved if separated by twice the half width at half maximum, or $2w$. The dispersion is

$$D \equiv \frac{d\theta_B}{d\lambda} = \frac{n_A}{2d \cos \theta_A} + \frac{n_B}{2d \cos \theta_B} \tag{20}$$

if the sign of n_B is chosen according to a convention suggested previously by Allison and Williams. Using Eqs. (19) and (20) we find

$$\frac{\lambda}{d\lambda} = \frac{D\lambda}{2w} = \frac{D\lambda}{2(w_A^2 + w_B^2)^{1/2}} \tag{21}$$

Eq. (21) represents the highest resolving power attainable in the double spectrometer for any given values of n_A and n_B. This can actually be attained without too great loss of energy in the (1, 1) position, where 14.1 becomes

[10] See Table V of the paper of Allison and Williams previously referred to. In the (1, 1) position the geometric half width at half maximum was 0.34″, whereas the rocking curve half width at half maximum due to crystal diffraction patterns was 3.0″. It would easily have been possible to decrease the vertical divergence further, but due to the large natural line width, nothing would be gained.

$$\frac{\lambda}{d\lambda} = \frac{(2)^{1/2} \tan \theta}{2w_c} . \tag{22}$$

Here w_c is the half width at half maximum of the single crystal diffraction pattern in the first order, and θ is the corresponding glancing angle.

By a comparison of Eqs. (22) and (17) we see that the maximum resolving power attainable by the double spectrometer in the (1, 1) position is 1.4 times that obtainable photographically in the first order from the same crystals. This conclusion has been previously stated by Valasek.[2] It is, of course, futile to pretend that the equations for resolving power developed here will be of

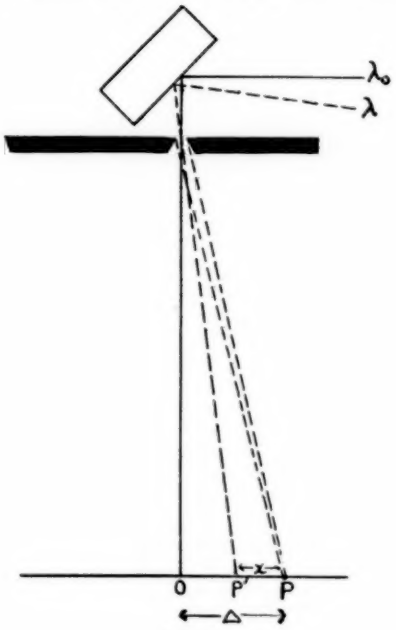

Fig. 3.

great importance to the investigator seeking to resolve a given pair of x-ray lines. Many other factors, such as their shapes, their relative intensities, and the acumen of the observer, enter. The real use of the equations is their ability to serve as a criterion of the relative resolving powers of different instruments and methods.

The Photographic Measurement of Line Breadths

In order to set up equations for the measurement of line breadths photographically, we must solve the problem of Eq. (15) in the case in which the spectrum, instead of being monochromatic, consists of a continuous distribution of energy over a range of wave-lengths.[11] We will limit our considerations

[11] Valasek has corrected his observed line widths by merely subtracting from them a value of the monochromatic width obtained by adding the angular slit width and the full width at half maximum of the observed rocking curve on the double spectrometer. In the opinion of the author, this method is open to criticism, and an attempt is here made to outline a better method of correction.

to a spectrum line and assume that the energy is dstributed in a Gaussian error curve, represented by

$$I_\lambda = e^{-(\lambda-\lambda_0)^2 \log 2/w_\lambda^2} \tag{23}$$

where I_λ is the intensity of wave-length λ in terms of the maximum which occurs at λ_0, and w_λ is the half width at half maximum of the line. In Fig. 3 consider the intensity at point P on the photographic plate due to a wave-length range $d\lambda$ about λ. P' is the intersection on the photographic plate of a line passing through the center of the slit aperture and making a glancing angle θ on the crystal (Eq. (2)). If I_λ is the intensity of this wave-length in the original spectrum, an intensity $I_\lambda d\lambda$ will be derived from the spectral range $d\lambda$. This will be spread out on the photographic plate in an impression the width of which is determined from Eq. (15), and the contribution to the intensity at P may be written

$$dI_p = I_\lambda d\lambda \int_{-(a-2x)/2R}^{(a+2x)/2R} e^{-(\log 2)/we^2)\xi^2} d\xi \tag{24}$$

where x is now the distance PP' and not OP as in Fig. 1. The integral in Eq. (24) will be one of the curves in Fig. 2; which one depending on the ratio $(a/2R)/w_e$ which is appropriate to the apparatus being used. Let us assume that this integral in a particular case is $F(x/R)$. Let $\overline{OP}/R$ in Fig. 3 be Δ, then if D is the angular dispersion,

$$x/R = \Delta - D(\lambda - \lambda_0) \tag{25}$$

and Eq. (24) becomes

$$dI_p = I_\lambda d\lambda F\{\Delta - D(\lambda - \lambda_0)\} \tag{26}$$

or

$$I_p = \int_{-\infty}^{\infty} I_\lambda F\{\Delta - D(\lambda - \lambda_0)\} d\lambda. \tag{27}$$

The extension of the limits of λ to $\pm\infty$ is justified by the narrowness of the lines compared to the spectral range which can get through the slit. Unless the form of $F(\Delta - D(\lambda - \lambda_0))$ is known, the problem cannot be carried out further. For suggestions as to the form of this function we may inspect Fig. 2. If we assume that for angular slit widths up to $a/2R = w_e$ the function can be sufficiently well represented by a Gaussian error curve we can get an approximate solution of Eq. (27). Setting

$$F\{\Delta - D(\lambda - \lambda_0)\} = e^{-\log 2/w^2\{\Delta - D(\lambda-\lambda_0)\}^2} \tag{28}$$

we obtain from Eq. (27) the result

$$I_p \sim e^{-\Delta^2 \log 2/(w^2 + w_\lambda^2 D^2)} \tag{29}$$

in which a factor similar to that under the radicle sign in Eq. (10) has been omitted. If W is the half width at half maximum of the line as observed on the photographic plate, in angular units, it follows from Eq. (29) that

$$W = (w^2 + D^2 w_\lambda^2)^{1/2} \tag{30}$$

Application to Experimental Results

Valasek[2] and Duane[8] have recently reported results obtained with high resolving power photographic spectrometers. In the case of Duane's work, the slit to plate distance R was 472.5 cm, but the slit width is not given, hence the resolving power cannot be calculated.

In Valasek's work results are given for measurements of Mo$K\alpha_1$, Mo$K\beta_1$, Ag$K\alpha_1$ and Cu$K\alpha_1$ in the first order from a high resolving power spectrometer constructed in Siegbahn's laboratory. Measurements in the second order for the $K\alpha$ lines of Fe, Ni, Co, and Cu are also given. Discussion here will be confined to the experiments on Mo$K\alpha_1$ in the first order, as for the other values so little is known at present about w_c that speculation is very precarious. We can, however, assume that the crystal used by Valasek had a w_c equal to that reported by Allison and Williams, and proceed to calculate the resolving power. The value of R was 296 cm, of a, 0.003 cm, hence $a/2R$ was 5.06×10^{-6}. Allison and Williams' value of w_c is 2.1 seconds of arc, or 1.02×10^{-5} radans. Hence $(a/2R)/w_c$ was 0.496 in Valasek's experiment. We now look to Fig. 2 to find the type of monochromatic impression on the photographic plate to be expected. We see that the curve will be of approximately Gaussian error curve shape and of angular width $w=1.09w_c=1.11\times10^{-5}$. Applying Eq. (16) we find that $\lambda/d\lambda=5350$. Valasek's own estimate of his resolving power is 4720. The maximum resolving power obtainable from a double spectrometer having equally good crystals in the (1, 1) position is is 8100.

We now proceed to the calculation of w_λ from the widths of the photometer curves observed by Valasek for the Mo$K\alpha_1$ line. We apply Eq. (30). Valasek's value of W observed was 0.20X.U. In order to apply Eq. (30) we must change the value of w in Eq. (30) to wave-lengths. The angular dispersion of calcite for Mo$K\alpha_1$ (1) is 34.28 seconds per X.U., hence the w of the preceding paragraph corresponds to 0.066 X.U. Applying Eq. (30) we find $w_\lambda=0.19$ X.U. for Mo$K\alpha_1$.

The value of w_λ calculated by this method is considerably larger than that calculated by Valasek from his own results (0.13 X.U.). If the method of treatment in this paper is valid, however, his method of correcting the observed W's, which consists in simply subtracting values of w from them, is erroneous.

The value of the half width at half maximum of Mo$K\alpha_1$ calculated here from Valasek's results (0.19 X.U.) is considerably larger than that obtained by the most recent results by the double spectrometer method. The value obtained by Allison and Williams was 0.147 X.U., and recently Mark and von Susich[12] have obtained the values 0.163 and 0.144 X.U. with calcite and topas crystals respectively. The discrepancy between the photographic and ionization double spectrometer methods may be due to lateral spreading of the image on the photographic plate due to secondary x-rays, or to photoelectrons ejected from the plate substance. Also the effective slit width of the microphotometer used in taking the blackening curve would contribute to the estimated W, tending to increase it.

[12] Mark and von Susich, Zeits. f. Physik **65,** 253 (1930).

500 KILOVOLT CATHODE RAYS

By R. E. Vollrath*
California Institute of Technology

(Received June 2, 1931)

Abstract

The high potential x-ray tube at the California Institute has been modified so as to permit either x-rays or cathode rays to be produced. Electron currents up to 35 microamperes have been obtained through an aluminum window. A typical magnetic velocity spectrum of the high speed electrons passing out of an aluminum window is presented. The high velocity limit corresponds to about 500 kilovolts when the transformer voltage is 600 kilovolts peak. The velocity spectrum appears to be continuous and no absorption anomalies due to aluminum and lead foil are evident. The time required to obtain a velocity spectrum was reduced to a few minutes by allowing the electrons after being magnetically deflected, to pass through a copper foil into the air. The outside of the foil is coated with calcium tungstate and the photographic plate is placed in contact with the tungstate. It is noted that part of the photographic action of the high speed electrons is due to fluorescence of the glass backing of the photographic plates.

Introduction

IT WAS shown in a previous paper[1] that it is possible to operate the high potential x-ray tube at the California Institute of Technology with a hot cathode at about 600 kv alternating current. Electron currents of at least 3 milliamperes can be handled in this type of tube; and therefore it appeared feasible to obtain, through a Lenard window, cathode rays corresponding to the above voltage and of sufficient intensity to permit magnetic velocity spectra to be recorded photographically in short exposures. This paper is a report of some preliminary work on these cathode rays and involves (1) the measurement of the potential difference between the electrodes of the tube and (2) the velocity spectrum of the electrons.

The measurement of the maximum or peak potential difference between the electrodes is a matter of considerable difficulty at these high voltages; and it was thought most reliable to determine it by calculation from the high velocity limit of the magnetic velocity spectrum of the electrons. The intensity of the cathode rays obtained made it possible to obtain the velocity spectrum of high speed electrons which had passed through foils of different substances for the purpose of discovering possible absorption edges due to quantum jumps higher in energy than the K x-ray limit.

Apparatus

In order to permit the tube to be used for the production of either x-rays or cathode rays the new electrode system in Fig. 1 designed by Dr. Lauritsen

* National Research Fellow.

[1] Lauritsen and Cassen, Phys. Rev. **36**, 988 (1930).

was used. The remainder of the tube was unchanged so that only the electrodes will be shown in Fig. 1. The upper or high potential electrode was furnished with a tungsten target which could be bombarded to produce x-rays by electrons coming from a hot filament in the lower or grounded electrode. The upper electrode also had mounted in it a tungsten filament which could be heated by means of a 6 volt storage battery on top of the tube. The current through this filament is controlled by a rheostat in the filament circuit oper-

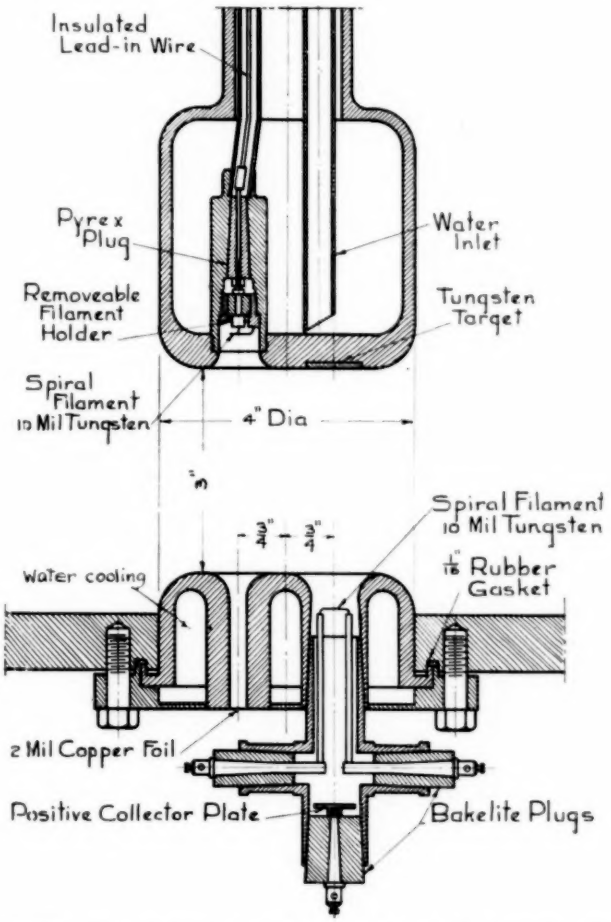

Fig. 1. Electrode system for producing either cathode rays or x-rays.

ated from the ground by means of long cords. Owing to the focussing effect of the recess in which the filament is mounted, electrons leave the upper electrode in a narrow beam which passes through the hole in the lower electrode and then through a thin copper window into the air.

At first mica and metal foils were fastened with sealing wax in the position shown in Fig. 1. However foils fastened in this manner were very easily punctured, probably due to deficient cooling. This difficulty was eliminated by using aluminum foil 0.004 cm thick clamped between the flanges of Fig. 2.

This arrangement was threaded into the hole formerly closed off by the copper foil of Fig. 1. Electron currents up to 35 microamperes were obtained through this foil without damaging it. Whether this is anywhere near the maximum that can be sent through the foil cannot at present be stated because the

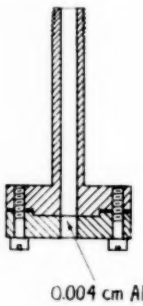

Fig. 2. Holder for aluminum window.

upper and lower electrodes were not sufficiently aligned and most of the electrons, amounting to 3 milliamperes, struck the walls of the hole. A few microamperes coming from the window into the air could be seen as a cone of bluish luminescence extending almost a meter away from it.

Velocity Spectrum

In the velocity determination, the electrons entered an evacuated magnetic spectrograph through an aluminum foil 0.004 cm thick. The foil of the tube and that of the spectrograph were separated by a distance of 1 cm, so that the velocity spectrum represents electrons which have passed through 0.008 cm of aluminum and 1 cm of air. Within the spectrograph a system of steel slits served to separate a beam of electrons 0.005 cm wide and 3 mm long

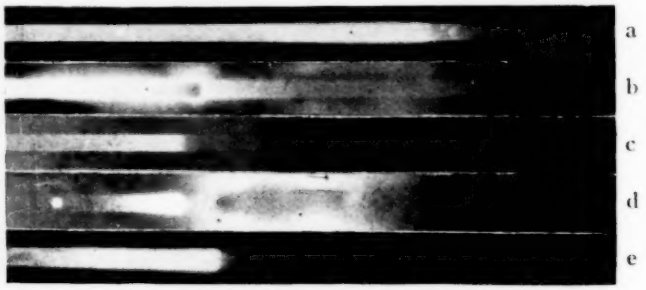

Fig. 3. Velocity spectra.

which was then bent into a semicircle by a magnetic field and fell on a photographic plate. The radius of curvature corresponding to a given position in the spectrum on the plate was determined from the position of a small spot photographed on the plate at a known distance from the slits. The magnetic field was measured after each exposure by means of a Grassot fluxmeter. The velocity was calculated from the measured radius of curvature of the electron

beam and the magnetic field, making use of the relativistic mass of the electron. Spectrograms of sufficient intensity could be obtained in 20 minutes with 2 microamperes coming out of the aluminum window. Fig. 3a is a typical spectrum obtained in this way. The high velocity limit in this corresponds to 567 kv. The voltage at the transformer terminal during this run was 650 kv. The difference 83 kv is most probably accounted for by a voltage drop in the water resistance in series with the tube and by a loss of velocity of the electrons passing through the foils. Spectrum *b* shows the effect of overexposure resulting in the well known decrease of blackening when the plate is overexposed. Spectrum *c* was obtained with the transformer voltage 630 kv. Here the high velocity limit was calculated to be 541 kv. Spectrum *d* was obtained

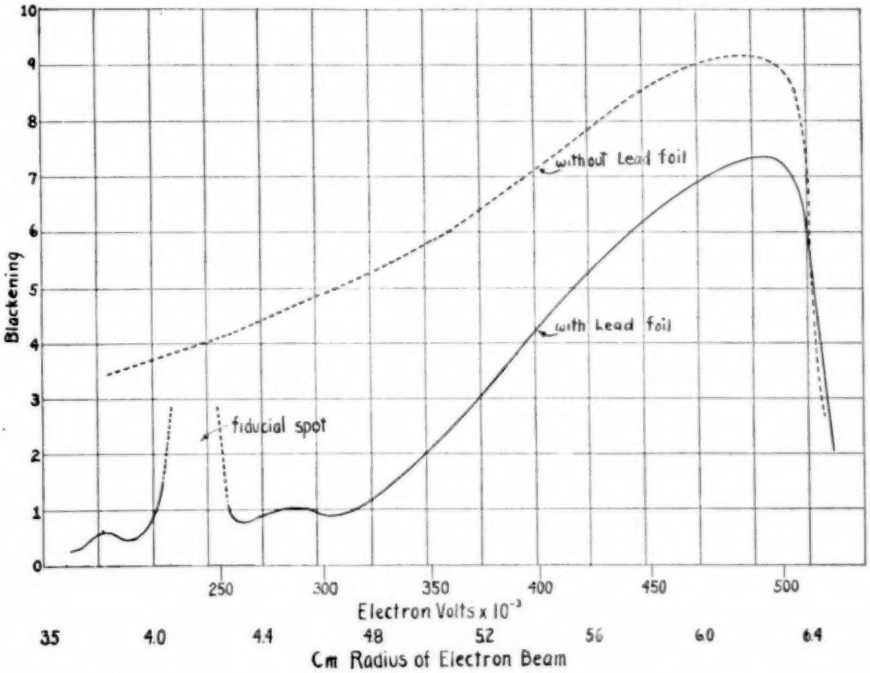

Fig. 4. Photometer record of electrons before and after passing through lead foil.

with the same voltage on the tube and the same magnetic field in the spectrograph, but the electrons were allowed to pass through a 0.003 cm lead foil before entering the spectrograph. A photometer record of spectrum *c* and *d* is shown in Fig. 4. Plate *d* was exposed for 45 minutes while *c* was exposed 15. The peculiar haze beyond the high velocity limit on *d* is due to stray light entering an amber plug in the spectrograph. A close examination of the original negative showed no absorption discontinuities and this is verified by the photometer record. Similar plates were taken with copper and iron foils and here also no absorption anomalies were evident.

On most of the plates the spectrum was surrounded by a pronounced haze. Plate *b* in Fig. 3 shows this most plainly. It was at first thought that this was due to x-rays resulting from the impact of the electrons on the photo-

graphic plate, and thus to serve as a means of investigating the efficiency of excitation of x-rays as a function of electron velocity. But the blackening was found to be due to visible fluorescence produced in the glass of the photographic plates by impact of electrons passing through the gelatine layer. A piece of black paper was placed over the photographic plate in the spectrograph and another plate placed on top of the paper with the sensitive gelatine layer in contact with the paper as in Fig. 5. After 20 minutes exposure the upper plate showed no blackening. But when the black paper was omitted the upper plate showed a blackening which was of the same order of intensity as the blackening produced by the electrons in the lower plate. Apparently a considerable fraction of the blackening in the electron spectrograms is due to this fluorescence. It is of course well known that glass fluoresces under the influence of electron bombardment. This fluorescence must be considered in any work on the blackening of photographic layers by high speed electrons.

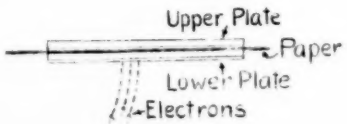

Fig. 5. Absorption of fluorescence by black paper.

With such high velocity electrons it was found feasible to obtain a velocity spectrum on a photographic plate outside of the spectrograph very much as oscillograms are obtained in the recently developed cathode ray oscillographs equipped with thin windows. The electrons after having been magnetically deflected were allowed to pass through a copper foil stretched over the gap between the semicircular pole faces of the electromagnet and to fall on a photographic plate placed with its sensitive layer in contact with the foil. A further improvement consisted in coating the outer surface of the copper foil with a thin film of collodion having suspended in it finely divided calcium tungstate. Electrons coming through the foil excited the tungstate to luminescence, and the velocity spectrum could be observed visually in a darkened room. Plate *e* was obtained in 5 minutes when placed in contact with the tungstate layer while 2 microamperes were emitted from the window of the tube.

The writer wishes to thank Professor Millikan for placing the facilities of the laboratory at his disposal.

X-RAY ABSORPTION COEFFICIENTS OF MERCURY VAPOR IN THE REGION OF ITS *L*-ABSORPTION DISCONTINUITIES

By Fred M. Uber
University of California, Berkeley

(Received June 8, 1931)

Abstract

An apparatus is described which is suitable for absorption measurements up to 2 or more angstroms. The absorber, which was in the form of superheated vapor whose density could be calculated on the assumption of perfect gas behavior, was contained in an all-glass chamber. The windows were constructed of thin glass films in such a way as to withstand atmospheric pressure from either side. The mass absorption coefficients, μ/ρ, of mercury in the wave-length region 0.74 to 1.4A were determined by an ionization method. They were found to obey the relation $\mu/\rho = A\lambda^c$, where the constants A and c vary from branch to branch of the μ/ρ, λ curve. The value of c is 2.56 on the short and 2.66 on the long wave-length side of the L discontinuities. The magnitudes, δ, of the three L absorption discontinuities, where δ is defined as the ratio of μ/ρ (the scattering coefficient being neglected) on the short and long wave-length sides of an absorption limit, are

$$\delta L_{\mathrm{I}} = 1.18 \qquad \delta L_{\mathrm{II}} = 1.39 \qquad \delta L_{\mathrm{III}} = 2.45$$

Introduction

THE magnitude, δ, of an absorption discontinuity (in case the absorption due to scattering is relatively small and may be neglected in comparison with the true or fluorescent absorption) is defined as the ratio of the mass absorption coefficients on the short and long wave-length sides of an absorption limit. Values for the magnitude of the K discontinuity have been determined for a large number of elements by Richtmyer,[1] Allen,[2] Jönsson,[3] and others. These have been found to decrease with increasing atomic number. Few researches have been published on the magnitudes of the three L discontinuities. Dauvillier[4] worked on gold, Kellström[5] on silver, and Backhurst[6] on gold and platinum.

Such paucity of data in this wave-length region is due to the lack of x-ray intensity and to the difficulties involved in preparing and measuring uniform absorbing screens of 0.0005 cm thickness. These difficulties have been obviated in the present research by the design of the apparatus and by using mercury in the vapor state, the latter making it possible to obtain the equivalent thickness of the absorber from accurate temperature and pressure measurements.

[1] F. K. Richtmyer, Phys. Rev. **27,** 1 (1926); **30,** 755 (1927).
[2] S. J. M. Allen, Phys. Rev. **28,** 907 (1926).
[3] E. Jönsson, Upsala Universitets Arsskrift, 1928, Mathematik och Naturvetenskap 1.
[4] A. Dauvillier, C. R. **178,** 476 (1924).
[5] G. Kellström, Zeits. f. Physik **44,** 269 (1927).
[6] Ivor Backhurst, Phil. Mag. (7) **7,** 353 (1929).

Apparatus

The high potential for operating the x-ray tube was furnished by a transformer-kenetron-capacity set, to which 500 cycle current was supplied from a 5 kw motor-generator. The field current for the generator was supplied by storage batteries. The tube voltage was read on an electrostatic voltmeter of the repulsion type, calibrated by using the short wave-length limit of the continuous x-radiation.

The x-ray tube and absorption chamber were of Pyrex glass and were combined into a single unit as shown in Fig. 1. All three compartments of the system were evacuated through a liquid air trap at the same time by a mercury diffusion pump. The target holder *W* was fitted on a ground glass joint

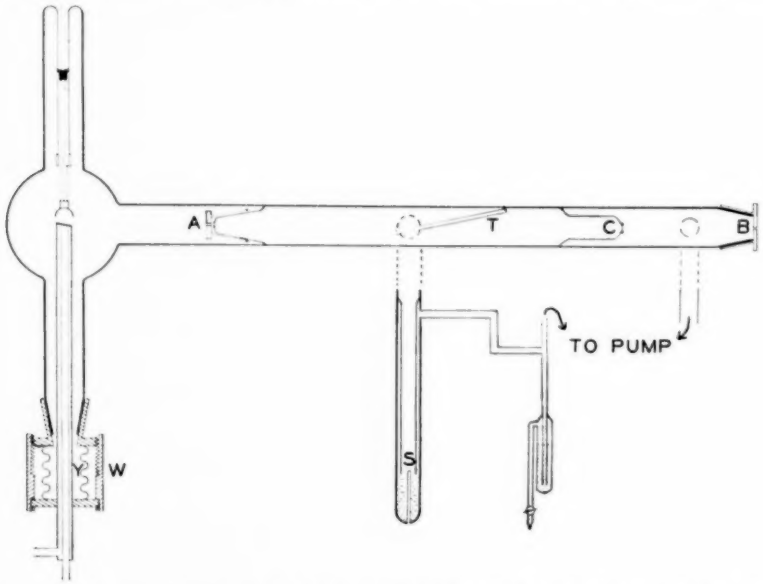

Fig. 1. Horizontal cross section of the x-ray tube and absorption chamber, and vertical cross section of the tube containing the liquid mercury.

to the x-ray tube and was made vacuum tight with deKhotinsky cement. The water-cooled tungsten target was made adjustable by the use of corrugated extensible copper tubing at *Y* so that the focal spot could be lined up with the fixed slits. The anticathode being grounded, the position of the target could be varied while the tube was in operation. The constancy of the focal spot was assured by using a cone-type filament holder at a distance of 1 cm from the face of the target, the latter making an angle of 12 degrees with the slit system. The current through the tungsten filament was supplied by storage batteries and was controlled by a continuously variable mercury resistance of the Kirkpatrick[7] type.

The x-ray beam was defined by two steel slits, *A* and *B*, each being 0.2 by 10 mm, placed 65 cm apart, giving an angular width to the beam of ap-

[7] P. Kirkpatrick, J.O.S.A. and R.S.I. **7**, 195 (1923).

proximately 2′ of arc. The corresponding spreads in wave-length were 0.45 and 0.25 percent at 0.8 and 1.4 *A* respectively. The resolution obtained was ample for separating the L_{III} edge of mercury and the γ_4 line of tungsten, which have an angular separation of 11′.

The absorption chamber was 3.5 cm in diameter and 40.4 cm in length. The windows were also made of Pyrex by sealing glass films 0.0025 cm thick on narrow glass slits. Glass tubing was flattened at one end to make a slit 0.1 by 1.5 cm. With the edge of this slit heated to incandescence, a thin glass film was pressed gently against it—there being sufficient heat present to fuse the two together. A small flame was used to melt in thoroughly the edges of the film and to give a finished appearance to the product. Satisfactory pieces of nearly curvature free film were obtained by blowing large glass bulbs. Skillfully prepared windows would withstand atmospheric pressure in either direction. The liquid mercury was contained in a tube 2 cm in diameter and 22 cm in depth, which projected from the bottom of the vapor chamber. After evacuation the absorption chamber was closed off by driving in sufficient mercury from a side tube to fill the trap at *S*. The temperature of the liquid at *S*, then, determined the vapor pressure of the system. This temperature was measured by inserting a thermocouple in the small tube just below the surface of the mercury. A thermocouple in the upper tube at *T*, as shown in the figure, measured the temperature of the vapor. To secure steady temperatures, the absorption tube was surrounded with a layer of 1.5 mm copper, which projected about 10 cm beyond the glass windows in order to prevent condensation. Heat insulation was provided by a large cylindrical furnace of 22 cm internal diameter and 62 cm length made of magnesium oxide. Four heating coils were strung lengthwise in this air space and maintained a temperature of 270°C. The liquid mercury container was insulated in a similar manner and electrically heated with current supplied by storage batteries.

The e.m.f. of the copper-constantan thermocouples was read on a potentiometer whose smallest scale division was 5 microvolts, which corresponds to a temperature difference of 0.1°C. A Weston standard cell was used for the reference voltage. The thermocouples were calibrated and used with the cold end in ice shavings. Fixed points for calibration were checked with thermometers recently certified by the U. S. Bureau of Standards. The boiling point of naphthalene was taken as 217.95°C from the Smithsonian Physical Tables. In practice, temperatures were determined by using a deviation curve in conjunction with a standard e.m.f.-temperature curve for copper-constantan, the latter being plotted from data in the International Critical Tables.[8] Data from the same source[9] were used in plotting on the same graph the vapor pressure-temperature curve of mercury. Each millimeter scale division on the chart corresponded to 0.1 degree or to 4 microvolts.

The ionization chamber followed in design and operation the descriptions of Williams and Allison[10] and of Hicks[11]. It was of Pyrex glass 3.5 cm

[8] International Critical Tables, Vol. I, p. 58.
[9] International Critical Tables, Vol. III, p. 206.
[10] J. H. Williams and S. K. Allison, J.O.S.A. and R.S.I. **18,** 473 (1929).
[11] Victor Hicks, Phys. Rev. **36,** 1273 (1930).

in diameter and 35 cm in length and was filled with methyl iodide and argon at partial pressures of 14 and 62 cm of mercury respectively. The window of the chamber, 2 by 20 mm, was covered with thin mica and was at a distance of 5 cm from the axis of the spectrometer table. The scale of the Bragg-type spectrometer could be read to 30″ of arc. The Compton electrometer was used heterostatically with a voltage sensitivity of 3500 mm/volt at a scale distance of 3 meters. The calcite crystal was one previously used by Allison for relative intensity measurements of x-ray measurements.

Method

The absorption tube was kept always at a temperature of about 270°C. Several hours before each series of measurements the liquid mercury was raised to a steady temperature which ranged from 205 to 230°C, depending on the wave-length region being investigated. The corresponding vapor pressures ranged from 25 to 40 mm of mercury. Temperature changes were always in one direction and were not greater than one degree per hour.

The voltage applied to the x-ray tube varied from 17 to 24 kv, in each case being sufficiently low to prevent excitation of radiation which would reflect in the second order. Tube currents ranged from 6.5 to 17.5 m.a. Both current and voltage could be kept constant to within one percent. The tube was operated for a period of two hours before any readings were recorded. Each series of readings consisted of from 8 to 12 positions of the crystal and required about two hours. Electrometer deflections were timed over the same range of the scale for a distance of 10 cm for all crystal positions. Individual readings varied from their average by about one percent. The temperature of the liquid mercury was read for each electrometer deflection. Then the furnace was removed and the liquid mercury cooled to below room temperature. Rates of deflection for the unweakened beam were measured for the same angular settings of the crystal and ranged from 2 to 7 mm/sec. From 0.4 to 0.8 of the original intensity was absorbed.

Calculations and Results

The mass absorption coefficient is given by the equation

$$\frac{\mu}{\rho} = \frac{\ln (I_0/I)}{\rho x}$$

where I_0 is the original intensity of the monochromatic beam of x-rays and I is the intensity after penetrating to a depth x in an absorbing medium of density ρ. Assuming that superheated mercury vapor behaves as a perfect gas, we will make use of the equation

$$pV = (m/M)RT$$

so that

$$\rho = \frac{m(\text{grams})}{V(\text{cm}^3)} = \frac{M(\text{grams/mole})\,p(\text{mm of } Hg.)\,A_n(\text{dynes/cm}^2)}{R(\text{ergs/deg/mole})(T_0 + t)760}$$

where A_n is the normal atmosphere. The constants used have the values: $A_n = 1.01325 \times 10^6$ dynes/cm², $R = 8.3136 \times 10^7$ ergs/deg/mole, $M = 200.61$ grams/mole = at. wt. of mercury, $T_0 = 273.18$ C, $x = 40.4$ cm = length of absorbing column, giving now as our final equation

$$\frac{\mu}{\rho} = \frac{T \ln (I_0/I)}{0.12997 p} \text{ or}$$

$$\log \frac{\mu}{\rho} = \log T + \log (\log (I_0/I)) - \log p + 1.24870$$

I_0 and I are proportional to the rates of deflection of the electrometer due to the ionization produced. T is the absolute temperature of the absorbing vapor and p its pressure in mm of mercury as determined from the vapor pressure-temperature curve of the liquid.

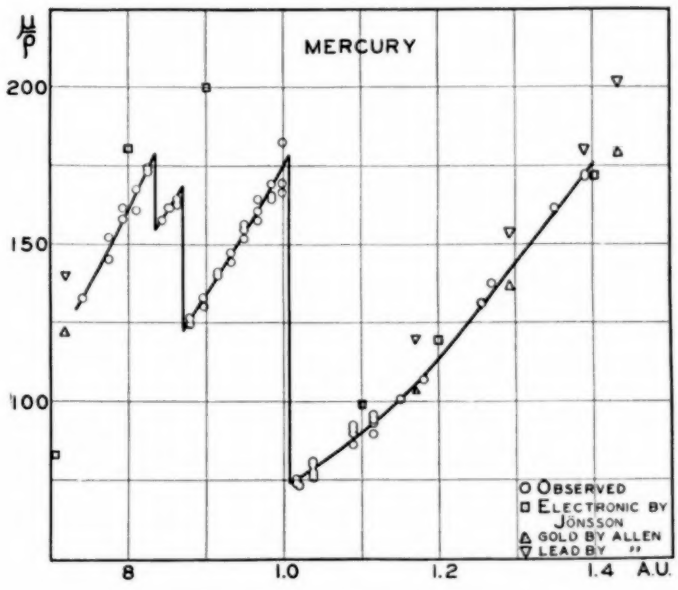

Fig. 2. The variation of the mass absorption coefficient of mercury with wave-length.

The observed points are plotted in Figs. 2 and 3. The wave-length corresponding to each position of the crystal has been obtained by interpolation from the tables in Siegbahn's Spectroscopy of X-rays. When several points are indicated for the same wave-length, they refer to observations made on different days under varying conditions of temperature, pressure, and perhaps current and voltage also. Edvin Jönsson[3] has proposed a universal formula for x-ray absorption which is based on the average absorption per electron. He finds this electronic absorption coefficient to be a function of $N\lambda$ for all elements, where N is the atomic number. Several values of μ/ρ for mercury, calculated from the tables of Jönsson, have been plotted for comparison in Fig. 2. There is no particular agreement except on the long wave-length side. The

mass absorption coefficients for gold and lead from the results of Allen[2] are seen to be consistent with the data for mercury.

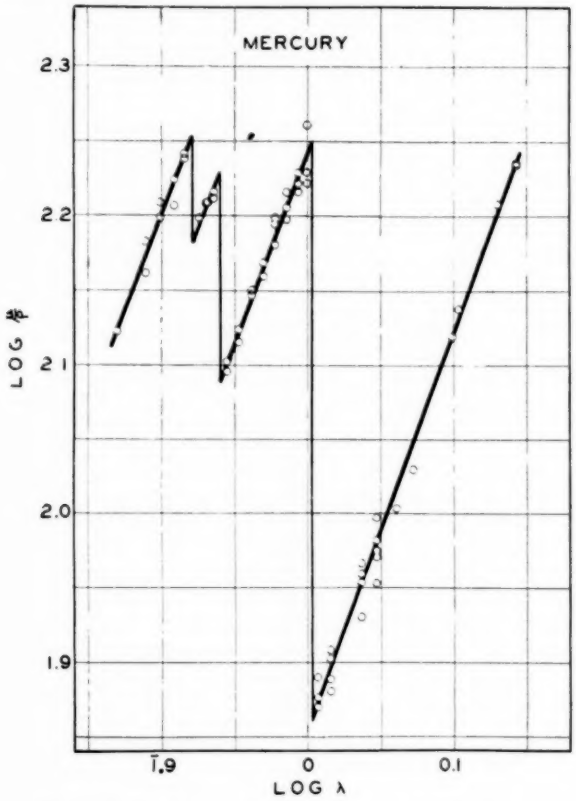

Fig. 3. Log μ/ρ as a function of log λ for mercury.

Within the limits of experimental error, the mass absorption coefficients have been found to obey the empirical law:

$$\frac{\mu}{\rho} = A\lambda^c$$

where A and c are constants whose values change from branch to branch of the absorption curve. In Fig. 3, log μ/ρ is plotted against log λ and the resulting equations for the four straight lines are

$$\log\left(\frac{\mu}{\rho}\right)_{L_{\mathrm{I}}} = 2.456 + 2.557 \log \lambda$$

$$\log\left(\frac{\mu}{\rho}\right)_{L_{\mathrm{II}}} = 2.384 + 2.557 \log \lambda$$

$$\log\left(\frac{\mu}{\rho}\right)_{L_{\mathrm{III}}} = 2.242 + 2.586 \log \lambda$$

$$\log\left(\frac{\mu}{\rho}\right)_{M_{\mathrm{I}}} = 1.856 + 2.656 \log \lambda$$

where λ is in Angstroms. The L_{II} branch has been assigned the same slope as L_I. Corresponding slopes for other elements are given in Table I. These slopes give good agreement with each other except for the short wave-length branch of gold. Allen finds that his data fit best a $c=2.92$ curve for L_I and a $c=2.6$ curve for M_I absorption for the elements W, Au, Pt, and Pb. Wingardh,[12] on the other hand, obtains 2.58 for Pb on the L_I branch. There is need for more experimental data.

TABLE I. *Slopes of the log μ/ρ, log λ curve for several elements.*

Element	Branch of curve				Observer
	L_I	L_{II}	L_{III}	M_I	
Silver (47)	2.6	2.6	2.6	2.6	Kellström[5]
Platinum (78)	2.6	2.6	2.6	2.64	Backhurst[6]
Gold (79)	2.91	2.91	2.64	2.61	Backhurst[6]
Mercury (80)	2.56	2.56	2.59	2.66	The author

The total mass absorption coefficient is the sum of two components—the fluorescence coefficient, τ/ρ, and the scattering coefficient, σ/ρ. The absorption due to scattering is supposed to be a continuous function of the wave-length and is believed to be relatively slight at long wave-lengths for elements of high atomic number, probably not greater than unity. Since μ/ρ is large under such conditions, σ/ρ is generally considered as negligibly small in comparison. It is τ/ρ that suffers a discontinuity at the absorption limits and so we define the magnitude of an absorption discontinuity as the ratio of τ/ρ on the short and long wave-length sides of a limit. If we neglect σ/ρ, then δ becomes equal to the corresponding ratio of the total mass absorption coefficients. The wave-lengths of the L limits of mercury, as recently measured by Sandström,[13] are

$$L_I = 0.8342A \quad L_{II} = 0.8708A \quad L_{III} = 1.0075A.$$

Values taken from the curve in Fig. 3 give the following for the magnitudes of the three L absorption discontinuities,

$$\log \delta L_I = 0.072 \quad \text{or} \quad \delta L_I = 1.183$$
$$\log \delta L_{II} = 0.142 \quad \text{or} \quad \delta L_{II} = 1.387$$
$$\log \delta L_{III} = 0.390 \quad \text{or} \quad \delta L_{III} = 2.455.$$

The discontinuity magnitudes for mercury are compared with those for other elements in Table II. Dauvillier used a photographic method and assumed a λ^3 law in arriving at his results. The only striking singularity in the atomic number sequence 78, 79, 80 is δL_I of mercury, which is decidedly lower than the corresponding values for gold and platinum. δL_{III} is also somewhat lower. One would expect a decrease in δ with increasing atomic number from an analogy with the K discontinuities. There are not sufficient data available, however, to allow conclusions to be drawn for the L absorption spectrum.

[12] K. A. Wingardh, Dissertation at Lund, 1923.
[13] Arne Sandström, Zeits. f. Physik **66**, 784 (1930).

Edvin Jönsson[3] has found that δK and δL obey the relation

$$\delta K = E_K/E_{L_1} \quad \text{and} \quad \delta L = E_{L_1}/E_{M_1}$$

where E represents the ν/R value of the designated absorption limit and δL is the product of the three separate magnitudes δL_{I}, δL_{II} and δL_{III}. How well this holds for mercury and several other elements can be seen from Table II also.

TABLE II. *Magnitudes of the L absorption discontinuities for several elements.*

Element	E_{L1}/E_{M1}	δL	δL_{I}	δL_{II}	δL_{III}	Observer
Silver (47)	5.24	5.82	1.25	1.47	3.17	Kellström[5]
Platinum (78)	4.22	4.26	1.25	1.37	2.47	Backhurst[6]
Gold (79)	4.20	4.20	1.24	1.39	2.48	Dauvillier[4]
	4.20	4.25	1.26	1.36	2.53	Backhurst[6]
Mercury	4.16	4.02	1.18	1.39	2.45	The author

As has been pointed out frequently in the literature,[1,2] none of the classical theories of x-ray absorption,—as formulated by Thomson, Compton, Kramers and deBroglie, represents satisfactorily the experimental data. The λ^3 law, which is contained in all of them, gives fair agreement for certain wave-length regions, however. The quantum-theoretical treatments of the problem by Oppenheimer[14] and Wentzel[15] allow more latitude in the value of the exponent of λ, but they are unable to predict definite values for a given wave-length region. More recently, Nishina and Rabi[16] and Roess[17] have worked out formulas on the basis of the Schrödinger and Dirac mechanics, respectively, but with only fair agreement with experiment. All these later theories, however, were developed for the K electrons, so that the L absorption still remains practically untouched from the theoretical viewpiont.

The original suggestion and mode of attack of this problem are due to Professor Samuel K. Allison, to whom the author wishes to express his sincere gratitude. The willing cooperation of Professor Robert B. Brode in furthering the experimental work is worthy of my heartiest thanks. I am also indebted to the University of California for the appointment to a Harold Whiting Fellowship in Physics during the course of the investigation.

[14] J. R. Oppenheimer, Zeits. f. Physik **41,** 268 (1926).
[15] G. Wentzel, Zeits. f. Physik **40,** 574 (1926).
[16] Y. Nishina and Rabi, Verh. d. D. Phys. Ges. (3) **9,** 6 (1928).
[17] L. C. Roess, Phys. Rev. **37,** 532 (1931).

MANY-ELECTRON SELECTION RULES

By S. Goudsmit and L. Gropper
University of Michigan

(Received May 11, 1931)

Abstract

Selection rules for many-electron transitions are derived by taking into account the first order perturbed eigenfunctions. The perturbations considered are the electrostatic interactions between the pairs of electrons, and the spin-orbit interaction of each electron. It was found that the possibly occurring terms in the first order eigenfunction were narrowly limited, and that this limitation provided the selection rules as follows: No more than three electrons can jump at a time. (a) when three electrons jump all change their n by an arbitrary amount, one changes its l by ± 1, the others by δ and ϵ, $\delta+\epsilon$ being even. (b) when two electrons jump both can change their n arbitrarily, one changes its l by $\delta \pm 1$, the other one by ϵ. Breaking off the series expansion for $1/r_{FG}$ in the electrostatic interaction after the second term gives for δ and ϵ only the values 0, ± 1. The Heisenberg two-electron selection rule is therefore to be considered as a special case of (b). The Laporte rule is verified making use only of the properties of spherical harmonics. Qualitative rules have been derived to tell when many-electron transitions may be expected to be strong. The first order terms also cause anomalies in the intensities of one-electron transitions.

I. Introduction

IN A recent paper* Condon considered the influence which neighboring electron configurations have upon each other when one treats the first order perturbation of the eigenfunctions. Condon also mentioned that the occurrence of two-electron transitions was closely connected with this mutual influence. In this paper we propose to study somewhat more in detail the possibilities for many-electron transitions by means of the method used by Condon. For our purpose it is necessary to investigate what type of terms occurs in the first order expansion of the eigenfunctions. The perturbations we shall consider are the electrostatic interaction between the different electrons, and the spin-orbit interaction for each electron.

2. One-Electron Transitions in the Many-Electron Problem

We shall first discuss the outline of the way in which our results were obtained, and at the end of the paper give the more detailed derivations and remarks.

Let

$$\psi^0(n_1 l_1;\ n_2 l_2;\ \cdots\ n_f l_f) \tag{2.1}$$

be a zeroth order eigenfunction for an f-electron problem, stabilized with respect to the electrostatic interaction between the different electrons, and for the spin-orbit interaction of each electron. For convenience we also assume

* Condon, Phys. Rev. **36**, 1121 (1930).

that these functions are stabilized for the interaction with a homogeneous magnetic field. This symbol thus stands for a linear combination of eigenfunctions, each one being the product of single-electron eigenfunctions for all electrons. The single-electron eigenfunctions are the usual Schrödinger central field eigenfunctions with spin,

$$R_{nl}(r)P_l^{m_l}e^{im_l\phi}S(m_s/l).$$

The different terms of such a linear combination will all contain the same set of quantum numbers, n_i, l_i, but will differ in the permutations of the coordinates over these states. Moreover the same permutation will occur several times in the linear combination, each time with a different choice for the magnetic quantum numbers, m_l and m_s for each electron. This choice is restricted, however, by the fact that the total projection, M, given by,

$$M = \sum m_l + m_s$$

is the same for all terms of the linear combination and is a characteristic of the state under consideration. For our problem the magnetic quantum numbers are of no further interest. That is why we do not use them in the designation of the eigenfunctions.[1]

The intensity of a transition between two states, each one characterized by such a zeroth order eigenfunction, depends upon integrals of the form

$$\int \bar{\psi}^0(n_1'l_1';\ n_2'l_2';\ \cdots\ n_f'l_f')X\psi^0(n_1l_1;\ n_2l_2;\ \cdots\ n_fl_f)d\tau. \tag{2.2}$$

Primes are used for the quantum numbers of the final state. Here X stands for any one of the quantities

$$\begin{aligned} &\sum_F r_F \sin\theta_F e^{i\phi_F} \\ &\sum_F r_F \cos\theta_F \\ &\sum_F r_F \sin\theta_F e^{-i\phi_F}. \end{aligned} \tag{2.3}$$

Considering the angles[2] θ_F one can derive first of all the well-known selection rule for M. For the first choice of X the integral (2.2) vanishes unless $M' = M+1$, for the second choice unless $M' = M$, and for the third choice unless $M' = M-1$. The middle choice gives a Zeeman component which is linearly polarized, parallel to the direction of the external field, the others give the circularly polarized components.

[1] In the derivations at the end the magnetic quantum numbers will be included for the sake of clarity.

[2] One should not confuse the coordinates of the first, second . . . Fth electron, with the quantum numbers, e.g., n_1, n_2, n_3, $\cdots$ n_f. The number of quantum number sets f, of course equals the number of electrons F, but there is no connection between n_1, and r_I, n_2 and r_{II} etc. Because of the permutations n_1 is connected with all the r_I, r_{II}, $\cdots$ r_F. Similarly for n_2, n_3, $\cdots$ n_f. The difference is further brought out by using Roman numerals for subscripts of the coordinates and the capital letter for the running index.

After the M's for initial and final state have been fixed it is very essential for our purpose to remark that the integral (2.2) will vanish anyhow unless just one of the l_i' of the final state differs by $+1$ or -1 from one of the l_i of the initial state. All other l and n must be the same for both states, except that the n_i' with the same index as the differing l_i' may be different from n_i by an arbitrary amount. (See note A). If we denote the quantum numbers which differ by the index 1 we can write for the non-vanishing case

$$\int \bar{\psi}^0(n_1', l_1 \pm 1; n_2, l_2; \cdots n_f, l_f) X \psi^0(n_1, l_1; n_2, l_2; \cdots n_f, l_f). \qquad (2.4)$$

In the language of the atomic model this result would mean that only one electron could jump at a time, when we consider only zeroth order eigenfunctions, and that it's l changes by $+1$ or -1 and its n by an arbitrary amount.[3]

3. Terms Occurring in the First Order Eigenfunctions

3. In order to account for two-electron jumps we must now investigate what happens if we take the first order terms into account. For a qualitative discussion we need to consider such terms only in the initial or the final state; taking them for both states would not result in anything new. The first order eigenfunction will be of the form

$$\psi^1(n_1, l_1; \cdots n_f, l_f) = \psi^0(n_1, l_1; \cdots n_f, l_f) + \lambda \sum_a{}' c_a \psi^0(n_1^a, l_1^a; \cdots n_f^a, l_f^a) + \mu \sum_b{}'' d_b \cdot \psi^0(n_1^b, l_1^b; \cdots n_f^b l_f^b) \qquad (3.1)$$

The first sum with the coefficient λ we assume to arise from the spin-orbit interactions, the second sum with μ from the electrostatic interactions. *It is just these terms which cause the many electron transitions and therefore we are very much interested in finding out what terms may occur and what terms are excluded.* Though it does not help us in getting the many-electron transition selection rule, as a first limitation on the terms occurring in the two sums, we may cite the well-known matrix mechanics theorems that only such terms will occur that have the same total M, and J. Next, the primes at the summation signs mean that all eigenfunctions except the unperturbed one may occur in the sum. As we are dealing here with an originally degenerate system we must look at this fact more closely, since the prime excludes different eigenfunctions from the first than from the second sum. If we take for instance extreme Russell-Saunders coupling, the smaller spin-orbit interaction causes the splitting up of each multiplet (due to the Russell-Saunders coupling) into its levels. In the first sum are therefore excluded such eigenfunctions

[3] It is perhaps not superfluous to note that this way of expressing our result may lead to the confusion mentioned in the footnote (2). One cannot say that one particular electron changes its quantum numbers, as all permutations of the electrons over the quantum numbers occur. If we consider the quantum state of the many-electron problem to be built up of a number of single electron states over which the electrons are distributed, one can say that in a transition only one electron *state* changes and the others remain unchanged.

of the different terms which belong to one and the same multiplet, but levels of other multiplets from the same configurations, that is, having the same[4] n's and l's may occur, as well as the eigenfunctions with different n's and l's.

The larger electrostatic interaction excludes from the sum all such eigenfunctions which belong to levels which fall together without this interaction. These are the multiplets with the same set of n's and l's. Thus the second sum will not contain eigenfunctions having this set of n's and l's. For extreme (jj) coupling on the other hand, the second sum may now contain terms having the same set of n's and l's as the unperturbed eigenfunction; the spin orbit sum (thus far) may or may not have the same set of l's, but must have at least one n different. These statements hold, of course, in extreme coupling only, in which case one can think of the perturbations as applied consecutively, the large one first and then the smaller.

For the spin-orbit interaction the perturbation is of the form,

$$\sum_F \frac{l_F \cdot s_F}{r_F{}^3} \cdot \tag{3.2}$$

This requires that in the first sum only such terms remain that have all l's the same as the zeroth order eigenfunctions, and one of the n's but not more may different.[5] (See Note B.)

The electrostatic perturbation is of the form

$$\sum_{FG} \frac{e^2}{r_{FG}} \cdot \tag{3.3}$$

This necessitates that only such terms occur in the second sum for which two and no more than two of the l's may be different from two of the l's of the zeroth order eigenfunction. (See Note C_1.)

If we denote these changes by ∂ and ϵ their sum must be even. (see Note C_2.)

If we restrict ourselves to the first term of the expansion of the electrostatic perturbation in spherical harmonics, we find that none of the l's may change, and that one of the n's may be different.[6] (See Note C_3.)

The next term in the expansion for $1/r_{FG}$ gives two l's different, each by $+1$ or by -1, and the n's connected with them maybe different by an arbitrary amount.[7] (See Note C_4.)

The results of this section may then be summed up as follows: If we take

[4] In the case that *all* the n's and l's are the same, the eigenfunction in the sum must be a different linear combination than the unperturbed one, namely, a combination belonging to another multiplet of the same configuration.

[5] As mentioned just before with reference to Note B, for extreme (jj) coupling one of the n's *must* be different.

[6] This is the same result that we got from the spin-orbit interaction.

[7] In general, if we consider the kth term of the expansion, taking the two differing l's as the first two, and calling them l_{1b}, l_{2b}, we find that in order that the integral does not vanish, l_1, l_{1b}, k, must be the side of a triangle of even perimeter; Similarly for l_2, l_{2b}, k. Thus, for example, $l_1 - l_{1b}$, may have the values, k, $k-2$, $k-4 \cdots$. The n's again are arbitrary. See Gaunt, Camb. Phil. Trans. 1929.

as an example those terms out of the sums for which the first quantum numbers are different, we may write them[8]

$$\begin{aligned}
&\lambda c\psi^0(n_1'', l_1; \cdots n_f, l_f) \text{ first order spin orbit terms} \\
&\left.\begin{aligned}
&\mu d_0\psi^0(n_1''', l_1; \cdots n_f, l_f) \\
&\mu d_1\psi^0(n_1^{\mathrm{IV}}, l_1 \pm 1; n_2^{\mathrm{IV}} l_2 \pm 1; \cdots n_f l_f) \\
&\quad\cdots\cdots\cdots\cdots\cdots\cdots \\
&\mu d_k\psi^0(n_1^{\mathrm{V}}, l_1 + \partial_k; n_2^{\mathrm{V}} l_2 + \partial_k; \cdots n_f, l_f)
\end{aligned}\right\}
\begin{aligned}
&\text{first order} \\
&\text{electrostatic} \\
&\text{terms} \\
&(\partial + \epsilon = \text{even}).
\end{aligned}
\end{aligned} \tag{3.4}$$

At this point we need say nothing more about the terms occurring in the spin-orbit sum (we again refer the reader to note B). But about the terms of the second sum we can say something further not only about what terms are excluded, but with what relative strength the allowed terms may occur. This is due to the fact that the coefficients of the terms of the second sum involve a product of two integrals, each of which contains a product of three spherical harmonics, the harmonic on which we sum occurring in the same way in both integrals (see notes C_1 and C_2). This latter property is the important one in excluding certain states from the sum and assigning the relative strength with which others occur. As mentioned in note C_2, the integral of a product of

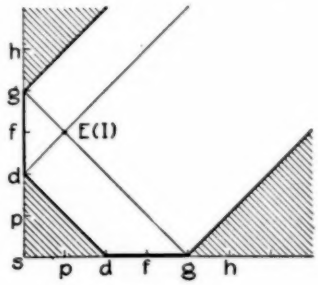

Fig. 1.

three spherical harmonics vanishes unless the absolute value of any two of the l's is equal to or less than the third l. This fact lends itself nicely to a chess-board diagram. We give the results which can easily be verified by examining the integrals for a few cases.

In Fig. 1 the abscissas and ordinates stand for the two l's (of the terms of the electrostatic interaction sum) which are allowed to be different from two of the unperturbed eigenfunction. Pick out any initial point or state, $E(I)$. Draw the two forty-five degree lines through it and complete the figure as shown by the heavy lines. Then

(a) the states which can occur in the sum, with respect to the chosen initial state, lie within the region bounded by the heavy line. Those, in the shaded region, are excluded by reason of the vanishing of the integrals.

[8] It can be understood from what follows that the terms for which all quantum numbers are the same as those of the unperturbed state, do not contribute to two-electron jumps, but are important in accounting for anomalies in one-electron intensities.

(b) states lying within the region bounded by the heavy lines, but which have $\partial+\epsilon \neq$ even, are also excluded. This gives the Laporte rule when one considers the transitions. One can easily show that the Laporte rule holds for higher perturbations as well, since for these perturbations the same type of integrals is involved.

(c) To find the relative strength with which the allowed states occur in the sum we proceed by the following rule: Go by the shortest number of unit "bishop's moves" from the initial state $E(I)$ to any allowed state in the sum. The number of unit moves which it takes to get there gives the lowest term in the expansion with which this state occurs (it may occur also in the higher terms). The states which are only one unit bishop move away occur with the largest coefficients, and are those which enter to give the Heisenberg selection rule.

4. Two-Electron and Three-Electron Transitions

We now consider a final state of which we take only a zeroth order eigenfunctions. We chose it such that that there would be no transitions if we had taken also only the zeroth order eigenfunction of the initial state; thus we take more than just one l and n different for the two states. We now investigate under what conditions the above given first order terms will cause the following integral, which governs the intensities, not to vanish

$$\int \bar{\psi}^0(n_1', l_1'; \cdots n_f', l_f') X \psi^1(n_1, l_1; \cdots n_f l_f) d\tau. \tag{4.1}$$

Substituting for ψ^1 leads to integrals of the following type

$$\lambda c \int \bar{\psi}^0(n_1', l_1'; \cdots n_f', l_f') X \psi^0(n_1'', l_1''; \cdots n_f l_f) d\tau \tag{4.2}$$

$$\mu d \int \bar{\psi}^0(n_1', l_1'; \cdots n_f', l_f') X \psi^0(n_1''', l_1 + \partial; n_2''', l_2 + \epsilon; n_3, l_3; \cdots n_f l_f) d\tau \tag{4.3}$$

and another integral like (4-2) due to the first term of $1/r_{FG}$. Of such integrals we know already that they will vanish, unless we have chosen the quantum numbers of the final state just right. Just one of the l's of the final state must differ by $+1$ or -1 from one of the l's of the other eigenfunction under the integral, the n's associated with these two l's may differ by an arbitrary amount, but all other l's and n's must be the same.

One will only get transitions with first order eigenfunctions when the quantum numbers of the final state are in a certain relation to the quantum numbers of the series expansion of the initial state.[9] Now we have seen that the quantum numbers in these series were related to the quantum numbers in the zeroth order eigenfunction, the quantum numbers by which we usually denote the state under consideration. It follows that one will only find transitions when the quantum numbers of the final state are related in a

[9] A similar statement will be true if we interchange initial and final state.

certain way to those of the initial as required by the condition that at least one of the integrals (4.2), (4.3), does not vanish. This can be provided for in a number of different ways and one can without much difficulty verify the following results, from which we omit the cases which give rise to an ordinary one-electron transition.

Combining statements just preceding references to notes A, B, and C_1, one finds that due to the first order terms of both the spin-orbit interaction and the first term of the electrostatic interaction, transitions may occur between two states:

(a) when there is a change in *two* electron states, one changing only its n, the other changing its l by $+1$ or -1, and its n by an arbitrary amount, thus:

$$\psi^1(n_1, l_1; \cdots n_f, l_f) \rightarrow \psi^0(n_1', l_1; n_2', l_2 \pm 1; \cdots n_f, l_f).$$

Combining statements just preceding references to notes A, C_2, C_3, C_4, one finds that due to the first order terms in the electrostatic interaction a transition may occur between two states,

(b) when there is a change in three electron states, all changing their n's by arbitrary amounts, two of them changing their l's by ∂ and ϵ ($\partial+\epsilon=$even), the third one changing its l by $+1$ or -1. The values of $+1$ and -1 for ∂ and ϵ will be more probable. Thus,

$$\psi^1(n_1, l_1; \cdots n_f, l_f) \rightarrow \psi^0(n_1', l_1 + \partial; n_2', l_2 + \epsilon; n_3', l_3 \pm 1; \cdots u_f, l_f).$$

(c) when there is a change in two electron states, both changing their n's by arbitrary amounts, the one changing its l by ∂, the other changing its l by $\epsilon \pm 1$ ($\partial+\epsilon=$even). Again the values $+1$, -1 for ∂ and ϵ will be more probable. Thus,

$$\psi^1(n_1, l_1; \cdots u_f, l_f) \rightarrow \psi^0(n_1', l_1 + \partial; n_2', l_2 + \epsilon \pm 1; n_3, l_3; \cdots n_f, l_f)$$

Case a (together with case c) if we choose ∂ and ϵ equal to ± 1 gives the well-known Heisenberg selection rule[10] for a two electron jump. All cases verify the Laporte rule.

5. Qualitative Remarks on Intensities of Many-Electron Transitions

5. Though it is difficult to give quantitive statements about the intensities of the two or more electron jumps, we can tell in which cases we can expect them to be strong. At the outset we can state that the three-electron transitions will be less probable, since an atom with three excited electrons is in a very high and improbable energy state, often corresponding to an energy higher than that of the ionized atom. The coefficients with which $E(I^a)$ occurs in the electrostatic expansion of $E(I)$ are given by,

$$\int \bar{\psi}^0(n_1^a, l_1^a; n_2^a, l_2^a; \cdots n_f^a, l_f^a) \frac{l^2}{r_{FG}} \psi^0(n_1, l_1; n_2, l_2; \cdots n_f l_f) d\tau$$

[10] W. Heisenberg, Zeits. f. Physik. **32,** 841 (1925).

The superscript, a, is used to denote the quantum numbers of the a^{th} eigenfunction occurring in the first expansion.

One of the conditions that the coefficients be large is that the levels $E(I)$ and $E(I^a)$ lie near together. This is a necessary but not a sufficient condition. For even though two states may lie close together they will only disturb each other when the quantum numbers obey the demands of (a) and (b) of section 3. We may say that the coefficients will be larger or smaller according to (c) of section 3.

The results obtained in Section 4 can be given the following interpretation. In order that a many electron transition between a state $E(I)$ and a state $E(II)$ be possible, it is necessary that there exist a state $E(I^a)$ which occurs in the first order expansion of $E(I)$ and which has the property that there can be a one electron transition between $E(I^a)$ and $E(II)$. The larger the coefficient and the stronger the one electron transition is, the more probable it will be to actually observe the many electron transition.

6. Notes

Note A.

The expression (2.2) written out completely is, if we take the first of (3:1) as an example,

$$\sum_{\substack{\alpha k \beta j \\ F}} \int d\tau \left[P_\alpha p_{\alpha k} \psi_1(m_1{}^k/x_1) \cdots \psi_f(m_f{}^k/x_f)\right] r_F \sin\theta_F e^{i\phi_F} \left[P_\beta q_{\beta j} \psi_{1'}(m_{1'}{}^j/x_1) \cdots \psi_{f'}(m_{f'}{}^j/x_F)\right]$$

Here:

1. $m_1{}^k, \cdots, m_f{}^k$ are the m's occurring in the k^{th} combination giving $\Sigma m = M$

2. $m_{1'}{}^j, \cdots, m_{f'}{}^j$ are the m's occurring in the j^{th} combination giving $\Sigma m' = M'$. Primes denote quantum numbers of the final state.

3. The subscripts of the ψ's stand for the n, l of the eigenfunctions.

4. P_α stands for the α^{th} permutation (of the coordinates) of each combination of the initial state.

5. P_β stands for the β^{th} permutation (of the coordinates) of each combination of the final state.

6. It must be remembered that $m_1{}^k = m_{l_1}{}^k + m_{s_1}{}^k$;

7. $p_{\alpha k}$ and $q_{\beta j}$ are the coefficients of each product of ψ's in the linear combinations forming stabilized eigenfunction, ψ)

Fix all the summation indices except j and let us look at the first term of the sum on F, namely, $r_I \sin\theta_I e^{i\phi_I}$. The integral vanishes unless $m_{s_1}{}^j = m_{s_1}{}^k$; $m_{l_1}{}' + 1 = m_{l_1}{}^k$; $l_1' = l_1 \pm 1$; $\psi_{2'} = \psi_2$; $\cdots$, $\psi_{f'} = \psi_f$. With these fixed conditions all the other integrals of the sums over F and j vanish either because of the ϕ or the θ part of the eigenfunctions. It is obvious that instead of starting with $r_I \sin\theta_I e^{i\phi_I}$ we might have started with any $r_F \sin\theta_F{}^{i\phi_F}$ and the result would have been the same.

Similar reasoning will show that the integral is zero unless the permutation β is the same as α (for the sake of clearness the integral as written has been taken for the case $\alpha=\beta$). For each k one will have for each term the same conditions $l_1'=l_1\pm1;\psi_{2'}=\psi_2;\cdots,\psi_{f'}=\psi_f$. Thus the 5-fold sum reduces to a 2-fold sum over the permutations α and the combinations k

$$\sum_{\alpha k}P_\alpha p_{\alpha k}q_{\alpha k}\int d\tau\bar{\psi}_{n_1}l_1(m_1{}^k/x_\alpha)r_\alpha\sin\theta_\alpha e^{i\phi_\alpha}\psi_{n_1'l_1\pm1}(m_1{}^k-1/x_\alpha).$$

The calculations show there is no restriction on $n_1'-n$. Similar computations show that the rule $l_i'=l_i\pm1$ is the same for the cases (3:2) and (3:3).

Note B.

The perturbed part of the eigenfunction due to the spin-orbit interaction will now be written more fully,

$$\lambda\sum_a{}'c_a\psi^0(n_1{}^a,l_1{}^a;\cdots n_f{}^a,l_f{}^a)$$

$$\equiv\lambda\sum_a{}'c_a\Big(\sum_{\beta t}q_{\beta t}\psi_{1a}(m_{1a}{}^t/x_1)\cdots\psi_{fa}(m_{fa}{}^t/x_F)\Big).$$

If one carries out the spin-orbit perturbation the coefficients of the λ part of the eigenfunction are given by,

$$c_a=\sum_{\substack{\alpha\beta kt\\F}}{}'P_\alpha P_\beta p_{\alpha k}q_{\beta t}\int d\tau[\psi_{1a}(m_{1a}{}^t/x_1)\cdots\psi_{fa}(m_{fa}{}^t/x_p)]\frac{l_F\cdot s_F}{r_F{}^3}[\psi_1(m_1{}^k/x_1)\cdots\psi_f(m_F{}^k/x_F)]$$

$$\overline{\qquad\qquad E_a-E\qquad\qquad}$$

Here

1. c_a stands for the coefficient occurring with the a^{th} set of n's and l's in the first order expansion. The bracket under the integral to the right of $l_F\cdot s_F/r_F{}^3$ is the given unperturbed eigenfunction, and hence does not need a running subscript with it's ψ's.

2. $m_{1a}{}^t,\cdots,m_{fa}{}^t$ are the m's occurring in the t^{th} combination of this product (state), giving a definite $\Sigma m_a=M_a$

3. P_β stands for the β^{th} permutation over the coordinates of this combination.

4. $m_1{}^k,\cdots,m_f{}^k$ are the m's occurring in the k^{th} combination of the unperturbed state giving a definite $\Sigma m=M$

5. P_α stands for the α^{th} permutation over the coordinates of this combination.

6. As given the states are for the $\alpha=1$ and $\beta=1$ permutations.

Let us fix our attention on $l_I\cdot s_I/r_I{}^3$. This operator does not work on $\psi_2,\cdots,\psi_f$. Thus the integral vanishes unless $\psi_{2a}=\psi_2,\cdots,\psi_{fa}=\psi_f$. We are left with the one-electron integrals

$$\sum_{\alpha} P_{\alpha} p_{\alpha k} q_{\alpha t} \frac{\int d\tau \bar{\psi}_{1a}(m_{1a}{}^{t}/x_{\alpha}) \dfrac{l_{\alpha} \cdot s_{\alpha}}{r_{\alpha}{}^{3}} \psi_{1}(m_{1}{}^{k}/x_{\alpha})}{E_{a} - E}$$

which are easily shown to vanish unless $m_{1a}{}^{t} = m_{1}{}^{k}$, $l_{1a} = l_{1}$. (In passing it might be mentioned that this demonstrates the fact that the Σm occurring in the perturbed terms, as well as in the unperturbed terms, must be the same.) One gets the same conditions starting with any other $l_F \cdot S_F / r_F{}^{3}$. n_{1a} may or may not be different from n_1. Let $n_{1a} = n_1$. With this condition and the fixed conditions $l_{1a} = l_1$; $\psi_{2a} = \psi_2$; $\cdots$, $\psi_{fa} = \psi_f$, the integrations over the other $l_F \cdot S_F / r_F{}^{3}$ will *not* vanish. This is the case mentioned in footnote 4. Although in this paper we are not interested in this case, for it provides only for one-electron jumps, it indicated at least the cause for the anomalies in the intensities of one-electron transitions; this is so because we see here that the coefficient of this first order term will be large, for in general the energy separations between multiplets of the same configuration (the case we have here) will be smaller than the energy separations between multiplets of different configurations.

It also must be mentioned that this case can occur only for extreme Russell-Saunders coupling. For extreme (jj) coupling, for example neon, one of the n's must be different.

With $n_{1a} \neq n_1$ and the other fixed conditions the integrations over the other $l_F \cdot s_F / r_F{}^{3}$ vanish. Thus, the conditions for the non-vanishing of the coefficients are the same as in the case $n_{1a} = n_1$, but this time the coefficients will be much smaller.

Note C_1.

The perturbed part of the eigenfunction due to the electrostatic interaction will now be written more fully

$$\mu \sum_{b}{}'' d_b \psi^{0}(n_1{}^{b}, l_{1j}{}^{b} \cdots n_f{}^{b}, l_f{}^{b})$$

$$\equiv \mu \sum_{b}{}'' d_b \Big(\sum_{\gamma r} P_{\gamma} u_{\gamma r} \psi_{1b}(m_{1b}{}^{r}/x_1) \cdots \psi_{fb}(m_{fb}{}^{r}/x_F) \Big).$$

If one carries out the electrostatic perturbation the coefficients of the μ part of the eigenfunction are given by

$$d_b = \sum_{\substack{\alpha\gamma k r \\ FG}}{}'' P_{\alpha} P_{\beta} p_{\alpha k} u_{\gamma r} \frac{\int d\tau \overline{[\psi_{1a}(m_{1a}{}^{2}/x_1) \cdots \psi_{fa}(m_{fa}{}^{r}/x_F)]} \dfrac{e^{2}}{r_{FG}} [\psi_{1}(m_1{}^{k}/x_1) \cdots \psi_{f}(m_f{}^{k}/x_F)]}{E_b - E}.$$

The explanation of the symbols is the same as that given in note B.

Let us fix our attention on $e^{2}/r_{I\,II}$. With the given permutation the integral vanishes unless $\psi_{3b} = \psi_3, \cdots, \psi_{fb} = \psi_f$. With these fixed conditions the integra-

tions over all the other e^2/r_{FG} give zero. Further one sees that the integral is zero unless $\alpha=\beta$. It is obvious that starting with any other e^2/r_{FG} we get the same results, namely, that only such coefficients occur for which two and no more than two of the n's and l's of the terms of the sum may be different from two of the n's and l's of the unperturbed eigenfunction. The summation reduces to

$$\sum_{\alpha kr} P_\alpha p_{\alpha k} u_{\alpha r} \frac{\int d\tau \psi_{1b}(m_{1a}{}^r/x_{\mathrm{I}})\psi_{2b}(m_{2a}{}^r/x_{\mathrm{II}})\dfrac{e^2}{r_{\mathrm{I\,II}}}\psi_1(m_1{}^k/x_{\mathrm{I}})\psi_2(m_2{}^k/x_{\mathrm{II}})}{E_b - E}.$$

Note C_2.

Now puting in the value

$$\frac{1}{r_{\mathrm{I\,II}}} = \sum_{im} \frac{(i-|m|)!}{(i+|m|)!}\frac{r(I)^i}{r(II)^{i+1}} P_i{}^{|m|}(\cos\theta_{\mathrm{I}})P_i{}^{|m|}(\cos\theta_{\mathrm{II}})e^{im(\phi_{\mathrm{I}}-\phi_{\mathrm{II}})}$$

where $r(I)$, $r(II)$ are the radial distances of the two electrons, $(r(I)<r(II))$, the non-radial part of the integral may be written, (dropping the denominator E_b-E)

$$\sum_{im}\sum_{\alpha kr} P_\alpha p_{\alpha k} u_{\alpha r} \int [P_{l_{(1b)}}{}^{m_{l_{(1b)}}{}^r}(\theta_{\mathrm{I}})P_{l_{(1)}}{}^{m_{l_{(1)}}{}^k}(\theta_{\mathrm{I}})P_i{}^{|m|}(\theta_{\mathrm{I}})]$$

$$[P_{l_{(2b)}}{}^{m_{l_{(2b)}}{}^r}(\theta_{\mathrm{II}})P_{l_{(2)}}{}^{m_{l_{(2)}}{}^k}(\theta_{\mathrm{II}})P_i{}^{|m|}(\theta_{\mathrm{II}})]d(\cos\theta_{\mathrm{I}})d(\cos\theta_{\mathrm{II}})$$

$$\times \int [S(m_{s_{(1b)}}{}^r)S(m_{s_{(1)}}{}^k)][S(m_{s_{(2b)}}{}^r)S(m_{s_{(2)}}{}^k)]$$

$$\times \int e^{-i(m_{l_{(1b)}}{}^r - m_{l_{(1)}}{}^k - |m|)\phi_{\mathrm{I}}} \cdot e^{-i(m_{l_{(2b)}}{}^r - m_{l_{(2)}}{}^k + m)\phi_{\mathrm{II}}} d\phi_{\mathrm{I}} d\phi_{\mathrm{II}}.$$

One sees first that the integral is zero unless

$$m_{s_{(1b)}}{}^r = m_{s_{(1)}}{}^k; \qquad m_{s_{(2b)}}{}^r = m_{s_2}{}^k$$

$$m_{l_{(1b)}}{}^r - m_{l_{(1)}}{}^k = |m| = m_{l_{(2)}}{}^k - m_{l_{(2b)}}{}^r \quad \therefore \quad m_{l_{(1)}}{}^k + m_{l_{(2)}}{}^k = m_{l_{(1b)}}{}^r + m_{l_{(2b)}}{}^r.$$

With the spin-orbit interaction we saw that only those terms might enter in the sum with $\Sigma m =$ constant. Here the limitation is stricter, namely only those terms enter into the sum that have common Σm_l and Σm_s.

Now the important thing to notice is that the same $P_i{}^{|m|}$ comes in with both angles. Each of the product of the two integrals will vanish unless the sums of the three lower indices be an even number.[11] This fact in conjuction with the statement just preceding requires that if $\delta=|l_{1b}-l_1|$ and $\epsilon=|l_{2b}-l_2|$ that $\delta+\epsilon$ be even. This verifies the Laporte rule after one considers transitions.

Another important property of the integral of a product of three spherical harmonics, given by Gaunt, is that it vanishes unless the absolute value of the difference of any two of the subscripts is equal to or less than the third.

[11] Gaunt, Cambridge Phil. Trans. 1929.

Note C_3.

For the first term of the expansion of $1/r_{I\,II}$, $i=0$, the non-radial part of the integral reduces to

$$\int [P_{l_{(1b)}}{}^{m}(\theta_{\mathrm{I}})P_{l_{(1)}}{}^{m}(\theta_{\mathrm{I}})][P_{l_{(2b)}}{}^{m}(\theta_{\mathrm{II}})P_{l_{(2)}}{}^{m}(\theta_{\mathrm{II}})]d(\cos\theta_{\mathrm{I}})d(\cos\theta_{\mathrm{II}}).$$

(We can now use the simple m, instead of $m_1{}^k$ etc., and leave off the summation sign since it does not affect the argument.)

This vanishes unless $l_{(b)}=l_{(1)}$; $l_{(2b)}=l_{(2)}$. The term $r(I)^i/r(II)^{i+1}$ reduces to $1/r(II)$. Thus in addition to the conditions for the l's and the initial conditions $\psi_{3b}=\psi_3;\ \cdots,\ \psi_{fb}=\psi_f$, in order that the radial part of the integral is not zero, one pair of n's must be equal. If both pair are equal we have the same situation mentioned in Note B, about one electron-jumps.

Note C_4.

The expansion of $1/r_{I\,II}$ decreases fairly rapidly because of the presence of the factor $(i-|m|)!/(i+|m|)!$. If we go to the second term of the expansion $i=1$, this approximation is sufficient to give the Heisenberg selection rule. The two possible integrals are

$$\int [P_{l_{(1b)}}{}^{m}(\theta_{\mathrm{I}})P_{l_{(1)}}{}^{m}(\theta_{\mathrm{I}})\cos\theta_{\mathrm{I}}][P_{l_{(2b)}}{}^{m}(\theta_{\mathrm{II}})P_{l_{(2)}}{}^{m}(\theta_{\mathrm{II}})\cos\theta_{\mathrm{II}}]d(\cos\theta_{\mathrm{I}})d(\cos\theta_{\mathrm{II}})$$

$$\int [P_{l_{(1b)}}{}^{m}(\theta_{\mathrm{I}})P_{l_{(1)}}{}^{m-1}(\theta_{\mathrm{I}})\sin\theta_{\mathrm{I}}][P_{l_{(2b)}}{}^{m}(\theta_{\mathrm{II}})P_{l_{(2)}}{}^{m-1}(\theta_{\mathrm{II}})\sin\theta_{\mathrm{II}}]d(\cos\theta_{\mathrm{I}})d(\cos\theta_{\mathrm{II}})$$

which do not vanish under the same conditions, namely, $l_{1(b)}=l_{(1)}\pm 1$, $l_{(2b)}=l_{(2)}\pm 1$. The n's are arbitrary in the radial part. As explained in the body of the paper this condition gives the Heisenberg rule, and in addition, the possibility of three and (up to this approximation) not more than three-electron transitions.

THE QUANTUM THEORY OF THE EQUATION OF STATE

By J. C. Slater
Massachusetts Institute of Technology

(Received May 21, 1931)

Abstract

It is shown that the quantum theory analogue to the quantity $e^{-\epsilon_{pot}/kT}$ giving the distribution in coordinates of systems at temperature T can be easily set up. Similarly in quantum theory the computation of the free energy can be reduced to the integration of such a function over the coordinates, as in classical theory. The result is applied to a qualitative discussion of the equation of state of an imperfect gas, showing that He and H_2 may be expected to show quantum effects in their equations of state, but hardly any other gases.

QUANTUM statistics have been mostly developed on the basis of the older quantum theory, rather than of wave mechanics. As a result of this, full use has not been made of the essentially statistical form of the present quantum mechanics. It is the purpose of the present note to point out how naturally, and simply, in principle at least, one can treat such problems as the equation of state of an imperfect gas by quantum theory. As a preliminary, we discuss the analogue in quantum theory to the expression $e^{-\epsilon_{pot}/kT}$ in classical statistics, giving the probability of finding a system, at temperature T, in a position where the potential energy is ϵ_{pot}.

Suppose we have given a wave function ψ. Then by the fundamentals of the statistical interpretation of quantum mechanics, the probability of finding a system of the sort described by ψ, in the small element of volume dq_1-dq_n, is $\psi^*\psi dq_1-dq_n$. If, in particular, $\psi=\Sigma_i C_i u_i(q_1-q_n)e^{-(2\pi i/h)E_i t}$, then the probability becomes $\Sigma_{ij}C_i^*C_j u_i^* u_j\, e^{-(2\pi i/h)(E_i-E_j)t}\, dq_1-d8_n$. By either of two procedures, we can eliminate the terms varying with time ($i\neq j$): we can average over time; or we can assume that we have sort of an ensemble of ψ's (each separate ψ being almost as general as a whole ensemble in classical statistics), in which the different C_i's are statistically independent in phase, and we can average over this ensemble. In either case, the result is that the remaining terms of the probability are $\Sigma_i C_i^* C_i u_i^* u_i dq_1-dq_n$, or, if the c's and u's are real, $\Sigma_i C_i^2 u_i^2(q_1-dq_n)dq_1-dq_n$.

On the other hand, given a classical distribution function $f(q_1-q_n, p_1-p_n)$ giving the probability of finding the system in a given point of phase space, we can at once pass to the probability of finding it at a given point of coordinate space by integrating over momenta: $[\int-\int\int dp_1-dp_n]\, dq_1-dq_n$. This should then correspond to the quantum expression of the last paragraph.

In particular, in thermal equilibrium at temperature T, we assume in either classical or quantum statistics the canonical ensemble. In classical statistics, this is given by $f=\text{constant}\times e^{-\epsilon(q_1-p_n)/kT}$, where $\epsilon(q_1-p_n)$ is the energy as function of coordinates and momenta. If, as in ordinary mechanical

problems, $\epsilon = \epsilon_{pot}\ (q_1 - q_n) + \Sigma p^2/2m$, then we can carry out explicitly the integration over the momenta, and the result is that the probability of finding the system in $dq_1 - dq_n$ is constant $\times \Pi_n (2\pi mkT)^{1/2} \times e^{-\epsilon pot/kT}\ dq_1 - dq_n$, the product being over all degrees of freedom. Thus, at constant temperature, the distribution in space is given by $e^{-\epsilon pot/kT}$.

In quantum mechanics, on the other hand, the canonical ensemble is given by supposing that the number of systems in the i^{th} stationary state is proportional to $e^{-E_i/kT}$, (all degenerate levels being separately counted). It is to be noted that this is true, quite apart from the question as to whether the system obeys Boltzmann, Einstein-Bose, or Fermi-Dirac, statistics. The latter arise from the existence of identical particles within the system, they show themselves only in changing the allowed stationary states, and appear as a change in the statistics only when viewed in the μ space, not as we are working here in the Γ space. Now the number of systems in the i^{th} state is proportional to C_i^2. Hence on quantum mechanics the probability of finding a system at $q_1 - q_n$ is $\Sigma_i e^{-E_i/kT} u_i^2 (q_1 - q_n)\ dq_1 - dq_n$. It is this function which should agree with the classical expression above. As a matter of fact, we can get complete agreement if we divide the classical expression by h^n. Thus we should have

$$\prod_n \left(\frac{(2\pi mkT)^{1/2}}{h} \right) e^{-\epsilon pot/kT} = \sum_i e^{-E_i/kT} u_i^2 (q_1 \cdots q_n).$$

The relation above may be expected to hold only in the limiting case of high quantum numbers; for it is a form of correspondence between classical and quantum distributions. Thus we expect that, for low temperatures, where only low states are excited, it will be a very inperfect correspondence; but at high temperatures it should become more and more exact. We may show the actual nature of the agreement by examples.

Suppose we consider a collection of systems, each consisting of a single particle of mass m moving in a one dimensional box of length L, the potential being zero while the particle is in the box, infinite outside. Then the normalized wave functions are $u_n(x) = (2/L)^{1/2} \sin\ n\pi x/L$, and the energies are $E_n = n^2h^2/8mL^2$. Our distribution function on classical theory is then $(2\pi mkT)^{1/2}/h$ within the box, zero outside. On quantum theory it is

$$\sum_{n=1}^{\infty} e^{-n^2h^2/8mL^2kT} \frac{2}{L} \sin^2 \frac{n\pi x}{L}$$

within the box, zero outside. In Fig. 1, we plot this function for various temperatures, comparing with the constant classical value. It is seen that in the center of the box, for reasonably high temperatures, the quantum distribution approaches the classical one extraordinarily closely. Near the boundary, however, this is not true. The reason is that in the center there are waves superposed in all sorts of phases, and only their amplitudes are of significance, not their wave-lengths. Near the edges, however, on account of the fact that all waves reduce to zero on the boundary and are hence in phase, there is a

sort of interference, and within a wave-length of the edges the distribution shows characteristic quantum effects. If the temperature is T, and the average kinetic energy $\frac{1}{2}kT$, then a sort of average wave-length is given by setting $p^2/2m = \frac{1}{2}kT$, $\lambda = h/p = h/(mkT)^{1/2}$. Thus the distance in which the distribution is anomalous is independent of the size of the box, and depends only on

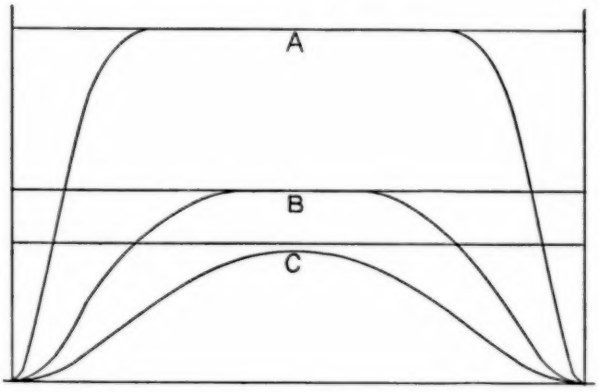

Fig. 1. Curves $\int e^{-\epsilon/kT}dp = f(T)e^{-\epsilon_{pot}/kT}$ for a free particle in a box (straight lines) and the quantum analogy to the same quantity (curves) as functions of position in the box. Temperatures are so chosen that in (A) there are 0.9 as many particles in the second quantized state as in the lowest state, in (B) 0.7, and in (C) 0.5 as many.

the mass of the particle and the temperature. For example, for a hydrogen atom at 100°K, the distance is 3.69A. The exact distribution around an edge of the box can be found, in the limiting case when L is large. For then, for small x compared with L, the summation can be replaced by an integration:

$$\int_0^\infty e^{-n^2h^2/8mL^2kT}\frac{2}{L}\sin^2\frac{n\pi x}{L}\,dn = \frac{(2\pi mkT)^{1/2}}{h}\left\{1 - \exp\left[-8\pi^2\left(x\frac{(mkT)^{1/2}}{h}\right)^2\right]\right\}.$$

For x large compared to $h/(mkT)^{1/2}$, the exponential reduces to zero, and we have the classical, constant value. On the other hand, for x small, the distribution decreases to zero at the boundary.

Similarly in Fig. 2 we plot several distribution curves, obtained from the two methods, for the linear oscillator. Here there is not such marked possibility of interference as with a sharp wall of potential, and the two methods agree more exactly. It is only at quite low temperatures, when only the lowest state is appreciably excited, that there is large discrepancy. Here the quantum distribution is of course simply that of the lowest vibrational level.

These two examples should indicate that in general, the quantum distribution agrees with the classical one except at such low temperatures, and correspondingly long average wave-length, that the potential changes greatly in a single wave-length. We can in fact give a simple proof of this by the method of Kramers, Wentzel, etc., worked out for this case by Van Vleck.[1]

[1] Van Vleck, Proc. Nat. Acad. Sci., **14,** 178 (1928).

This method treats the amplitude of the wave function, showing how it varies with the potential. VanVleck shows, for a general mechanical system, that $u_i^2(q_1-q_n)$, if we take the average over the sinusoidal oscillations of the function, is proportional to the limit to the integral over the momenta of the distribution $f(q_1-q_n\ p_1-p_n)$ for a microcanonical ensemble of energy E_i. Since our summation $\Sigma_i e^{-E_i/kT}u_i^2$ corresponds to a canonical ensemble made up of microcanonical ones of all different energies, it would then be proportional to

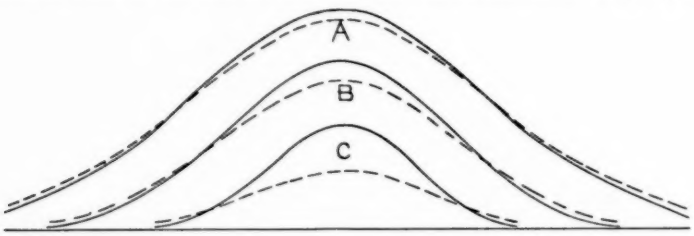

Fig. 2. Curves $j(T)e^{-\epsilon_{pot}/kT}$ for a linear oscillator (full lines) and quantum analogy to the same quantity (dotted lines) as function of displacement from position of equilibrium. Temperatures are chosen so that in (*A*) there are 0.5 as many oscillators in each state as in the one below, in (*B*) 0.3, in (*C*) 0.05 as many.

the integral over momenta of the distribution f for a canonical ensemble, which is what we wished to show.

Having discussed the analogue of the Boltzmann function $e^{-\epsilon_{pot}/kT}$ in quantum theory, we can proceed to the related problem of the equation of state. This is ordinarily found by computing the free energy ψ, given by the equation

$$e^{-\psi/kT} = \frac{1}{h^n}\int\!\!-\int e^{-\epsilon/kT}dq_1\cdots dp_n$$

or

$$= \sum_i e^{-E_i/kT}$$

on classical and quantum theory, respectively. Then by differentiating ψ, we can find specific heat and pressure. The quantum form has been often used for computing specific heat, but not for equation of state. For the latter purpose, with the classical form, we ordinarily integrate first over the momenta, obtaining

$$\prod_n \frac{(2\pi mkT)^{1/2}}{h}\int\!\!-\int e^{-\epsilon_{pot}/kT}dq_1\cdots dq_n.$$

The integral over the coordinates is then evaluated. For an imperfect gas at low density, for example, ϵ_{pot} is zero in most parts of the coordinate space, and $e^{-\epsilon_{pot}/kT}=1$. Only in those particular regions of space where two atoms are close together do we have an integrand different from unity. By considering only single collisions, as in the computation of the second virial coefficient, we can consider separately the various parts of coordinate space where two

molecules are in collision, reducing the whole problem to a set of separate ones each dealing with a single collision, and these can be easily treated. The problem leads eventually to the valuation of an integral $\beta = \iiint (1 - e^{-\epsilon_{pot}'/kT})\, dv$, where ϵ_{pot}' is the potential energy of one molecule in the field of another fixed one. In terms of $B = (N/2)\beta$, when N is the number of molecules, the final result is

$$e^{-\psi/kT} = \left(\frac{(2\pi mkT)^{1/2}}{h}\right)^{3N} (V - B)^N,$$

$\psi = -(3N/2)kT \log (2\pi mkT/h^2) - NkT \log (V-B)$, from which

$$C_v = -T\left(\frac{\partial^2 \psi}{\partial T^2}\right)_V = (3/2)Nk, \quad P = -\left(\frac{\partial \psi}{\partial V}\right)_T = \frac{NkT}{V - B}.$$

In the quantum theory, in a corresponding way, we may write $e^{-\psi/kT}$ as an integral over coordinates. We do this by substitution of $\Sigma_i e^{-E_i/kT} u_i^2(q_1 - q_n)$ for the corresponding classical expression $\Pi_n (2\pi mkT)^{1/2}/h e^{-\epsilon_{pot}/kT}$. The result is then

$$e^{-\psi/kT} = \int \sum_i e^{-E_i/kT} u_i^2(q_1 \cdots q_n)\, dq_1 \cdots dq_n$$

by exact analogy with the classical case. Taking the summation outside, integrating, and making use of the normalization of the u's, this reduces at once to the form $\Sigma_i e^{-E_i/kT}$ given above. But in practice it is more practicable not to do this, but to proceed as in the classical case. For the imperfect gas, for example, we know at once that the quantum density distribution approaches the classical except where the potential changes greatly in a single wave-length. Thus our integrand is practically $\Pi_n (2\pi mkT)^{1/2}/h$, throughout the whole of configuration space except on the walls of the vessel (which is unimportant) and in the regions where two molecules are in collision. The whole argument of separating out the different colliding pairs goes through as in classical statistics, and the only change comes when we compute β. Then, instead of putting in the classical expression $e^{-\epsilon_{pot}'/kT}$ for the interaction of a pair of molecules, we must use the corresponding quantum theory value. To work this out, we must solve the problem of the interaction of two molecules. If for example they are monatomic, or for any other reason spherically symmetrical, this problem will be one of two particles acting on each other by central forces, which can be solved, if necessary by numerical methods, when the interatomic potential is known. Having found the stationary states and wave-functions (including of course the continuous ones), we square, multiply by the corresponding $e^{-E_i/kT}$ and add. The resulting distribution will be similar to $e^{-\epsilon_{pot}'/kT}$, and must be used in its place.

The actual calculation, as we readily see, is much more tedious than in classical mechanics, since it involves finding many wave-functions. It is then fortunate that in general the results will agree closely with those of classical mechanics, so that a classical calculation suffices. We can see this by examin-

ing the potential curve for the interaction of the molecules. The potential will of course have a negative region, where the molecules attract, and then at shorter distances they all repel. There will be in general discrete vibrational and rotational states, of negative energy, and continuous ones of positive energy. We can get a very rough idea of the number of vibrational levels as follows: it should equal $\int pdq/h$, where the integral is over the region where the potential is definitely negative. If we let the length of this region be L, and let $\bar{p}$ be a sort of average p, the result is $2L\bar{p}/h$. But now take the worst case, where the particles on separation have no kinetic energy. Then p is related to the energy of dissociation of the aggregate of two molecules, and this energy is approximately given by the critical temperature, so that very roughly we may write $\bar{p}=(mkT_c)^{1/2}$. Thus this approximation gives $[2L(mkT_c)^{1/2}/h]$ for the number of levels. If we take $L=3$A, a reasonable value, and substitute numerical values, we have $0.162\ (MT_c)^{1/2}$, where M is the molecular weight. Thus for He we have less than one state, for H_2 one only, for Ne 4 or 5, for N_2 9 or 10. The result for He can be checked from the actual potential, and calculation actually seems to show that no discrete levels exist. The other values are highly tentative, but probably of the right order of magnitude. Thus we see that, with the exception of He and H_2, the other gases all have several vibrational levels, which of course are all excited under ordinary conditions in the gas above the critical point. We may anticipate then that for all gases except these two, the wave-length is short enough in proportion to the size of the potential minimum, and the states are sufficiently excited, so that classical statistics will give a good approximation.

For the two light gases, however, and particularly for He, we shall expect deviations from the classical statistics of molecular interaction. This has already been noticed by London,[2] without however indicating the proper method of correcting it. It is evident, as London points out, that on account of the lack of negative levels, the attraction cannot be as effective as it would be classically, and the second virial coefficient B must be larger than if we used a classical calculation. It is no doubt significant in this connection that the values of B for He, as computed by Kirkwood and Keyes,[3] using classical statistics, lies below the experimental values, at low temperatures. It is to be hoped that a detailed calculation, using quantum statistics, will show an improvement of the agreement.

[2] F. London, Zeits. f. Physik **63**, 259 (1930).

[3] J. G. Kirkwood and F. G. Keyes, Phys. Rev. 37, 832 (1931).

QUANTUM THEORY AND ELECTRON PAIR BOND

By W. Heitler
Universitaet Goettingen, at present Ohio State University

(Received May 21, 1931)

Abstract

It is shown for some simple examples that the stable molecular quantum state of a polyatomic system, is nearly identical with a state, by which there are built so many electron pairs between each pair of atoms, as the corresponding chemical formula shows.

1. THE aim of the following note is to point out more definitely the connection between the quantum theory and the Lewis' electron pair idea for some simple examples of poly-atomic molecules. In principle this paper contains nothing new; the principles have all been developed in recent papers published by G. Rumer and the writer[1] and by H. Weyl.[2] It seems to the writer, however, that the results of the following calculations, while indeed very simple, might be of interest.

The quantum theory leads to a full justification of the electron pair conception for diatomic molecules. Let us consider two atoms A and B with n_a and n_b free electrons of parallel spin (spin angular momenta $n_a/2$ and $n_b/2$) and let us assume for simplicity that the orbital angular momenta are zero. For every value of the spin momentum of the whole system s between $(n_a+n_b)/2$ and $|(n_a-n_b)/2|$ there exists just one interaction term with an energy ϵ_s.

Instead of s we can introduce the number of *pairs* p of electrons with *antiparallel spin* between A and B defined by

$$p = \frac{n_a + n_b}{2} - s$$

Lewis' electron pairs are just these pairs of electrons with antiparallel spin. In the chemical picture, p would be the number of valence-dashes between A and B. If we further introduce the number of *free* valences, which go out from the atom A

$$\nu_a = n_a - p$$

then the energy will assume the simple form

$$\epsilon_p = J_E + (p - \nu_a\nu_b)(AB) \quad p = 0, 1, \cdots n_b \text{ if } n_b \leqq n_a \qquad (1)$$

where J_E is the Coulomb interaction of the two atoms, (AB) the well-known exchange integral between A and B. By the usual assumptions of the sign of

[1] W. Heitler and G. Rumer, Zeits. f. Physik 68, 12 (1931).
[2] H. Weyl, Gott. Nachr. 1931, in press.

(AB), [(AB) negative] which are now justified in many cases, ϵ_p assumes the largest negative value (strongest bond) if p has the largest value ($=n_b$). If p becomes smaller, the bond energy will become smaller and finally negative (if $p=0$) corresponding to repelling atoms.

2. This simple theory cannot be extended to the general case of polyatomic molecules. If we have several atoms A, B, C—with n_a, n_b, n_c—electrons, we get in the general case *several*, say f_s, interaction terms (not only one) belonging to a specified s. One could define for all these f_s terms an entire number of electron pairs

$$p = \frac{n_a + n_b + n_c + \cdots}{2} - s$$

but one cannot say, how these f_s terms differ one from the other (except the interaction energy value of course) and further, one cannot say, how many of these p electron pairs are built between two *specified atoms* A and B. Just this question, however, is answered in Lewis' theory.

In the previously mentioned papers. it has been shown, that one can use for the unperturbed system certain unperturbed wave-functions, such that by each of them is built a certain number of electron pairs (or valence-dashes) p_{ab} between each pair of two atoms A and B etc. If this wave-function belongs to a certain value p the sum of the p_{ab} must be equal to p

$$p_{ab} + p_{ac} + p_{bc} + \cdots = p$$

Such a wave-function we will denote by

$$\psi_1 = [AB]^{p_{ab}}[AC]^{p_{ab}} \cdots .$$

There exist f_s independent wave-functions $\psi_1 \cdots \psi_{f_s}$ which differ by the distribution p_{ab}, $p_{ac} \cdots$ of the valence dashes between the atoms, but all have the same *sum* p of valence dashes. Weyl calls such a function a "*pure valence state*," because the valence dashes are here strictly localized between the atoms.

The wave-functions $\phi_1, \cdots \phi_{f_s}$ belonging to the f_s different energy states $\epsilon_1 \cdots \epsilon_{f_s}$ are, however, *not* identical with these pure valence states. In the zeroth order of approximation they are linear combinations of the ψ's.

$$\phi_i = \sum_k c_{ik}\psi_k. \tag{2}$$

The coefficients c_{ik} in Eq. (2) depend on the ratio of the exchange integrals, and therefore on the distances of the atoms.

A pure energy state is a superposition of some pure valence states, or, in the language of the quantum mechanics the energy is not permutable by the valence-dash-configuration.

It seems, that the valence-dash picture should no longer have a place in the quantum theory. We will now show, that it can again assume a certain meaning.

If the coefficients (2) are determined, one can easily work out the *probabilities* of any pure valence state ψ_k if the system is in a definite energy state ϕ_i and vice versa. This probability is

$$w_{ik} = \left| (\phi_i \psi_k) \right|^2$$

where $(\phi_i \psi_k)$ is the integral $\int \phi_i \psi_k$ integrated over all space and spins (scalar product of ϕ_i and ψ_k).

We will show, for some simple examples, that these probabilities for a definite state ϕ are all *small* except for *one* valence state ψ_k in which case these probabilities are *nearly* equal to unity. To a certain energy state there corresponds therefore *nearly* a certain valence state; for the *stable molecular state* it will be just this valence state, which one expects from the *chemical standpoint.*

It is first necessary to make mention of some properties of the valence states. If one builds all valence states, by giving all possible values to the numbers p_{ab}, p_{ac} (while the sum is the same of course) one gets more than f_s valence states. Some of them are therefore linearly dependent. Further two such valence states will not be orthogonal $(\psi_i \psi_k) \neq 0$. The pure valence states do not exclude one another. There is always a certain probability $\left|(\psi_i \psi_k)\right|^2$ for the tate ψ_k if the system is in the state ψ_i.[3]

3. Let now for instance A_1 and A_2 be two atoms with two valence electrons each, H_1 and H_2 be two atoms with one valence electron. We consider the atom configuration

$$H_1 A_1 A_2 H_2$$

and neglect the exchange integrals between non-neighbours. The other exchange integrals will be of the same order of magnitude. Let the distances be chosen so, that they are equal

$$(H_1 A_1) = (A_1 A_2) = (A_2 H_2).$$

One can build three pure valence states

$$\psi_1 = [A_1 A_2][A_1 H_1][A_2 H_2] \qquad H - A - A - H$$

$$\psi_2 = [A_1 A_2][A_1 H_2][A_2 H_1] \qquad H \quad A - A \quad H$$

$$\psi_3 = [A_1 A_2]^2[H_1 H_2] \qquad H \quad A = A \quad H$$

On the right hand side is given the corresponding "chemical formula." ψ_1 alone would, of course, correspond to a usual chemical molecule.

If these three ψ's are normalized the following relation holds[1,2]

$$\psi_1 - \psi_2 - \frac{2}{3^{1/2}} \psi_3 = 0.$$

[3] It is then possible that for a specified ϕ_i the probabilities for *two* valence states ψ_k, ψ_l are nearly equal to unity. See the second example in the text.

The exact meaning of $|(\phi_i \psi_k)|^2$ is the probability to find the valence state ψ_k and *not* an other state, which is in *contradiction* (*orthogonal*) to ψ_k. In general ψ_l will not be in contradiction to ψ_k.

We get therefore two energy states ϕ_1, ϕ_2 one of which, namely ϕ_1, leads to an attraction of the atoms while the other, ϕ_2 leads to a repulsion.[1] For the scalar products have been found the following values.

$$(\phi_1\psi_1) = 0.98 \quad (\phi_2\psi_1) = 0.19$$
$$(\phi_1\psi_2) = 0.17 \quad (\phi_2\psi_2) = 0.99$$
$$(\phi_1\psi_3) = 0.72 \quad (\phi_2\psi_3) = -0.70$$

One sees that $(\phi_1\psi_1)$ is ~ 1 and on the other hand also $(\phi_2\psi_2)$ is ~ 1. One could therefore use for the stable molecular state ϕ_1 *nearly* the chemical formula

$$H - A - A - H$$

in agreement with chemical expectations. For the repelling state one could use the formula

$$\overbrace{H \quad \overbrace{A - A}^{2} \quad H}^{1}.$$

The state ψ_3 has, however, for ϕ_1 and ϕ_2 a probability $\sim \frac{1}{2}$. It is a superposition of the two above formulae.[4]

Now let N be an atom with three electrons and B an atom with two electrons, and let us consider the configuration

$$B \quad N \quad N \quad B.$$

One can build six pure valence states corresponding to six valence-dash-configurations:

$$\psi_1 \sim B = N - N = B$$
$$\psi_2 \sim \overbrace{B \quad \overbrace{N - N}^{2} \quad B}^{1}$$
$$\psi_3 \sim \overbrace{B - \overbrace{N - N}^{2} - B}^{1}$$
$$\psi_4 \sim \overbrace{B \quad \overbrace{N = N}^{2} \quad B}^{1}$$
$$\psi_5 \sim \overbrace{B - \overbrace{N = N}^{2} - B}^{1}$$
$$\psi_6 \sim \overbrace{B \quad \overbrace{N \equiv N}^{2} \quad B}^{1}$$

Of these only three are linearly independent, and there exist therefore three energy states ϕ_1, ϕ_2, ϕ_3, of which ϕ_1 represents a stable molecular state[1] and ϕ_2, ϕ_3 represent repelling states. Of the latter two ϕ_3 has the greater forces of repulsion.

Making the same assumptions about the exchange integrals, the scalar products are:

$$(\phi_1\psi_1) = 0.95 \quad (\phi_2\psi_1) = -0.33 \quad (\phi_3\psi_1) = 0.08$$
$$(\phi_1\psi_2) = -0.02 \quad (\phi_2\psi_2) = -0.33 \quad (\phi_3\psi_2) = 0.94$$
$$(\phi_1\psi_3) = 0.16 \quad (\phi_2\psi_3) = -0.98 \quad (\phi_3\psi_3) = 0.18$$
$$(\phi_1\psi_4) = 0.15 \quad (\phi_2\psi_4) = -0.37 \quad (\phi_3\psi_4) = -0.92$$
$$(\phi_1\psi_5) = 0.94 \quad (\phi_2\psi_5) = 0.37 \quad (\phi_3\psi_5) = -0.02$$
$$(\phi_1\psi_6) = 0.58 \quad (\phi_2\psi_6) = 0.55 \quad (\phi_3\psi_6) = 0.60.$$

[4] If the exchange integrals are not equal, the above numbers will be changed. If for instance $z = (A_1A_2)/(A_1H_1) + (A_2H_2)$ becomes equal to zero, $(\phi_1\psi_1) = 1$, if $z = \infty$ $(\phi_1\psi_3) = 1$.

It is here remarkable, that one can use for the molecular state ϕ_1 *two* chemical formulae, which are both near to ϕ_1

$$\psi_1 \sim B = N - N = B \text{ or } \psi_5 \sim \underline{B - N = N - B}.$$

The first one is to be expected. The second one, however, seems from the chemical standpoint also to be reasonable.

Corresponding to ϕ_2 the formula $\overline{B-N-N-B}$ could be used, and to ϕ_3 the formula $\boxed{B \quad N-N \quad B}$ or $\boxed{B \quad N=N \quad B}$; it is apparent that these last formulae are quite alien to the chemist, since such states represent states of repulsion.

NOTE ON THE CALCULATION OF ZERO ORDER EIGENFUNCTIONS

By Newton M. Gray and Lawrence A. Wills
Department of Physics, New York University, New York, New York

(Received June 1, 1931)

Abstract

An elementary procedure is outlined for obtaining zero approximation eigenfunctions of many electron problems. The procedure allows a calculation of these functions as linear combinations of products of functions, each involving one electron only. The proper combination of products for one of the terms of highest multiplicity may, as a rule, be obtained by inspection; the remaining functions are obtained from this by the use of angular momentum operators. The "strong field" eigenfunctions for equivalent and non-equivalent electrons are obtained first, and from these are found the "weak field" eigenfunctions. The usual solution of the secular equation is unnecessary wherever the resultant states may be interpreted as having a definite and known kind of vector coupling (e.g. Russell-Saunders, or (jj)).

THE solution of quantum mechanical problems involving many electrons is usually carried out by means of a perturbation calculation. In the case of degenerate systems the direct method of performing the calculation involves the solution of the secular determinant. This step is frequently awkward. In some cases it may be avoided by the use of the method of sums. In other cases it is possible to use general theorems about the form of angular momentum matrices, as for instance in the derivation of the Landé g factor. The method of sums is however not always sufficient to solve a given problem, and the use of matrices is often difficult. We describe below a systematic and elementary way of automatically solving the secular equation, i.e. removing the degeneracy, for any case in which the angular momenta of the resultant states are known. For such cases the "zero approximation functions," which are linear combinations of the complete set of functions describing the degenerate problem, may be formed directly by a simple application of certain angular momentum operators. Having the "zero approximation" eigenfunctions the perturbation energies are obtainable by direct integration. Needless to say, this method is applicable only for cases of definite and known vector coupling, such as Russell Saunders or (jj), and not for unknown intermediate couplings.

The general method can be explained by considering a single p electron which gives rise to ^2P states. If the coupling between the orbital motion and the spin is weak, the following "strong field" eigenfunctions may be constructed: $^2P_{1,\frac{1}{2}}$, $^2P_{0,\frac{1}{2}}$, $^2P_{-1,\frac{1}{2}}$, $^2P_{1,-\frac{1}{2}}$, $^2P_{0,-\frac{1}{2}}$, $^2P_{-1,-\frac{1}{2}}$ where the first subscript gives the value of the orbital magnetic quantum number m_l, and the second gives the spin quantum number m_s. If the possible orbital functions are denoted by u_1, u_0, u_{-1}, and the two spin functions by s_+ and s_-, the $^2P_{1,\frac{1}{2}}$ term must be

represented by $e^{i\theta}\, u_1 s_+$ where θ is a real number. For simplicity we let $\theta = 0$. In order to form the other functions we use the formulas:[1]

$$
\begin{aligned}
(J_x + iJ_y)\psi(j, m) &= (j + m)^{1/2}(j - m + 1)^{1/2}\psi(j, m - 1)\\
(L_x + iL_y)u(l, m_l) &= (l + m_l)^{1/2}(l - m_l + 1)^{1/2}u(l, m_l - 1)\\
(S_x + iS_y)s(s, m_s) &= (s + m_s)^{1/2}(s - m_s + 1)^{1/2}s(s, m_s - 1)\\
(J_x - iJ_y)\psi(j, m) &= (j - m)^{1/2}(j + m + 1)^{1/2}\psi(j, m + 1)\\
(L_x - iL_y)u(l, m_l) &= (l - m_l)^{1/2}(l + m_l + 1)^{1/2}u(l, m_l + 1)\\
(S_x - iS_y)s(s, m_s) &= (s - m_s)^{1/2}(s + m_s + 1)^{1/2}s(s, m_s + 1).
\end{aligned}
$$

Here $\psi(j, m)$ denotes the "weak field" eigenfunction containing both spatial and spin coordinates, (the symbols j, m are here suffixes), and represents a state of total angular momentum j, and total magnetic quantum number m. The function $u(l, m_l)$ contains only spatial coordinates and represents a state of total orbital angular momentum l, and orbital magnetic quantum number m_l. Similarly $s(s, m_s)$ contains only spin coordinates and represents a state of total spin s, and spin magnetic quantum number m_s. Again l, m_l, s, m_s are suffixes.

$$(J_x, J_y, J_z) = (L_x + S_x, L_y + S_y, L_z + S_z)$$

where by definition the components of the total angular momentum operator $\boldsymbol{J}$ are the sums of the components of orbital and spin operators $\boldsymbol{L}$ and $\boldsymbol{S}$.

Successive applications of the operators $L_x + iL_y$ and $S_x + iS_y$ starting with ${}^2P_{1,\frac{1}{2}}$, will give immediately all the "strong field" functions, but in this simple case the "strong field" functions can be written down at once without use of the operators.

The "weak field" function ${}^2P_{3/2}\,(m = 3/2)$ must be equal to the "strong field" function ${}^2P_{1,\frac{1}{2}}$ since a stationary state in which the value of m is a maximum can arise only when m_l and m_s have their maximum values. The ${}^2P_{3/2}\ (m = \frac{1}{2})$ eigenfunction will be a linear combination of the "strong field" eigenfunctions ${}^2P_{1,-\frac{1}{2}}$ and ${}^2P_{0,\frac{1}{2}}$. Applying the operator $(J_x + iJ_y)$ to the term ${}^2P_{3/2}\,(m = 3/2)$ gives the proper combination of these terms and automatically the proper normalization factor. Further applications of the operator lead to the remaining "weak field" functions for the ${}^2P_{3/2}$ term. The ${}^2P_{\frac{1}{2}}\ (m = \frac{1}{2})$ term may be obtained by constructing a combination of ${}^2P_{0,\frac{1}{2}}$ and ${}^2P_{1,-\frac{1}{2}}$ which is normal, and orthogonal to ${}^2P_{3/2}\ (m = \frac{1}{2})$. The ${}^2P_{\frac{1}{2}}\ (m = -\frac{1}{2})$ term may be obtained from this by operating with $(J_x + iJ_y)$ or by constructing a function orthogonal to ${}^2P_{3/2}\ (m = -\frac{1}{2})$ in a way similar to the above. All the ${}^2P$ eigenfunctions are listed in Table I. In this and the following tables the symbol representing the term stands for the corresponding eigenfunction also.

When dealing with states arising from two or more non-equivalent electrons, different orbital functions must be used. Thus for the combination of a p and a d electron which gives rise to singlet and triplet P, D and F terms, there appear the orbital functions u_1, u_0, u_{-1} for the p electron and v_2, v_1, v_0,

[1] H. Weyl, Gruppentheorie und Quantenmechanik, Kapitel IV.

TABLE I. ^2P *eigenfunctions arising from a p electron.*

"Strong field"	"Weak field"	
$^2P_{1,\frac{1}{2}}=u_1s_+$	$^2P_{3/2}(m=3/2)=^2P_{1,\frac{1}{2}}$	$=u_1s_+$
$^2P_{0,\frac{1}{2}}=u_0s_+$	$^2P_{3/2}(m=\frac{1}{2})=1/3^{\frac{1}{2}}(2^{1/2}\,^2P_{0,\frac{1}{2}}+\,^2P_{1,-\frac{1}{2}})$	$=1/3^{1/2}(2^{1/2}u_0s_++u_1s_-)$
$^2P_{-1,\frac{1}{2}}=u_{-1}s_+$	$^2P_{3/2}(m=-\frac{1}{2})=1/3^{\frac{1}{2}}(^2P_{-1,\frac{1}{2}}+2^{1/2}\,^2P_{0,-\frac{1}{2}})$	$=1/3^{1/2}(u_{-1}s_++2^{1/2}u_0s_-)$
$^2P_{1,-\frac{1}{2}}=u_1s_-$	$^2P_{3/2}(m=-3/2)=^2P_{-1,-\frac{1}{2}}$	$=u_{-1}s_-$
$^2P_{0,-\frac{1}{2}}=u_0s_-$	$^2P_{\frac{1}{2}}(m=\frac{1}{2})=1/3^{1/2}\,^2P_{0,\frac{1}{2}}-2^{1/2}\,^2P_{1,-1})$	$=1/3^{1/2}(u_0s_+-2^{1/2}u_1s_-)$
$^2P_{-1,-\frac{1}{2}}=u_{-1}s_-$	$^2P_{\frac{1}{2}}(m=-\frac{1}{2})=1/3^{\frac{1}{2}}(2^{1/2}\,^2P_{-1,\frac{1}{2}}-\,^2P_{0,-\frac{1}{2}})$	$=1/3^{1/2}(2^{1/2}u_{-1}s_--u_0s_-)$

v_{-1}, v_{-2} for the d electron. To satisfy the exclusion principle, the total eigenfunction must be made antisymmetric, and since the only combination of spin functions giving $m=1$ is $s_+^{\mathrm{I}}s_+^{\mathrm{II}}$, the antisymmetric orbital combination $1/2^{1/2}(u_1^{\mathrm{I}}v_2^{\mathrm{II}}-u_1^{\mathrm{II}}v_2^{\mathrm{I}})$ must be used to obtain $^3F_{3,1}$

$$^3F_{3,1}=\frac{1}{2^{1/2}}\begin{vmatrix} u_1^{\mathrm{I}}s_+^{\mathrm{I}} & u_1^{\mathrm{II}}s_+^{\mathrm{II}} \\ v_2^{\mathrm{I}}s_+^{\mathrm{I}} & v_2^{\mathrm{II}}s_+^{\mathrm{II}} \end{vmatrix}.$$

The superscripts refer to the number of the electron. Operating on $^3F_{3,1}$ with $\sum_{\mathrm{I,II}}(L_x+iL_y)$ gives

$$\sum_{\mathrm{I,II}}(L_x+iL_y)\,^3F_{3,1}=6^{1/2}\,^3F_{2,1}$$

$$=\frac{1}{2^{1/2}}\begin{vmatrix} 2^{1/2}u_0^{\mathrm{I}}s_+^{\mathrm{I}} & u_1^{\mathrm{II}}s_+^{\mathrm{II}} \\ 2v_1^{\mathrm{I}}s_+^{\mathrm{I}} & v_2^{\mathrm{II}}s_+^{\mathrm{II}} \end{vmatrix}+\frac{1}{2^{1/2}}\begin{vmatrix} u_1^{\mathrm{I}}s_+^{\mathrm{I}} & 2^{1/2}u_0^{\mathrm{II}}s_+^{\mathrm{II}} \\ v_2^{\mathrm{I}}s_+^{\mathrm{I}} & 2v_1^{\mathrm{II}}s_+^{\mathrm{II}} \end{vmatrix}$$

The sum of these two determinants is equal to the sum of two other determinants

$$\frac{1}{2^{1/2}}\begin{vmatrix} 2^{1/2}u_0^{\mathrm{I}}s_+^{\mathrm{I}} & 2^{1/2}u_0^{\mathrm{II}}s_+^{\mathrm{II}} \\ v_2^{\mathrm{I}}s_+^{\mathrm{I}} & v_2^{\mathrm{II}}s_+^{\mathrm{II}} \end{vmatrix}+\frac{1}{2^{1/2}}\begin{vmatrix} u_1^{\mathrm{I}}s_+^{\mathrm{I}} & u_1^{\mathrm{II}}s_+^{\mathrm{II}} \\ 2v_1^{\mathrm{I}}s_+^{\mathrm{I}} & 2v_1^{\mathrm{II}}s_+^{\mathrm{II}} \end{vmatrix}$$

These new determinants are obtained by expanding each of the former by the column changed by the operator and then recombining by rows. The result of this expansion and recombination is directly obtained by applying the operators to the rows instead of to the columns. It is seen that this is applicable to all the cases considered. The advantage of the second form is that the columns of any one determinant are all the same except for the electron index. Thus the notation can be abridged by writing only one column of each determinant. For example:

$$^3F_{3,1}=\frac{1}{2^{1/2}}\begin{vmatrix} u_1s_+ \\ v_2s_+ \end{vmatrix};\quad \sum_{\mathrm{I,II}}(L_x+iL_y)\,^3F_{3,1}=\begin{vmatrix} u_0s_+ \\ v_2s_+ \end{vmatrix}+2^{1/2}\begin{vmatrix} u_1s_+ \\ v_1s_+ \end{vmatrix}\ \text{etc.}$$

All the ^3F terms can be obtained from $^3F_{3,1}$ by operating with $\sum_{\mathrm{I,II}}(L_x+iL_y)$ and $\sum_{\mathrm{I,II}}(S_x+iS_y)$.

The procedure outlined above applies in general with the obvious generalization of using three kinds of orbital functions in the case of three electrons, etc. Two electron eigenfunctions may be separated into products of spin and orbital functions. For triplet states there are three symmetric spin

functions $s_1 = s_+^{\mathrm{I}} s_+^{\mathrm{II}}$, $s_0 = 1/2^{1/2}(s_+^{\mathrm{I}} s_-^{\mathrm{II}} + s_-^{\mathrm{I}} s_+^{\mathrm{II}})$, $s_{-1} = s_-^{\mathrm{I}} s_-^{\mathrm{II}}$, and for singlet states there is only one antisymmetric function

$$\hat{s}_0 = \frac{1}{2^{1/2}}(s_+^{\mathrm{I}} s_-^{\mathrm{II}} - s_-^{\mathrm{I}} s_+^{\mathrm{II}}).$$

To satisfy the exclusion principle, the orbital eigenfunctions for triplet states must be antisymmetric, and may be represented by determinants. For singlet states the orbital functions must be symmetric and may be written as "permanents" thus:

$$\begin{pmatrix} u_1 \\ v_2 \end{pmatrix} = u_1^{\mathrm{I}} v_2^{\mathrm{II}} + u_1^{\mathrm{II}} v_2^{\mathrm{I}}.$$

The ${}^3F$ eigenfunctions arising from the combination of a p and a d electron are listed in Table II.

TABLE II. *"Strong field" ${}^3F$ eingenfunctions arising from the combination of a p and a d electron. The subscript i can take the values 1, 0, −1, where s_1, s_0 and s_{-1} have the values given above.*

$$
\begin{aligned}
{}^3F_{3,i} &= 1/(2)^{1/2} \begin{vmatrix} u_1 \\ v_2 \end{vmatrix} s_i \\
{}^3F_{2,i} &= 1/(6)^{1/2} \left\{ 2^{1/2} \begin{vmatrix} u_1 \\ v_1 \end{vmatrix} + \begin{vmatrix} u_0 \\ v_2 \end{vmatrix} \right\} s_i \\
{}^3F_{1,i} &= 1/(60)^{1/2} \left\{ (12)^{1/2} \begin{vmatrix} u_1 \\ v_0 \end{vmatrix} + 4 \begin{vmatrix} u_0 \\ v_1 \end{vmatrix} + 2^{1/2} \begin{vmatrix} u_{-1} \\ v_2 \end{vmatrix} \right\} s_i \\
{}^3F_{0,i} &= 1/(20)^{1/2} \left\{ 2^{1/2} \begin{vmatrix} u_1 \\ v_{-1} \end{vmatrix} + 6^{1/2} \begin{vmatrix} u_0 \\ v_0 \end{vmatrix} + 2^{1/2} \begin{vmatrix} u_{-1} \\ v_1 \end{vmatrix} \right\} s_i \\
&\cdots\cdots\cdots

$^3D_{2,1}$ is orthogonal to $^3F_{2,1}$ and is obtained from it by changing the sign between the determinants. The other ^3D functions are obtained from $^3D_{2,1}$ by use of the operators, and are listed in Table III.

For two non-equivalent p electrons the procedure is exactly like the above except that now there are orbital functions u_1, u_0, u_{-1} and v_1, v_0, v_{-1}. If, however, the two p electrons are equivalent, simplifications occur since the orbital functions for the two electrons are the same. Consider first the ^1D state arising from this configuration. For the $^1D_{2,0}$ state only the combinations $u_1^{\mathrm{I}}\, s_+^{\mathrm{I}} u_1^{\mathrm{II}}\, s_-^{\mathrm{II}}$ and $u_1^{\mathrm{I}}\, s_-^{\mathrm{I}}\, u_1^{\mathrm{II}}\, s_+^{\mathrm{II}}$ may be used, and their antisymmetric combination, written in the abbreviated notation is

$$^1D_{2,0} = \frac{1}{2^{1/2}} \begin{vmatrix} u_1 s_+ \\ u_1 s_- \end{vmatrix}.$$

All the ^1D eigenfunctions may be obtained from $^1D_{2,0}$ by successive applications of the operator $\sum_{\mathrm{I,II}}(L_x + iL_y)$ or from $^1D_{-2,0}$ by use of $\sum_{\mathrm{I,II}}(L_x - iL_y)$. The ^1D eigenfunctions are found to be:

$$^1D_{1,0} = \frac{1}{2}\left\{ \begin{vmatrix} u_0 s_+ \\ u_1 s_- \end{vmatrix} + \begin{vmatrix} u_1 s_+ \\ u_0 s_- \end{vmatrix} \right\},$$

$$^1D_{0,0} = \frac{1}{12^{1/2}}\left\{ \begin{vmatrix} u_{-1} s_+ \\ u_1 s_- \end{vmatrix} + 2 \begin{vmatrix} u_0 s_+ \\ u_0 s_- \end{vmatrix} + \begin{vmatrix} u_1 s_+ \\ u_{-1} s_- \end{vmatrix} \right\} \cdots .$$

The ^3P eigenfunctions may be obtained from either $^3P_{1,1}$ or $^3P_{-1,1}$. Either one of these can be constructed by inspection as was done for $^1D_{2,0}$. Having either of them the remaining ^3P eigenfunctions are obtained by using $\sum_{\mathrm{I,II}}(L_x + iL_y)$ and $\sum_{\mathrm{I,II}}(S_x + iS_y)$ or $\sum_{\mathrm{I,II}}(L_x - iL_y)$ and $\sum_{\mathrm{I,II}}(S_x - iS_y)$. These eigenfunctions are found to be:

$$^3P_{1,i} = \frac{1}{2^{1/2}} \begin{vmatrix} u_1 \\ u_0 \end{vmatrix} s_i, \quad ^3P_{0,i} = \frac{1}{2^{1/2}} \begin{vmatrix} u_1 \\ u_{-1} \end{vmatrix} s_i, \quad ^3P_{-1,i} = \frac{1}{2^{1/2}} \begin{vmatrix} u_0 \\ u_1 \end{vmatrix} s_i.$$

$^1S_{0,0}$ must be a linear combination of the three eigenfunctions having a resultant m_l and m_s equal to zero, so

$$^1S_{0,0} = A \begin{vmatrix} u_1 s_+ \\ u_{-1} s_- \end{vmatrix} + B \begin{vmatrix} u_{-1} s_+ \\ u_1 s_- \end{vmatrix} + C \begin{vmatrix} u_0 s_+ \\ u_0 s_- \end{vmatrix}.$$

Since $^1S_{0,0}$ must be orthogonal to $^1D_{0,0}$ and $^3P_{0,0}$ and must be normalized there are three conditions for determining the coefficients A, B, and C, namely:

$$\int (^1S_{0,0})^* (^1D_{0,0})\, dv = 0; \quad \int (^1S_{0,0})^* (^3P_{0,0})\, dv = 0;$$

$$\int (^1S_{0,0})^* (^1S_{0,0}) dv = 1.$$

These conditions determine $^1S_{0,0}$ to within a factor of absolute magnitude one, and it is found that

$$^1S_{0,0} = \frac{1}{6^{1/2}}\left\{ \begin{vmatrix} u_1 & s_+ \\ u_{-1}s_- \end{vmatrix} - \begin{vmatrix} u_0s_+ \\ u_0s_- \end{vmatrix} + \begin{vmatrix} u_{-1}s_+ \\ u_1 & s_- \end{vmatrix} \right\}.$$

The method outlined above can be very simply extended to a combination of three or more electrons. For n electrons the determinants are of order n.

If the electrons are non-equivalent, a different orbital function must be used for each, and the calculation may become clumsy. It is always definite however, and if the electrons are equivalent, the calculation is very much abridged. Eigenfunctions for three equivalent p electrons, calculated by this method, are listed in Table IV.

TABLE IV. *^2P and ^2D "strong field" eigenfunctions arising from the combination of three equivalent p electrons.*

$$^2D_{2,\frac{1}{2}} = 1/6^{1/2} \begin{vmatrix} u_1s_+ \\ u_1s_- \\ u_0s_+ \end{vmatrix} \qquad ^2D_{2,-\frac{1}{2}} = 1/6^{1/2} \begin{vmatrix} u_1s_+ \\ u_1s_- \\ u_0s_- \end{vmatrix}$$

$$^2D_{1,\frac{1}{2}} = 1/12^{1/2}\left\{ \begin{vmatrix} u_1s_+ \\ u_0s_- \\ u_0s_+ \end{vmatrix} + \begin{vmatrix} u_1s_+ \\ u_1s_- \\ u_{-1}s_+ \end{vmatrix} \right\} \qquad ^2D_{1,-\frac{1}{2}} = 1/12^{1/2}\left\{ \begin{vmatrix} u_0s_+ \\ u_1s_- \\ u_0s_- \end{vmatrix} + \begin{vmatrix} u_1s_+ \\ u_1s_- \\ u_{-1}s_- \end{vmatrix} \right\}$$

$$^2D_{0,\frac{1}{2}} = 1/6\left\{ \begin{vmatrix} u_1s_+ \\ u_{-1}s_- \\ u_0s_+ \end{vmatrix} + 2\begin{vmatrix} u_1s_+ \\ u_0s_- \\ u_{-1}s_+ \end{vmatrix} + \begin{vmatrix} u_0s_+ \\ u_1s_- \\ u_{-1}s_+ \end{vmatrix} \right\} \qquad ^2D_{0,-\frac{1}{2}} = 1/6\left\{ \begin{vmatrix} u_{-1}s_+ \\ u_1s_- \\ u_0s_- \end{vmatrix} + 2\begin{vmatrix} u_0s_+ \\ u_1s_- \\ u_{-1}s_- \end{vmatrix} + \begin{vmatrix} u_1s_+ \\ u_0s_- \\ u_{-1}s_- \end{vmatrix} \right\}$$

$$^2D_{-1,\frac{1}{2}} = 1/12^{1/2}\left\{ \begin{vmatrix} u_0s_+ \\ u_0s_- \\ u_{-1}s_+ \end{vmatrix} + \begin{vmatrix} u_1s_+ \\ u_{-1}s_- \\ u_{-1}s_+ \end{vmatrix} \right\} \qquad ^2D_{-1,-\frac{1}{2}} = 1/12^{1/2}\left\{ \begin{vmatrix} u_{-1}s_+ \\ u_1s_- \\ u_{-1}s_- \end{vmatrix} + \begin{vmatrix} u_0s_+ \\ u_0s_- \\ u_{-1}s_- \end{vmatrix} \right\}$$

$$^2D_{-2,\frac{1}{2}} = 1/6^{1/2} \begin{vmatrix} u_0s_+ \\ u_{-1}s_- \\ u_{-1}s_+ \end{vmatrix} \qquad ^2D_{-2,-\frac{1}{2}} = 1/6^{1/2} \begin{vmatrix} u_{-1}s_+ \\ u_0s_- \\ u_{-1}s_- \end{vmatrix}$$

$$^2P_{1,\frac{1}{2}} = 1/12^{1/2}\left\{ \begin{vmatrix} u_1s_+ \\ u_0s_- \\ u_0s_+ \end{vmatrix} + \begin{vmatrix} u_1s_+ \\ u_{-1}s_+ \\ u_1s_- \end{vmatrix} \right\} \qquad ^2P_{1,-\frac{1}{2}} = 1/12^{1/2}\left\{ \begin{vmatrix} u_1s_- \\ u_0s_- \\ u_0s_+ \end{vmatrix} + \begin{vmatrix} u_1s_+ \\ u_{-1}s_- \\ u_1s_- \end{vmatrix} \right\}$$

$$^2P_{0,\frac{1}{2}} = 1/12^{1/2}\left\{ \begin{vmatrix} u_1s_+ \\ u_{-1}s_- \\ u_0s_+ \end{vmatrix} + \begin{vmatrix} u_0s_+ \\ u_{-1}s_+ \\ u_1s_- \end{vmatrix} \right\} \qquad ^2P_{0,-\frac{1}{2}} = 1/12^{1/2}\left\{ \begin{vmatrix} u_1s_- \\ u_0s_- \\ u_{-1}s_+ \end{vmatrix} + \begin{vmatrix} u_1s_+ \\ u_{-1}s_- \\ u_0s_- \end{vmatrix} \right\}$$

$$^2P_{-1,\frac{1}{2}} = 1/12^{1/2}\left\{ \begin{vmatrix} u_1s_+ \\ u_{-1}s_- \\ u_{-1}s_+ \end{vmatrix} + \begin{vmatrix} u_0s_+ \\ u_{-1}s_+ \\ u_0s_- \end{vmatrix} \right\} \qquad ^2P_{-1,-\frac{1}{2}} = 1/12^{1/2}\left\{ \begin{vmatrix} u_1s_- \\ u_{-1}s_- \\ u_{-1}s_+ \end{vmatrix} + \begin{vmatrix} u_0s_+ \\ u_{-1}s_- \\ u_0s_- \end{vmatrix} \right\}$$

The "weak field" eigenfunctions for a particular state can be obtained from the "strong field" eigenfunctions of that state by forming linear combinations in the proper way. Since the weak and strong field levels are the same for singlet states, the weak and strong field eigenfunctions are the same for singlet states. For states of multiplicity higher than one the procedure is as follows: the "weak field" eigenfunction having the largest value of j and the maximum value of the corresponding m is the same as the "strong field" eigenfunction with the maximum values of m_l and m_s, i.e. $^3P_2(m=2) = {}^3P_{1,1}$. The $^3P_2$ eigenfunctions for the other values of m may be obtained from the $^3P_2(m=2)$ eigenfunction by applying the operator $\sum(J_x+iJ_y)$. The $^3P_2$ $(m=-2)$ eigenfunction might have been obtained by inspection and the re-

maining eigenfunctions calculated by means of the operator $\sum(J_x - iJ_y)$. This affords a check on the work. It is seen that the use of the $\sum(J_x + iJ_y)$ or $\sum(J_x - iJ_y)$ operators is equivalent to making linear combinations of the "strong field" eigenfunctions. These operators give the proper linear combinations and normalization factors automatically as well as checking each other. The ${}^3P_1(m=1)$ eigenfunction must be a linear combination of the two "strong field" eigenfunctions for which $m_l + m_s = 1$, that is of ${}^3P_{1,0}$ and ${}^3P_{0,1}$. Since the ${}^3P_1(m=1)$ eigenfunction must be orthogonal to ${}^3P_2(m=1)$ and is to be normalized, it can be determined to within a factor of absolute magnitude one. Successive applications of $\sum(J_x + iJ_y)$ will give all the ${}^3P_1$ eigenfunctions. It will be found that there will be just enough conditions to determine the ${}^3P_{0,0}$ eigenfunction. It is easy to see that this procedure is applicable in general. This "weak field" eigenfunction for ${}^3P$ states arising from the combination of two equivalent p electrons are:

$$
\begin{aligned}
{}^3P_2(m=2) &= {}^3P_{1,1}, \\
{}^3P_2(m=1) &= \frac{1}{2^{1/2}}\left\{{}^3P_{1,0} + {}^3P_{0,1}\right\} \cdots {}^3P_2(m=-2) = {}^3P_{-1,-1}; \\
{}^3P_1(m=1) &= \frac{1}{2^{1/2}}\left\{{}^3P_{0,1} - {}^3P_{1,0}\right\} \\
{}^3P_0(m=0) &= \frac{1}{3^{1/2}}\left\{{}^3P_{1,-1} + {}^3P_{0,0} - {}^3P_{-1,1}\right\}
\end{aligned}
$$

It is to be observed that the proper linear combination of "strong field" eigenfunctions to form "weak field" eigenfunctions for a given state is independent of the electron configuration giving rise to that state. In the calculation of "weak field" functions it is also not necessary to write out the "strong field" functions explicitly, but it is sufficient to apply the operators to a "strong field" function $\phi(m_l, m_s)$, the operators $L_x + iL_y$ and $L_x - iL_y$ applying to the first index m_l, $S_x + iS_y$, $S_x - iS_y$ applying to the second, m_s.

We appreciate the assistance of Professor G. Breit who suggested to us the use of angular momentum operators and kindly advised us during the preparation of the paper.

CALCULATION OF INTERACTION BETWEEN ATOMS WITH s-ELECTRONS

By N. Rosen
Massachusetts Institute of Technology

(Received May 20, 1931)

Abstract

An attempt is made to systematize the general calculation of the interaction energy of a pair of atoms each of which has one or two equivalent *s*-electrons outside of closed shells. General expressions for this energy are set up in terms of certain integrals and these integrals are evaluated for wave functions of Slater's type in terms of functions which are either tabulated or derivable from those in the accompanying tables. The method is applied to the calculation of some of the constants of a normal Na_2 molecule (which show fair agreement with the experimental values) and the repulsion energy of two normal helium atoms.

I. Introduction

THE interaction between two hydrogen atoms insofar as it is obtainable from a first-order calculation of the perturbation energy was determined by Heitler and London in their paper[1] which opened the way to molecular calculations. The investigation of the interaction between two atoms other than hydrogen is considerably more complicated due to the greater number of electrons and the increased number and complexity of the wave functions. In this paper an effort is made to systematize such calculations for the case of two atoms each of which has one or two equivalent *s*-electrons in its outermost shell. While the calculations are long in some cases they are not particularly difficult; and to judge from the examples worked out, the results are fairly good.

II. Theory

The theory for the type of interaction considered in this paper was first set forth by Heitler and London. However, it may be of some interest to develop it again at this time using the method of J. C. Slater in his paper on "Theory of Complex Spectra."[2]

1. Assumptions.

In the first place it is assumed that the functions of the atoms can be represented by products (or sums of products) of wave functions of the individual electrons, each such function being formed of one factor depending on the space quantum numbers and the electron coordinates and one factor on the spin quantum number and the spin coordinate, the latter being the component of the spin vector along the line joining the nuclei of the two atoms

[1] Heitler and London, Zeits. f. Physik **44**, 455 (1927)
[2] Slater, Phys. Rev. **34**, 1293 (1929).

involved. In accordance with the Pauli principle the complete wave function for each atom is taken as a determinant the elements of which are the individual wave functions with all possible permutations of electron coordinates. This wave function is assumed to satisfy the wave equation for the given atom. Similarly the wave function for the system of two atoms is taken as a determinant involving the individual wave functions of both atoms (zero'th order approximation). The electron spin serves only to determine the symmetry but does not affect the energy in this approximation. Questions of nuclear symmetry or spin are not considered here.

Another assumption made is that closed shells contribute nothing to the interaction. Strictly speaking, closed shells cause a repulsion through the interaction of each with the outer electrons of the other atoms and—a much smaller force—through their interaction with each other. The repulsive effect becomes rapidly smaller the deeper the shells in question are located within the atoms. For ordinary molecular distances this repulsion is small compared to the forces between the outer electrons.

The attraction between the atoms due to their mutual polarization (Van der Waals force) is not treated in this paper. It is known[3] that this polarization force varies practically as $1/R^6$ (R the distance between centers of atoms) whereas the "exchange" force considered here varies exponentially. Consequently for large distances the polarization force predominates and causes an attraction. For small distances it becomes relatively unimportant. For this reason it can be left out in calculations involving atoms in an "attractive" state where the equilibrium distance is small. In this case there is moreover a cancellation between the polarization force and the repulsion due to inner shells which may cause calculated results to be fairly accurate for the heavier atoms. But for "repulsive" states the distance between atoms is larger and the Van der Waals force must be taken into account; in fact there could be no equilibrium without it. If wanted it can be obtained by a separate calculation and added to the results obtained by the calculation treated here.

Finally, it is assumed that closed shells completely shield the nucleus insofar as effects on another atom are concerned. That is, the effective charge (which is to be understood hereafter whenever charge is mentioned) is the nuclear charge less the charge of all the electrons in closed shells. For the usual molecular distances this is certainly valid. In cases where the atoms are exceptionally close together, the effective charge may have to be corrected for incomplete shielding; but the formal results obtained below remain unchanged.

2. Notation.

We consider two atoms A and B with nuclei a and b and effective nuclear charges Z_a and Z_b. The two possible orientations of each electron spin vector will be denoted by $\bar{\alpha}$ and $\bar{\beta}$ (corresponding to $m_s = +1/2$, $m_s = -1/2$). The coordinates of the various electrons will be specified by numbers. The individual space wave-functions will be designated by $u(a)$ and $u(b)$; if the spin

[3] Eisenschitz and London, Zeits. f. Physik **60**, 491 (1930).

and the electron are to be distinguished, by $u(a\bar{\alpha}1)$ for example. Combined wave functions will be indicated by u with subscripts. The internuclear distance will be denoted by R, other distances by r with appropriate subscripts. In integrations the element of volume in the total coordinate space will be denoted by $d\tau$ and that in the coordinate space of a single electron by dv (with a subscript if necessary). Then

$$d\tau = dv_1 dv_2 \cdots .$$

Furthermore, let

$$I = \int u(a)u(b)dv, \tag{1}$$

$$K_1(a) = \int \frac{[u(b)]^2}{r_a} dv, \text{ etc.}, \tag{2}$$

$$K_2 = \int \frac{[u(a1)]^2[u(b2)]^2}{r_{12}} d\tau, \tag{3}$$

$$J_1(a) = \int \frac{u(a)u(b)}{r_a} dv, \text{ etc.}, \tag{4}$$

$$J_2 = \int \frac{u(a1)u(b1)u(a2)u(b2)}{r_{12}} d\tau \tag{5}$$

$$J_3(a) = \int \frac{[u(a1)]^2 u(a2)u(b2)}{r_{12}} d\tau, \text{ etc.} \tag{6}$$

Other symbols or quantities will be defined as needed.

3. Development.

It is convenient to break up the general problem into three cases that may arise depending on the number of electrons involved (outside of closed shells).

(a) *One electron on each atom.* The spin vectors of the two electrons may be either parallel or anti-parallel. In the first case the resultant vector S will be of one unit magnitude and hence will give three possible spin components, $M_s = 1, 0, -1$, according to its orientation, resulting in a triplet term ($^3\Sigma$). In the second case $S = 0$ and hence $M_s = 0$, giving a singlet term ($^1\Sigma$). Hence wave functions for $M_s = \Sigma m_s = \pm 1$ correspond to the triplet. But those for $\Sigma m_s = 0$ may belong to either the triplet or singlet. The possible wave functions are

Wave Function	$m_s(a)$	$m_s(b)$	Σm_s	Multiplicity
$u_1 = u(a\bar{\alpha}1)u(b\bar{\alpha}2) - u(a\bar{\alpha}2)u(b\bar{\alpha}1)$	$\frac{1}{2}$	$\frac{1}{2}$	1	3
$u_2 = u(a\bar{\alpha}1)u(b\bar{\beta}2) - u(a\bar{\alpha}2)u(b\bar{\beta}1)$	$\frac{1}{2}$	$-\frac{1}{2}$	0	1 or 3
$u_3 = u(a\bar{\beta}1)u(b\bar{\alpha}2) - u(a\bar{\beta}2)u(b\bar{\alpha}1)$	$-\frac{1}{2}$	$\frac{1}{2}$	0	
$u_4 = u(a\bar{\beta}1)u(b\bar{\beta}2) - u(a\bar{\beta}2)u(b\bar{\beta}1)$	$-\frac{1}{2}$	$-\frac{1}{2}$	-1	3

We can now set up the secular equation to determine the energy levels. In doing this, we note first that as Slater showed,[2] the energy operator will have no components (to the degree of approximation considered here) between states of different Σm_s. Secondly we see that u_2 and u_3 are not orthogonal to each other. The secular equation becomes

$$\begin{vmatrix} W - H_{11} & 0 & 0 & 0 \\ 0 & W - H_{22} & W\delta_{23} - H_{23} & 0 \\ 0 & W\delta_{32} - H_{32} & W - H_{33} & 0 \\ 0 & 0 & 0 & W - H_{44} \end{vmatrix} = 0$$

where

$$H_{ij} = \int u_i H u_j d\tau \Big/ \left(\int u_i^2 d\tau \int u_j^2 d\tau \right)^{1/2}$$

$$\delta_{ij} = \int u_i u_j d\tau \Big/ \left(\int u_i^2 d\tau \int u_j^2 d\tau \right)^{1/2}$$

The Hamiltonian operator H is given by

$$H = -\frac{h^2}{8\pi^2 m}(\nabla_1^2 + \nabla_2^2) + e^2\left(\frac{Z_a Z_b}{R} - \frac{Z_a}{r_{a1}} - \frac{Z_a}{r_{a2}} - \frac{Z_b}{r_{b1}} - \frac{Z_b}{r_{b2}} + \frac{1}{r_{12}}\right). \tag{7}$$

In this expression each nuclear charge is to be considered as a function of the electron coordinates in the sense that it has two values: one for the case where the electron in question is in the same atom (when the shielding by the inner electrons is incomplete), the second when the electron is in the other atom (when the shielding by the inner electrons is practically complete).

Now the individual wave functions satisfy equations involving the atomic Hamiltonians. For example

$$H_{a1} u(a1) = E_{0a} u(a1), \tag{8}$$

where

$$H_{a1} = -\frac{h^2}{8\pi^2 m}\nabla_1^2 - \frac{Z_a e^2}{r_{a1}}.$$

Using the fact that individual wave functions with opposite spins are orthogonal, one gets by a simple calculation

$$H_{11} = H_{44} = E_{0a} + E_{0b} + e^2\left\{\frac{Z_a Z_b}{R} + \frac{K_2 - [Z_a K_1(a) + Z_b K_1(b)] - [J_2 - I(Z_a J_1(a) + Z_b J_1(b))]}{1 - I^2}\right\} \tag{9}$$

$$H_{22} = H_{33} = E_{0a} + E_{0b} + e^2\left\{\frac{Z_a Z_b}{R} + K_2 - [Z_a K_1(a) + Z_b K_1(b)]\right\} \tag{10}$$

$$H_{23} = H_{32} = -I^2\left[E_{0a} + E_{0b} + e^2\frac{Z_aZ_b}{R}\right] - e^2[J_2 - I(Z_aJ_1(a) + Z_bJ_1(b))] \quad (11)$$

$$\delta_{23} = \delta_{32} = -I^2. \quad (12)$$

The roots of the secular equation are given by

$$W_1 = H_{11}, \quad (13)$$

$$W_2 = H_{44} = H_{11}, \quad (14)$$

and by the roots of

$$\begin{vmatrix} W - H_{22} & W\delta_{23} - H_{23} \\ W\delta_{32} - H_{32} & W - H_{33} \end{vmatrix} = 0,$$

which are

$$W_3 = \frac{H_{22} + H_{23}}{1 + \delta_{23}} = H_{11}, \quad (15)$$

and

$$W_4 = \frac{H_{22} - H_{23}}{1 - \delta_{23}} = E_{0a} + E_{0b} + e^2\left\{\frac{Z_aZ_b}{R} + \frac{K_2 - [Z_aK_1(a) + Z_bK_1(b)] + J_2 - I[Z_aJ_1(a) + Z_bJ_1(b)]}{1 + I^2}\right\}. \quad (16)$$

The energy given by the roots $W_1 = W_2 = W_3$ is that of the triplet, the three levels having the same energy because the spin is not present in the Hamiltonian. The root W_4 gives the energy of the singlet.

If one determines the wave functions corresponding to W_3 and W_4 one finds by the usual theory that they are given (to within an arbitrary factor) by

$$\tilde{u}_2 = u_2 + u_3, \quad (17)$$

$$\tilde{u}_3 = u_2 - u_3, \quad (18)$$

where $\tilde{u}_2$ is the wave function belonging to the triplet and $\tilde{u}_3$ to the singlet.

Heitler and London[1] pointed out that the functions of the triplet were all antisymmetric in the two nuclei and hence would have a node in the region between the nuclei, whereas the singlet function was symmetrical and would not, and hence concluded that the singlet would have a lower energy than the triplet. This means that

$$J_2 - I(Z_aJ_1(a) + Z_bJ_1(b)) < 0 \quad (19)$$

and this has been verified in a number of calculations for typical cases involving neutral atoms, i.e. those for which

$$Z_a = Z_b = 1.$$

It is found in general that for neutral atoms the triplet energy rises monotonically as the atoms approach each other and hence there is repulsion between them. The singlet energy, it turns out, has a minimum for some particular distance between the atoms, and thus a pair of atoms with electron spins anti-parallel will attract each other until they arrive to within this distance.

(*b*) *One atom with one electron, the other with two.* For this case the only energy level is a doublet because of the two possible spin orientations of the single electron; since in the two-electron atom the spins must be opposite because the space wave functions are the same. Hence there are only two functions possible. If A is the atom with one electron these functions are

$$u_1 = \begin{vmatrix} u(a\bar{\alpha}1) & u(a\bar{\alpha}2) & u(a\bar{\alpha}3) \\ u(b\bar{\alpha}1) & u(b\bar{\alpha}2) & u(b\bar{\alpha}3) \\ u(b\bar{\beta}1) & u(b\bar{\beta}2) & u(b\bar{\beta}3) \end{vmatrix} \tag{20}$$

and

$$u_2 = \begin{vmatrix} u(a\bar{\beta}1) & u(a\bar{\beta}2) & u(a\bar{\beta}3) \\ u(b\bar{\alpha}1) & u(b\bar{\alpha}2) & u(b\bar{\alpha}3) \\ u(b\bar{\beta}1) & u(b\bar{\beta}2) & u(b\bar{\beta}3) \end{vmatrix}.$$

The energy is given by

$$W = \int u_1 H u_1 d\tau \Big/ \int u_1^2 d\tau = \int u_2 H u_2 d\tau \Big/ \int u_2^2 d\tau \tag{22}$$

where

$$H = -\frac{h^2}{8\pi^2 m}\sum_{i=1}^{3}\nabla_i^2 + e^2\left\{\frac{Z_a Z_b}{R} - Z_b\sum_{i=1}^{3}\frac{1}{r_{ai}} - \sum_{i=1}^{3}\frac{1}{r_{bi}} + \sum_{i>j=1}^{3}\frac{1}{r_{ij}}\right\}. \tag{23}$$

Making use of the facts that matrix components of H between functions with opposite spins are zero, and that the integrals are independent of the electron labels, it follows readily that

$$\int u_1 H u_1 d\tau = 3!\left\{\int u(a1)u(b2)u(b3)Hu(a1)u(b2)u(b3)d\tau - \int u(a2)u(b1)u(b3)Hu(a1)u(b2)u(b3)d\tau\right\}$$

$$\int u_1^2 d\tau = 3!\left\{\int [u(a1)u(b2)u(b3)]^2 d\tau - \int u(a1)u(b1)u(a2)u(b2)[u(b3)]^2 d\tau\right\}.$$

By means of the relation

$$Hu(a1)u(b2)u(b3)$$
$$= \left\{E_{0a} + E_{0b} + e^2\left[\frac{Z_aZ_b}{R} - \frac{Z_a}{r_{a2}} - \frac{Z_a}{r_{a3}} - \frac{Z_b}{r_{b1}} + \frac{1}{r_{12}} + \frac{1}{r_{13}}\right]\right\}u(a1)u(b2)u(b3)$$

one obtains

$$W = E_{0a} + E_{0b} + e^2\left\{\frac{Z_aZ_b}{R}\right.$$
$$\left. + \frac{2K_2 - Z_aK_1(a)(2 - I^2) - Z_bK_1(b) - [J_2 + I(J_3(b) - Z_aJ_1(a) - Z_bJ_1(b))]}{1 - I^2}\right\}. \quad (24)$$

Because of the fact that the two atoms can behave in only one way, that is, because there is nothing in the atom B to distinguish the two possible spin orientations of the electron in atom A, the force between the atoms must be repulsive.[1] Another way of putting it is that an atom with a closed shell will exert a repulsion on any other whatever the state of the latter may be.

(*c*) *Each atom with two electrons.* For this case there is only one possible wave function corresponding to a singlet ($^1\Sigma$) state

$$u = \begin{vmatrix} u(a\bar{\alpha}1) & u(a\bar{\alpha}2) & u(a\bar{\alpha}3) & u(a\bar{\alpha}4) \\ u(a\bar{\beta}1) & u(a\bar{\beta}2) & u(a\bar{\beta}3) & u(a\bar{\beta}4) \\ u(b\bar{\alpha}1) & u(b\bar{\alpha}2) & (ub\bar{\alpha}3) & u(b\bar{\alpha}4) \\ u(b\bar{\beta}1) & u(b\bar{\beta}2) & u(b\bar{\beta}3) & u(b\bar{\beta}4) \end{vmatrix}. \quad (25)$$

The energy is given by

$$W = \int uHud\tau \Big/ \int u^2 d\tau$$

where H has a form similar to (23).

Expanding gives

$$\int uHud\tau = 4!\left\{\int u(a1)u(a2)u(b3)u(b4)Hu(a1)u(a2)u(b3)u(b4)d\tau\right.$$
$$- 2\int u(a3)u(a2)u(b1)u(b4)Hu(a1)u(a2)u(b3)u(b4)d\tau$$
$$\left. + \int u(a3)u(a4)u(b1)u(b2)Hu(a1)u(a2)u(b3)u(b4)d\tau\right\},$$
$$\int u^2 d\tau = 4!\left\{\int [u(a1)u(a2)u(b3)u(b4)]^2 d\tau\right.$$
$$- 2\int u(a1)u(b1)u(a3)u(b3)[u(a2)u(b4)]^2 d\tau$$
$$\left. + \int u(a1)u(b1)u(a2)u(b2)u(a3)u(b3)u(a4)u(b4)d\tau\right\}.$$

Proceeding as before one gets

$$W = E_{0a} + E_{0b} + e^2\{Z_aZ_b/R + (K_2(4 - 2I^2) - 2(1 - I^2)(Z_aK_1(a) + Z_bK_1(b)) + 2I[(1 - I^2)(Z_aJ_1(a) + Z_bJ_1(b)) - (J_3(a) + J_3(b)) - J_2(2 - 4I^2)])/(1 - I^2)^2\}. \quad (26)$$

This can be written also in the form

$$W = E_{0a} + E_{0b} + e^2\left\{\frac{Z_aZ_b}{R} + 4\frac{K_2 - [(Z_a/2)K_1(a) + (Z_b/2)K_1(b)] - J_2 - I[Z_a/2)J_1(a) + (Z_b/2)J_1(b)]}{1 - I^2} + \frac{I^2K_2 + J_2 - I[J_3(a) + J_3(b)]}{(1 - I^2)^2}\right\}. \quad (27)$$

The term in braces is analogous to the perturbation energy obtained for the case of two one-electron atoms. For two neutral atoms ($Z_a = Z_b = 2$) it is in fact 4 times this corresponding energy. The last term is a correction term of the same order of magnitude as the preceding.

The force between the atoms in this case is repulsive just as in the previous case.

III. Integrals

We now come to the question of determining the numerical values of the expressions set up in the preceding section. For this purpose it is necessary first of all to choose atomic wave functions which are simple enough in form so as not to complicate the calculations excessively and yet have sufficient accuracy for the purpose. In general the accuracy required in molecular problems is less than that for atomic problems because the theory itself is less accurate.

The best form of wave function for the present purpose is that given by Slater,[4] of the form $r^{n-1}e^{-((Z-s)/na_0)r}$ where $a_0 = 0.529$A, n is the effective quantum number and s is a shielding constant, both of the latter being assigned by rules proposed by him. In the case of a stable molecule, i.e. for a pair of atoms in an attractive state, these wave functions are to be used as given by Slater with one exception, namely that n is to have only integral values. In those cases for which Slater's n is not an integer there are two ways of proceeding. Either one can calculate the quantities for the two nearest values of n and interpolate or—and this is the better procedure—one can approximate the wave function in the important region, i.e. where there is most overlapping, by using the nearest integral value of n and then readjusting the shielding constant to get a good fit.

In the case of "repulsive" states, Slater's rules for setting up wave functions are not accurate for the larger distances involved. One can either use the real quantum number for n and take for s one less than the total number of electrons in the atom; or one can determine the wave function by some

[4] Slater, Phys. Rev. **36**, 57 (1930).

other method, for example that of Hartree, and having determined, fit to it a wave function of the form given above by choosing suitable values of n and s. This will be made clearer in an example to follow.

In any case one can write the wave function in the form $r^{n-1}e^{-\alpha r}$ where α is a known constant. In the molecular problem the wave function is then normalized. For the repulsion problem this is not advisable, it being better to adjust the multiplying constant to get the best approximation to the true wave function *in the important region*. In the latter case one can then assume that enough of the electron charge (either positive or negative) is concentrated at the center of the atom to make up one electron. In what follows the multiplying factor will be denoted by N if the wave function is normalized, otherwise by C.

For the problem on hand we consider two wave functions, one for each atom

$$\begin{aligned} u(a) &= N_a r^{m-1} e^{-\alpha r} \\ u(b) &= N_b r^{n-1} e^{-\beta r}. \end{aligned} \tag{28}$$

From the condition

$$\int [u(a)]^2 dv = 4\pi N_a^2 \int_0^\infty r^{2m} e^{-2\alpha r} dr = 1$$

it follows that

$$N_a = \left(\frac{(2\alpha)^{2m+1}}{4\pi (2m)!} \right)^{1/2}, \tag{29}$$

and an analogous expression holds for N_b.

The integrals defined in the previous section can be calculated by a few simple devices, such as the use of elliptic coordinates, the fact that the potential of a spherical shell is constant inside the shell and outside is the same as if concentrated at the center, and the Neumann expansion of $1/r_{12}$ in terms of Legendre functions.[5] The integrals can be separated into two groups according as to whether $\alpha = \beta$ or $\alpha \neq \beta$.

In evaluating the integrals use is made of certain functions given by Guillemin and Zener,[6] which are most conveniently defined as follows

$$A_n(\alpha) = A_n(1, \alpha) = \int_1^\infty x^n e^{-\alpha x} dx = \frac{n! e^{-\alpha}}{\alpha^{n+1}} \sum_{\nu=0}^{n} \frac{\alpha^\nu}{\nu!} \tag{30}$$

$$A_n(-1, \alpha) = \int_{-1}^\infty x^n e^{-\alpha x} dx = \frac{n! e^{\alpha}}{\alpha^{n+1}} \sum_{\nu=0}^{n} \frac{(-\alpha)^\nu}{\nu!} \tag{31}$$

$$B_n(\alpha) = \int_{-1}^{1} x^n e^{-\alpha x} dx = A_n(-1, \alpha) - A_n(1, \alpha) \tag{32}$$

$$\begin{aligned} F_n(\alpha) &= \int_1^\infty x^n e^{-\alpha x} Q_0(x) dx = \tfrac{1}{2} \int_1^\infty x^n e^{-\alpha x} \ln \left(\frac{x+1}{x-1} \right) dx \\ &= \tfrac{1}{2} \left[(\ln 2\alpha + C) A_n(1,\alpha) - Ei(-2\alpha) A_n(-1,\alpha) \right] - \theta(n,\alpha) \end{aligned} \tag{33}$$

[5] Sugiura, Zeits. f. Physik **45,** 484 (1927).

[6] Zener and Guillemin, Phys. Rev. **34,** 999 (1929). Their notation has been changed slightly.

where

$$C = 0.577216 \cdots \text{ (Euler's constant)}$$

and

$$\theta(n, \alpha) = \frac{e^{-\alpha}}{\alpha} \sum_{\nu=0}^{n} C_\nu{}^n \alpha^{-\nu}, \tag{34}$$

the coefficients $C_\nu{}^n$ being defined by the relations

$$C_\nu{}^{n+1} = C_\nu{}^n + \nu C_{\nu-1}{}^n + \frac{[1 + (-1)^{n-\nu}]}{2} \frac{n!}{(n-\nu+1)!}, \quad 0 < \nu \leq n \tag{35}$$

$$C_0{}^n = 0.$$

In addition to these we define the coefficients $p_\tau{}^i$ and $q_\tau{}^i$ by means of the identities

$$P_\tau(x) = \sum_{i=0}^{\tau} p_\tau{}^i x^i, \tag{36}$$

$$Q_\tau(x) = Q_0 \sum_{i=0}^{\tau} p_\tau{}^i x^i + \sum_{i=0}^{\tau} q_\tau{}^i x^i, \tag{37}$$

where $P_\tau(x)$ and $Q_\tau(x)$ are Legendre functions of the first and second kind respectively of order τ ($Q_0(x) = 1/2\ ln\ (x+1)/(x-1)$).

These coefficients satisfy recursion formulae which follow from the relations between Legendre functions

$$p_\tau{}^j = \left(\frac{2\tau - 1}{\tau}\right) p_{\tau-1}^{j-1} - \left(\frac{\tau - 1}{\tau}\right) p_{\tau-2}^{j}, \quad (0 < j \leq \tau, \tau > 1) \tag{38}$$

$$p_\tau{}^0 = -\left(\frac{\tau - 1}{\tau}\right) p_{\tau-2}^{0}, \qquad (\tau > 1)$$

$$p_0{}^0 = p_1{}^1 = 1,$$

and

$$q_\tau{}^j = \left(\frac{2\tau - 1}{\tau}\right) q_{\tau-1}^{j-1} - \left(\frac{\tau - 1}{\tau}\right) q_{\tau-2}^{j}, \quad (0 < j \leq \tau, \tau > 1) \tag{39}$$

$$q_\tau{}^0 = -\left(\frac{\tau - 1}{\tau}\right) q_{\tau-2}, \qquad (\tau > 1)$$

$$q_0{}^0 = 0, \ q_1{}^1 = -1.$$

The coefficients D_p^{mn} are defined by the identity

$$(x + y)^m (x - y)^n = \sum_{p=0}^{m+n} D_p^{mn} x^{m+n-p} y^p,$$

so that

$$D_p^{mn} = \sum_k (-1)^k \binom{m}{p-k}\binom{n}{k}. \tag{40}$$

They satisfy the following relations

$$D_p^{mn} = D_p^{m-1,n} + D_{p-1}^{m-1,n} = D_p^{m,n-1} - D_{p-1}^{m,n-1}, \quad (0 < p \leq m+n) \tag{41}$$

$$D_p^{mn} = (-1)^p D_p^{nm}, \quad D_{m+n-p}^{mn} = (-1)^n D_p^{mn},$$

$$D_{2k+1}^{mm} = 0, \quad D_{2k}^{mm} = (-1)^k \binom{m}{k},$$

$$D_p^{m,0} = \binom{m}{p},$$

$$D_0^{mn} = 1.$$

Finally we require several more quantities, as follows

$$R_\tau^n = \int_{-1}^{1} x^n P_\tau(x)\,dx, \tag{42}$$

$$= \frac{2^{\tau+1} n! \left(\frac{n+\tau}{2}\right)!}{\left(\frac{n-\tau}{2}\right)!(n+\tau+1)!}, \text{ if } n-\tau \geq 0 \textit{ and } \text{even},$$

$$= 0, \qquad \text{if } n-\tau < 0 \textit{ or } \text{odd},$$

$$G_\tau^n(\alpha) = \int_{-1}^{1} x^n e^{-\alpha x} P_\tau(x)\,dx, \tag{43}$$

$$= \sum_{i=0}^{\tau} p_\tau^i B_{n+i}(\alpha),$$

$$A_n^m(\alpha) = \sum_{\nu=0}^{m} \frac{\alpha^\nu}{\nu!} A_{n+\nu}(\alpha) \tag{44}$$

$$F_n^m(\alpha) = \sum_{\nu=0}^{m} \frac{\alpha^\nu}{\nu!} F_{n+\nu}(\alpha). \tag{45}$$

In Tables I-VII[7] are given some of the values of

$$A_n(1,\alpha),\ A_n(-1,\alpha),\ C_\nu^n,\ R_\tau^i,\ p_\tau^i,\ q_\tau^i, \text{ and } D_p^{mn}.$$

By means of the defining equations and recursion formulae the tables can be extended if necessary. Although it would be convenient to have tables of the

[7] Tables I and II were prepared by Dr. S. Ikehara to whom I am indebted. Bartlett (Phys. Rev. **37**, 507 (1931)) has given a smaller table of $A_n(1,\alpha)$. Part of Table III is given in reference (6).

TABLE I. $A_n(1, \alpha)$

α	n								
	0	1	2	3	4	5	6	7	8
1.5	$1.48753 \cdot 10^{-1}$	$2.47922 \cdot 10^{-1}$	$4.79317 \cdot 10^{-1}$	1.10739	3.10178	1.04880·10	4.21009·10	$1.96620 \cdot 10^{2}$	$1.04879 \cdot 10^{3}$
2.0	$6.76676 \cdot 10^{-2}$	1.01501	1.69169	$3.21421 \cdot 10^{-1}$	$7.10510 \cdot 10^{-1}$	1.84394·1	5.59950·1	1.96660·10	$7.87313 \cdot 10^{2}$
2.5	3.28340	$4.59676 \cdot 10^{-2}$	$6.96081 \cdot 10^{-2}$	1.16364	2.19016	$4.70866 \cdot 10^{-1}$	1.16291	3.28899·1	1.05576·10
2.75	2.32465	3.16998	4.63009	$7.37565 \cdot 10^{-2}$	1.30529	2.60571	$5.91766 \cdot 10^{-1}$	1.52957	4.47288·1
3.0	1.65957	2.21276	3.13474	4.79431	$8.05198 \cdot 10^{-2}$	1.50795	3.18186	$7.59031 \cdot 10^{-1}$	2.04068
3.25	1.19305	1·56015	2·15314	3·18057	5.10760	$9.05090 \cdot 10^{-2}$	1.79024	3.97521	$9.90443 \cdot 10^{-1}$
3.5	$8.62782 \cdot 10^{-3}$	1.10929	1.49666	2.14564	3.31494	5.59841	1.04601	2.17829	5.06553
3.75	6.27140	$7.94377 \cdot 10^{-3}$	1.05081	1.46779	2.19278	3.55084	$6.30849 \cdot 10^{-2}$	1.24030	2.70869
4.0	4.57891	5.72364	$7.44073 \cdot 10^{-3}$	1.01595	1.47384	2.30019	3.90817	$7.29719 \cdot 10^{-2}$	1.50523
4.25	3.35629	4.14601	5.30735	$7.10266 \cdot 10^{-3}$	1.00111	1.51694	2.47719	4.41571	$8.64755 \cdot 10^{-2}$
4.5	2.46867	3.01726	3.80967	5.00845	$6.92062 \cdot 10^{-3}$	1.01582	1.60130	2.73778	5.11402
5.0	1.34759	1.61711	1.99443	2.54425	3.38299	$4.73058 \cdot 10^{-3}$	$7.02428 \cdot 10^{-3}$	1.11816	1.92381
6.0	$4.13125 \cdot 10^{-4}$	$4.81980 \cdot 10^{-4}$	$5.73785 \cdot 10^{-4}$	$7.00018 \cdot 10^{-4}$	$8.79801 \cdot 10^{-4}$	1.14630	1.55942	$2.23245 \cdot 10^{-3}$	$3.38972 \cdot 10^{-3}$
7.0	1.30269	1.48879	1.72806	2.04328	2.47028	$3.06717 \cdot 10^{-4}$	$3.93169 \cdot 10^{-4}$	$5.23438 \cdot 10^{-4}$	$7.28484 \cdot 10^{-4}$
8.0	$4.19328 \cdot 10^{-5}$	$4.71744 \cdot 10^{-5}$	$5.37264 \cdot 10^{-5}$	$6.20802 \cdot 10^{-5}$	$7.29729 \cdot 10^{-5}$	$8.75409 \cdot 10^{-5}$	1.07589	1.36073	1.78006
8.5	2.39375	2.67536	3.02324	3.46077	4.02234	4.75983	$5.75363 \cdot 10^{-5}$	$7.13203 \cdot 10^{-5}$	$9.10624 \cdot 10^{-5}$
9.0	1.37122	1.52358	1.70979	1.94115	2.23395	2.61231	3.11276	3.79225	4.74211
10.	$4.53999 \cdot 10^{-6}$	$4.99399 \cdot 10^{-6}$	$5.53879 \cdot 10^{-6}$	$6.20163 \cdot 10^{-6}$	$7.02064 \cdot 10^{-6}$	$8.05032 \cdot 10^{-6}$	$9.37018 \cdot 10^{-6}$	1.10991	1.34193
12.	$5.12018 \cdot 10^{-7}$	$5.54686 \cdot 10^{-7}$	$6.04465 \cdot 10^{-7}$	$6.63134 \cdot 10^{-7}$	$7.33062 \cdot 10^{-7}$	$8.17460 \cdot 10^{-7}$	$9.20748 \cdot 10^{-7}$	$1.04912 \cdot 10^{-6}$	$1.21143 \cdot 10^{-6}$
14.	$5.93949 \cdot 10^{-8}$	$6.36374 \cdot 10^{-8}$	$6.81860 \cdot 10^{-8}$	$7.40705 \cdot 10^{-8}$	$8.05579 \cdot 10^{-8}$	$8.81656 \cdot 10^{-8}$	$9.71802 \cdot 10^{-8}$	$1.07985 \cdot 10^{-7}$	$1.21101 \cdot 10^{-7}$

TABLE I. $A_n(1, \alpha)$

α	n							
	9	10	11	12	13	14	15	16
3.0	6.13863·1	2.04787·1	7.51051·10	$3.00437 \cdot 10^{2}$	$1.30191 \cdot 10^{3}$	$6.07560 \cdot 10^{4}$	$3.03780 \cdot 10^{4}$	$1.62016 \cdot 10^{5}$
3.5	1.31111	3.75467·1	1.18090	4.04967·10				
4.0	$3.43255 \cdot 10^{-1}$	$8.62716 \cdot 10^{-1}$	2.37705·1	7.13573·1	2.31957·10	8.11895·10	$3.04465 \cdot 10^{2}$	$1.21787 \cdot 10^{3}$
4.25	1.86481	4.42135	1.14771	3.24394				
4.5	1.04749	2.35245	$5.77511 \cdot 10^{-1}$	1.54250	4.45857·1	1.38736		
5.0	$3.59762 \cdot 10^{-2}$	$7.33000 \cdot 10^{-2}$	1.62608	$3.91606 \cdot 10^{-1}$	1.01952	2.85601·1	8.56938·1	2.74234·10
6.0	$5.49771 \cdot 10^{-3}$	$9.57598 \cdot 10^{-3}$	$1.79691 \cdot 10^{-2}$	$3.63513 \cdot 10^{-2}$	$7.91743 \cdot 10^{-2}$	$1.85153 \cdot 10^{-1}$	$4.63296 \cdot 10^{-1}$	1.23587·1
7.0	1.06689	1.65440	$2.73004 \cdot 10^{-3}$	$4.81034 \cdot 10^{-3}$	$9.06375 \cdot 10^{-3}$	$1.82578 \cdot 10^{-2}$	$3.92541 \cdot 10^{-2}$	$8.98538 \cdot 10^{-2}$
8.0	$2.42189 \cdot 10^{-4}$	$3.44669 \cdot 10^{-4}$	$5.15853 \cdot 10^{-4}$	$8.15712 \cdot 10^{-4}$	8.36747	$2.43500 \cdot 10^{-3}$	$4.60755 \cdot 10^{-3}$	$9.25704 \cdot 10^{-3}$
8.5	1.20356	1.65533	2.38157	3.60159	$5.74769 \cdot 10^{-4}$	$9.70616 \cdot 10^{-4}$	1.73679	3.27319
9.0	$6.11333 \cdot 10^{-5}$	$8.16381 \cdot 10^{-5}$	1.13492	1.65035	2.52096	4.05862	$6.90148 \cdot 10^{-4}$	1.24064
10.	1.66174	2.11573	$2.78131 \cdot 10^{-5}$	$3.79157 \cdot 10^{-5}$	$5.38304 \cdot 10^{-5}$	$7.99025 \cdot 10^{-5}$	1.24394	$2.03570 \cdot 10^{-4}$
12.	$1.42059 \cdot 10^{-6}$	$1.69584 \cdot 10^{-6}$	$2.06654 \cdot 10^{-6}$	$2.57856 \cdot 10^{-6}$	$3.30546 \cdot 10^{-6}$	$4.36838 \cdot 10^{-6}$	$5.97250 \cdot 10^{-6}$	$8.47535 \cdot 10^{-6}$
14.	$1.37245 \cdot 10^{-7}$	$1.57427 \cdot 10^{-7}$	$1.83088 \cdot 10^{-7}$	$2.16327 \cdot 10^{-7}$	$2.60270 \cdot 10^{-7}$	$3.19665 \cdot 10^{-7}$	$4.01893 \cdot 10^{-7}$	$5.18701 \cdot 10^{-7}$

TABLE II $A_n(-1, \alpha)$

α	n								
	0	1	2	3	4	5	6	7	8
1.5	2.98779	$-9.95931\cdot10^{-1}$	1.65988	$3.31977\cdot10^{-1}$	3.87306	9.92242	4.26775·10	$1.96174\cdot10^{2}$	$1.04925\cdot10^{3}$
2.0	3.69453	1.84726·1	1.84726	$-9.23632\cdot10^{-1}$	1.84726	$1.84726\cdot10^{-1}$	6.46542·1	1.89345·10	7.94323·10
2.5	4.87300	2.92380	2.53396	1.83225·1	1.94140	$-9.90194\cdot10^{-1}$	2.49653	2.11729·1	1.16483
2.75	5.68823	3.61978	3.05566	2.35478	2.26309	1.57352·1	2.25510	$-5.20320\cdot10^{-2}$	5.83959·1
3.0	6.69518	4.46345	3.71954	2.97564	2.72767	2.14907	2.39704	$-1.10209\cdot1$	3.75628
3.25	7.93549	5.49380	4.55469	3.73116	3.34343	2.79196	2.78109	1.94544	3.14671
3.5	9.46156	6.75826	5.59970	4.66182	4.13377	3.55618	3.36525	2.73105	3.21916
3.75	1.13390·10	8.31523	6.90416	5.81562	5.13562	4.49146	4.15262	3.58739	3.68585
4.0	1.36495	1.02372·10	8.53096	7.25132	6.39822	5.65176	5.17190	4.59872	4.45209
4.25	1.64954	1.26141	1.05593·10	9.04174	7.98551	7.10067	6.47092	5.83741	5.50733
4.5	2.00038	1.55585	1.30889	1.12779·10	9.97904	8.91599	8.11582	7.37920	6.88524
5.0	2.96826	2.37461	2.01842	1.75721	1.56249·10	1.40577·10	1.28134·10	1.17439·10	1.08924·10
6.0	6.72381	5.60318	4.85609	4.29577	3.85997	3.21554	3.21664	2.97107	2.76239
7.0	$1.56662\cdot10^{2}$	$1.34282\cdot10^{2}$	$1.18296\cdot10^{2}$	$1.05964\cdot10^{2}$	9.61112	8.80110	8.12238	7.54380	7.04470
8.0	3.72620	3.26042	2.91109	2.63453	$2.40893\cdot10^{2}$	$2.22062\cdot10^{2}$	$2.06073\cdot10^{2}$	$1.92305\cdot10^{2}$	$1.80314\cdot10^{2}$
8.5	5.78208	5.10184	4.58165	4.16503	3.82207	3.53381	3.28763	3.07462	2.88832
9.0	9.00343	8.00305	7.22497	6.59510	6.07227	5.62994	5.25013	4.91999	4.63010
10.	$2.20265\cdot10^{3}$	$1.98238\cdot10^{3}$	$1.80617\cdot10^{3}$	$1.66080\cdot10^{3}$	$1.53833\cdot10^{3}$	$1.43348\cdot10^{3}$	$1.34256\cdot10^{3}$	$1.26286\cdot10^{3}$	$1.19236\cdot10^{3}$
12.	$1.35629\cdot10^{4}$	$1.24327\cdot10^{4}$	$1.14908\cdot10^{4}$	$1.06902\cdot10^{4}$	9.99950	9.39644	8.86468	8.39184	7.96834
14.	8.59003	7.97646	7.45054	6.99349	$6.59189\cdot10^{4}$	$6.23578\cdot10^{4}$	$5.91755\cdot10^{4}$	$5.63125\cdot10^{4}$	$5.37217\cdot10^{4}$

TABLE II. $A_n(-1, \alpha)$

α	n							
	9	10	11	12	13	14	15	16
3.0	4.57366	2.19407·10	7.37541·10	$3.01712\cdot10^{2}$	$1.30072\cdot10^{3}$	$6.07673\cdot10^{3}$	$3.03770\cdot10^{4}$	$1.62017\cdot10^{5}$
3.5	−1.18372	6.07951·1	−9.64548·1	4.25318·10				
4.0	3.63232	4.56873	−1.08554	1.03929	2.01275·10	8.40957·10	$3.01710\cdot10^{2}$	$1.22049\cdot10^{3}$
4.25	4.83281	5.12407	3.23308	7.36669·1				
4.5	6.23333	6.15196	4.96569	6.76198	−4.69204·1	1.85441·10		
5.0	1.00763·10	9.53011	8.71639	8.76330	6.89806	1.03681	1.42159·1	3.42317·10
6.0	2.58023	2.42343·10	2.28086·10	2.16210·10	2.03926·10	1.96554	−1.80996·10	1.89725
7.0	6.60872	6.22516	5.88379	5.57969	5.30390	5.05838	4.82680	$4.54473\cdot10$
8.0	$1.69766\cdot10^{2}$	$1.60412\cdot10^{2}$	$1.52053\cdot10^{2}$	$1.44540\cdot10^{2}$	$1.37742\cdot10^{2}$	$1.31571\cdot10^{2}$	$1.25925\cdot10^{2}$	$1.20770\cdot10^{2}$
8.5	2.72386	2.57754	2.44644	2.32828	2.22118	2.12367	2.03443	1.95257
9.0	4.37333	4.14418	3.93832	3.75233	3.58339	3.42926	3.28800	3.15810
10.	$1.12952\cdot10^{3}$	$1.07313\cdot10^{3}$	$1.02221\cdot10^{3}$	9.75996	9.33852	8.95254	8.60432	8.25956
12.	7.58664	7.24070	6.92559	$6.63731\cdot10^{3}$	$6.37248\cdot10^{3}$	$6.12833\cdot10^{3}$	5.90248	$5.69139\cdot10^{3}$
14.	$5.13649\cdot10^{4}$	$4.92111\cdot10^{4}$	$4.72345\cdot10^{4}$	$4.54136\cdot10^{4}$	$4.37305\cdot10^{4}$	$4.21698\cdot10^{4}$	4.07184	$3.93650\cdot10^{4}$

TABLE III. C_ν^n

n	ν								
	0	1	2	3	4	5	6	7	8
0	0								
1	0	0							
2	0	1	0						
3	0	1	4	0					
4	0	2	6	1.8·10	0				
5	0	2	1.4·10	3.6	9.6·10	0			
6	0	3	1.8	9.8	$2.40\cdot10^2$	$6.00\cdot10^2$	0		
7	0	3	3.0	$1.52\cdot10^2$	7.52	$1.800\cdot10^3$	$4.320\cdot10^3$	0	
8	0	4	3.6	2.84	$1.360\cdot10^3$	6.400	$1.5120\cdot10^4$	$3.5280\cdot10^4$	0
9	0	4	5.2	3.92	2.832	$1.3200\cdot10^4$	6.0240	$1.41120\cdot10^5$	$3.22560\cdot10^5$
10	0	5	6.0	6.20	4.400	3.0384	$1.39440\cdot10^5$	6.23280	$1.45152\cdot10^6$
11	0	5	8.0	8.00	7.600	5.2384	3.51984	$1.59936\cdot10^6$	7.04256
12	0	6	9.0	$1.150\cdot10^3$	$1.0800\cdot10^4$	9.8304	6.66288	4.39589	$1.98374\cdot10^7$
13	0	6	$1.14\cdot10^2$	1.420	1.6720	$1.52301\cdot10^5$	$1.35115\cdot10^6$	9.05990	5.89962
14	0	7	1.26	1.918	2.2400	2.53064	2.26498	$1.97535\cdot10^7$	$1.31475\cdot10^8$
15	0	7	1.54	2.296	3.2256	3.65064	4.02360	3.56083	3.06801
16	0	8	1.68	2.968	4.1440	5.59104	6.21398	6.73771	5.91667

TABLE III. C_ν^n

n	ν						
	9	10	11	12	13	14	15
9	0						
10	$3.26592\cdot10^6$	0					
11	$1.63296\cdot10^7$	$3.62880\cdot10^7$	0				
12	8.63654	$1.99584\cdot10^8$	$4.39085\cdot10^8$	0			
13	$2.64902\cdot10^8$	$1.14307\cdot10^9$	$2.63451\cdot10^9$	$5.74802\cdot10^9$	0		
14	8.47760	3.79210	$1.62461\cdot10^{10}$	$3.73621\cdot10^{10}$	$8.09513\cdot10^{10}$	0	
15	$2.03104\cdot10^9$	$1.20962\cdot10^{10}$	5.79592	$2.46845\cdot10^{11}$	$5.66659\cdot10^{11}$	$1.22050\cdot10^{12}$	0
16	5.05170	3.33066	$2.11815\cdot10^{11}$	9.42356	$3.99360\cdot10^{12}$	9.15372	$1.96151\cdot10^{13}$

TABLE IV. R_τ^i

i	τ										
	0	1	2	3	4	5	6	7	8	9	10
0	2.00000										
1		0.666667									
2	0.666667		0.266667								
3		0.400000		0.114286							
4	0.400000		0.228571		0.0507937						
5		0.285714		0.126984		0.0230880					
6	0.285714		0.190476		0.0692641		0.0106560				
7		0.222222		0.121212		0.0372960		$0.0^2497280$			
8	0.222222		0.161616		0.0745921		0.0198912		$0.0^2234014$		
9		0.181818		0.111888		0.0447552		0.0105307		$0.0^2110849$	
10	0.181818		0.139860		0.0745921		0.0526532		$0.0^2554245$		$0.0^3527852$

TABLE V. p_τ^i

τ	i										
	0	1	2	3	4	5	6	7	8	9	10
0	1.										
1		1.									
2	−0.5		1.5								
3		−1.5		2.5							
4	0.375		−3.75		4.375						
5		1.875		−8.75		7.875					
6	−0.3125		6.5625		−19.6875		14.4375				
7		−2.1875		+19.6875		−43.3125		26.8125			
8	0.273438		−9.84375		54.14063		−93.84375		50.27344		
9		2.46094		−36.09375		140.76563		−201.09375		94.96094	
10	−0.246094		13.53516		−117.30469		351.91406		−427.32422		180.42578

TABLE VI. q_τ^i

τ	i										
	0	1	2	3	4	5	6	7	8	9	10
0	0										
1	−1.										
2		−1.5									
3	0.666667		−2.5								
4		2.29167		−4.375							
5	−0.533333		6.125		−7.875						
6		−2.8875		14.875		−14.4375					
7	0.457143		−10.6125		34.375		−26.8125				
8		3.38371		−32.91406		77.08594		−50.27344			
9	0.406349		15.95138		−92.72656		169.44010		−94.96094		
10		−3.81740		59.68973		−245.55781		367.18229		−180.42578	

TABLE VII. D_p^{mn}

m	n	p										
		0	1	2	3	4	5	6	7	8	9	10
0	0	1										
	1	1	−1									
	2	1	−2	1								
	3	1	−3	3	−1							
	4	1	−4	6	−4	1						
	5	1	−5	10	−10	5	−1					
1	0	1	1									
	1	1	0	−1								
	2	1	−1	−1	1							
	3	1	−2	0	2	−1						
	4	1	−3	2	2	−3	1					
	5	1	−4	5	0	−5	4	−1				
2	0	1	2	1								
	1	1	1	−1	−1							
	2	1	0	−2	0	1						
	3	1	−1	−2	2	1	−1					
	4	1	−2	−1	4	−1	−2	1				
	5	1	−3	1	5	−5	−1	3	−1			
3	0	1	3	3	1							
	1	1	2	0	−2	−1						
	2	1	1	−2	−2	1	1					
	3	1	0	−3	0	3	0	−1				
	4	1	−1	−3	3	3	−3	−1	1			
	5	1	−2	−2	6	0	−6	2	2	−1		
4	0	1	4	6	4	1						
	1	1	3	2	−2	−3	−1					
	2	1	2	−1	−4	−1	2	1				
	3	1	1	−3	−3	3	3	−1	−1			
	4	1	0	−4	0	6	0	−4	0	1		
	5	1	−1	−4	4	6	−6	−4	4	1	−1	
5	0	1	5	10	10	5	1					
	1	1	4	5	0	−5	−4	−1				
	2	1	3	1	−5	−5	1	3	1			
	3	1	2	−2	−6	0	6	2	−2	−1		
	4	1	1	−4	−4	6	6	−4	−4	1	1	
	5	1	0	−5	0	10	0	−10	0	5	0	−1

other functions available, it did not appear advisable to go to the labor of preparing them in view of the fact that the present theory is probably of a temporary nature. From the tables given here, the other functions for specific values of the arguments can be computed in a reasonably short time.

Using the functions and quantities mentioned, the integrals can be evaluated and are listed below. Those which can be obtained by interchanging a and b, α and β, and m and n in integrals already listed are omitted. The integrals given are for normalized wave functions. Corresponding integrals for unnormalized functions can be obtained from those below by multiplying I and $J_1(b)$ by C_aC_b/N_aN_b, $K_1(b)$ by C_a^2/N_a^2, J_2 and K_2 by $C_a^2C_b^2/N_a^2N_b^2$ and $J_3(a)$ by $C_a^3C_b/N_a^3N_b$.

1. $\alpha = \beta$

$$I = \frac{(\alpha R)^{m+n+1}}{((2m)!(2n)!)^{1/2}} \sum_{k=0}^{\leq (m+n)/2} \frac{D_{2k}^{mn}}{2k+1} A_{m+n-2k}(\alpha R), \tag{46}$$

$$K_1(b) = \frac{1}{R} + \frac{(2\alpha R)^{2m}}{(2m)!R}\left[(2\alpha R - 2m)A_{2m-1}(2\alpha R) - e^{-2\alpha R}\right], \tag{47}$$

$$K_2 = K_1(b) - \frac{\alpha(\alpha R)^{2m}}{n(2m)!}\sum_{\nu=0}^{2n-1}\frac{2n-\nu}{\nu!}(\alpha R)^{\nu}\sum_{p=0}^{\leq m+(\nu-1)/2}\frac{D_{2p}^{2m-1,\nu}}{2p+1}A_{2m+\nu-1-2p}(2\alpha R), \tag{48}$$

(or the same with atomic quantities interchanged),

$$J_1(b) = \frac{2\alpha(\alpha R)^{m+n}}{((2m)!(2n)!)^{1/2}}\sum_{k=0}^{\leq(m+n-1)/2}\frac{D_{2k}^{m,n-1}}{2k+1}A_{m+n-1-2k}(\alpha R), \tag{49}$$

$$\begin{aligned} J_2 = {} & \frac{\alpha(\alpha R)^{2m+2n+1}}{(2m)!(2n)!}\sum_{\tau=0}^{m+n}\sum_{s=0}^{m+n}D_{\tau}^{mn}D_{s}^{mn}\sum_{\tau=0}^{\leq r,s}(2\tau+1)R_{\tau}^{r}R_{\tau}^{s} \\ & \Bigg\{\sum_{j=0}^{\tau}\sum_{i=0}^{\tau}p_{\tau}^{\,i}A_{m+n-s+j}(\alpha R)\left[p_{\tau}^{\,i}F_{m+n-r+i}(\alpha R) + q_{\tau}^{\,i}A_{m+n-r+i}(\alpha R)\right] \\ & - \sum_{j=0}^{\tau}\sum_{i=0}^{\tau}p_{\tau}^{\,j}(m+n-s+j)!(\alpha R)^{-(m+n-s+j+1)} \\ & \left[p_{\tau}^{\,j}F_{m+n-r+i}^{m+n-s+j}(2\alpha R) + q_{\tau}^{\,i}A_{m+n-r+i}^{m+n-s+j}(2\alpha R)\right]\Bigg\}, \end{aligned} \tag{50}$$

$$\begin{aligned} J_3(b) = {} & J_1(b) - \frac{\alpha(\alpha R)^{2m}}{n((2m)!(2n)!)^{1/2}}\sum_{\nu=0}^{2n}\frac{2n-\nu}{\nu!}(\alpha R)^{\nu} \\ & \sum_{k=0}^{\leq(m+n+\nu-1)/2}\frac{D_{2k}^{m,n+\nu-1}}{2k+1}A_{m+n+\nu-1-2p}(2\alpha R). \end{aligned} \tag{51}$$

2. $\alpha \neq \beta$

$$I = \tfrac{1}{2}\left(\frac{(\alpha R)^{2m+1}(\beta R)^{2n+1}}{(2m)!(2n)!}\right)^{1/2}\sum_{p=0}^{m+n}D_{p}^{mn}B_{p}\left(\frac{R}{2}(\alpha-\beta)\right)A_{m+n-p}\left(\frac{R}{2}(\alpha+\beta)\right), \tag{52}$$

$$K_1(b) = \frac{1}{R} + \frac{(2\alpha R)^{2m}}{(2m)!R}\left[(2\alpha R - 2m)A_{2m-1}(2\alpha R) - e^{-2\alpha R}\right], \tag{53}$$

$$\begin{aligned} K_2 = {} & K_1(b) - \frac{\alpha(\alpha R)^{2m}}{2(2m)!n}\sum_{\nu=0}^{2n}\frac{2n-\nu}{\nu!}(\beta R)^{\nu} \\ & \sum_{p=0}^{2m-1+\nu}D_{p}^{\,2m-1,\nu}B_{p}(R(\alpha-\beta))A_{2m-1+\nu-p}(R(\alpha+\beta)), \end{aligned} \tag{54}$$

$$\begin{aligned} J_1(b) = {} & \frac{1}{R}\left(\frac{(\alpha R)^{2m+1}(\beta R)^{2n+1}}{(2m)!(2n)!}\right)^{1/2} \\ & \sum_{p=0}^{m+n-1}D_{p}^{\,m,n-1}B_{p}\left(\frac{R}{2}(\alpha-\beta)\right)A_{m+n-1-p}\left(\frac{R}{2}(\alpha+\beta)\right), \end{aligned} \tag{55}$$

$$J_2 = \frac{(\alpha R)^{2m+1}(\beta R)^{2n+1}}{(2m)!(2n)!R} \sum_{r=0}^{m+n} \sum_{s=0}^{m+n} D_r^{mn} D_s^{mn}$$

$$\sum_{\tau=0}^{\infty} (2\tau + 1) G_\tau^r \left(\frac{R}{2}(\alpha - \beta)\right) G_\tau^s \left(\frac{R}{2}(\alpha - \beta)\right)$$

$$\left\{ \sum_{j=0}^{\tau} \sum_{i=0}^{\tau} p_\tau^{ij} A_{m+n-s+j}\left(\frac{R}{2}(\alpha + \beta)\right) \left[p_\tau^{ij} F_{m+n-r+i}\left(\frac{R}{2}(\alpha + \beta)\right) \right.\right.$$

$$\left. + q_\tau^{ij} A_{m+n-r+i}\left(\frac{R}{2}(\alpha + \beta)\right)\right]$$

$$- \sum_{j=0}^{\tau} \sum_{i=0}^{\tau} p_\tau^{ij} (m + n - s + j)! \left[\frac{R}{2}(\alpha + \beta)\right]^{-(m+n-s+j+1)}$$

$$\left. [p_\tau^{ij} F_{m+n-r+i}^{m+n-s+j}(R(\alpha + \beta)) + q_\tau^{ij} A_{m+n-r+i}^{m+n-s+j}(R(\alpha + \beta))] \right\}, \tag{56}$$

$$J_3(b) = J_1(b) - \frac{1}{2nR}\left(\frac{(\alpha R)^{2m+1}(\beta R)^{2m+1}}{(2m)!(2n)!}\right)^{1/2} \sum_{\nu=0}^{2n} \frac{2n - \nu}{\nu!} (\beta R)^\nu$$

$$\sum_{p=0}^{m+n-1+\nu} D_p^{m,n-1+\nu} B_p(R(\alpha - \beta)) A_{m+n-1+\nu-p}(R(\alpha + \beta)). \tag{57}$$

It is to be noted that the expression for J_2 for $\alpha \neq \beta$ involves an infinite (convergent) summation. The term at which this is to be cut off depends of course on the accuracy desired. The error involved in cutting off the expansion at the term $\tau = k$ is measured by the error in cutting off the expansion of $\mu^s e^{-(R/2)(\alpha-\beta)\mu}$ in a series of Legendre polynomials $P_\tau(\mu)$ at the kth term. From the theory of expansions in terms of orthogonal functions it follows that the root mean square error over the interval $(-1, +1)$, which results in cutting off this series at the kth term is less than that for the corresponding situation in an expansion in terms of any other polynomials, in particular in a power series. Now in the expansion

$$\mu^s e^{-(R/2)(\alpha-\beta)\mu} = \sum_{\tau=0}^{\infty} \frac{\left[\frac{R}{2}(\beta - \alpha)\right]^\tau}{\tau!} \mu^{s+\tau}$$

it is known from elementary theory that the error in the function in the range $(-1, +1)$ on cutting off at the kth term is less than

$$\frac{\left|\frac{R}{2}(\beta - \alpha)\right|^{k+1}}{(k+1)!}.$$

Consequently the magnitude of this can be taken as a rough measure of the error in the approximate expansion above, and may be helpful in determining the number of terms to keep in the series.

From Eqs. (46), (48) and (51) and the analogous equations in the second group, bearing in mind the definitions of the various functions, one can see that in most cases the following approximations may be made

$$I^2K_2 \sim I^2/R, \tag{58}$$

$$IJ_3(b) \sim IJ_1(b). \tag{59}$$

IV. Applications

It may be well to say a few words on the technique of these calculations. The most essential point is to be systematic. All the functions required should be calculated for the values of the arguments needed before beginning the lengthy summations that occur in some of the integrals. The summations should be carried out in tabular form; and it is wise to carry along the calculations for the various values of the argument simultaneously. This helps to avoid mistakes. Finally one should carry perhaps two or three more significant figures through the work than are required in the final result, because of the large number of subtractions of nearly equal quantities that occurs.

In the actual calculation again there are two different procedures depending on whether the problem is one of attraction or repulsion. In the first case what one generally desires is the equilibrium distance between the atomic nuclei, the energy at this position, and often the fundamental vibration frequency. Consequently one calculates the interaction energy for a number of values of the distance until one finds three consecutive values (fairly close together) such that the energy for the middle one is less than that for the other two. One can then assume that the energy as a function of the distance can be represented by a parabola in this region and thus determine the minimum energy and the corresponding distance R_0. If now the parabola is represented in the form

$$E = \tfrac{1}{2}k(R - R_0)^2 + E_0,$$

one can determine k and then get the fundamental frequency (in wave numbers) by the relation

$$\omega_0 = \frac{1}{2\pi c}\left(\frac{k}{M}\right)^{1/2},$$

where M is the reduced mass

$$M = \frac{M_aM_b}{M_a + M_b},$$

and c the velocity of light.

In the case of a repulsion problem, what is generally desired is a knowledge of the energy as a function of the distance. One can therefore calculate it for a number of values of the distance (choosing them so as to have the arguments of the functions among the values found in the tables in order to avoid interpolation) and make a plot. It is advisable to plot log E against the distance because of its rapid rate of change; it is generally found that this will give a curve not differing greatly from a straight line.

As illustration of the method we may consider two typical calculations:

1. Sodium molecule ($^1\Sigma$ state)

Using Slater's rule it is found that for a sodium atom the outer electron has a shielding constant of 8.8, and quantum number $n=3$, so that

$$\alpha = \frac{Z}{na_0} = 1.385 \times 10\, A^{-1}.$$

Carrying out the calculation one finds the following values for the energy ($\Delta E = W - E_0$):

αR	R(in A)	ΔE(in volts)
4.00	2.888	−0.831
4.25	3.069	. 837
4.50	3.249	.801

From these values one gets for the minimum energy $\Delta E_m = -0.84$ electron-volts, at a distance of separation $R_0 = 3.01$A. and a fundamental vibration frequency of 1.7×10^2 cm^{-1}. These compare favorably with the experimental values -1.0 ± 0.1 volts, 3.07A., and 158 cm^{-1}, as given by Loomis.[8] Incidentally, the present tendency is to consider Loomis' value for the energy as too high, about 0.8 volts being thought correct.[9] In particular Kinsey[10] finds it to be $0.85\pm.02$ volts. For comparison, it might be mentioned that the calculated energy of the triplet has values for the distances given above of +1.11, 0.78, and 0.68 volts.

At this point the question naturally arises as to what is the effect of the inner shells, the interactions of which had been neglected, on the energy. To give an accurate answer to this question would involve considerable calculation but we can set up a rough argument to indicate the order of magnitude of the energy due to the inner shells. By the latter is meant the interaction between the outer electron of each atom with the inner shell of the second, for the interaction between the two inner shells must be exceedingly small. The argument is based on the fact that the interaction between two atoms having electrons with wave functions of the form $r^{m-1}e^{-\alpha r}$ and $r^{n-1}e^{-\beta r}$ gives rise to an energy of the form $Pe^{-(\alpha+\beta)R}$ where P is a polynomial in R which changes relatively little compared to the change in the exponential for changes in R or even in the kinds of atoms. Consequently, in calculating orders of magnitude one may assume P constant. Now consider the interaction between a neon atom and an argon atom. Although such atoms have not been treated in the theory of this paper, for such a rough calculation one may assume that the repulsion will be of the same form as in the cases that have been considered. Slater's rule (which can be used here for the accuracy desired, even if this is a repulsion problem) gives for neon $Z-s=5.85$, $n=2$ (so that $\alpha=5.52\text{A}^{-1}$) and for argon $Z-s=11.25$, $n=3$ ($\beta=4.25\text{A}^{-1}$), whence

[8] Loomis, Phys. Rev. **29**, 607 (1927) and **31**, 323 (1928). See Birge, Int. Crit. Tab. V, pp. 415, 418, New York (1929).

[9] Ladenburg and Thiele, Zeits. f. Physik. Chem. **7**, 161 (1930).

[10] Kinsey, Proc. Nat. Acad. Sci. **15**, 37 (1929).

$$\Delta E \sim Pe^{-9.77R}$$

Now the kinetic theory radii for neon and argon are 1.1 and 1.3A respectively.[11] Hence a neon and an argon atom approach to about 2.4A at ordinary temperature; so that this distance corresponds to an energy of about 10^{-2} volts. For $R=3$A this gives, considering P unchanged (it certainly cannot change by more than a small factor),

$$\Delta E \sim 10^{-5} \text{ volts}.$$

Now for the interaction between the outer shell of each of two sodium atoms with the inner shell of the other for the same value of R, the energy will be different because of the different values for α and β, because the number of electrons is less (we can make a rough allowance for this by dividing the results obtained by 4) and because P is different. Neglecting the change in P which cannot be very large since the atoms are not very different in kind from the preceding, we need only to consider the change in the exponential factor. For the inner shell, Slater's rule gives $\alpha=6.47\text{A}^{-1}$, for the outer, $\beta=1.39\text{A}^{-1}$. Hence the exponential in this case is $e^{-7.86R}$ instead of $e^{-9.77R}$ as above. Taking this into account and also the decreased number of electrons

$$\Delta E \sim 10^{-3} \text{ volts}$$

which is negligible.

Admittedly this is a very rough calculation but it should serve to give the right order of magnitude. If for some reason the energy is somewhat larger than this estimate, no harm is done for it tends to balance the effect of polarization of the outer shells which has not been considered.

2. Helium atoms.

If each electron of a helium atom A has a wave function $u(a)$, then the charge at any point is given by $2u^2(a)$. If now one uses Hartree's charge distribution for helium in the range 0.5A to 2A and one assumes a simple exponential form for the wave function one finds as a good approximation

$$u = 3.20e^{-1.48r/a_0}$$

where r is measured in A. However, this wave function is not normalized; it is too low in the inner part of the atom. This can be compensated by imagining additional electron charge concentrated at the center of the atom. The exact position of the charge is not important for its effect on the result is small. The simplest way of proceeding at this point is to use the expressions for the integrals given in III modified by a appropriate factors C_a/N_a etc., as indicated there, with the exception that the terms $1/R$ are not to be changed. It can be verified that this implies neglecting a small part of the interaction between the inner portion of the wave function of one atom and the outer part of the other with respect to the integral K_2, and also it neglects the contribution of this inner part to the J_1 and J_2 integrals. But these are quite small and tend to balance each other.

[11] Rankine, Phys. Zeits. **11**, 745 (1910); Phil, Mag. **29**, 554 (1915).

Carrying out the calculation according to the theory of III, 3, one obtains the following values for the interaction energy:

αR	R(in A)	ΔE(in ergs)	Slater's value
4	1.430	6.38×10^{-13}	1.08×10^{-12}
5	1.787	1.55×10^{-13}	2.09×10^{-13}
6	2.144	3.43×10^{-14}	4.06×10^{-14}
8	2.859	1.37×10^{-15}	1.5×10^{-15}
10	3.574	4.68×10^{-17}	5.8×10^{-17}

In the last column are included for comparison the values calculated by Slater's formula[12]

$$\Delta E = 7.7 \times 10^{-10} e^{-2.43(R/a_0)}.$$

It can be seen that the order of magnitude of the two sets of results is the same and they are nearly equal in the region of 3A. It is difficult deciding which is the more correct.[13]

The writer wishes to express his indebtedness to Professor J. C. Slater and to Professor R. M. Langer for their ever helpful advice and criticism.

[12] Slater, Phys. Rev. **32,** 349 (1928).
[13] Cf. Gentile, Zeits f. Phys., **63,** 795 (1930).

LOW VELOCITY INELASTIC COLLISIONS

By Clarence Zener*
California Institute of Technology
Pasadena, California.

(Received June 1, 1931)

Abstract

The probability that a low velocity collision be inelastic is shown to depend in a relatively simple manner upon three factors: the magnitude of the change in total internal energy, ΔE; the matrix element, with respect to the initial and final states, of the interaction energy at the closest distance of approach, W_{12}; and the "time of collision," τ, a function of the relative velocity and of the sharpness of the collision. An approximation to this probability is

$$P=\left[\frac{2\pi W_{12}}{h}\tau\,(1+\epsilon_1\beta^{\epsilon_2})e^{-\epsilon_3\beta}\right]^2$$

where $\beta=2\pi\tau\Delta E/h$ and ϵ_1, ϵ_2, ϵ_3 are nearly unity, their precise values depending upon the characteristics of the particular collision.

I. Introduction

THE Born method of treating a system involving a perturbation dependent on the time has frequently been applied with success in the study of high velocity collisions. Similar success has not been met in low velocity collisions. This failure is due in part to the reluctance of modern theoretical physicists to work with classical methods even when their use is justifiable. This is illustrated by the problem of the transfer of energy between atoms. If the atoms are replaced by sets of linear oscillators, as in the dispersion theory, the classical equations give results qualitatively better than the approximate quantum mechanical treatment of Kallman and London,[1] and , in the most interesting cases, identical with the more exact quantum mechanical results of Rice.[2] Again, the author[3] has shown how to calculate the transfer of vibrational energy between molecules. His wave equations were so complex that in order to obtain numerical results crude approximations had to be made. With the introduction of classical concepts these approximations are unnecessary.

The major difficulty in a precise quantum mechanical treatment, as given by Rice and the author, occurs in operations involving the relative coordinates of the centers of gravity of the two colliding systems. But the centers of gravity may be described approximately by classical equations. In this paper it is shown how a large class of low velocity inelastic collisions may be readily treated starting from that wave equation of the internal coordinates in which the relative coordinates occur as parameters and depend upon time

* National Research Fellow

[1] Kallman and London, Zeits. f. physik. Chem B. **2,** 207 (1929).

[2] O. K. Rice, Proc. Nat. Acad. **17,** 34 (1931).

[3] C. Zener, Phy. Rev. **37,** 556 (1931).

in a manner determined by Newtonian equations. In these Newtonian equations the potential is taken to be the exact interaction potential averaged over all the internal coordinates.

II. General Theory

Let H_0 be the unperturbed Hamiltonian of the internal coordinates of the two systems, ψ_n and E_n the corresponding eigenfunctions and eigenwerte. The subscript refers to the total aggregate of internal quantum numbers. The mutual interaction V is appreciably different from zero only during a finite interval of time. Hence the transition probability, obtained by the variation of constants method, approaches a constant value at infinite time. This limiting value, representing the probability of a transition during a collision in which $n' \rightarrow n''$ is

$$P = \left| \frac{2\pi}{h} \int_{-\infty}^{\infty} V_{n'n''}\{X(t)\} e^{2\pi i t \Delta E/h} dt \right|^2. \tag{1}$$

Here $V_{n'n''}(X) = \int \psi_{n''}^* V \psi_{n'} dv$, and $\Delta E = |E_{n'} - E_{n''}|$. Let E be the constant total energy of the system. Then the relative coordinates X are to be obtained as functions of time by solving the classical equation of motion whose potential energy and total energy are $(V_{n'n'} + V_{n''n''})/2$ and $E - (E_{n'} + E_{n''})/2$ respectively. The arbitrariness of this determination of the relative coordinates increases with the differences $|V_{n'n'} - V_{n''n''}|$ and $|E_{n'} - E_{n''}|$, so that this method becomes inapplicable when these differences are large.

Let the origin of time be chosen at the moment of closest approach, so $V_{n'n''}(t)$ has the maximum value $W_{12} = V_{n'n''}(0)$. With each inelastic collision we may associate a time of collision defined as that time interval τ whose product with W_{12} is equal to the integrated value of $V_{n'n''}(t)$, i.e. $W_{12}\tau = \int_{-\infty}^{\infty} V_{n'n''}(t) dt$. We may then write

$$P = \left| \frac{2\pi W_{12}}{h} \tau S \right|^2$$

where

$$S = \frac{1}{W_{12}\tau} \int_{-\infty}^{\infty} V_1''(t) e^{2\pi i t \Delta E/h} dt$$

We see that S has the maximum value of unity when $\Delta E = 0$, and that it decreases rapidly as $2\pi \Delta E \tau / h$ becomes large. Before examining in detail the dependence of S upon ΔE, it will be interesting to review the classical concepts of energy interchange.

We consider the energy interchange between two linear oscillators A, B, with angular frequencies w_1, w_2. Let only B be initially oscillating, and let the coupling be suddenly introduced. A will start oscillating with a phase lag with respect to B. If $w_1 = w_2$, this phase difference will remain constant until all the energy of B has been given to A. The situation is then reversed, B will start oscillating with a phase lag, and gradually regain its initial energy. However, if $w_1 \neq w_2$, the phase differences will be continually changing. B will start lagging in phase before all its energy has been lost, and hence A will

never acquire all the energy of B. The maximum energy of A will decrease with increasing $|w_1-w_2|$. This maximum energy will also depend upon the strength of the coupling. Hence if this coupling changes from zero to a maximum and then to zero so gradually that its change during the time interval $1/|w_1-w_2|$ vanishes, the total energy transferred to A approaches zero. Thus increasing $|w_1-w_2|$ has the double effect of reducing the maximum energy of A and of reducing the ratio of the final energy of A to this maximum energy. To obtain a quantitative idea of these effects in actual collisions, we shall consider B to move past A with a constant velocity v and a closest distance of approach p. The coordinates of the oscillators A, B namely ξ, η are taken to be normal to the plane of p and v. Then the interaction energy $e^2\xi\eta(p^2+v^2\xi^2)^{-3/2}$ gives rise to a transfer of energy from B to A of magnitude[4]

$$\Delta w = \frac{1}{2m}\left[\frac{e^2\eta_0}{vp^2}\beta K_1(\beta)\right]^2 \backsimeq \frac{1}{2m}\left[\frac{e^2\eta_0}{vp^2}(1+\beta^{1/2})e^{-\beta}\right]^2$$

provided we may consider B as undisturbed by A. Here $\beta=(P/v)|w_1-w_2|$, η_0 is the amplitude of η, and m is the mass associated with ξ. If we now translate these classical results into quantum language by defining $P=2\pi\Delta W/hw_1$ as the probability that A become excited, and $W_{12}=e^2\xi^1{}_0\eta_0/p^3$ where $\xi^1{}_0$ is the matrix element of ξ over the normal and first excited states we obtain

$$P \backsimeq \left[\frac{2\pi W_{12}}{h}\tau(1+\beta^{1/2})e^{-\beta}\right]^2$$

where now $\tau=p/v$, $\beta=\tau|w_1-w_2|=2\pi\tau\Delta E/h$. Here we have used the quantum result that $4\pi m(\xi_0{}^1)^2w_1/h=1$. It is interesting to note that a formula identical to this is obtained from the quantum mechanics, as we should expect from the dispersion theory.

As a function of τ, P has the maximum value $(2W_{12}/\Delta E)^2$ when $\tau=\tau_0\equiv h(2\pi\Delta E)^{-1}$. In the classical picture, when $\tau=\tau_0$ the oscillators are effectively separated just before A begins to return energy to B. As τ becomes much smaller than τ_0, the systems do not remain in contact long enough for much energy to be transferred. When $\tau\gg\tau_0$, energy fluctuates many times between A and B, the maximum energy of A gradually decreasing as the systems are separated.

III. Applications

Inelastic low velocity collisions in actual experiments are too complex to solve in a straightforward manner by quantum mechanics. We must replace these collisions by simpler collisions in which irrelevant elements are omitted. But in deciding which elements are important we must use our physical intuition which is based on classical mechanics. In the previous section we found that the classical mechanics, supplemented by the quantum conditions of dispersion theory, gives results identical to the quantum mechanics in the simple collision of two linear oscillators. Moreover, we were able to interpret the

[4] This may be obtained by a method analogous to that of N. Bohr, Phil. Mag. **25**, 10 (1913).

results in terms of elementary concepts. Hence if we are able to express the probability of an inelastic collision in a form similar to that for two linear oscillators, say as

$$P = \left[\frac{2\pi W_{12}}{h}\tau(1+\epsilon_1\beta^{\epsilon_2})e^{-\epsilon_3\beta}\right]^2$$

$$\beta = \frac{2\pi\Delta E}{h}\tau$$

we shall be able to form a physical picture of the collision, and thus see why only certain factors are important.

The efficiency of an inelastic collision is usually expressed by an effective cross section, σ_{eff}. Let r_E be the closest distance of approach in a head-on collision whose relative kinetic energy is E. Then if $\sigma_{\text{eff}} > \pi r_E^2$, an approximation may be obtained by the method of Rice.[2] That closest distance of approach p_0 is found for which the transition probability is appreciable, say $\frac{1}{2}$. Then $\sigma_{\text{eff}} \cong \pi p_0^2$. This is justified since the transition probability diminishes rapidly when the closest distance of approach becomes larger than p_0. If $\sigma_{\text{eff}} \ll \pi p_0^2$, an upper limit may readily be found by calculating the transition probability P for a head-on collision. Then $\sigma_{\text{eff}} = \lambda P \pi r_E^2$, $\lambda \leqq 1$. The precise value of λ varies with different collisions, ranging from 0.1 to 0.5 for those collisions which have been examined.

When the effective cross section σ_{eff} is larger than πr_E^2, we need consider only those collisions whose closest distance of approach p is so large that the centers of gravity of the two systems may be taken to move in straight lines. If p is so large that the interaction between two atoms is essentially that of dipoles, the probability of an energy transfer between an excited and normal atom is found from (1) to be approximately

$$P = \left[\frac{2\pi W_{12}}{h}\tau(1+4\beta^{3/2})e^{-\beta}\right]^2 \tag{2}$$

$$\beta = \frac{2\pi\Delta E}{h}\tau.$$

Here $W_{12} = e^2/2p^3\ (x_1 \pm iy_1)'\ (x_2 \pm iy_2)''$, $\tau = p/v$, and ΔE as usual refers to the magnitude of the change in the total internal energy. The formula of Kallman and London[1] is essentially obtained as the special case when v is so adjusted that $\beta = 1$, Hence their σ_{eff} decreases too slowly with increasing ΔE. When ΔE is small in comparison to the relative kinetic energy of translation, and when $\beta > 1$, (2) is identical to the formula of Rice.[2] Rice's formula is less general than (2), not being defined for $0 < \beta < 1$. Substitution of numerical values shows that at room temperature unless $\Delta E < 0.01$ volt, P is very small when $p \geqq 5 \times 10^{-8}$ cm. Hence the assumptions leading to (2) are rarely justified.

Since for nearly all inelastic collisions, $\sigma_{\text{eff}} \ll \pi r_E^2$, in most cases it will be sufficient to find P only for head-on collisions, and then set $\sigma_{\text{eff}} < P\pi r_E^2$.

In a head-on collision the only relative coordinate is r, the distance between the centers of gravity of the two systems. The interaction integrals V_{ij} depend upon r approximately as

$$V_{ij} = W_{12} e^{-\alpha(r-r_E)}, \tag{3}$$

where r_E is the closest distance of approach when the relative kinetic energy is E. The approximate dependence of r upon time is found by solving the classical equation of motion in which the potential is $Ee^{-\alpha(r-r_E)}$.[5] This solution is $r - r_E = (1/\alpha) \log\{(1 + \cosh \alpha v t)/2\}$. The velocity v is defined by $\frac{1}{2}mv^2 = E$, m being the reduced mass of the system. Substitution into (1) gives

$$P = \left[\frac{2\pi W_{12}}{h} \int_{-\infty}^{\infty} \frac{2e^{2\pi i t \Delta E/h}}{1 + \cosh \alpha v t} dt\right]^2$$

Integration gives, defining $\tau = 4\,(\alpha v)^{-1}$,

$$\begin{aligned} P &= \left[\frac{2\pi W_{12}}{h} \tau \frac{\beta}{\sinh \beta}\right]^2 \\ &\leqq \left[\frac{2\pi W_{12}}{h} \tau (1 + 2\beta) e^{-\beta}\right]^2 \qquad (4) \\ \beta &= \frac{2\pi \Delta E}{h} \cdot \frac{\pi \tau}{4}. \end{aligned}$$

Eqs. (4) may be applied to that large group of collisions in which the interaction energy may be written as (3). We see that the important factors of a low velocity inelastic collision are the relative velocity, the sharpness of the interaction potential, which together determine τ, the energy resonance ΔE, and the maximum value of the matrix element of the interaction energy, W_{12}. The precise form of the interaction potential is thus not very important. With a knowledge of these three quantities we may at once obtain the magnitude of σ_{eff}.

As a numerical example, let P be the probability that in a head-on collision at room temperature an excited diatomic molecule in its first vibrational state transfer its energy of excitation to a normal diatomic molecule. Here typical values are $W_{12} \leqq 0.0005$ volts, $\tau = 2 \times 10^{-13}$ secs, and $\Delta E = 0.02$ volts, which on substitution in Eq. (4) leads to $\beta = 6$ and $P = 2 \times 10^{-5}$.

[5] For a justification of this potential, see ref. 3, also London, Zeits. f. physik. Chem. B. **11**, 237 (1930), and Kirkwood, Phys. Rev. **37**, 835 (1931)

THE PROBABILITY LAW GOVERNING IONIZATION BY ELECTRON IMPACT IN MERCURY VAPOR

By Curtis R. Haupt
Department of Physics, University of California

(Received May 18, 1931)

Abstract

Despite several attempts, the unusual type of probability law found by Lawrence to govern inelastic impacts in mercury vapor just above the ionization potential, has not been verified by other observers. His experiment, making use of a magnetic separation of the electron beam and a Faraday cylinder type of ionization chamber, has been criticized on the basis that electron reflection from the walls and other spurious wall effects might account for the results. Since no theory has predicted such a probability law it seemed important that a new investigation be launched in an attempt to prove or disprove its validity. An apparatus providing an electron beam approaching in homogeneity that of the Maxwellian distribution should make such a test readily possible. An electron-gun type of ionization tube was devised, capable of high resolving power, and eliminating the objectionable features of the Lawrence method. Using a dull emitter cathode it was found possible to approach very closely the theoretical Maxwellian velocity distribution. With this arrangement the new critical potentials of Lawrence were checked and his probability law verified within the limits of experimental error. The values of these critical potentials are: 10.6; 11.3; 11.7; and 12.1 volts. Additional ionization potentials at 12.3; 12.45; 12.85; and 13.2 volts were also found. A search for critical potentials above 13.2 volts yielded negative results. The results indicate that the failure of other experimenters to detect this probability law was due to their wide distribution of electron velocities. Since this is true, the values which they have given for the probability of ionization in this region can be considered as correct only in order of magnitude. Evidence is presented to show that these critical potentials are a result of the ionization of metastable mercury atoms, the probability law indicating either a high concentration of such excited atoms, or a large collision cross section for a metastable atom toward an ionizing collision. Data concerned with the variation of ionization current with electron current density, seem to favor such an hypothesis but is not decisive in character. When mercury vapor is admitted to the tube, the widening of the velocity distribution indicates the existence of a new type of atomic collision process. In this process the electrons lose energies of only a small fraction of a volt. These low energy losses are now being investigated together with additional evidence concerning the metastable atom hypothesis.

Introduction

THE form of the probability law governing ionization in the region just above the minimum ionization potential was first subjected to close scrutiny by Lawrence.[1] His work indicated, first, the existence of several new critical potentials for inelastic impact, lying just above the minimum ionization potential, and, second, that the probability of ionization in this range was not a continuous monotonically rising function of the electron energy as had been concluded from the results of other investigations.[2,3,4,5,6] In fact,

[1] E. O. Lawrence, Phys. Rev. **28,** 947 (1926).
[2] A. L. Hughes and E. Klein, Phys. Rev. **23,** 111 (1924); **23,** 450 (1924).

the probability of ionization was not zero at the minimum ionization potential but had a finite value, which, with increase in electron energy, decreased to a point where it took on a sudden increment at the next critical potential. There was then a further decrease with a second subsequent increment, etc.

Later these so-called ultraionization potentials were again observed by Lawrence[7] and also by Morris,[5] and by Hughes and Van Atta[8] using the ordinary total current methods, but no evidence of the peculiar type of probability law, earlier found by Lawrence, was obtained. In fact, Morris concluded from the results of his experiment, that the probability law of Lawrence must be in error and offered the alternative hypothesis that the probability of ionization was proportional to the excess of energy of the electron over the amount required to produce a given ultrastate.

The purpose of this investigation was to see whether the existence of a probability law of the type proposed by Lawrence could be verified without using his technique of magnetic separation. This was important, since, as von Hippel[9] pointed out, the Lawrence method permits the possibility of an explanation of any new critical potentials on the basis of spurious effects, such as might arise, for example, from soft x-rays or secondary electrons emitted from the walls of the ionization chamber.

The factors which prevent precise determinations of critical potentials are well known. The initial distribution of electron velocities from the heated filament cathode is the most troublesome source of uncertainty and prevents sharp breaks in the ionization curve at the points where new critical potentials make their appearance. However, computations based on the assumed validity of the Lawrence probability law and the experimental realization of a Maxwellian velocity distribution, make it evident that under such conditions, the probability function ought to be amenable to experimental test.

Apparatus

A modified form of Farnsworth electron gun[10] was chosen as a basis for the apparatus inasmuch as it had shown itself capable of producing electron beams of an unusually high degree of homogeneity. A cross sectional view of the ionization tube, with circuit diagram is shown in Fig. 1. All metal parts were of nickel. The filament used in this investigation was of the coated type noted for its low work function and was furnished through the courtesy of the Bell Telephone Laboratories. The figure indicates the manner of connecting the filament to the tungsten leads and shows that the magnetic field due to the heating current in the filament was negligible. This was substanti-

[3] K. T. Compton and C. C. Van Voorhis, Phys. Rev. **26,** 436 (1925); **27,** 724 (1926).
[4] T. J. Jones, Phys. Rev. **29,** 822 (1927).
[5] J. C. Morris, Jr., Phys. Rev. **32,** 447 (1928).
[6] W. Bleakney, Phys. Rev. **35,** 140 (1930).
[7] E. O. Lawrence, Jour. of the Frank. Inst. **204,** 91 (1927).
[8] A. L. Hughes and C. M. Van Atta, Phys. Rev. **36,** 214 (1930).
[9] A. von Hippel, Ann. d. Physik **87,** 1035 (1928).
[10] H. E. Farnsworth, Jour. Opt. Soc. of Amer. **15,** 290 (1927).

ally an equipotential source, since, with 1.2 amperes heating current, the potential drop across the filament was less than 0.05 volts. The accelerating potential was, in effect, applied at the center of the filament by a potentiometer arrangement across the filament battery.

O is a focussing cylinder provided with a tight fitting sleeve for the purpose of facilitating renewals of the filament. The end of cylinder *B*, to which the electrons were accelerated, was extended a sufficient amount in order to cover the filament and focussing cylinder. This arrangement prevented electrons from passing around the outside of the cylinder where they might strike the glass walls of the tube and give rise to troublesome electrostatic effects. Cylinders *B*, *C* and *D* served to control the velocity of the electrons as well as to collimate the beam. In order to prevent electrons from striking the metal walls and at the same time allow for the natural widening of the beam, the

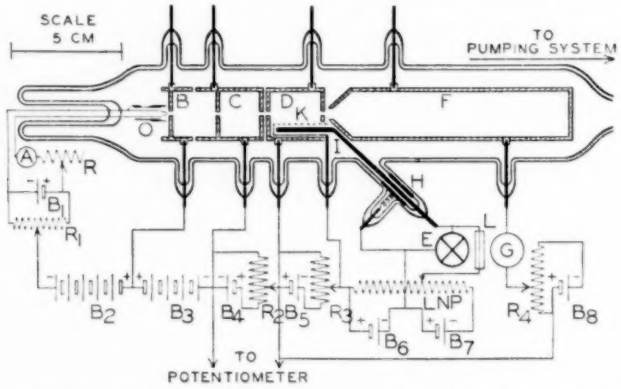

Fig. 1. Cross-sectional diagram of ionization tube showing a schematic arrangement of the electrical connections.

holes in successive cylinders were made with gradually increasing diameters. The circular opening in cylinder *B* was crossed by 10 minute nickel wires equally spaced. This made the accelerating field very uniform across the opening, and tended to prevent unfavorable modification of the velocity distribution of the emergent electrons.

It was decided to employ a Faraday cylinder to receive the electron beam inasmuch as investigations by Lawrence[11] had shown such a device to be an efficient electron absorber if its length were made sufficient to prevent reflection of slow electrons. The Faraday cylinder, *F*, was made 11 cm in length. Subsequent tests showed that it retained all entering electrons.

The usual precautions of removing occluded gases and water vapor by thoroughly outgassing the glass and metal parts, were taken.

The tube was mounted so that its axis was parallel to the lines of the earth's magnetic field. Thus there was no component of the earth's field tending to deflect the electrons from their course down the axis of the tube. In addition to this, the tube was placed at the center of a large pair of square coils. By suitably adjusting the orientation of these, and controlling the cur-

[11] E. O. Lawrence, Proc. Nat. Acad. Sci. **12,** 29 (1926).

rent through them, either the earth's field could be neutralized or they could be made to produce an axial field which would aid in defining the electron beam. Finally it was found desirable to wind a long solenoid on the outside of the tube for the same purpose.

The apparatus was kept on the pumps during all runs, the gas pressure being maintained at all times below the limits measurable on a McLeod gauge. The pressure of the mercury vapor was controlled by varying the temperature around a liquid air trap connected in the system at a point near the tube. Most of the runs were taken with a vapor pressure corresponding to a temperature of zero degrees centigrade, although some data were taken with a pressure corresponding to room temperature.

The electrometer used to measure the positive ions was of the Swann type, having a sensitivity of about 4000 mm per volt. The electron currents were detected by a Leeds and Northrup galvanometer having a sensitivity of about 2000 megohms. The potentials applied to cylinders B and C were measured by Leeds and Northrup precision voltmeters (not shown) accurate to 0.25 percent.

Experimental Method

As a rule, electrons were accelerated to B with about 15 volts velocity, retarded to C with about 5 volts velocity and given their final energy on passing into D. After colliding and producing ions in the field free space of the ionization chamber D, the electrons passed into the Faraday cylinder F, where they were collected. The positive ions formed in D, were accelerated by a small potential of a few tenths of a volt to the grid K and by a much larger potential to the ion collector I. This arrangement prevented electrons from reaching the ion collector and yet caused little distortion of the field in D. The variable accelerating potential applied to the beam as it entered the ionization chamber, was provided by battery B_4 shunted by potentiometer R_2, and its value was accurately fixed by a Leeds and Northrup potentiometer and standard cell. The method was to vary this accelerating potential in steps of 0.05 volts and to record the number of positive ions produced, as a function of this potential.

The method of measurement of the positive ion current was as follows. The collecting electrode I was attached to the free quadrant of the electrometer E and the accumulation of charge on the quadrants, was balanced by an equal and opposite current introduced by an attached india ink resistance L, of about 10^{11} ohms and a Leeds and Northrup potentiometer L. N. P. The readings of the potentiometer were then directly proportional to the positive ion current.

The velocity distribution of the electrons in the beam was determined by retarding potential measurements to the Faraday cylinder in the usual manner.

Experimental Results

Fig. 2 shows a plot of the probability law, formulated by Lawrence to explain the results of his experiments using the magnetic separation method. The equation of this probability law is:

$$P(e) = P_{e_0}\epsilon^{-10(e-e_0)/e_0} \tag{1}$$

where e is the energy of the impacting electron and e_0 is the associated critical potential. $P(e)$ is the relative probability of production of a given type of ion for an electron of energy e, and P_{e_0} is the relative maximum probability of the several types of inelastic impacts. These relative maximum probabilities together with the associated critical potentials as given by Lawrence are:

e_0	10.40	10.60	11.29	11.70
P_{e_0}	0.25	1.0	1.4	1.15

These probabilities are based on the arbitrary assignment of a probability of 1.0 to the 10.60 critical potential.

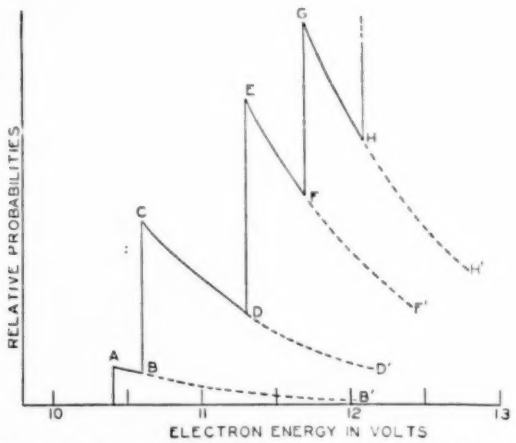

Fig. 2. Probability law of Lawrence for inelastic impacts in Hg vapor above 10.4 volts. The ordinates represent the relative probabilities of ionization of Hg vapor by electrons of energies corresponding to the abscissas. The heavy line $ABCDEF$, etc., represents the resultant ionization probability function while ABB' is the probability of 10.4 volt ionization and the ordinates between CDD' and ABB' represent the probability of ionization of the 10.60 volt type, etc.

It may be stated at the outset that no attempt was made to calculate the absolute value of the probability of production of an ion; that is, the number of ions formed per electron per unit path at unit pressure, divided by the total number of collisions made in this distance. Only relative values of the ionization probability were calculated in the present investigation.

$$P = I^+/I^- \tag{2}$$

gives the relative probability of ionization where I^+ is the positive ion current and I^- is the corresponding electron current.

Fig. 3 is typical of many ionization runs taken under the best experimental conditions. The filament was operated at a dull red heat. A current of 0.92 amperes which was passed through the magnetizing coils, produced a field of about 13 gauss which helped to collimate the beam. That the beam was exceptionally narrow is indicated by the fact that the ratio of the current

to the Faraday cylinder to that intercepted by the ionization chamber was 12.5/1 at the start of the run and at the end of the run no measurable current was intercepted by the ionization chamber. The black dots represent the experimental values of the relative probability of ionization (ordinate) as a function of the accelerating voltage between cylinders *C* and *D*. The liquid air trap controlling the pressure of the mercury in the apparatus, was maintained at 0° centigrade. At this temperature, the vapor pressure of mercury is 3.5×10^{-4} mm and the electronic mean free path is about 85 cm. The observed velocity distribution, which is about 0.7 volt in width, is only 0.3 volt wider than that estimated from the Maxwellian law for a filament burning at a dull red heat.

An examination of the experimental ionization curve *EI* indicates marked departure from the type of curves obtained by Lawrence[1] and Morris.[5] There

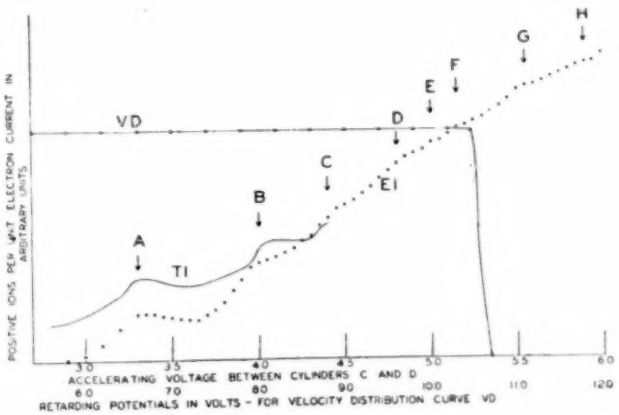

Fig. 3. The ordinates of *VD* are the electron currents entering the Faraday cylinder corresponding to the retarding potentials represented by the abscissas. The ordinates of *EI* record relative values of the ionization as a function of the accelerating potential applied to the ionization chamber, *D*. Curve *TI* is an ionization curve theoretically calculated from the velocity distribution assuming a succession of distinct types of ionization having the critical potentials 10.40, 10.60, 11.29 and 11.70 volts respectively, and the probability law plotted in Fig. 2. New critical potentials are indicated by the arrows, *E*, *F*, *G* and *H*.

is a very pronounced critical potential at the point indicated by the arrow *A*, another at *B* and less conspicuous potentials at *C*, *D*, etc. It seemed very evident from the contour of the ionization curve that a probability law of the type proposed by Lawrence, must be operative. The slope of the curve just beyond *A* actually passes through zero and becomes negative and again passes through zero. It was therefore decided to test the Lawrence probability law by computing the theoretical ionization curve from the measured velocity distribution, making use of Eq. (1). The results are shown by the solid curve *TI*. The ordinate scale for this graph has been displaced one unit in the positive direction in order to facilitate comparison with the curve *EI*. The agreement can be considered quite good for an experiment carried on

under conditions entirely different from those of the magnetic analysis method of Lawrence, and lends strong support to his law. The fit of the two curves is especially close over the region of the first ultraionization potential (point A) as would be expected since the separation of the latter from adjacent critical potentials is relatively great and any influences due to local experimental conditions would be noticeable to a less degree. That the agreement is not better may largely be attributed to the experimentally observed fact that the velocity distribution does not remain constant as the equivalent energy of the electrons is changed. No account can be taken of such variations in computing the theoretical ionization curve. The graphical methods of differentiation and integration used in obtaining TI involve approximations which are, of course, possible sources of error in computing the theoretical curve. The curve TI is not continued over the entire region covered by EI for the reason that Lawrence assigned values of the probability coefficients P_{e_0} only for the first three of the ultra-ionization potentials. Beyond the point where TI ends, the critical potential at D and higher ones begin to contribute to the number of positive ions so that to continue the curve farther would lead to erroneous conclusions. The critical potentials beyond C are not resolved sufficiently well to enable the assignment of values of the corresponding probability coefficients with any degree of certainty. It is evident however, from considerations of their separation and the velocity distribution that the probability coefficients are of the same order of magnitude as those of A, B and C.

The proper point at which to locate a critical potential on an ionization curve has always been a moot question. Some writers argue that the proper method is to draw tangents to the curve on either side of the break point, the intersection of these two tangents giving the location of the critical potential. Others take the point of inflection where the slope goes through a maximum and some assign the critical potential to the point of inflection where the slope goes through a minimum. It seems that the proper criterion to use will depend upon the probability law which is operative in a given case together with the velocity distribution of the electrons. If one is dealing with a probability law of the kind given by Lawrence, and if one has a very narrow distribution of velocities, the second method certainly is the proper one to employ. The number of ions formed will be governed largely by the velocities of a narrow band of electrons lying near the point of inflection of the distribution curve. The slower and faster electrons on either side of this band being relatively few in number cannot contribute greatly to the ionization current. Just as the given critical potential is passed, there is a great decrease in the probability of production of the ion, which makes itself evident in the ionization curve by a decrease in slope. Thus it appears that this decrease in slope should be the most logical point to designate as the critical potential. It is on this basis that the points A, B, C, D etc., have been located. The shape of the computed theoretical curve TI indicates that this procedure is justified for the point where a new inelastic impact occurs is precisely the point where the theoretical curve shows a decrease in slope.

The values of the critical potentials observed, are: 10.60 (assumed), 11.30, 11.70, 12.10, 12.30, 12.45, 12.85 and 13.20 volts, designated by the letters *A*, *B*, *C*, *D*, *E*, *F*, *G*, and *H* respectively. That these are the correct assignments is attested both by the agreement of the computed probability curve *TI*, and by the fact that the separation of the critical potentials was the correct amount to agree with the values given by Lawrence. The last four mentioned critical potentials are new. Ionization of the normal mercury atom begins, of course, at 10.4 volts. This point is not indicated in Fig. 3 but would be at 3.1 on the abscissa scale of curve *EI* in the graph. That part of the ionization curve to the left of this point is due to the faster components of the velocity distribution in the electron beam. Since numerous runs have checked these ionization potentials, it is strongly felt that, even though the changes in slope are small in some cases, they are genuine ultra-ionization potentials. It must be pointed out also that the data are more accurate than can be shown on a graph of such small dimensions, and if the readings were plotted on a scale consistent with the precision with which the values are known, these potentials would be much more evident.

The ionization probability curve beyond 13.3 volts has been explored only casually but no evidence of additional critical potentials was noted. However, there may be many more ionization potentials in this region which are closer together and cannot be resolved with this apparatus.

Errors

There are several possible sources of error which might influence the results in this experiment and a discussion of their significance is given below.

Contact electromotive forces

These may be of two kinds, (1) contact potentials between the electron stream and various electrodes and (2) contact potentials varying over the surface of a single electrode. The first type prevents a precise calculation of any critical potential from the accelerating and retarding potentials involved. Otherwise they do no harm unless they show variations during the course of a run. Such contact potentials were always present in these experiments. Contact potentials of the type (2) are very serious if present to any appreciable degree. They prevent the collisions from taking place in a field free space, making entirely uncertain, the energy exchanges involved. The high degree of uniformity in the results secured over a long interval of time indicates that contact e.m.f's of the first type were constant and that errors due to the second type were negligible.

Diffusion of positive ions

The presence of a sheath of positive ions in the neighborhood of the filament due to the accelerating potential applied to cylinder *B* tended to neutralize the space charge and to favorably increase the electron emission. It is important, however, to know whether any of these were accelerated into the ionization chamber by the retarding potentials applied to the electron beam. This was tested by varying the initial accelerating potential from

about 10 to 20 volts, keeping the equivalent energy of the electron beam entering D, at a value just below the ionization potential. It was found that no positive ions were collected in the ionization chamber when the initial accelerating potential was below 15 volts.

Photoelectrons

The ejection of photoelectrons from the ion collector, I, by radiation from excited atoms was reduced to insignificant proportions by making the collector of very small area. Also it was partially shielded by the surrounding grid K so that it could intercept but very little of the total radiation. That the currents measured were really positive ion currents, was demonstrated by making K slightly positive with respect to D, which caused the current intercepted by I to drop to zero.

Uniformity of field in ionization chamber

That saturation current was measured was apparent from the fact that the positive ion current remained unchanged as the potential applied between the grid K and the ionization chamber was changed from 0.05 to 1.0 volts. No reduction of the electron current to the Faraday cylinder could be detected when the small potential of 0.3 volts, ordinarily used to draw out the positive ions, was applied to the grid K.

Multiple collisions

In all cases, the mercury vapor pressure was kept so low that the electron mean free path was many times greater than the length of the ionization chamber. Even in the runs made at room temperature (25°C) the vapor pressure is 0.00184 mm and the mean free path about 9 cm. Under these conditions, therefore, multiple collisions could not have contributed to the effects observed.

Wall effects

These were rendered insignificant by designing the apparatus in such a way that the electron current intercepted by the walls of the ionization chamber was but a very small fraction of the total current intercepted by the ionization chamber. Since, in these cases, the ultraionization potentials were present with the same degree of prominence as in any data obtained, it is certain that von Hippel's suggested explanation of these phenomena on the basis of the production of secondary electrons, soft x-rays or photoelectrons, must be regarded as untenable. However, in order to further test this point, some runs were made with a magnetic field applied in such a direction and magnitude as to deflect the entire electron beam to the walls of the ionization chamber. If these ionization potentials were critical wall potentials, one should expect them to appear with unmistakable clarity under these more favorable conditions. Instead there was found but a slight suggestion of the 10.6 volts ionization potential and a faint trace of the 11.3 volt potential. This data must be regarded as giving strong support to the idea that these new potentials are genuine critical potentials of the mercury atom. The presence of the fine wire grid across the opening of the first cylinder undoubtedly gave

rise to some slow secondary electrons in the beam. These, however, were included in the measured velocity distribution to the Faraday cylinder, *F*.

Careful attention to circuit arrangements and details of technique tended to minimize experimental errors. Individual storage battery sources of potential were used in the different parts of the circuit. Each reading of the potential between cylinders *C* and *D* was checked against a standard cell. Since the values of the positive ion current could be taken in any order desired without altering the results, it is assumed that the experimental conditions were entirely satisfactory.

The values of the critical potentials given in this work are all based on the assignment by Lawrence of the 10.60 volt critical potential which has itself, a probable error of 0.2 percent. The first three ultraionization potentials recorded above, are probably correct to 0.5 percent and the others to 0.8 percent. These values are assigned from a consideration of the details of the experimental method, reproducibility of results, etc.

Discussion of Results

As regards any attempts to explain the origin of these effects, it should be noted at the outset that the experimental method precludes any interpretation which does not regard them as genuine critical potentials of the mercury atom. Among the more likely hypotheses which have been offered were those of Lawrence[1] who suggested that they might involve ejection of one electron in the usual manner and the simultaneous removal of another electron to a higher energy state, or that they might be critical potentials of the molecule and identified with energy levels associated with band spectra. To test the first hypothesis, one must turn to the spectrum of normal and ionized mercury. The removal of one of the optical electrons from the lowest level 1^1S_0 to infinity requires, of course, 10.39 volts. To raise the other from the lowest level 1^2S to the next higher level (a metastable level $^2D_3$) in the ionized atom would require 4.38 volts.[12] Thus the minimum amount of energy required to carry through a process such as this, would be 14.77 volts. Since the electron beams in these experiments were all of energies less than this amount, this hypothesis must be rejected.

The second explanation must be regarded as equally unlikely. Both on theoretical and experimental grounds, the relative concentration of molecules to atoms, at room temperature for instance, would be very small. The heat of dissociation of the mercury molecule is but slightly larger than the mean kinetic energy of a molecule at room temperature, which would prevent any appreciable concentration of molecules. However, in order to test this point, Morris[5] tried his experiment in superheated vapor at higher temperatures. On account of the low heat of dissociation, a slight increase in temperature should greatly decrease the relative concentration of molecules to atoms, and curves taken at higher temperatures should show critical potentials of molecular origin less prominently. No such effect was observed in the case of the ultraionizing potentials.

[12] F. Paschen, Akademie der Wissenschaften Berlin, Sitzungsberichte, **2**, 541-(1928).

Von Hippel[9] has suggested that these ultraionization potentials may be due to the ionization of metastable mercury atoms. It is possible and perhaps probable that on collision with a metastable atom an electron might ionize the atom by ejecting the metastable electron and utilize any additional energy in raising the other optical electron from its lowest level to any of the possible higher levels as obtained from the mercury spark spectrum.

Assume that we have a mercury atom with one valence electron in the normal 1^1S_0 state and the other in the metastable 2^3P_2 state. The energy required to ionize the atom by removing to infinity the metastable electron, would be 4.94 volts. The energy required to raise the other electron from its lowest level 1^2S to 2^2P_1 (which is a highly probable transition) would be 6.35 volts. If we add these two numbers to ascertain the energy required to cause both transitions to occur, we obtain 11.29 volts which is precisely the value of one of the ultraionization potentials as given by Lawrence. Other possible transitions are:

	Energy required
$2^3P_2 \rightarrow \infty + 1^2S \rightarrow 2^2P_2$	12.42 volts
$2^3P_0 \rightarrow \infty + 1^2S \rightarrow 2^2P_1$	12.09 volts
$2^3P_0 \rightarrow \infty + 1^2S \rightarrow 2^2P_2$	13.22 volts.

These values correspond within experimental error to four critical potentials which have been found in this and in previous work. The close numerical agreement between the observed and calculated values lends considerable support to an explanation of the critical potentials on this basis. Of course transitions might occur to higher terms than 2^2P_2 in the spark spectrum. The difficulty in resolving these closely spaced terms, together with the decreased probabilities of transitions to such levels probably accounts for their not having been observed.

The proposed hypothesis is, admittedly weakened by the fact that the same explanation will not serve for all of the critical potentials observed. However it is not inconceivable that two different types of phenomena might be operative in giving the same kind of experimental effect. There are four observed potentials which do not fit in with a metastable atom scheme. Professor J. R. Oppenheimer has suggested, in a private conversation, that they might be due to an Auger effect in the mercury atom, that is, to processes involving excitation without ionization, spontaneous ionization occurring later, with or without a collision of the second kind.

A further test of the metastable atom hypothesis is possible from measurements of the positive ion current as a function of the electron current density in the tube. The rate of formation of metastable atoms is proportional to the density of the electron beam. Thus if the rate of disappearance of metastable atoms is constant, their concentration would be proportional to the current density. Since the number of impacts between electrons and atoms is proportional to the current density, the number of positive ions formed by impacts with metastable atoms should increase as the square of the current density. Fig. 4 shows some curves which were taken to test this point.

It is seen that the positive ion current is approximately proportional to the electron current in a range varying from 10 to 20 on the ordinate scale. This linearity cannot be said to favor the metastable atom hypothesis. At greater current densities there is a marked departure from the straight line in the direction to be expected if a secondary effect were playing a role. This deviation cannot be attributed to space charge effects, since the maximum electron current to the Faraday cylinder was only on the order of 10^{-8} amperes. Thus we can only account for this turning by assuming some secondary effect such as the metastable atom hypothesis mentioned above. If this is the true state of affairs, it is evident that the experimental conditions will greatly affect the concentration of metastable atoms and therefore the observed results. Thus the complete lack of agreement among various observers who have tested the probability law in mercury, becomes understandable.

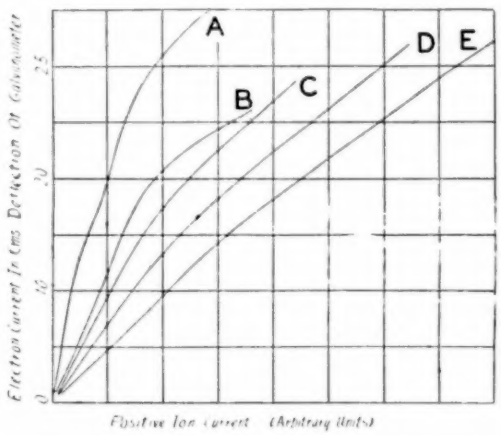

Fig. 4. The positive ion current as a function of the electron current density in the ionization chamber (ordinate scale). Curves *A*, *B*, *C*, *D* and *E* are taken for electron impact energies of 10.40, 10.60, 11.30, 11.70 and 12.10 volts respectively.

The double curvature exhibited by curve *A* near the ordinate 20, is interesting and can be explained as follows. This curve was taken for equivalent electron energies slightly above 10.4 volts. At this point the velocity distribution of the electron beam overlaps the 10.4 volt critical potential so that only part of the electron beam has sufficient energy for ionization. In the region from 0 to 17 on the ordinate scale the width of the velocity distribution remains nearly constant so that about the same fraction of the total number of electrons are producing positive ions in all cases. With increasing current density, the velocity distribution rapidly widens so that a greater relative proportion of the total number of electrons are now too slow to ionize and the rate of production of positive ions shows a decrease. At still higher current densities the curve again reverses itself showing that the velocity distribution becomes more nearly constant and secondary effects begin to predominate.

Thus the evidence secured, while not decisive, cannot be said to rule out the possibility of an explanation on the basis of metastable atoms. It must be

remembered that diffusion may play an important role in determining the number of metastable atoms present in the ionization chamber at any time. If it should be true that for low current densities, a much greater number of metastable atoms are diffusing in from outside regions than are being formed in the ionization chamber itself while at higher current densities the reverse is the case, then the straight portions of the curves of Fig. 4 would be explained. The number of metastable atoms present is also dependent on their rate of disappearance as well as on their rate of formation, and one cannot be certain that this rate of disappearance is constant. The strongest argument against a metastable atom hypothesis is the fact that there would be required either a very large concentration of such atoms or that the collision cross section of a metastable atom toward an ionizing collision should be very great in order to account for the magnitude of the effects observed. Indeed, inasmuch as the metastable atoms are neutralized on striking the walls, it is difficult to see how a sufficiently large concentration of metastable atoms could exist at these low pressures in the ionization chamber. Couliette[13] showed that metastable atoms of mercury diffuse thru mercury as if the effective radius of the metastable atom is 1.5 times that of the normal atom. This is in line with the above requirement.

Professor J. R. Oppenheimer, in a private conversation, has also pointed out that on this hypothesis, one should expect ionization potentials to be found at 4.94 and 5.74 volts, corresponding to simple ionization of the mercury atom. That such potentials have never been reported, may be due to the possible inefficient production of metastable atoms at those energies.

Various types of experiments have been devised to measure the energy lost by an electron on making inelastic collisions with atoms. Foard[14] working with mercury vapor, utilized the most elaborate apparatus for this purpose. He observed but one energy loss in the region covered by these ultraionizing potentials, namely that at 11.07 volts. He attributed this to a double electron jump of some sort. His wide distribution of velocities, 1.6 volts, would have prevented him from observing energy losses corresponding to these ultraionizing potentials. In fact, the existence of a single loss at 11.07 volts is questionable. It is more likely due to the superposition of several energy losses which lie in the region covered by his velocity distribution.

Several investigators,[15,16,17,18] have recently reported the observation of a series of ultraionization potentials in mercury, covering the region of this investigation. There is, in general, good agreement in the measurements reported, and those of the present investigation. However Smith reports about twice the number of critical potentials observed by the writer while Hughes and Van Atta and Nielsen and Potter report several that have not

[13] J. S. Couliette, Phys. Rev. **32,** 636 (1928).
[14] C. W. Foard, Phys. Rev. **35,** 1187 (1930).
[15] A. L. Hughes and C. M. Van Atta, Phys. Rev. **36,** 214 (1930).
[16] P. T. Smith, 166th Meeting of the American Physical Society, Phys. Rev. **37,** 808 (1931).
[17] W. M. Nielsen and R. D. Potter, Journal of the Elisha Scientific Soc. **44,** 31 (1928).
[18] W. M. Nielsen, Phys. Rev. **37,** 87 (1931).

been found in the present work. The reason why these several experiments differ so widely in the number of ionization potentials found, does not seem clear. Of these investigations, at least the first two showed no evidence of the Lawrence probability law but merely exhibited the ionization potentials as slight changes in slope of the ionization curve. The discrepancy in this regard, between the results of Smith and Hughes and those of the present work possibly may be due to a wider distribution of velocities in the electron beam in their experiments. Of course this possibility cannot be determined, since in their experiments, the distribution of velocities was not measured. The great difficulty the author had in obtaining a narrow distribution of velocities makes him feel that it is not very unlikely that Smith and Hughes and Van Atta did have a wider distribution of velocities than they thought. According to information received in a private communication from Nielsen, his experiment gave a qualitative evidence of a probability law of the Lawrence type. He observed a decrease in the number of positive ions with increasing electron energy at several of the critical potentials. Unfortunately the nature of his apparatus prevented a measurement of the electron velocity distribution so that he was not able to investigate the probability law operative.

The extreme difficulty in securing very narrow distributions of velocity in ionization experiments can be appreciated only by those who have worked in the field. The underlying causes of this difficulty appear not to have been generally recognized but became apparent to the writer during the course of a series of tests on the velocity distribution under varying conditions of mercury vapor pressure. When the mercury vapor was completely removed from the tube by using liquid air on the control trap, the range of velocities in the beam entering the Faraday cylinder immediately narrowed to that of the theoretical Maxwellian distribution. However, as soon as a slight amount of mercury vapor was admitted, the width of the distribution increased by about 0.2 volts. This can only be due to a series of inelastic collisions in which the electrons lose amounts of energy on the order of one or two tenths of a volt. This rather surprising conclusion has been confirmed by the writer by observation of a number of energy losses of this order of magnitude in the electron stream.

Further tests of the metastable atom hypothesis as well as detailed quantitative studies of these newly discovered low energy losses are now being made by the writer at the Physical Laboratories of Pomona College.

The writer desires to express his thanks to the Bell Telephone Laboratories who kindly lent the special filament wire used in this investigation; also to Mr. W. R. Stamper, instrument maker at the University of California Physical Laboratories and to Mr. L. B. Clark for his skill in performing an unusually difficult piece of glass blowing and to other members of the Department of Physics for their timely suggestions. Finally, the writer is happy to acknowledge his indebtedness to Professor E. O. Lawrence, who initiated the problem and who has maintained a constant and stimulating interest in the work since its beginning.

ON THE TEMPERATURE OF CATHODE IN VACUUM ARC

By R. Tanberg* and W. E. Berkey
Research Laboratories, Westinghouse Elec. and Mfg. Co., East Pittsburgh

(Received May 25, 1931)

Abstract

Pyrometric and spectroscopic tests show that the metal cathode spot in a vacuum arc is not at an extremely high temperature. The temperature of a copper cathode is measured by an optical pyrometer and found to be about 3000°K in a 20 ampere arc. Spectroscopic examination of the cathode spot shows only a faint continuous spectrum indicating that the temperature of the cathode is not high. A temperature of the above magnitude is shown to be sufficient to give the rate of vaporization required to account for observed loss of cathode material under extreme assumptions. The results show that the high speed of the vapor stream issuing from the cathode region cannot be due to high temperature of the cathode itself.

Introduction

ONE of the authors[1] has previously determined the average velocity of the vapor emitted from the copper cathode in a high vacuum arc. Calculations were based upon (1) the observed force of reaction on the cathode, with the loss in weight of the cathode, (2) the force of reaction upon a vane suspended 2 cm in front of the cathode with the increase in weight of the vane. Both methods gave mean velocities around 10^6 cm/sec. In order to emphasize the magnitude of this velocity the transformation was made into equivalent gas temperature by the equation $\frac{1}{2}\, mv^2 = 3/2\, KT$. The astounding values of 500,000°K resulted from this calculation.

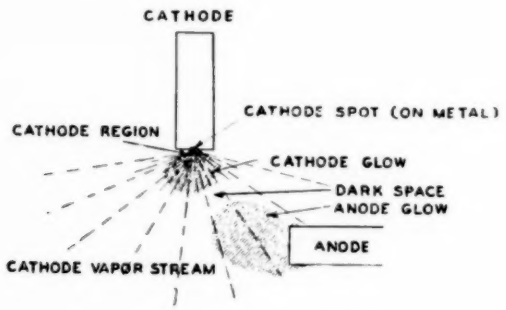

Fig. 1. Nomenclature of vacuum arc.

Recently Dr. K. T. Compton[2] has suggested a mechanism to account for the force of reaction upon the cathode. By means of an accommodation coefficient the incoming copper ions are neutralized at the cathode, but still

* R. Tanberg (Now of Drammen, Norway).
[1] R. Tanberg, Phys. Rev. **35,** 1080–1089 (1930).
[2] K. T. Compton, Phys. Rev. **36,** 706–708 (1930).

retain a fraction of their kinetic energy. These neutralized ions then rebound from the cathode with a random distribution of velocity forming the vapor stream.

Dr. J. Slepian and R. C. Mason[3] have pointed out that while Compton's theory may account for the reaction of the cathode, it does not account for the high speed of the vapor leaving the cathode region.

It is the purpose of this paper to show that the observed high mean velocity of the copper vapor cannot be due to temperature of the metal cathode spot itself.

In order to avoid misinterpretation of terms used, a nomenclature of the vacuum arc is shown in Fig. 1 and will be followed throughout this paper.

A. Distribution of Light in Vacuum Arc

Visual observation of the cathode region of an arc in vacuum reveals a high luminosity on the surface of the cathode, giving the impression that the

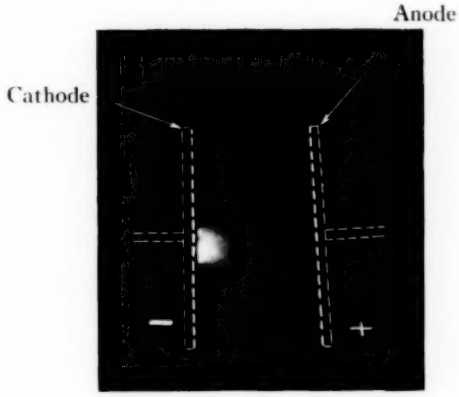

Fig. 2. Low voltage form of 7 amp. D.C. arc between copper plates. The cathode spot moved during the exposure which makes the glow at the cathode surface appear much broader than actually was the case.

the metal surface is incandescent at an extremely high temperature. However, a photographic cross section of the arc, shown in Fig. 2, indicates that the major portion of light comes from a comparatively small region close to the cathode. The light intensity outside this region falls off rapidly to no visible radiation in the dark space. Therefore the real location of the high energy indicated by the cathode vapor speed[1] may not be in the cathode spot on the metal, but more probably in a thin layer of gas immediately in front of the cathode spot.

B. Spectrographic Observations of Arc Cathode

A series of spectrograms were taken of the various portions of arc, with a small Hilger Constant Deviation Spectrograph, Model D. The experimental arrangement is shown in Fig. 3.

[3] J. Slepian and R. C. Mason, Phys. Rev. **37,** 779 (1931).

An observation of the spectrum in the visible region from the copper cathode, shows a faint continuous spectrum upon which high intensity emission lines are superimposed. When the cathode is moved to one side so that the cathode spot no longer faces directly into the slit both the continuous and line spectra vanish.

Many years ago J. Stark[4] made a similar observation on the cathode of a mercury arc. His results showed a continuous spectrum when the cathode spot faced directly into the spectroscope and a line spectrum when the slit was faced just outside the cathode spot. His conclusion was that the actual mercury which was acting as the cathode base was at a yellow or white heat.

A three mil copper wire was placed in vacuum and gradually heated by passing current through it .Just before the wire melted the continuous spectrum was about the same intensity as the continuous spectrum in the vacuum arc.

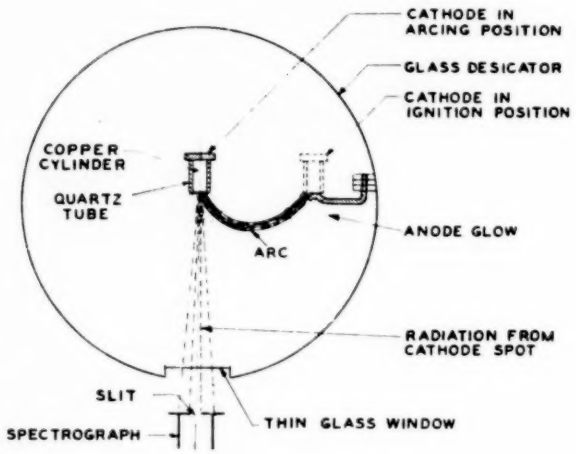

Fig. 3. Arrangement for spectrograms of cathode spot. Cathode was mounted on arm which extended to the outside through flexible bellows.

There may be some reason to believe the continuous spectrum from the cathode spot is due to emission of electrons or neutralization of ions at the cathode surface. But, due to the fact that the arc is drawn in a vacuum of 10^{-4} mm Hg, and that the arc is never held longer than 5 seconds, it seems improbable that the density of copper molecules could be great enough to account for the continuous spectrum.

Fig. 4a is a spectrogram of the high intensity lines from the cathode spot. The continuous spectrum is so weak that it does not show on the plate. Fig. 4b is the reference copper arc at atmospheric pressure, while 4c shows the emission lines of the anode glow. The presence of iron lines in Fig. 4a is probably due to impurities in the copper cathode. The strong mercury lines in the anode glow may be accounted for by mercury distilling over from the pumps.

[4] J. Stark, Phys. Zeits. **5,** 550 (1904).

The Fig. 4c shows that the anode glow exists primarily in the residual gases of the arcing chamber, and that the cathode vapor under the condition

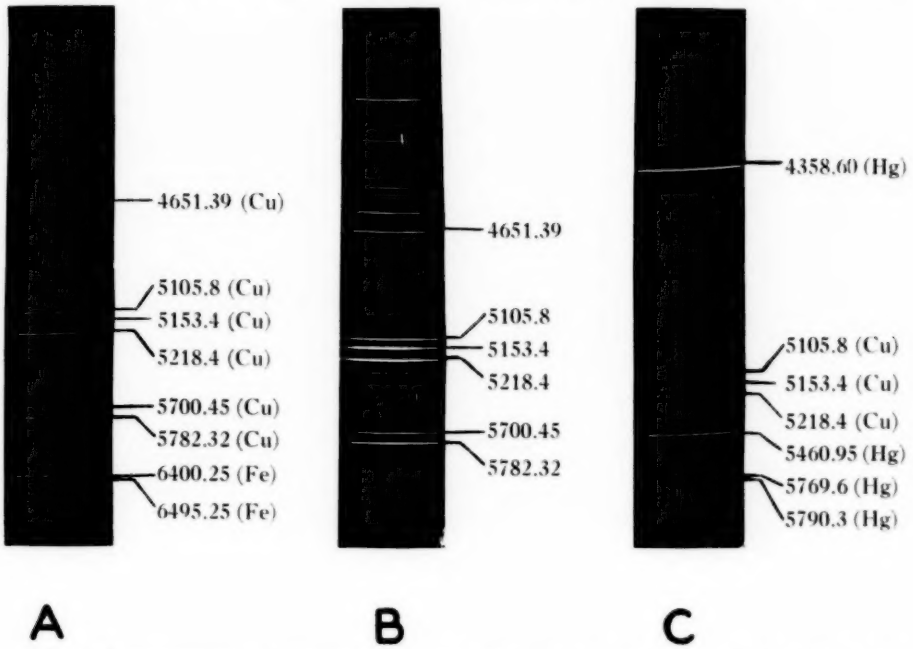

Fig. 4. Spectrograms of vacuum arc. A, cathode spot, vacuum arc between copper electrodes. B, copper arc, atmospheric pressure. C, anode glow, vacuum arc between copper electrodes.

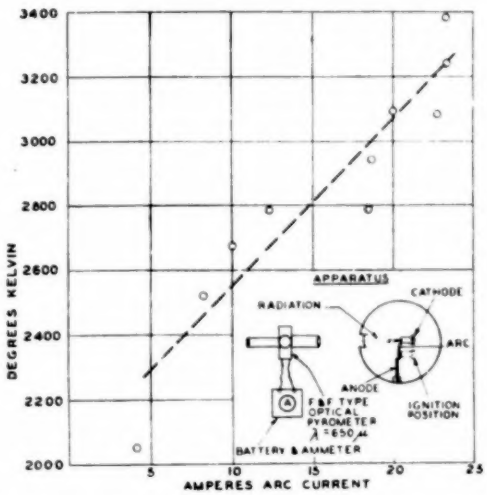

Fig. 5. Apparent temperature—arc current curve. Temperature by optical pyrometer. Emissivity, 0.15.

considered here does not directly sustain the arc in the region next to the anode.

C. Apparent Temperature of Cathode Spot by Optical Pyrometer

An optical pyrometer* F and F Type ($\lambda = 0.650\mu$) was set up as shown in in Fig. 5. This pyrometer was a constant filament current-variable wedge absorption type and calibrated in degrees centigrade against a standard lamp.

Fig. 5 shows the apparent temperature of the cathode spot as a function of the arc current after corrections have been made for an emissivity of 0.15, constant glass absorption of 50°K, and a linear correction for the copper deposit on the glass window. The maximum total correction was 800° and the minimum 379°. The maximum correction for the copper deposit was 250° and the minimum 25°.

Just what temperature the optical pyrometer measures at the cathode of an arc is questionable. The Brown-Boveri Company[5] has measured the temperature of the cathode spot in a mercury arc rectifier as being 2087 ± 25°C, by an optical pyrometer in a similar arrangement. However, they used a green filter and as there are several green emission lines in the mercury spectrum, their results may not be accurate. Other investigators[6] place the temperature of the cathode spot at 500°C in a mercury arc.

It seems unlikely that the temperature of the cathode spot is higher than the temperature measured by the optical pyrometer.

D. Vaporization of the Cathode

The current density at the cathode of a vacuum arc was determined by passing the arc over a highly polished cathode surface. A cross section of the arc path was selected and the width of individual trails measured by a cathotometer. A current density of 14,000 amperes per cm² was found, assuming the cathode spot to be circular. Fig. 6 shows the observed total rate of vaporization plotted against the arc current for a copper cathode. Assuming a current density of 14,000 amps/cm² a constant value of 0.21 grams/cm²/sec is found.

An equation is developed by Jones, Langmuir and Mackay[7] which gives the relation between the absolute temperature and the rate of vaporization of a metal in vacuum. Fig. 7 is plotted from their Eq. (22), namely,

$$\log_{10} M = \frac{A}{C} - \frac{\lambda_0 + E}{CT} - \frac{B}{C} \log_{10} T - \frac{DT}{C} \qquad (1)$$

where M = mass of metal evaporated per cm² per sec.

$A = 44{,}638$ for copper
$C = 4.577$ " "
$E = 370$ " "
$B = 3.126$ " "
$D = 0.0008$ " "

* Optical Pyrometer built by Scientific Materials Company. Distributed by Fisher Scientific Company.

[5] Brown Boveri Mitteilungen **16,** 61 (1929).

[6] E. Luebcke, Zeits. f. Tech. Physik **12,** 598, 603 (1929).

[7] Jones, Langmuir and Mackay, Phys. Rev. **30,** 201 (1927).

$\lambda_0 = 82{,}060$ " " = latent heat of vaporization per gram atom of metal at absolute zero.

T = absolute temperature.

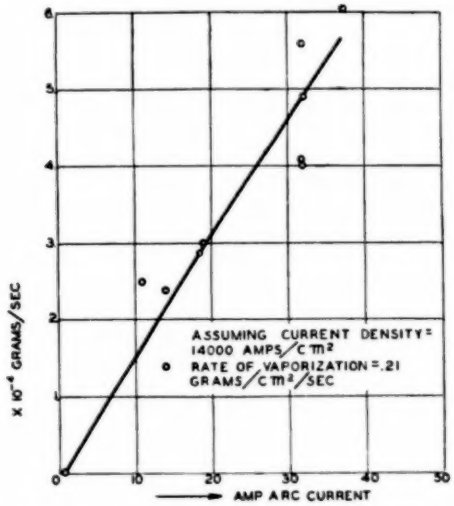

Fig. 6. Vaporization of copper cathode by arc in vacuum.

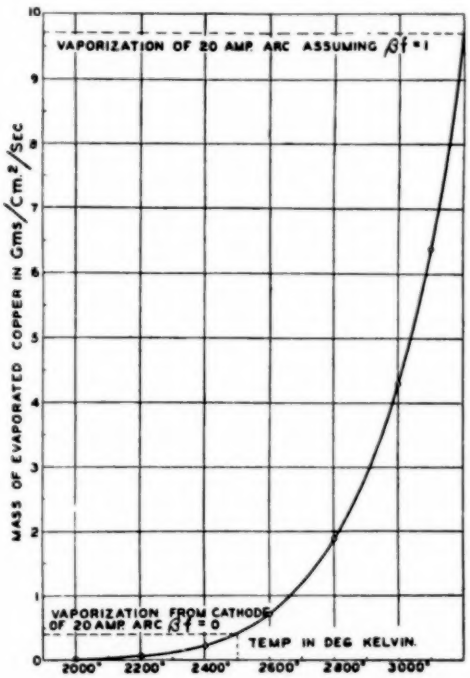

Fig. 7. Rate of vaporization as function of absolute temperature. Plotted from Eq. (22) Phys. Rev. 30, 210, Jones, Langmuir and Mackay.

If the measured rate of vaporization (0.21 gm/cm²/sec) based upon a current density of 14,000 amps/cm², represents the total vaporization at the

cathode, then a temperature of 2400°K is found from Fig. 7. However, this measured rate of vaporization may not be the total vaporization rate at the cathode spot.

If there exists a high energy region in the gas just outside the cathode spot, then a molecule emitted from the cathode spot will have a kinetic energy corresponding to the temperature of the cathode spot, until it reaches this cathode region. In the cathode region the molecule is so highly energized that its original kinetic energy is negligible compared to its kinetic energy in the cathode region. The velocity of thermal agitation is so great in the cathode region that the vapor molecules will be emitted in all directions according to their random motion.

Let m_1 = rate of vapor returning to the cathode from the cathode region and m_2 = net rate of loss of vapor away from the cathode. In Fig. 8 this condition is shown graphically.

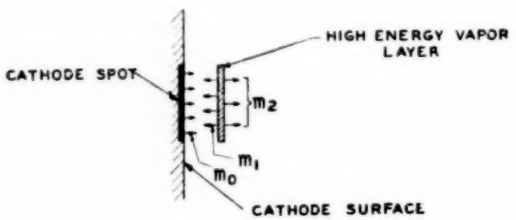

Fig. 8.

As an approximation it is initially assumed that $m_1 = m_2$ because the total surface of the cathode is large compared to the actual area of the cathode spot and the high temperature gas layer is very close to the cathode spot.

It then follows that $m_0 = m_1 + m_2$ where m_0 is the total rate of vaporization at the cathode. The measured rate of loss of cathode material is then $\frac{1}{2}$ the total rate, that is,

$$m_0 = 2m_2 \ . \tag{2}$$

Based upon this reasoning the actual rate of vaporization is 0.42 gm per cm^2 per sec, and the temperature of the cathode spot is 2500°K.

In the above discussion no account was taken of the part the positive ions play at the cathode. A modification of the above theory was suggested by R. C. Mason.

Let αm_0 = fraction of copper vapor which is ionized before it is permanently lost or returned to the cathode. After the arc has reached equilibrium

$$\alpha m_0 = n_+ \tag{3}$$

where n_+ is the number of positive ions returning to the cathode.

The copper vapor lost per second which constitutes the vapor stream previously mentioned is

$$m_2' = \tfrac{1}{2}(1 - \alpha)m_0 \tag{4}$$

while

$$m_1' = \alpha m_0 + \tfrac{1}{2}(1 - \alpha)m_0 \tag{5}$$

where m_2' is the net rate at which the vapor is lost and m_1' is the rate at which copper is returned to the cathode.

$$m_0 = \frac{2m_2'}{1-\alpha} \tag{6}$$

but

$$\alpha = \frac{n_+}{m_0}$$

therefore

$$2m_2' = m_0\left(1 - \frac{n_+}{m_0}\right) = m_0 - n_+$$

$$m_0 = 2m_2' + n_+. \tag{7}$$

If, however, there is an accommodation coefficient as suggested by K. T. Compton[2] not all the positive ions may be condensed. If β is the fraction of the positive ions actually condensed then

$$m_0 = 2m_2' + \beta n_+ \tag{8}$$

where $1 \geqq \beta \geqq 0$, and $n_+ = i_+/e = f\,i/e$. f is the fraction of current carried by the positive ions at the cathode.

$$1 \geqq f \geqq 0$$

$$m_0 = 2m_2' + \beta f \frac{i}{e}.$$

The previous assumption that $m_1 = m_2$ will be true only if

$$\beta f = 0$$

Assuming the other extreme $\beta f = 1$, then the rate of vaporization is

$$m_0 = 2m_2' + \frac{i}{e}$$

assuming singly ionized copper molecules

$$\frac{i}{e} = 9.30\ \text{gm/cm}^2\text{/sec}.$$

$$m_2' = 0.21\ \text{gm/cm}^2\text{/sec}.$$

$$m_0 = 9.72\ \text{gm/cm}^2\text{/sec}.$$

Extrapolating the curve of Fig. 7 shows that this rate of evaporation corresponds to a temperature of 3200°K, about 100° over the boiling point.[7] Thus the difference in temperature caused by choosing $\beta f = 0$ and $\beta f = 1$ is only 700°.

Conclusions

(1) Spectroscopic observation of the cathode spot discloses a weak continuous spectrum, which is of a strength comparable with that given by a 3 mil copper wire heated in vacuum just before the wire melts.

(2) Pyrometric readings of the temperature of the cathode spot give a temperature which may be too high due to the unknown effect of the ionized gas in front of the cathode spot.

(3) Temperatures calculated under extreme assumptions as to actual rates of vaporization are shown to agree in order of magnitude with those measured by an optical pyrometer.

(4) Further experiments have confirmed the existence of the high velocity vapor and since this high energy of the vapor cannot be attributed to the temperature of the cathode spot, then the vapor stream must acquire its high velocity in the cathode region.

The writers wish to express their appreciation to Dr. J. Slepian and Mr. R. C. Mason for helpful suggestions.

WAVE-LENGTH STANDARDS IN THE SPECTRA OF CARBON AND TIN IN THE SCHUMANN REGION

By R. V. Zumstein and D. S. Marston
Mendenhall Laboratory, Ohio State University

(Received May 28, 1931)

Abstract

In the region 2000 to 1500A the strong lines of C I and Sn II have been measured to about 0.02A by direct comparison with iron. The dispersion of the second order lines was 3A per mm and the carbon groups were well resolved. The 1930.93 line of carbon for the arc has a value as given by Selwyn which differs from the value found for the spark. For the carbon groups at 1656 and 1560 values are obtained very close to the accepted ones. The tin wave-lengths are 1899.875, 1831.75, 1811.206, 1757.91, 1699.39. For the last two the error is about 0.03A.

THE first wave-length measurements in the Schumann region were made by Lyman[1] and are described in his book. He used a one meter concave grating with the slit not far from the grating normal, an arrangement which has been followed by most later workers. The spectrum produced is nearly normal so that only a small number of standard wave-lengths is required. The standards which Lyman measured were considered reliable to within about 0.2A and were not improved upon for several years. In this article all discussion refers to the region of the spectrum between 1500A and 2000A. During the past ten years it has been necessary to increase the accuracy of the standards which was done by Smith and Lang,[2] Bowen and Ingram,[3] Birge and Hopfield[4] and others. Their method was to photograph the Schumann region in the second order along with the iron spectrum of the first order.

There is at present a strong tendency to use the grating with a large angle between the incident ray and the grating normal.[5] With this arrangement, which was used in the present experiments, the dispersion may be large and the spectrum far from normal. According to our experience the standards must not be over 50A apart. One cannot interpolate by a straight line between such standards but it is necessary to use some more complicated interpolation formula. At present we feel that there is a great need for a much larger number of standards. For this reason we have worked with the tin spectrum. There are five strong lines of Sn II which may be easily produced in the arc, spark and vacuum tube. Our spectrograph was similar to that described by Hoag. The angle of incidence was about 70° which is less than that used by Hoag. The grating was of about two meter radius of curvature and 15,000

[1] T. Lyman, Spectroscopy of the Extreme Ultraviolet.
[2] S. Smith and R. J. Lang, Phys. Rev. **28,** 36 (1926).
[3] I. S. Bowen and S. B. Ingram, Phys. Rev. **28,** 444 (1926).
[4] R. T. Birge and J. J. Hopfield, Astrophys. J. **68,** 266 (1928).
[5] J. B. Hoag, Astrophys. J. **66,** 225 (1927).

lines per inch. It was an old grating ruled by Rowland. The slit, grating and plate were mounted approximately on a circle of two meters diameter. The distance from the slit to the grating was 55 cm and from the grating to the plate 95 cm. The spectra were photographed with thick Schumann films 35 cm $\times$ 3.8 cm $\times$ 1.5 mm similar to those sold by Hilger. They were bent to a circle of two meters diameter so the spectrum was in focus over nearly the whole length of the plate. The slit width was 0.05 mm and the time of exposure about eight minutes. A carbon arc was used as the source. The lower carbon was 3.5 cm diameter. A shallow hole one cm diameter contained the tin. The upper carbon was a solid rod one cm diameter. The arc was usually in a nitrogen atmosphere at one cm pressure. The cyanogen bands were present with considerable intensity. If they interfered the arc was used in hydrogen at the same pressure. The arc was also tried at lower pressures but did not seem as steady and the carbon lines were not in general as sharp. If a higher pressure of 10 cm was used the strong tin spark lines were often reversed. The current was about 80 amperes and the distance between the carbon electrodes about 3 mm. A thin strip of cellophane (0.04 mm) covered the lower part of the plate.

An exposure was first taken with tin in the lower electrode, the spectrum extending from 4200A to 2400A. The strong tin lines could be identified by comparing the plate with Eder and Valenta's Atlas. There were strong lines present due to both Sn I and Sn II. The first order arc and spark lines were able to pass through the cellophane with reduced intensity. Five strong lines were present which were entirely absorbed by the cellophane. They are second lines of Sn II. Second order lines were also present due to carbon (C I). We were surprised to find the second order lines almost as strong as the first order lines. Our source only emits lines due to the arc and first spark spectrum. Very few lines have been observed due to the second spark spectrum. In this respect it is much better than the hot spark which is often so rich in lines of higher stages of ionization. A small quantity of iron was added to the tin and a new plate taken. It was not easy to identify the iron lines as the intensities for our source differ from those of the arc in air. The international normals were not present with the same intensity. A few were entirely absent. We are very much indebted to Dr. Keivin Burns[6] for sending a reprint of work with Dr. Walters on the wave-lengths of iron in the vacuum arc. We have used their wave-lengths entirely. Our intensities also agree much better with theirs so we feel confident that the iron lines have been correctly identified. Since the dispersion of our spectrum is not uniform it is necessary to use a more complicated method of interpolation than linear interpolation between the iron lines. We have used the method of divided differences.[7] This requires three standards about 50A apart. The wave-length is assumed to be a polynomial in x of the second degree (x is the position of the line on the photographic plate as measured with the dividing engine). Besides the stand-

[6] K. Burns and F. M. Walters, Publications of the Allegheny Observatory VI, No. 11 (1929).

[7] A. Henry, Calculus and Probability, p. 51 Layton (1927).

ards and second order lines other iron and tin lines were included in each measurement. The calculation of such wave-lengths showed how well the polynomial applied and served as a check on mistakes in the calculation. The first order lines so measured were correct to about 0.02A. The wave-lengths so determined are given in Table I.

TABLE I. *Wave-length standards.*

	C I			Sn II	
Int	λ (vac.)	error	Int	λ (vac.)	error
10	1930.93	0.02	15	1899.875	0.02
2	1658.12	0.02	10	1831.75	0.02
2	1657.90	0.02	10	1811.206	0.02
2	1657.37	0.02	8	1757.91	0.03
4	1656.97	0.03	6	1699.39	0.03
2	1656.27	0.02			
10	1561.39	0.02			
8	1560.69	0.02			
5	1560.30	0.02			

Three of the tin lines, 1899, 1831 and 1757 were very close to iron lines (no second order iron lines have been observed). Spectra were obtained with a mixture of tin and nickel in the arc. The values of Barnes[8] were used as far as possible otherwise values from the International Critical Tables, Vol. 5, p. 308. The influence of the close iron line could be reduced to a negligible value by diminishing the amount of iron in the arc. This sometimes left the line without three suitable standards. Traces of aluminum, manganese, copper and chromium were present as impurities or were added in small quantities and the sensitive lines of these elements used in part as standards if the wave length seemed known to 0.01A. Each wave-length in Table I is an average of values obtained by measuring from three to seven plates. About thirty plates were taken.

Sources of error.

First it should be mentioned that Rowland's method of coincidences was used. A second source of error is the pole effect. Burns and Walters state that the iron arc, at these low pressures, shows no pole effect with currents as large as 16 amperes. They did not investigate larger currents. Unfortunately we have been forced to use much larger currents so far. The pole effect can be reduced by using a long arc and taking the light from the central portion of the arc only. Our arc is very steady with a length of 15 mm but the second order lines are absent. It seems necessary to use the short arc to get the second order lines.

The values of the carbon wave-lengths should be compared with the work of Smith and Lang, Bowen and Ingram, Bowen[9] and Selwyn.[10] This compari-

[8] B. T. Barnes, Astrophys. J. **63,** 130 (1926).
[9] I. S. Bowen, Phys. Rev. **29,** 231 (1927).
[10] E. H. Selwyn, Proc. Phys. Soc. **41,** 392 (1929).

son seems to show that under good conditions it is possible to make measurements in this part of the spectrum which are accurate to a few hundredths of an angstrom. The 1930 lines of carbon from the arc have a lower wave-length than from the vacuum spark as noticed by Selwyn. It may be that the vacuum spark brings out a second line of slightly greater wave-length and the center of the two unresolved lines is measured. For the other carbon groups there is very good agreement. The values for tin may be compared with measurements by Lang quoted in a paper by Green and Loring[11] and should be more accurate than any other values for these tin lines. We wish to thank Dr. L. H. Thomas for calling our attention to interpolation by divided differences and also to Professor Alpheus W. Smith for his kind encouragement.

[11] J. B. Green and R. A. Loring, Phys. Rev. **30**, 574 (1927).

SOME REMARKS ON THE THEORY OF THE PHOTOELECTRIC EFFECT

By J. Frenkel
University of Minnesota

(Received May 28, 1931)

Abstract

1. It is shown that the theory of photoelectric effect in a hydrogen-like atom can be successfully developed on the basis of the representation of the ejected electrons by means of plane waves, the results being exact with regard to angular distribution of the ejected electrons and satisfactory with regard to the dependence of the ejection probability on the frequency of the light.

2. The theory is extended to take account of the mobility of the nucleus.

3. The Tam-Schubin theory of the selective photoelectric action in metals is critically examined and replaced by an improvement of Fowler's theory, in connection with a discussion of the selective transparency of surface electric fields to electrons.

THE calculation of the probability of the ejection of an electron from a hydrogen-like atom is extremely simplified if the motion of the ejected electron is represented by a *plane sine wave*. The results will have, of course, an approximative character only, but it seems that they are good enough to justify this method. It should be mentioned that a similar method is usually applied to the calculation of *collision* probabilities, the results being equivalent to those obtained by Born's method where the motion of the particle after collision is represented by a complicated function reducing at large distances to a spherical wave, the plane waves used in the alternative method (due to Dirac) being nothing else but extended portions of the spherical wave.

The value of the method in question as applied to the photoelectric effect consists in the fact that it enables one to determine in an extremely simple way the angular distribution of electrons ejected by light of very short wavelength, whereas the ordinary method based on the use of spherical waves[1] leads in this case to considerable complications.

We shall assume that the electron (or rather the atom formed by the electron and the nucleus) was initially in the normal state specified by the normalized wave function

$$\psi_1 = \left(\frac{\alpha^3}{\pi}\right)^{1/2} e^{-\alpha r}$$

The final state will be represented by the function $\psi_2 = \rho e^{ip \cdot r}$ where $h/2\pi p$ is the momentum of the electron after ejection and ρ a normalization coefficient. Defining the incident light-wave by means of the vector potential

[1] Or solutions in parabolic co-ordinates recently used by J. Fischer, Ann. d. Physik **8**, 821 (1931). Fischer's results obtained by means of complicated calculations are practically equivalent with those of this paper.

$$A = A_0 \cos(qr - \omega t) = \tfrac{1}{2}\left[A_0 e^{i(qr-\omega t)} + A_0 e^{-i(qr-\omega t)}\right].$$

We can retain but one of the two complex terms, namely that for which the resonance condition $W_1 - W_2 + h\nu = 0$ will be satisfied, and drop the time factor, specifying accordingly the perturbation energy by the following operator $V = (\epsilon/2cm)\,(h/2\pi i)\,e^{-iqr}(A_0 \cdot \Delta)$ where ϵ is the charge and m the mass of the electron.

The probability that the electron will be ejected in the direction of the vector p by light falling in the direction of the vector q will be thus measured by the square of the matrix element[2]

$$V_{12} = \int \psi_1^* V \psi_2 d\tau = C(A_0 \cdot p) \int e^{-\alpha r + i(p-q)\cdot r} d\tau$$

where

$$C = \left(\frac{\alpha^3}{\pi}\right)^{1/2} \cdot \rho \cdot \frac{\epsilon h}{4\pi c m}.$$

Putting $p - q = s$ and introducing polar coordinates with the axis in the direction of the vector s, we have $(p-q)\cdot r = sr\cos\theta$, $d\tau = 2\pi r^2 dr \sin\theta d\theta$, whence since

$$\int_0^\pi e^{isr\cos\theta} \sin\theta d\theta = \int_{-1}^{+1} e^{isr\xi} d\xi = 2\,\frac{\sin sr}{sr}$$

$$V_{12} = C(A_0 \cdot p)\,\frac{4\pi}{s} \int_0^\infty e^{-\alpha r} \sin sr \cdot r dr$$

or with the help of the relation

$$\int_0^\infty e^{-\alpha r} \sin sr \cdot r dr = -\frac{\partial}{\partial \alpha} \int_0^\infty e^{-\alpha r} \sin sr \cdot dr = -\frac{\partial}{\partial \alpha}\left(\frac{s}{\alpha^2 + s^2}\right)$$

$$V_{12} = 8\pi C \alpha (A_0 \cdot p)/(\alpha^2 + s^2)^2. \tag{1}$$

Denoting with θ_1 and θ_2 the angles formed by the vector p (direction of ejection) with A_0, (direction of electric vibrations, since $E = -1/c\ \partial/\partial t\ A$) and with q (direction of light propagation) respectively, we have

$$A_0 \cdot p = A_0 p \cos\theta_1, \quad s^2 = p^2 + q^2 - 2pq\cos\theta_2$$

so that finally

$$V_{12} = 8\pi C \alpha A_0 p \cos\theta_1 \cdot (\alpha^2 + p^2 + q^2 - 2pq\cos\theta_2)^{-2} \tag{1a}$$

The magnitude of the vector p is fixed by the resonance or energy condition $W_2 - W_1 = h\nu$, which in view of the equations

$$W_1 = -\frac{h_2 \alpha^2}{8\pi^2 m}, \quad W_2 = \frac{h^2 p^2}{8\pi^2 m}, \quad h\nu = \frac{hcq}{2\pi}$$

[2] Instead of V_{12} we could use $V_{21} = \int \psi_2^* V \psi_1, d\tau$ with $V = (\epsilon/2cm)\ (h/2\pi i) e^{+iqr}\ (A_0 \cdot \nabla)$. The calculations are a little more complicated in this case, but of course lead to the result $V_{21} = V_{12}^*$.

can be written in the form

$$\alpha^2 + p^2 = \frac{4\pi cm}{h} q \tag{2}$$

If we restrict ourselves to the electrons ejected in the plane of polarization of the light waves, then $\theta_1+\theta_2=\pi/2$.

The most probable direction of ejection is determined accordingly by the condition that the expression

$$f(\theta_1) = \frac{\cos\theta_1}{(\alpha^2 + p^2 + q^2 - 2pq\sin\theta_1)^2}$$

should have its maximum value. The corresponding value of θ_1 is easily found to be given by the equation $\sin^2\theta_1+\mu\sin\theta_1-2=0$

$$\sin\theta_1 = \frac{-\mu + (\mu^2+8)^{1/2}}{2} \tag{3}$$

where

$$\mu = \frac{\alpha^2 + p^2 + q^2}{2pq} \tag{3a}$$

For light of sufficiently high (but not too high) frequency, such as ordinary x-rays, p is very large when compared with α and q. In this case we have approximately

$$\mu \cong \frac{p}{2q} (\gg 1)$$

and

$$\sin\theta_1 = \frac{2}{\mu} = \frac{4q}{p},$$

Since $hp/2\pi$ is the total momentum imparted to the ejected electron by the light, while $hq/2\pi$ is the momentum of the light quantum, the preceding formula can be interpreted by saying that the average (or most probable) momentum communicated to the electron in the forward direction (i.e. direction of light propagation) is 4 times larger than the momentum of the corresponding proton. According to Sommerfeld and Schur[3] the former should be twice larger than the latter.

Our formula (1) agrees, however, *exactly* with the results obtained by J. Fischer.[4]

The expression (3a) for μ can be replaced according to (2) by the expression

$$\mu = \frac{q}{2p} + \frac{2\pi cm}{hp}. \tag{3b}$$

The first term of which, for light of moderate frequency, is very small compared with the second.

[3] Sommerfeld and Schur, Ann. d. Physik **4**, 409 (1930).

[4] Reference 1, p. 829, Eq. (11′), which is obtained from our equation (1) by squaring and using the relation $\cos\theta_1=\cos\theta_2\sin\phi$ ($\theta_2=\vartheta$). Fischer does not seem to perceive any discrepancy between his results (in the approximate form) and those of Sommerfeld

For very high frequency, relativity mechanics must be used so that the preceding expression becomes erroneous while (3a) remains valid.

In order to determine the absolute value of the ejection probability, we must fix the normalization coefficient ρ in $\psi_2=\rho e^{ip\cdot r}$. This coefficient would be equal to $(2\pi)^{-3/2}$ if the function ψ_2 was specified by the parameters p_x, p_y, p_z the normalization in question being defined by the condition $\int|\bar{\psi}_2|^2dv=1$ with

$$\bar{\psi}_2=\frac{1}{(\Delta p_x\cdot\Delta p_y\cdot\Delta p_z)^{1/2}}\int_{-\Delta p_x/2}^{+\Delta p_x/2}\int_{-\Delta p_y/2}^{+\Delta p_y/2}\int_{-\Delta p_z/2}^{+\Delta p_z/2}\psi dp_x dp_y dp_z$$

Introducing instead of p_x, p_y, p_z the kinetic energy of the ejected electron $W=h^2p^2/8\pi^2m$ and the angles θ, ϕ, defining the direction of ejection

$$(p_x=p\sin\theta\cos\phi,\quad p_y=p\sin\theta\sin\phi,\quad p_z=p\cos\theta)$$

we can replace $dp_xdp_ydp_z$ by

$$P^2dpd\Omega=\frac{1}{2}\left(\frac{8\pi^2m}{h^2}\right)^{3/2}W^{1/2}dwd\Omega$$

where $d\Omega=\sin\theta d\theta d\phi$ is the solid angle in which the direction of ejection is supposed to lie, and put accordingly $\rho^2=1/(2\pi)^3\tfrac{1}{2}(8\pi^2m/h^2)^{3/2}W^{+1/2}=\tfrac{1}{2}(2\pi)^3$ $8\pi^2mp/h^2$ i.e.

$$\rho^2=\frac{m}{2\pi h^2}P \tag{4}$$

Under this condition the probability of ejection in the direction $d\Omega$ per unit time is given by

$$Pd\Omega=\frac{4\pi^2}{h}|V_{12}|^2d\Omega \tag{5}$$

which gives according to (1)

$$P=\frac{4\pi^2}{h^2}\cdot(8\pi)^2\frac{\alpha^5}{\pi}\left(\frac{\epsilon h}{4\pi cm}\right)^2\rho^2\frac{(A_0\cdot p)^2}{(\alpha^2+s^2)^4}$$

that is

$$P=B\cdot\alpha^5p\frac{(A_0\cdot p)^2}{(\alpha^2+s^2)^4} \tag{6}$$

where B is a universal constant which we need not write down fully, so far as the dependence of P upon the frequency of the incident light $\nu=\omega/2\pi$ and the initial state (specified by α) are concerned.

For sufficiently low frequencies we can replace s by p (neglecting q compared with p) and put $\alpha^2+p^2=4\pi m/h\nu$ according to (2). We have further, introducing the amplitude of the electric force

$$E_0=\frac{2\pi\nu}{c}A_0$$

and putting

$$\alpha^2=\frac{4\pi m}{h}\nu_0$$

$$P \sim E_0^2 \frac{\nu_0^{5/2} P^3}{\nu^6} \sim E_0^2 \frac{\nu_0^{5/2}(\nu - \nu_0)^{3/2}}{\nu^6} \tag{6a}$$

or approximately, if p is large compared with α i.e., large compared with ν_0

$$P \sim E_0^2 \nu_0^{5/2} \nu^{-9/2}. \tag{6b}$$

The dependence of p both upon ν and ν_0 given by this formula is very similar to that obtained by J. Fischer.[5] The latter can be written approximately in the form

$$P \sim E_0^2 \frac{\nu_0^3}{\nu^5} \frac{1}{\sinh (\nu_0/\nu)^{1/2}}$$

which for $\nu \gg \nu_0$ reduces to (6b).

A similar result is obtained also by means of the approximate theory based upon the representation of the ejected electrons by means of a spherical wave.[6]

2. The Influence of the Mobility of the Nucleus

We are now going to extend the theory of the photoelectric effect in a hydrogen-like atom by *allowing for the motion of the nucleus*, the proton say, which is usually treated as a fixed center of force.

The normal state of the system, electron + nucleus will be represented by a function ψ_1 equal to the product of two factors, namely $(\alpha^3/\pi)^{1/2} e^{-\alpha r}$ representing the relative motion of the two particles and $\rho_0 e^{i p_0 \cdot r_0}$ representing the translatory motion of the center of gravity. Here $r = r_1 - r_2$ and $r_0 = m_1 r_1 + m_2 r_2 / m_1 + m_2$ the index 1 referring to one of the particles the electron say, and r_2 to the other (the nucleus). The photoelectric effect consists in the disintegration of the system, the final state being represented by the product

$$\psi_2 = \rho_1 e^{i p_1 \cdot r_1} \cdot \rho_2 e^{i p_2 \cdot r_2} \tag{7}$$

where each of the factors represents the translatory motion of the separate particles.

The perturbation energy must be defined by the operator

$$V = \frac{\epsilon_1}{2cm_1} \frac{h}{2\pi i} e^{-iqr_1}(A^0 \cdot \nabla_1) + \frac{\epsilon_2}{2cm_2} \frac{h}{2\pi i} e^{-iq \cdot r_2}(A^0 \cdot \nabla_2) \tag{8}$$

equal to the sum of the operators representing the action of light on the electron and nucleus taken separately.

The matrix element V_{12} is thus reduced to the sum of the two terms $V_{12}^{(1)}$ and $V_{12}^{(2)}$ where

[5] Reference 1, p. 832, Eq. (15); Fischer's n and αz correspond to our P and α respectively: the integration over all the direction of ejection in our case is equivalent to a multiplication of P with $4\pi/3$, giving Fischer's N/t.

[6] Cf.—J. Frenkel, Einführung in die Wellenmechanik p. 270, Eq. (43a). It is interesting to note that for small values of $(\nu - \nu_0)$ the latter expression is inversely proportional to $(\nu - \nu_0)^{1/2}$ whereas the expression (6a) is proportional to $(\nu - \nu_0)^{3/2}$ which seems to be in a better agreement with experimental facts, P remaining finite for $\nu = \nu_0$

$$V_{12}^{(1)} = C_1(A^0 \cdot f_1) \int\int e^{-\alpha r + i(p_1 \cdot r_1 + p_2 \cdot r_2 - p_0 \cdot r_0 - q \cdot r_1)} d\tau_1 d\tau_2 \Big\} \tag{8a}$$

and

$$V_{12}^{(2)} = C_2(A^0 \cdot f_2) \int\int e^{-\alpha r + i(p_1 \cdot r_1 + p_2 \cdot r_2 - p_0 \cdot r_0 - q \cdot r_1)} d\tau_1 d\tau_2 \Big\}$$

with

$$C_1 = \left(\frac{\alpha^3}{\pi}\right)^{1/2} \rho_0 \rho_1 \rho_2 \frac{\epsilon_1 h}{4\pi c m_1}, \quad C_2 = \left(\frac{\alpha^3}{\pi}\right)^{1/2} \rho_0 \rho_1 \rho_2 \frac{\epsilon_2 h}{4\pi c m_2}.$$

In the evaluation of $V_{12}^{(1)}$ it will be convenient to express r_0 and r_2 through r and r_1, using the coordinates x, y, z and x_1, y_1, z_1, as independent variables.

We have $r_2 = r_1 - r$ and

$$r_0 = \frac{m_1 r_1 + m_2 r_2}{m_1 + m_2} = r_1 - \frac{m_2}{m_1 + m_2} r$$

The Jacobian of the transformation r_1, $r_2 \to r_1$, r is equal to 1 (or -1 if the integration limits are not reversed) so that

$$V_{12}^{(1)} = C_1(A^0 \cdot p_1) \int e^{-\alpha r + i(\beta_2 p_0 - f^2) \cdot r} d\tau \int e^{i(p_1 + p_2 - p_0 - q) \cdot r_1} d\tau_1$$

where

$$\beta_2 = m_2/(m_1 + m_2)$$

This expression vanishes unless

$$p_1 + f_2 - p_0 - q = 0 \tag{9}$$

which is the equation for the conservation of total momentum. Under this condition $V_{12}^{(1)}$ turns out to be proportional to

$$\frac{\epsilon_1}{m_1}(A^0 \cdot p_1)\left[\alpha^2 + (\beta_2 f_0 - p_2)^2\right]^{-2}$$

or if p_2 is replaced by $p_0 + q - p_1$

$$\frac{\epsilon_1}{m_1}(A^0 \cdot p_1)\left[\alpha^2 + (p_1 - q - \beta_1 f_0)^2\right]^{-2} \tag{9a}$$

where

$$\beta_1 = 1 - \beta_2 = m_1/(m_1 + m_2)$$

If a coordinate system is used with respect to which the center of gravity of the atom in the initial state is at rest, this expression reduces to that investigated in the preceding section. It does not, however, determine the probability of the photoelectric effect since it has to be considered in conjunction with the expression

$$\frac{\epsilon_2}{m_2}(A^0 \cdot f_2)\left[\alpha^2 + (f_2 - q - \beta_2 p_0)^2\right]^{-2} \tag{9b}$$

which corresponds to the action of the light on the nucleus.

Since the coefficients of proportionality are the same for (9a) and (9b) and the two expressions contain arbitrary phase factors (not explicitly written down) which makes the average value of their product vanish, we can define the total probability of the photoelectric "disintegration" of the two particles by the sum of the squares of the two expressions. As the mass m_2 of the nucleus is very much larger than that of the electron, the second term will in general contribute but a small correction to the result represented by the fact and investigated in the preceding section.

Assuming the center of gravity to be initially at rest ($p_0=0$) we can put $p_2=q-p_1$ and consequently $A_0\cdot p_2=-A_0\cdot p_1$, since A_0 is perpendicular to q. The probability in question, apart from a coefficient of proportionality thus assumes the form

$$(A^0\cdot p_1)^2\left\{\left(\frac{\epsilon_1}{m_1}\right)^2[\alpha^2+(p_1-q)^2]^{-4}+\left(\frac{\epsilon_2}{m_2}\right)^2[\alpha^2+p_1{}^2]^{-4}\right\} \tag{10}$$

or approximately if q can be neglected when compared with p_1

$$(A^0\cdot p_1)^2\left[\left(\frac{\epsilon_1}{m_1}\right)^2+\left(\frac{\epsilon_2}{m_2}\right)^2\right](\alpha^2+p_1{}^2)^{-4}. \tag{10a}$$

3. Selective Photoelectric Effect in Metals

The theory of the photoelectric effect in a metallic body has been worked out for the first time by Wentzel,[7] who, however, made physically incorrect and inconsistent assumptions. This theory has been improved by Fröhlich[8] and especially by Tamm and Schubin[9] who in a recent paper have given a very illuminating discussion of the subject. So far, however, as Tamm and Schubin's work is supposed by the authors to give the solution of the problem of the selective photoelectric action and is introducing in this connection the notion of free electrons of two types, completely free "Sommerfeld electrons" and partially bound "Bloch electrons," it is open to grave criticism.

The selective maximum is obtained by Tamm and Schubin in a way similar to that of Wentzel, namely, as a result of the gradual decrease of the probability of ejection of an electron with increase of the frequency of light beyond the threshold value ν_0 in connection with the increase of the number of electrons which can be ejected, i.e., with a threshold value $\nu_0<\nu$, these threshold values being distributed according to Fermi's law between $\nu_g=\nu_a-\bar{\nu}$ for the fastest electrons and ν_g for the slowest ones (where $h\bar{\nu}$ is the maximum kinetic energy of the completely free electrons (at $T=0$) and $h\nu_a$ is the jump of potential energy across the surface of the metal. After ν has been increased beyond ν_g, the magnitude of the photoelectric effect (i.e. the total number of electrons ejected from the metal in unit time) should decrease as shown on the full curve, Fig. 1. As a matter of fact the selective max-

[7] Sommerfeld's Testschrift, 1928, p. 20.
[8] Fröhlich, Ann. d. Physik **7**, 103 (1930).
[9] Tamm and Schubin, Zeits. f. Physik **68**, 97 (1931).

imum is by no means always observed, and is known to depend very largely upon the condition of the metal's surface (adsorbed gases etc.). Moreover, if it is observed, it is followed by a further increase of photoelectric emission as shown by the dotted curve, Fig. 1. And finally, the position of the maximum ν_m does not at all coincide as Tamm and Schubin believe it, with the theoretical value derived from the above consideration if due account is taken of the fallacy of the Fermi theory to give an accurate absolute value for the kinetic energy of the free electrons.

The maximum of this energy as given by Fermi's formula turns out to be of the order of magnitude of 1 volt. Tamm and Schubin obtain for potassium $\bar{\lambda} = c/\bar{\nu} = 620 m\mu$, whereas $\bar{\lambda}_\varrho$ is equal experimentally to $605 m\mu$ which would mean that $h\nu_a = h(\bar{\nu} + \nu_\varrho)$ the potential energy jump across the surface of the metal must be about twice as large as ν_ϱ i.e., amount to about 2 volts. This is

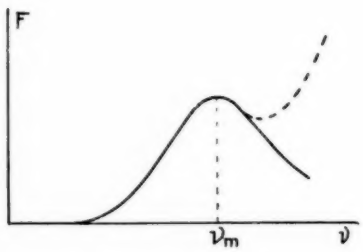

Fig. 1.

contradicted by the experimental evidence on cathode-ray diffraction, which indicates that the intrinsic potential of the various metals, as measured by $h\nu_a$ varies between 12 and 20 volts for different metals.

As has been shown by the present writer[10] it is possible with the help of the virial theorem to establish a simple relationship between the two energies $h\bar{\nu}$ and $h\nu_a$, namely

$$\bar{\nu} = \tfrac{1}{6}\nu_a$$

which, together with the experimental value of the difference

$$\nu_a - \bar{\nu} = \nu_\varrho$$

enables one to calculate the absolute values of $\bar{\nu}$ and ν_a. The latter comes out in this way in good agreement with the experimental data whereas the former turns out to be about 3 times larger than that obtained from Fermi's distribution law on the hypothesis of completely free electrons.

If, instead of using this erroneous "theoretical" value for $\bar{\nu}$ Tamm and Schubin used the correct one, their "selective maximum" would appear far in the ultraviolet region at frequencies about three times as large as those for which it is actually observed for alkali metals.

[10] Frenkel, Zeits. f. Physik 1928. Elementare theorie der elektrischen und magnetischen Eigenschaften der Metalle beim absoluten Nullpunkt der Temperatur.

Further, it would have been impossible to explain the subsequent rise of the curve $F(\nu)$ beyond the selective maximum, without assuming that there are besides the absolutely free electrons another group of relatively bound (Bloch's) electrons, which enter into play at a threshold frequency $\nu_0' > \nu_0$. Such a hypothesis is actually made by Tamm and Schubin. It seems, however, very artificial and inconsistent with the fact that Sommerfeld's "completely free" electrons simply do not exist and are but an approximation to the more real "relatively bound" electrons of Bloch. It seems, however, possible to use Sommerfeld's picture as a basis for the calculation of photoelectric action, if due allowance is made to the fact above referred of the inadequacy of the theoretical estimate of $\bar{v}$.

The theory of Tamm and Schubin, if corrected in this way, does not thus give any explanation of the *selective* photoelectric action. A theory of the latter taking account of the prominent role of the surface condition of the metal (i.e., the presence of adsorbed layers) has been recently proposed by R. Fowler.[11] The fundamental idea of Fowler's theory, which ascribes the selec-

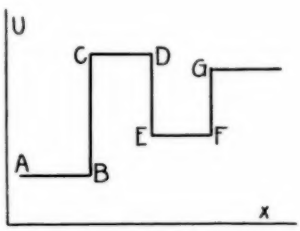

Fig. 2.

tive photoelectric action to a "selective transparence" of the metal's surface layer for electrons of a particular velocity (in the direction of the normal to the surface) is undoubtedly correct. What seems wrong about it is the very special character of the potential energy curve in the surface layer which Fowler thought it necessary to assume in order to explain this selective transparence. Fowler's curve is shown on Fig. 2, the characteristic part of it being a drop *DEFG*, attributed to the influence of an adsorbed layer and responsible for the selective transparence, the condition for the latter amounting to the principle that the wave length of the electron in this region should be a submultiple of its length. *ABCD* is the "jump" of potential energy by means of which the normal condition of the metallic surface is usually described.

One of the arguments that can be raised against Fowler's theory of selective transparence is that the finer details of the potential energy curve such as local maxima or minima do not matter in the surface layer any more than inside. The metal where they have the same order of magnitude and where they are nevertheless neglected so far as Sommerfeld's picture of the free electrons is adopted, on which Fowler's theory of selective transparence is based.

[11] R. Fowler, Proc. Roy. Soc., 1930.

Now it can be shown, and this is the main point of the present section, that a selection transparence must exist as a rule *for any type of surface field involving a transition of the potential energy from one (constant) level U_1 inside the metal to another constant level U_2 outside it*, irrespective of the presence or absence of any local maxima or minima.

It is certainly a great simplification of the surface field of force of a metal to represent it by an energy jump of the type ABC, Fig. 2. Actually this field possesses a definite extension $\Delta x = x_2 - x_1$ and can be represented rather by an inclined than by a vertical line, the slope of the line being determined by the ratio $\Delta u/\Delta x (\Delta u = u_2 - u_1)$ Fig. 3. If this line is replaced by a two-step line (broken line in Fig. 3) representing two simple jumps of the preceding type and the transmission coefficient D for the electrons whose initial energy W is higher than $u_2 - u_1$ is calculated, it turns out that D as a function of W displays a series of minima and maxima. The latter obviously corresponding to "selectivity" of the type desired. The oscillations of D gradually diminish as the energy increases while D is tending to the limiting value 1.

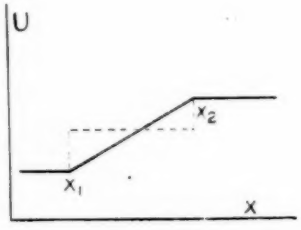

Fig. 3.

Similar results have been recently obtained by a rather laborious numerical calculation by Mr. W. Wetzel[12] for the case represented by the full line of Fig. 3 and corresponding to the passage of electrons through an electric condenser of the width Δx. So long as $W < U_2$ the reflection coefficient for electrons entering into the field from the left side is equal to zero. When this kinetic energy increases, the reflection coefficient first drops, then rises again, which corresponds to a local maximum of the transmission coefficient, the succeeding maxima being but slightly pronounced under conditions roughly corresponding to those actually found for metals (with $\Delta x \leq$ a few Ängstrom units and Δu 10–20 volts).

Results of the same character have been obtained by Dr. E. Hill[13] for a potential energy of a type $u = A + B/(x-a)^2$ which is not very different from a straight line for not too large widths of the field. According to Hill the reflection coefficient $R = 1 - D$ can be represented in this case by a formula of the type

$$R = \frac{\sinh^2 \tfrac{1}{2}\omega(1-\xi^2)^{1/2}}{-\xi^2 + \cosh^2 \tfrac{1}{2}\omega(1-\xi^2)^{1/2}}$$

[12] Of this department. Mr. Wetzel's results will be published separately with some detail about the method of calculation.

[13] Hill's calculation will be published separately.

where $\xi = 4\pi\Delta x/(\lambda_1 - \lambda_2)$ and $\omega = \log \lambda_1/\lambda_2$, $\lambda_{1,2}$ being the wave length of the electron inside and outside of the metal respectively. If $\xi < 1$ and

$$R = \frac{\sin^2 \frac{1}{2}\omega(\xi^2 - 1)^{1/2}}{\xi^2 - \cos^2 \frac{1}{2}\omega(\xi^2 - 1)^{1/2}}$$

in the case $\xi > 1$.

The latter formula in connection with the relation $4\pi^2/\lambda_{1,2}^2 = 2m(w - u_{1,2})$ shows that under certain conditions R displays a variation with W of a periodic type, with a minimum which is the deeper both absolutely and compared with the following minima, the nearer ξ is to 1 (remaining larger than 1). If ξ is much larger than 1 wh'ch corresponds to a very thick surface layer (large Δx) or very large kinetic energies (small $\lambda_1 - \lambda_2$) R decreases with W in a nearly monotonous way thanks to the term ξ^2 in the preceding formula. It increases likewise monotonously with decrease of W in the region for which $\xi \leqq 1$.

We thus see that a pronounced selective transparence can be met with in the case of such metals only, whose surface layer—naturally, or a result of the presence of some adsorbed substance, has a thickness of a suitable order of magnitude corresponding to the wave-length difference $\lambda_1 - \lambda_2$ for some of the free electrons, λ_1, being the wave-length obtained by them after the absorption of the light quantum $h\nu$ and enabling them to escape from the metal.

These results are just what we might expect from very simple physical considerations, which permit to interpret the selective transparence of a field of force of a limited length as a kind of "resonance" between this length and the wave-length of the electrons passing through it (actually it is not so much the wave-length itself as the difference of the wave-lengths that matters).[14]

In conclusion it should be mentioned that in the calculation of the probability of the ejection of an electron from the metal by the action of light, the function ψ_2 must be defined not as a plane line wave, but as a combination of such a wave emerging from the metal with the incident and reflected wave which remain within it. It is only through this combination, together with the normalization condition, that the transmission coefficient D appears in the expression of the probability defined in the usual way as proportional to the square of the matrix element

$$\int \psi_1^* (A_0 \nabla) \psi_2 d\nu.$$

As has been shown by Tamm and Schubin, it is only the outside part of the integral which matters for the probability in question (the inner part corresponding to free electrons gives practically no contribution to it). In this

[14] Eckart, Phys. Rev. July, (1930) has solved the problem of the transmission of the electrons through a field of the type $u = e\alpha x/e\alpha x + 1$ with the result that the transmission coefficient increases monotonously with the energy. This result seems to be specific for the type of field considered and to represent an exceptional case.

external part we must put $\psi_1 = e^{-\alpha x}$ where x is the distance from the surface and $\psi_2 = D(W)e^{ip \cdot r}$, the value of the energy W corresponding to the momentum p. For a detailed discussion the reader is referred to the work quoted and that of Fröhlich. The particular question which interested us in this connection was the character of the function $D(W)$ as the key to the explanation of the selective photoelectric effect.

PHOTOELECTRIC PROPERTIES OF THIN UNBACKED GOLD FILMS

By Ralph P. Winch
Department of Physics, University of Wisconsin

(Received May 25, 1931)

Abstract

Unbacked films of gold 2×10^{-6} cm thick were produced and studied to determine their photoelectric behavior. These films did not hold a constant photo-emission, but showed a rapid increase in emission with exposure to ultraviolet light. The increase in photo-current was 136 fold and was accompanied by a shift in long wave limit of 576A. Solid gold and silver were given similar treatment and showed a like effect. This increase is explained on the basis of outgassing caused by ejected electrons removing gas from the surface. The final long wave limit reached by the gold films is compared with that for the mass metal when outgassed by severe heat treatment.

THIS work was undertaken with the view of comparing the characteristics of free films with the results of previous workers[1] who used films of metal backed with quartz. Their results showed interesting differences between the photo-emission from the incident and emergent sides of a metal film. The effect of the backing was uncertain so it seemed worth while to attempt the same study using unbacked films.

Unfortunately the thinnest films which it was found possible to remove from their backing were 2×10^{-6} cm thick. Compton and Ross[1] found, for backed films of gold, that films thinner than 8×10^{-7} cm were imperfectly conducting due to isolated regions not in conducting contact with the rest of the film. Since the unbacked films must be sufficiently homogeneous to support themselves, and for photoelectric studies must be large enough so that the image of the source may be focused entirely on them, it is not surprising that they must be considerably thicker than the limit set by Compton and Ross.

The films were produced by a method suggested by Laub and Ruppert.[2] The method was, in brief, to sputter the metal on the surface of a polished rock salt crystal and dissolve the rock salt in water leaving the film free. This film was then caught on a copper ring which gave it rigidity for handling and mounting. The films for which data is given here were approximately 2×10^{-6} cm thick. The thickness was measured by light absorption[3] using data obtained by Meier[4] and Hagen and Rubens.[5]

[1] Compton and Ross, Phys. Rev. **13,** 374–391 (1919); Stuhlman, Phys. Rev. **13,** 109 (1919); **2,** 199 (1913); **4,** 195 (1914). Robinson, Phil. Mag. **32,** 421–425 (1916); **25,** 115–132 (1913).

[2] Laub and Ruppert, Phys. Zeits. **27,** 452.

[3] Wood, "Physical Optics," p. 465.

[4] Meier, Ann. d. Physik **31,** 1017 (1919).

[5] Hagen and Rubens, Deutsch Phys. Ges. **4,** 5 55–63 (1902).

The vacuum apparatus and electrometer were the same as used for the study of the photoelectric properties of silver.[6] Pressures of 10^{-7} mm of Hg or less were maintained throughout the experiment. The long wave length limit tests were made by placing absorption cells in the path of the incident light and immediately photographing the spectrum of the transmitted light using a quartz spectrograph. Solutions of various concentrations of tartaric acid in distilled water were found to cut off quite sharply in the desired region of the spectrum. In this way the longest effective wave-length could be found.

Photoelectric Outgassing

The photo-emission from these gold films did not remain constant but increased very rapidly on exposure to ultraviolet. This effect was noted first by Millikan[7] while studying silver, zinc, iron, nickel, and copper in the solid form.

With prolonged exposure of the film to ultraviolet under conditions for photo-emission the long wave limit shifted from about 2000A to 2482A. Long continued exposure failed to make 2537A effective and the emission remained constant during this time.

With an identical film under conditions as nearly identical as could be determined the field about the film was reversed so that emitted electrons travelled against the field until their kinetic energy was lost and then returned to the film. This time the long wave limit shifted on exposure to ultraviolet, more rapidly than before and, although it started at the same place, it ended near 2576A. While in the former case 2482A was the longest wave-length to become effective with continued exposure, in this case 2537A became effective in 64 hours and, when equilibrium was reached after 250 hours of exposure, 2576A was the longest effective line. One hundred hours additional exposure did not change either the long wave limit or the emission. During this latter change of long wave limit the photo-current increased 136 fold.

Photographs, with a quartz spectrograph, showed that the films were transmitting light down to a wave-length of 2259A but that only approximately 10 percent of the energy in the lines below 2537A was being transmitted.

While the incident face of the film was being exposed as discussed above the opposite face was affected only by the transmitted light. It showed an increase in emission proportional to the ultraviolet transmitted by the film but no such increase as shown by the incident face. The second face was now exposed for 32 hours through a filter which absorbed all wave lengths below 2800A but which transmitted 55 percent of the total energy of the arc as measured with a thermopile. During this time there was no change in the emission. At the end of the 32 hours the filter was removed and the emission immediately began to increase changing by 5.6 fold in the next 32 hours. Continued exposure of this face showed a very close repetition of the change discussed for the former face.

[6] Winch, Phys. Rev. **37,** 1269–1275 (1931).

[7] Millikan, Phys. Rev. **30,** 287–288 (1910); **29,** 85 (1909); **34,** 68–70 (1912).

A repetition of this experiment using a disk of solid gold showed an increase in photo-emission, and shift of long wave limit from 2000A to 2482A which took place much more slowly than with the thin films.

After 360 hours exposure of the film and 160 hours exposure of the solid gold the light from the arcs was cut off and frequent readings taken to determine the change of emission on standing without exposure to ultraviolet. The film was found to hold a constant emission for about 3 hours, and then gradually decrease. The solid gold held constant for about 1.5 hours and then gradually decreased. This shows that the equilibrium gas conditions change very slowly. Similar curves taken earlier in the process showed a more rapid falling off of emission on standing unexposed.

A filament of silver, 0.025 mm thick and 3 mm wide, was given treatment similar to that given the gold films and solid gold in order to determine whether this effect of ultraviolet light is unique with gold. The increase in emission was analogous and was accompanied by a shift in long wave limit. There was one marked difference between the silver and gold. For gold there was a rather abrupt increase in photo-current each time the shift in long wave limit took in a new line of the mercury arc followed by nearly constant emission until the next line was reached. However in the case of silver the emission increased continuously whether a new line became effective or not. As an example of this, after seven hours of exposure of the silver to ultraviolet, 2482A was the last effective line; and careful tests made after 15 hours showed that it was still the last effective line, but the emission had doubled during this time. The long wave limit is undoubtedly shifting continuously and for silver the "quantum efficiency" apparently shifts continuously as well. The change of the silver specimen was never carried as far as it would go.

Conclusions

This increase in emission and shift of long wave limit is analogous to that observed when metals are given heat treatment for outgassing.[6] The evidence given here points to the theory that electrons ejected photoelectrically remove gas molecules from the surface of the metal. Heating due to absorbed radiation, could not explain the results since the two faces of so thin a film would be at nearly the same temperature and hence would increase in emission together. This was not the case. Also the increase in temperature of the mass metals, under the conditions used for this study, would be very small. The fact that the exposure of the film, through the filter which cut out all light effective for photo-emission, did not produce an increase points to the fact that photo-emission is the cause of the outgassing. If ejected electrons remove gas from the surface it is conceivable that returning electrons should do the same. The part of the experiment where the field was reversed showed this to be the case.

Morris[8] showed that the long wave limit of thoroughly outgassed gold at room temperature is near 2560A. The final value arrived at for gold films

[8] Morris, Phys. Rev. **37,** 1263–1268 (1931).

after long continued exposure was near 2576A. The long wave limit is a rather indeterminate quantity since the curves for emission per unit light intensity against wave-length show an exponential tail along the wave-length axis. Consequently these two values for long wave limit at room temperature are in good agreement, rather better agreement than one would expect from the history of the specimens previous to their determination. It will be noted in Morris' work that the emission for gold increased very rapidly to a high maximum with heating and then decreased finally settling down to a steady value. At the same time the long wave limit shifted first to above 3000A and then back to the stable value of 2560A. This is quite in contrast with the behavior of the thin films where the emission increased and the long wave limit shifted in one direction continuously with exposure to ultraviolet ultimately settling down at the final value. Since the film is so thin that light passes entirely through it and the exposure was long continued on both surfaces it is not inconceivable that the film is in the same stable condition reached by the solid gold subjected to severe heat treatment. On the other hand it is also possible that the final condition of the film corresponds to an early stage in the outgassing process when the long wave limit is on its way toward 3000A. In this case one would have to conclude that the film was not outgassed. The first great increase in sensitivity of the solid gold specimen is probably due to the particular combination of gas (coming from the interior or on the surface) and metal existant at that time and is not characteristic of the metal. This high maximum has been shown by other metals given similar heat treatment.[6] It is possible that with the thin film the combination for the high maximum never existed but that the final condition was the same as with the solid gold.

Dillon[9] of this laboratory has used this method of outgassing on a single crystal of zinc which was made in vacuum and hence had gas only on the surface. The method is particularly useful for those cases where outgassing by heat treatment cannot be employed. By such treatment a stable condition is reached, but its relationship to the stable condition reached by heat treatment must be more carefully studied.

In conclusion the writer wishes to express his appreciation of the many suggestions and continued help generously given by Professor C. E. Mendenhall, under whose direction this work was carried out.

[9] Dillon, Phys. Rev. August 1, 1931.

NOTE ON THE STRUCTURE OF THE GROUPS XO_3

By J. C. Slater
Massachusetts Institute of Technology

(Received May 21, 1931)

Abstract

The structure of such radicals as $(NO_3)^-$ on the one hand, $(ClO_3)^-$ on the other, is discussed on the basis of their being partly valence compounds, the oxygen being in the form of O^{-1} with one valence bond. The directional properties of the valence lead to a coplanar structure for the first type of radical, a pyramidal one for the second, as is observed. The energy relations are discussed, it is shown that the valence model will be bound in a stable structure, and that it is stabler and hence nearer the real model than the purely ionic structure.

Directional Properties

THE structures of a number of radicals of the form XO_3 have been investigated by x-ray methods, and it has been pointed out by Zachariasen[1] that some of them apparently form plane groups, others pyramidal ones. The criterion governing this is very simple: those groups for which the number of valence electrons is 24 form plane configurations ($(NO_3)^{-1}$, $(CO_3)^{-2}$, $(BO_3)^{-3}$), while those with 26 valence electrons form pyramids ($(ClO_3)^{-1}$, $(BrO_3)^{-1}$, $(SO_3)^{-2}$, $(AsO_3)^{-3}$). If one assumes that those compounds are purely ionic, then as Zachariasen shows we can get an explanation of the difference in behavior. For this purpose we assume that the oxygens form ions O^{-2}. This leaves the positive ions in the first case without valence electrons, since the oxygen ions use up all 24 electrons, while in the second case the positive ions are left with two valence electrons, presumably *s* electrons. As a result the positive ion in the latter case is much more polarizible, and this polarizibility proves to be enough to make a pyramidal structure more stable than the plane one.

Now it has been pointed out by the present writer,[2] and independently by Pauling,[3] that an explanation of many directional properties in valence bonds can be given on the basis of wave mechanics. Many things suggest that in the groups XO_3 the bonds are partly of a homopolar nature, and it is the purpose of the present note to point out how this explanation fits in with the generalization of Zachariasen. Of course, this is not a new explanation of these compounds; it has been discussed, for example, by Lewis, Huggins,[4] and Pauling.[3] The principal contribution of the present note is to point out that the two explanations, the homopolar and the ionic ones, are not necessarily antago-

[1] Zachariasen, Norske Vid. Akad. Skr. Oslo, 1928, No. 4, p. 90; J. Am. Chem. So., now in press; Phys. Rev. **37**, 775 (1931).

[2] J. C. Slater, Phys. Rev. **37**, 481 (1931).

[3] Linus Pauling, J. Am. Chem. Soc. **53**, 1367 (1931).

[4] M. L. Huggins, Phys. Rev. **37**, 1177 (1931).

nistic, but that the real situation is undoubtedly a combination of the two, in proportions, or with probabilities, which can be computed, rather than being the subject of arguments. A suggestive, though very rough, calculation of these relative proportions shows that the homopolar model is the more likely one in the actual case treated.

Let us take $(NO_3)^{-1}$, $(ClO_3)^{-1}$ as examples of the two groups. We can explain $(NO_3)^{-1}$ as being made of the ions $N^{+5}(O^{-2})_3$, or $N^{+2}(O^{-1})_3$, and (ClO_3^{-1}) as being made of $Cl^{+5}(O^{-2})_3$, or $Cl^{+2}(O^{-1})_3$. The first explanation in either case is that in which the attraction is wholly ionic, and it is this which Zachariasen discusses. But the second explanation as well seems plausible, and we wish to show that it leads to the same results. First we take $(NO_3)^{-1}$. The ion N^{+2} contains three valence electrons, and can therefore have three valence bonds; O^{-1} lacks one electron from a complete shell, and so has one bond. Thus there can be a regular valence compound, the N being held by valence bonds to each O, the valences being reinforced by the ionic attractions which still remain. Now we consider the directional properties of the valences. The normal state of N^{+2} would have two *s* electrons, one *p*, and would be monovalent. Since we wish a trivalent form, one of the *s* electrons must be raised to a *p* state, so that we have one *s*, two *p* electrons. Now in the previous paper it was shown that three *p* electrons and an *s* can form four functions of tetrahedral symmetry. In the same way two *p*'s and an *s* could form three functions of triangular symmetry, the valence bonds sticking out in a plane, forming angles of 120° with each other. This form of valence bond could lead to the coplanar form of the nitrate ion, and of the other ions of that structure. Or perhaps, as Pauling suggests, the form could be slightly pyramidal, with the nitrogen or carbon ion oscillating from one side of the plane of the oxygens to the other.

The other group of ions, of which $(ClO_3)^{-1}$ is an example, differs in having two more electrons. The Cl^{+2} has five valence electrons, two *s*'s and three *p*'s, the former not contributing to valence, the latter furnishing three bonds. These bonds, as usual when there are three *p* valences, tend to be at right angles to each other, so that the radical is pyramidal. The distinction between the two structures thus proves to be just in agreement with observation.

Examination of other radicals containing oxygen shows that the model formed of O^{-1} ions is always possible, and that it leads to valence bonds as well as ionic attractions, and hence to directional properties. For instance, it has just been found by Ziegler[5] that the nitrite ion, $(NO_2)^{-1}$, is angular rather than collinear. If we assume this made of N^{+1} and $(O^{-1})_2$, the nitrogen has four valence electrons, two *s*'s and two *p*'s, giving two *p* valences to link with the two oxygens, and hence an angular model. In general, in such a radical, we are to assume the oxygens to be in the form of O^{-1} ions, and to assume the other electrons to be located on the positive ions. Then we find that there are just enough valence bonds to go around, and from the nature of the electrons concerned in these valence bonds we can determine the directional properties by the rules of the previous paper.

[5] G. E. Ziegler, Washington Meeting of American Physical Society, April 30, 1931.

Energy Relations

It is possible to answer in a fairly definite way the question as to which model of the radical is right, the purely ionic one or the one involving valence bonds. The answer has already been discussed in the previous paper: if both models seem possible, the real situation is a combination of both. Thus if ψ_1 represents the wave function of the purely ionic case, ψ_2 of the case involving valence, the wave-function will be of the form $a\psi_1+b\psi_2$, where the relative sizes of a and b determine which model is nearer the truth. We can get information about these magnitudes by considering the energies of the two models. If, for example, the state ψ_2 lies much below ψ_1, then for the low state of the radical we shall have b large compared with a, and the correct model will be the second, with energy accordingly. On the other hand, if the two energies are nearly the same, a and b will be nearly the same, and the true model will be midway between the two. We can actually make fairly accurate estimates of the energies, and they illustrate our points very nicely.

Suppose we consider the energy of the nitrate ion as a function of the distance R from the nitrogen to any one of the oxygens, supposing that it changes its size while leaving its shape unaltered. We expect the curve of energy against R to resemble those for diatomic molecules. At infinite separation the energy is that of the separate atoms or ions. Take as zero of energy the configuration N^-+3O, which is presumably the lowest level of the separated ion, and the one into which the lowest level of the radical will go at large enough R. Then state $N^{+5}+3O^{-2}$ lies very high above this, by an amount which we can estimate from the shielding constants suggested by the author.[6] It requires about 19.0×13.53 volts to remove the five valence electrons from nitrogen (effective nuclear charge for an L electron in nitrogen $=7-2(0.85)-4(0.35)=3.90$, energy $=5(3.90/2)^2\times13.53$ volts). Further, the energy of the negative ion is very nearly the same as of the corresponding neutral atom. (For O^{-2}, nuclear charge $=8-2(0.85)-7(0.35)=3.85$, energy $=8(3.85/2)^2=29.6$; for O^{-1}, charge $=4.20$, energy $=7(4.20/2)^2=30.8$; for O, charge $=4.55$, energy $=6(4.55/2)^2=31.0$. According to this, O is more stable than O^{-1} by 0.2, and more stable than O^{-2} by 1.4. Similarly for N^{-1}, charge $=3.55$, energy $=6(3.55/2)^2=18.9$, so that N is more stable by 0.1). Thus the height of our ionic state is about 19.0 units above the zero or more precisely $18.9+3(1.4)=23.1$ units. The other state does not lie nearly as high at infinite R, for we have to remove only two electrons, giving N^{+2} (requiring energy $18.9-3(4.60/2)^2=3.1$ units) and join these to the O atoms (requiring 0.6 more), so that this level is only 3.7 units up from our zero.

As R decreases, both energy levels become lower, on account of the electrostatic attractions between ions, and the polarizations. The energies thus can become lower than those for infinite separation, giving binding. Further, the ionic level decreases so much faster that at the actual dimensions of the radical the two energies are of the same order of magnitude. To compute the energy at distance R, we proceed as follows. There is first the electro-

[6] J. C. Slater, Phys. Rev. **36**, 57 (1930).

static attraction of the nitrogen for the three oxygen ions at distance R. Next there is the mutual electrostatic repulsion of the oxygens, at distance $R\sqrt{3}$ Finally there is the polarization energy of the oxygens, $\frac{1}{2}\alpha F^2$ for each, where α is the polarizibility, F the field. The former is 1.55×10^{-24} cc[7] for the O^{-2} ion; we assume the same for O^{-1}, although this is not very accurate. The field at an oxygen ion is composed of two parts, the attraction from the nitrogen, equal to the charge on the nitrogen over R^2; and the repulsions form the two other oxygens, the components of each along the resultant being the charge over $\sqrt{3}R^2$. Combining all terms, we have for the whole energies the following expressions. Here R is in units of a_0, energies in units 13.53 volts, and the factor 2 in the potential energy takes care of these units.

(1) *Ionic case*:

$$23.1 - \frac{2}{R}\left(3\times2\times5 - \frac{3\times2\times2}{\sqrt{3}}\right) - \frac{2}{R}\cdot\frac{\alpha}{R^3}\cdot\frac{3}{2}\left(5 - \frac{2\times2}{2\sqrt{3}}\right)^2$$

$$= 23.1 - \frac{4.62}{R} - \frac{44.4}{R}\,\frac{\alpha}{R^3}.$$

(2) *Valence case*:

$$3.7 - \frac{2}{R}\left(3\times1\times2 - \frac{3}{\sqrt{3}}\right) - \frac{2}{R}\,\frac{\alpha}{R^3}\,\frac{3}{2}\left(2 - \frac{2}{2\sqrt{3}}\right)^2$$

$$= 3.7 - \frac{8.5}{R} - \frac{2.5}{R}\,\frac{\alpha}{R^3}.$$

Now in the actual equilibrium position, $R\sqrt{3}$, the distance between oxygens, equals about 2.70A, so that $R = 1.56\text{A} = 2.93\ a_0$, and $\alpha/R^3 = 0.415$. Thus for this part of the energy we have

(1) *Ionic case:* $23.1 - \dfrac{4.62}{2.93} - \dfrac{44.4}{2.93}\times .415 = 1.1$ unit

(2) *Valence case:* $3.7 - \dfrac{8.5}{2.93} - \dfrac{2.5}{2.93}\times .415 = 0.0$ units.

In other words, the two levels have both come down nearly to the zero of energy.

In addition to the energies already considered, there are two others to be added in. First is the repulsion arising from the exclusion principle. This begins to be appreciable at about the distance of equilibrium, and causes both curves to turn up again sharply as R decreases still further. The second is the valence attraction in case 2. This will reduce the energy still further in the neighborhood of the minimum, bringing it safely below the zero of energy, and ensuring a stable radical.

[7] See Debye, Polar Molecules, for similar calculations, and tables of polarizibilities

When we consider all the terms in the energy, we see that the valence model seems to correspond to the lower energy, and to stable binding; but the ionic model gives an energy not far above for small R's, although at large R's it goes much higher. We conclude, therefore that the true state of affairs is nearer the valence case although suggesting both; approaching, however, the lowest state, $N^- + 3O$, at very large R. As R is increased, the ionic case becomes less likely. This latter statement is interesting when we look at it in another light: as R is decreased, and the nuclei are pushed together, the oxygens become more highly charged negatively. This is as if the electrons did not follow the nuclei as they approached, but rather formed a cloud of more or less stationary dimensions, and allowed the nuclei to be pushed through them. This is as we should expect, when R becomes quite small; the exclusion principle requires that the electrons stay a reasonable distance apart from each other.

Finally we can get an interesting light on the structure by considering the electric moment of the polarized oxygen ions, which is equal to αF. In the first case, this is $\alpha/R^3 \times eR \times (5 - 2/\sqrt{3}$, where e is the charge on the electron, and in the second case it is $\alpha/R^3 \times eR \times (2 - 1/\sqrt{3}$. Substituting, this gives for the equilibrium value of R the two moments 1.60 eR and 0.59 eR respectively. These have an interesting interpretation: in the first case the polarization of each O^{-2} is what we should have if 1.60 electrons moved from the oxygen to the nitrogen, and in the second case if 0.59 moved, leaving in either case about half an electron on each oxygen. Or we can say, in case 1 one electron shifts from oxygen to nitrogen (bringing us to case 2 automatically), and the second extra electron shifts from the oxygen to the position midway between oxygen and nitrogen, as if it were held in a double bond. These results are only suggestive, for of course the oxygen has many electrons, and all can be displaced. Nevertheless they point in the direction of assuming that the structure of the radicals is one in which the separate ions are only moderately charged, and are held together at least partially by valence forces.

THE EFFECT OF TEMPERATURE UPON THE ULTRAVIOLET BAND SPECTRUM OF OZONE AND THE STRUCTURE OF THIS SPECTRUM

By Oliver R. Wulf and Eugene H. Melvin
Bureau of Chemistry and Soils, Washington, D. C.

(Received June 4, 1931)

Abstract

The ultraviolet absorption of ozone in the region 3400 – 2300A consists of a large number of bands appearing against a background of continuous absorption. The effect of temperature upon this spectrum has been studied over the range −78° to 250°C. A definite though small effect has been observed. Grossly it manifests itself as an increase in contrast with decreasing temperature. Photometric results show this to be a decrease in absorption between the bands, all of the bands appearing to come from normal vibrational levels of very low if not the lowest energy. Though somewhat diffuse, the bands tend to degrade to the red. The observed influence of temperature can be explained as a decrease of intensity in the continuous background, and also in the higher rotational absorption of the bands, with decreasing temperature. Discontinuities in the intensity relations and the regular spacing of certain of the bands have led to a partial vibrational analysis indicating two active vibrational degrees of freedom in the excited electronic state. The observed change in the absorption with temperature may affect somewhat the estimates which have been made of the amount of ozone existing in the upper atmosphere, and may possibly afford a method of estimating the temperature of the upper atmosphere.

FOLLOWING plans mentioned in an earlier report upon the visible absorption spectrum of ozone[1] the authors have made a study of the influence of temperature upon the ozone spectrum working with the absorption which lies in the ultraviolet. The ultraviolet absorption of ozone consists of a large number of rather diffuse bands appearing against a background of continuous absorption.[2] It is not one of the most promising spectra for the study of triatomic molecules, but it is an important spectrum because of the several fields in which the ozone molecule is of interest. The limitation of the solar and stellar spectra in the ultraviolet is due to the ozone of the upper atmosphere, and the determination of the amount and variation in amount of this atmospheric ozone has, to the present, been done chiefly through a study of its ultraviolet absorption spectrum as it shows on the short wave-length edge of the solar spectrum. Furthermore, the reversion of ozone to oxygen is a chemi-

[1] Wulf, Proc. Nat. Acad. Sci. **16,** 507 (1930).

[2] Hartley, Jour. Chem. Soc. **39,** 57 (1881); Huggins, Proc. Roy. Soc. **48,** 216 (1890); Meyer, Ann. d. Physik **12,** 849 (1903); Ladenburg and Lehmann, Ibid. **21,** 305 (1906); Krüger and Moeller, Physik. Zeits. **13,** 729 (1912); Fabry and Buisson, Jour. de physique et le radium **3,** 196 (1913); Fowler and Strutt, Proc. Roy. Soc. **93,** 729 (1917); Shaver, Proc. Roy. Soc. Canada **15,** Sec. III, 5 (1921); Lambert, Dejardin and Chalonge, Compt. rend. **183,** 800 (1926); Lauchli, Zeits. f. Physik **53,** 92 (1929); Lambry and Chalonge, Gerland's Beiträge z. Geophysik **24,** 42 (1929); Dutheil and Dutheil, Jour. de physique et le radium **7,** 414 (1926).

cal reaction which has received a great deal of attention in both thermal and photochemical kinetics, making important a knowledge of the energy levels and processes of dissociation of the molecule. The molecule is probably a result of the combination of the normal reactive $^3\Sigma$ state of oxygen molecule with the normal ^3P state of oxygen atom, the two sets of unpaired electrons pairing, leaving the normal state of ozone diamagnetic.[3]

The infrared data for ozone[4] indicates vibrational states[1] which might lead to an appreciable temperature effect in its electronic absorption at ordinary temperatures. If such did occur in ozone it would be important[5] for it might alter somewhat the estimation of the amount of ozone present in the upper atmosphere, and part of the apparent variation in the amount of this ozone might be simply a variation in the temperature of the atmosphere at the height of the ozone layer. It might, furthermore, lead to a direct method of estimating the temperature at this altitude. And any knowledge of the influence of temperature on the spectrum should aid in understanding its structure.

We have studied the effect of temperature upon this absorption over the region 3400–2300A. The region 3400–2900A has been studied from about −78°C to room temperature, while in the region of stronger absorption, i.e., 2550A, it has been photographed as high as 250°C. The former region has, however, been studied in most detail.

A definite influence of temperature has been observed though it is small and hence difficult to measure. Grossly it manifests itself as an increase in contrast with decreasing temperature, perceivable with the eye alone on the original plates. The work has been done on two Hilger spectrographs, one the familiar E2, the other of the Féry design. The continuous spectrum of hydrogen was used as a background, and the absorption of ozone, produced in a silent discharge ozonizer and of a wide variation of concentrations, was photographed in quartz and pyrex cells at the temperature of solid carbon dioxide and at a series of higher temperatures. In the work at the low temperature the cells were packed in crushed solid carbon dioxide, being fitted in most cases with projecting auxiliary cells at both ends containing dry air and phosphorus pentoxide to prevent frosting at the windows. In the case of the bands at the extreme red a two meter cell was used, its windows projecting from the cold pack and being kept at room temperature, thus nearly all but not strictly all of the path of gas being at the low temperature in this case.

A photometric study of the plates has been made against a series of exposures of the same source weakened by calibrated screens.[6] In this study,

[3] Lewis, Valence and the Structure of Atoms and Molecules, Chem. Cat. Co., 1923, pp. 130, 147 et seq; Chem. Rev. **1,** 234 (1924); Wulf, Proc. Nat. Acad. Sci. **13,** 744 (1927); Vaidyanathan, Indian Journ. Phys. **2,** 422 (1928).

[4] E. Ladenburg and E. Lehmann, Ann. d. Physik (4), **21,** 305 (1906); Verh. d. deutsch. Phys. Ges. **8,** 125 (1906).

[5] R. Ladenburg, Gerlands Beiträge z. Geophysik **24,** 40 (1929); Ruedy, ibid. **24,** 49 (1929); See also Ref. (1).

[6] The authors are indebted to Dr. F. S. Brackett for the use of the recording microphotometer of the Smithsonian Institution.

constant exposure time was used and the series of comparison exposures using the screens were made on the same plate as the exposures of the absorption of ozone. From the calibration exposures, density was plotted against the logarithm of the transmission, and the transmission of the ozone in the experimental exposures under any particular conditions was read from this, the density being determined from direct measurements on the photometer curves. The results over the region 3400A to 2900A show that the bands all behave the same within the accuracy of measurement, exhibiting a strengthening in the maxima with decreasing temperature and a weakening of absorption in the space between the bands. The temperature effect appears to be essentially the same whether carried out at constant total gas density (closed absorption cell) or at constant pressure (cell open to atmosphere), in both cases the same number of ozone molecules in the path. A blank run showed no appreciable photochemical ozone decomposition over the time of an experiment. The continuous background, which builds up strongly as one goes from 3400A to 2900A, decreases in strength with decreasing temperature. At 3100A the bands are almost negligible compared to the background and the absorption here shows a decrease over this temperature range of about 10 percent. Passing to longer wave-lengths, where the bands come more in evidence, the maxima tend to increase against the background with decreasing temperature while in the space between bands the absorption falls away more strongly. This is shown in Table I which contains the results of the most re-

TABLE I. *Temperature effect in band maxima and minima.*

Band	Wave-length A	$\frac{\alpha_{195°K}}{\alpha_{295°K}}$	Band	Wave-length A	$\frac{\alpha_{195°K}}{\alpha_{295°K}}$
6:7	3058	0.90	5:4	3155	0.95
7:5	3066	0.91			0.81
		0.89	4:5	3169	0.96
6:6	3081	0.90	5:3	3175	0.99
7:4	3088	0.90			0.84
		0.86	4:4	3194	0.97
6:5	3102	0.88	5:2	3199	0.98
7:3	3113	0.91			0.85
		0.89	4:3	3220	1.11
5:5	3135	0.96	5:1	3226	1.09
		0.82			0.91

liable measurements. The figures in the third and sixth columns are the ratios of the absolute values of the absorption coefficient at the two temperatures, 195°K and 295°K at the points of band maxima and minima. The bands are designated by the number of the group to which they appear to belong and their number in that group, this numbering being further explained later on. Thus it appears that all of the bands that have been studied come from vibrational states of very low if not the lowest energy. Bands from a vibrational level of as high as 400 cm^{-1} would show a change of a few fold in intensity over this range of temperature, and of course much more from a level as high as 1000 cm^{-1}.[1] A general picture of the whole absorption is given in Fig. 1.

The bands, though somewhat diffuse with no rotational structure resolved,[7] tend to degrade to the red in the near ultraviolet region. This can be seen best by a careful study of the photometer curves given in Fig. 2. Thus

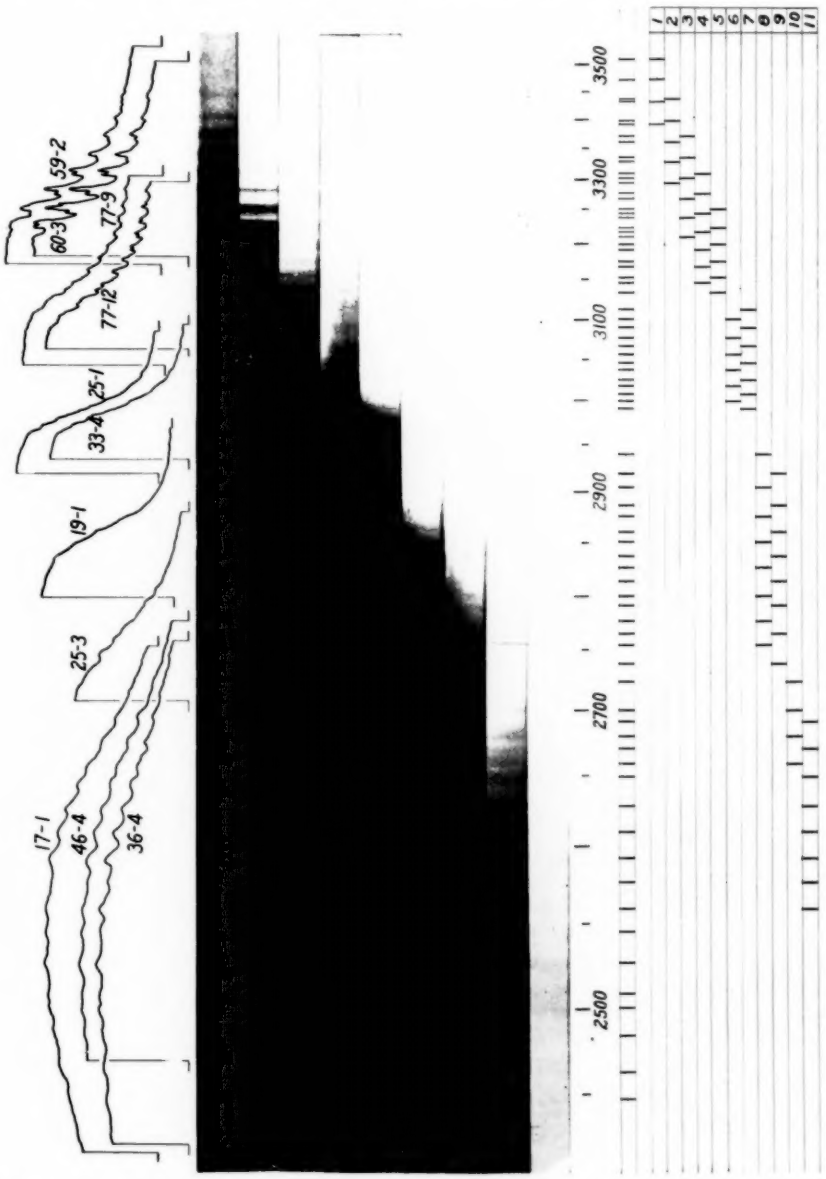

Fig. 1. Scale of wave-lengths in Angstroms. Above are tracings of photometer curves; where two are given the lower is at 195°K and the upper at 295°K. In the 2500A region the third and upper curve is at approximately 525°K. Below is diagram illustrating the tendency toward regularity in certain groups of the bands. A scratch on plate shows at about 2750A in the two lowest exposures.

[7] Fowler and Strutt, Proc. Roy. Soc. **93,** 582 (1917).

the absorption between two bands is apparently due partially to the rotational structure of the bands lying just to shorter wave-lengths, chiefly of course to that of the adjacent band. Partially it appears to be due also to the overlying continuous absorption, and in an amount which increases with decreasing wave-length. The observed change of absorption with temperature can thus be explained as a decrease in the absorption of the continuous background, and a decrease in the higher rotational absorption of the bands with decreasing temperature.

Certain groups of the bands show a decided tendency toward regular spacing;[8] also several discontinuities occur in the intensity change from band to band within such groups, appearing to identify a series of partial progressions. We have used this fact to afford a numbering for the bands, each band being designated by two numbers, the first its partial progression number and the second (starting with zero) its position in the progression. These groups with the wave-lengths of the bands as we have observed them are given in Table

TABLE II. *Band groups.*

Band Number	Partial Progression Number 1	2	3	4	5	6	7	8	9	10	11
0	3513	3439	3371	3310	3254			2945	2930	2724	2666
1	3473	3401	3337	3278	3226			2907	2890	2700	2646
2	3432	3362	3302	3247	3199			2876	2862	2678	2629
3	3394	3333	3270	3220	3175		3113	2852	2837	2658	2611
4			3240	3194	3155		3088	2827	2814		2594
5			3213	3169	3135	3102	3066	2801	2789		2579
6				3145		3081	3045	2778	2766		2560
7						3058	3025	2753	2738		
8						3039	3008				
9						3020	2990				
10						3000					

II. At the beginning of the absorption in the near ultraviolet the bands comprise five groups having a band separation within the groups of the order of 300 cm^{-1} and a displacement between the groups of the order of 600 $cm.^{-1}$ These are shown in Fig. 2 with two photometer curves above them, the upper at the high and the lower at the low temperature. Consistent intensity relations between the bands within the partial progressions lend further support for this grouping. Somewhat further in the ultraviolet are two more groups that have fairly closely the same band separation and may belong with these. The first members of these may not have been observed because of their low intensity and the lack of contrasty plates in this region of strong continuous background. It is to be noted that while the absolute numbering of these partial progressions is arbitrary, the relative numbering and especially the absolute

[8] Kondratjew, Zeit. f. physik. Chem. B, **7**, 70 (1930), has taken six of the bands as measured by Fowler and Strutt as representing a series. As will be seen later the last five of these are members of our partial progression 4, while the first we have not observed, the nearest to this being band 2 of partial progression 3. Partial progression 5 shows a close resemblance to 4, but 2 and 3 are not so evidently similar. Within the low accuracy of placing such poorly defined bands it does not seem possible to go much further with the extrapolation of the progressions.

numbering of the bands within these progressions is not. The latter depends on the intensity discontinuities at the start of each partial progression, the next band to the red being absent. This is best seen in progressions 3, 4, and 5. All these bands appear to exhibit the same behavior with respect to tem-

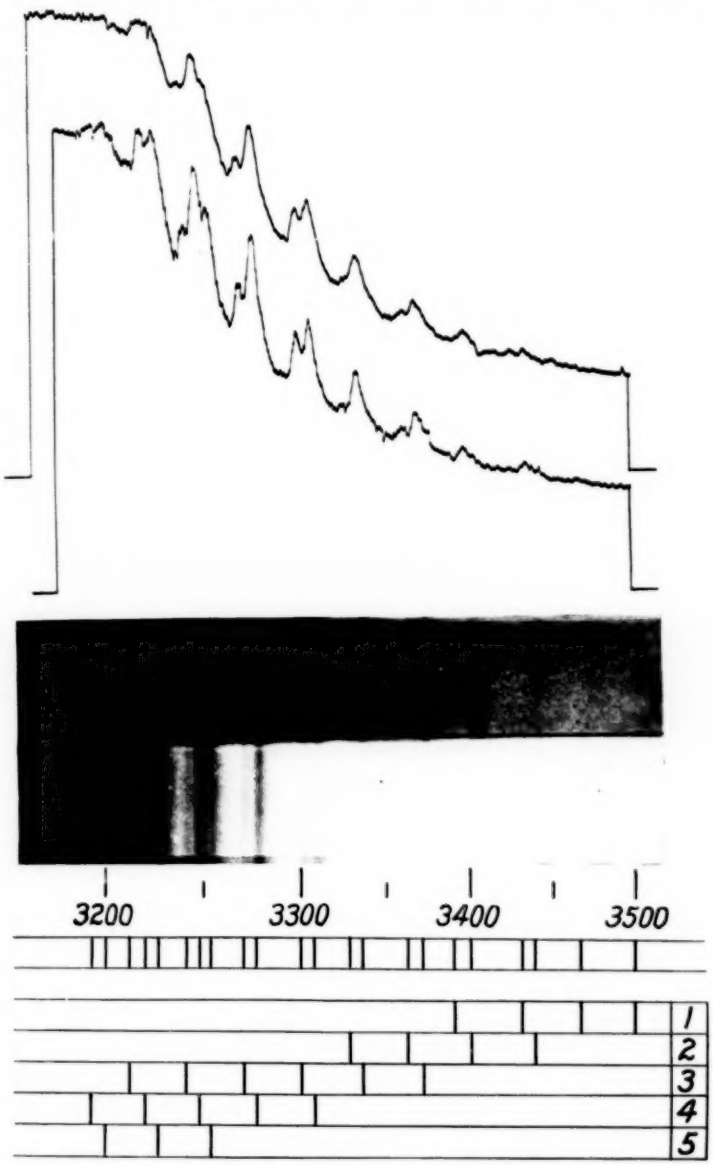

Fig. 2. Beginning of the bands in the near ultraviolet. Original photometer curves showing change in contrast, the lower at 195°K, the upper at 295°K. Note that these are not records of the illustrative exposures shown below which are of different times and both at the low temperature.

perature. Considerably further in the ultraviolet are a number of bands which, while they show some tendency toward regular spacing, may not be con-

nected with the others. These bands appear to exhibit a similar behavior with respect to temperature, though this is not certain. It seems possible that the ultraviolet absorption of ozone may consist of two electronic transitions overlaying one another. The bands in the near ultraviolet appear to establish two vibrational degrees of freedom in one excited electronic state, the transitions, as stated above, being from normal vibrational levels of very low if not the lowest energy, probably the latter.

This situation seems to offer a possible explanation for the abnormally high absorption coefficient of ozone. Its value[9] is $\alpha = 1/x \log_{10} I_0/I = 123$ at the maximum where x is in cm of pure ozone at n.t.p., while for bromine[10], for instance, a very colored gas, it is but 7. For every one transition from the lower state to one of the upper vibrational levels of a diatomic molecule there is the possibility of a series of transitions to one of the upper vibrational levels of one degree of freedom in the triatomic case and to a number of upper vibrational levels in the other degree of freedom. These bands and the continuous beyond them will overlap closely the similar sets built on the other vibrational levels of the first degree of freedom due to the small energy separation of the vibrational levels, leading, it would seem, to the possibility of a very much higher over all absorption coefficient than would be expected for a similar transition in a diatomic molecule.

This influence of temperature upon the ozone spectrum may affect somewhat the estimation of the amount of ozone in the upper atmosphere which depends upon the values of absorption coefficients measured in the laboratory. While the effect is not large it may be of importance, especially in the method of estimation which uses the difference in intensity of solar radiation at two wave-lengths at one time. The effect would be greatest if these wave-lengths happened to be located one in a band edge and the other well in a minimum of absorption between bands. The measurements indicate at present that this might be as great as a variation of ten percent in the ratio of $\log I_1/I_2$ for the range from room temperature down to $-78°$C. If such a variation in temperature occurs in the ozone layer this effect could account for a part of the apparent variations in the amount of ozone from day to day. It might also account in part for any differences found to exist in the values determined for a series of wave-lengths on any one day from a number of photographs. Depending of course upon the actual variations in temperature of the upper atmosphere the effect might be correspondingly greater or less than that estimated above for a temperature range of 100° in the neighborhood of 0°C.

It should be pointed out particularly that only the temperature effect has been considered here and that if there is also an effect of pressure upon the absorption this would further complicate the matter. (See Ladenburg, ref. 2.)

In conclusion, it does not seem hopeless to attempt to obtain some idea of the temperature of the atmospheric ozone from a study of the intensity distribution in the ozone bands at the edge of solar or stellar spectra. The change

[9] Fabry and Buisson, ref. 2.

[10] Ribaud, Ann. de phys. **12,** 107 (1919).

in contrast shows sufficiently on the laboratory plates to judge, for example, whether the ozone used in a particular exposure was at a temperature considerably below zero centigrade or considerably above.[11] Thus, unless the presence of the Fraunhofer lines and some further factor such as a pressure effect complicates the procedure too much, it should be possible to gain a rough idea of the temperature at the height of the ozone layer from a careful comparison of the ozone bands on solar plates with those taken under known conditions of temperature in the laboratory.

[11] An observation of Fowler and Strutt is of interest in this connection. They state "The bands as a whole are more diffuse in the photograph of Sirius than in the laboratory spectra, · · · " (Proc. Roy. Soc. **93**, 584 (1917)). Thus, barring other complications, this might be taken as indicating a temperature greater than room temperature in the ozone layer at some 50 km altitude. This is, of course, an observation made at night.

CONCERNING THE REFLECTION POWER OF METALS IN THIN LAYERS FOR THE INFRARED

By R. Bowling Barnes* and M. Czerny
Physikalisches Institut der Universität Berlin

(Received May 8, 1931)

Abstract

The reflection power of metals for the infrared and the visible spectra has been studied with special regard to the dependence of R upon the thickness of the reflecting layer. A new equation governing this relation has been developed.

THE annoying fact that silvered surfaces, such as those used in infrared spectroscopy, tarnish rather rapidly when exposed to the gases usually present in laboratory air, has started many infrared experimenters on the search for a remedy or a substitute for silver. The results of these investigations are much varied. Some have found relief by simply covering the freshly silvered surface with an extremely thin protective film of collodion. Others[1] have suggested distilling a thin layer of quartz upon the surface in order to prevent the harmful gases from coming into contact with the metal. The majority of investigations however have been concerned with the use of some metal other than silver, such as gold, platinum, steel, antimony and many alloys.

We found here in this institute an antimony mirror which had been exposed to laboratory gases for two years. As this still appeared perfectly fresh and showed absolutely no traces of tarnish, we at once decided to antimony our spectrometer mirrors. The process which we used, distillation in high vacuum, though apparently simple, presented a number of very interesting complications which we wish to describe at this time.

The apparatus used embodied the essential features described in the papers of Pohl and Pringsheim,[2] Pfund,[3] Burger and van Cittert,[4] and Murmann.[5] It consisted chiefly of a bell jar, evacuated to approximately 10^{-4} mm, in which the distillation was effected. Bits of metallic antimony were contained in a small quartz tube or oven of 2 mm inside diameter, which was heated to a bright red by a spiral of tungsten wire. Above this oven, which was mounted vertically, the glass surface which was to be coated with antimony was supended. To obtain a deposit of uniform thickness the distance from the oven to the glass surface had to be about 10 cm. Precaution had to be taken in heating the oven, for if it was too rapidly or too unevenly heated the bits of antimony were shot out as if from a cannon.

* International Research Fellow.

[1] H. C. Burger and P. H. van Cittert, Zeits. f. Physik **66,** 218 (1930).

[2] R. Pohl and P. Pringsheim, Verh. d. D. Phys. Ges. **14,** 46 (1912).

[3] A. H. Pfund, R.S.I. **1,** 397 (1930).

[4] H. C. Burger and P. H. van Cittert, reference 1.

[5] Hans Murmann, Zeits. f. Physik **54,** 741 (1929).

As the process begins the antimony condenses as a thin highly transparent metallic film, of a light brownish color. This gradually increases in opacity and reflection power remaining always quite uniform in its appearance. At a certain stage in the process, depending upon the speed with which the distillation is carried on, the surface remains no longer uniform but becomes covered with spots. These are always round, more opaque than the surrounding layer, and have a relatively high reflection power. With the appearance of these spots the process should at once be interrupted and the mirror removed from the apparatus. If this is done at the right time, these spots, which we shall refer to as the second modification of antimony, increase in number, and expand always however remaining circular in form. They merge one with another to form larger areas, and after a period of time varying from 5 minutes to half an hour, this process completes itself and the mirror is composed entirely of the second modification. This is obviously the desired modification for it is more opaque and possesses for visible light a much higher reflection power than the first layer which forms. By gently warming the glass the speed of this transformation from the first modification into the second can be greatly increased.

If, however the distillation process is allowed to continue after the formation of these spots, another series of changes takes place. While the process is going on the spots increase in size and number and merge to form larger spots just as before. In addition, however, some kind of a "third modification" begins to form as a dark speck at the centers of the original spots. These specks, usually about 0.5 mm in diameter, do not increase in size, but remain fixed. When the mirror is finally taken out of the vacuum the second modification grows a bit, but usually not sufficiently to cover the entire mirror, with the result that in the end one has a mirror consisting of what is apparently three distinct forms of antimony.

This process of spot formation is exactly the same that found by Murmann[6] and described by him in detail. He investigated carefully some of the optical and electrical properties of the first and second forms of the antimony and as a result of his studies believed that the first form was an unstable amorphous modification which changed over into the stable crystalline second form. Evidence was also found by him for the existence of two analogous modifications in the case of silver. In all cases he found that the physical properties of the various modifications were radically different.

The spectrometer was equipped with three concave and two plane mirrors prepared in the manner described above, all five being of the so-called second form of antimony. These mirrors appeared to be optically perfect, however, when the instrument was tested for radiation of 52μ wave-length, the microradiometer deflections were entirely unsatisfactory, being extremely small. This suggested that one or more of the mirrors had for these wave-lengths an exceptionally low reflection power, for the same instrument equipped with silver mirrors had previously given nice deflections.

[6] Hans Murmann, reference 5.

In order to investigate this point a rocksalt reststrahlen apparatus, shown in Fig. 1, was assembled and for each of the mirrors the percentage reflection was roughly determined. Each mirror was in turn substituted for the freshly silvered plane mirror M_2, whose reflection power was assumed to be 100 percent. Since the effect for which we were looking was so large, the errors introduced by the approximations made in these measurements played a very small role. The results were rather surprising. The four antimony mirrors had reflection powers ranging from 42 percent to 80 percent, while a platinum mirror had $R=92$ percent and an old badly tarnished silver mirror, 96 percent.

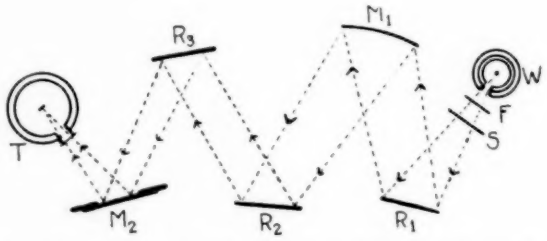

Fig. 1. Reststrahlen apparatus. W = Welsbach mantel, F = soot filter, R = rock-salt plates, T = microradiometer, S = glass shutter, M = silver mirrors.

The well-known formula for the reflection power of metals taken from Drude, reads

$$R = 100 - \frac{200}{(\sigma T)^{1/2}}$$

where σ is the conductivity expressed in e.s.u., and T is the period of the incident electromagnetic wave. This can also be expressed in the form,

$$R = 100 - \frac{36.5}{(x\lambda)^{1/2}}$$

where x is the reciprocal of the resistance in ohms for a conductor 1 m long and 1 mm cross-section, and λ is the wave-length expressed in μ. Taking for x the value $1/0.4$ or 2.5, we should expect antimony to have a reflection power for $\lambda = 50\mu$ of 96.7 percent. Rubens and Hagen[7] in their work on the reflection power of metals did not measure antimony. However, from their work on other metals we know that the above formulas are accurate, and therefore theoretically we should expect an antimony mirror to have a reflection power throughout the far infrared of over 90 percent. Why then these particularly low values at 52μ?

The value taken for x, the conductivity, in the above equation was of course measured on massive antimony. If in such thin sheets prepared as described above the conductivity should be exceptionally low, then such low values of R could result. Indeed Murmann found that the resistances of mirrors of the first modification of antimony were in the order of 10^5 ohms. These

[7] H. Rubens and E. Hagen, Ann. d. Physik **8**, 1 (1902).

same mirrors, after the transformation to the second modification was complete, showed resistances of only 10^2 ohms. This, assuming that the thicknesses were in the two modifications the same, indicated that the value of the conductivity of the first form was extremely small in comparison with that of the second modification. Our mirrors, though all of the second form may still have possessed smaller values of x than 2.5.

Further discussion of this problem, however, led us to a new and entirely different question regarding the reflection power of metals. To just what extent and in what manner does the reflection power depend upon the thickness of the reflecting layer? From Drude we took as a starting point the equation expressing the ratio of the reflected amplitude to the incident amplitude in the case of non-absorbing substances.* This formula, as stated by Drude in his "Lehrbuch der Optik," reads

$$\frac{E_n}{E_i} = \frac{(e^{ip} - e^{-ip})(\epsilon_1 - \epsilon_2)}{e^{ip}(\epsilon_1^{1/2} + \epsilon_2^{1/2})^2 - e^{-ip}(\epsilon_1^{1/2} - \epsilon_2^{1/2})^2}. \tag{1}$$

where E_r is the reflected amplitude; E_i the incident amplitude; ϵ_1 the dielectric constant of medium 1; ϵ_2 the dielectric constant of medium 2; $p = 2\pi d/\lambda(n - ik) = \alpha - i\beta$; $\alpha = 2\pi nd/\lambda$; $\beta = 2\pi kd/\lambda$. In our particular example, i.e., a metal surface in air, we can set

$$\epsilon_1 = 1 \text{ and } \epsilon_2^{1/2} = n - ik$$

where n and k are the optical constants of the metal in question. Rewriting Eq. (1), we get

$$\frac{E_r}{E_i} = \frac{(e^{i\alpha}e^{\beta} - e^{-i\alpha}e^{-\beta})(1 - n^2 + k^2 + 2ink)}{e^{i\alpha}e^{\beta}(1 + n - ik)^2 - e^{-i\alpha}e^{-\beta}(1 - n + ik)^2}. \tag{2}$$

If this equation is now multiplied by its complex conjugate, we then have

$$\frac{E_r^2}{E_i^2} = \frac{[e^{2\beta} + e^{-2\beta} - 2\cos(2\alpha)][(1 - n^2 + k^2)^2 + 4n^2k^2]}{e^{2\beta}[(1+n)^2+k^2]^2+e^{-2\beta}[(1-n)^2+k^2]^2-2\cos(2\alpha)[(1-n^2-k^2)^2-4k^2]} \\ \overline{-2\sin(2\alpha)[4k(1 - n^2 - k^2)]}. \tag{3}$$

Setting

$$[(1 + n)^2 + k^2] = U$$
$$[(1 - n)^2 + k^2] = V$$

and introducing an angle ψ, defined by

$$\tan\psi = \frac{2k}{n^2 + k^2 - 1}$$

Eq. (3), by the application of a trigonometric transformation, becomes,

$$R = \frac{E_r^2}{E_i^2} = \frac{[e^{2\beta} + e^{-2\beta} - 2\cos(2\alpha)]UV}{e^{2\beta}U^2 + e^{-2\beta}V^2 - 2UV\cos(2\psi)\cos(2\alpha) + 2UV\sin(2\psi)\sin(2\alpha)} \tag{4}$$

* This equation takes into account possible interference effects arising from multiple reflection of the radiation between the two surfaces of the non-absorbing body.

or

$$R = \frac{[e^{2\beta} + e^{-2\beta} - 2\cos(2\alpha)]UV}{e^{2\beta}U^2 + e^{-2\beta}V^2 - 2UV\cos 2(\alpha+\psi)} \tag{5}$$

Applying now the formula

$$\cos 2x = 1 - 2\sin^2 x$$

we get the final expression

$$R = R_\infty \frac{(e^{\beta} - e^{-\beta})^2 + 4\sin^2\alpha}{(e^{\beta} - R_\infty e^{-\beta})^2 + 4R_\infty \sin^2(\alpha+\psi)} \tag{6}$$

where

$$R_\infty = \frac{(n-1)^2 + k^2}{(n+1)^2 + k^2} = \frac{V}{U}$$

$$\alpha = \frac{2\pi n}{\lambda} d \qquad \beta = \frac{2\pi k}{\lambda} d$$

$$\tan\psi = \frac{2k}{n^2 + k^2 - 1}$$

This Eq. (6), is the general expression giving the reflection power of a plane parallel plate of an absorbing substance as a function of the plate thickness, d. That it expresses correctly the extreme cases can easily be seen. Since d enters only in α and in β it is clear that

(1) when $d \ll \lambda$, i.e. an extremely thin plate, α and β will each be equal to zero, and therefore R will be also zero.

(2) when $d \ll \lambda$, or in case of a very thick plate, the terms $4\sin^2\alpha$ and $(4R_\infty \sin^2(\alpha+\psi))$ may be neglected in comparison with the exponential terms. Also the negative exponentials vanish, leaving the result $R = R_\infty$.

Using this equation we have made calculations of several interesting numerical examples. With values of n and k so chosen as to typify both good and

TABLE I. *Calculated reflection powers and percentage transmissions as functions of the thickness of the metal layer. d = thickness in μ, R = percentage reflection, D = percentage transmission.*

← λ = 0.59μ →						← λ = 25μ →								
$n=0.18$, $k=3.67$			$n=3.04$, $k=4.94$			$n=k=40$			$n=k=70$			$n=k=200$		
d	R	D	d	R	D	d	R	D	d	R	D	d	R	D
.0051	12.98	82.3	.0019	6.8	58.3	.001	12.7	79.0	.00056	16.8	33.8	.00019	40.7	11.4
.0128	48.0	45.4	.0095	42.2	13.7	.005	44.6	11.0	.00284	61.0	4.7	.00099	81.4	9.0
.0256	79.2	14.7	.019	64.7	4.4	.01	65.4	4.0	.00568	77.5	1.5	.00199	90.1	2.5
.0503	93.1	1.8	.0285	68.4	1.48	.02	79.0	1.2	.0114	88.3	.4	.0039	94.7	.7
.128	95.1	—	.038	70.0	.6	.05	90.9	.2	.0284	97.0	—	.0099	97.6	—
						.10	94.3	—	.0568	97.1	—	.0199	98.7	—

← λ = 50μ →														
$n=k=10$			$n=k=30$			$n=k=60$			$n=k=100$			$n=k=300$		
d	R	D	d	R	D	d	R	D	d	R	D	d	R	D
.0398	4.47	31.0	.01	28.3	22.0	.0066	61.5	6.9	.0008	20.3	38.5	.00026	62.7	8.1
.0797	13.25	13.2	.0265	54.9	6.1	.0132	72.5	2.6	.0039	69.5	2.6	.0013	89.4	.4
.1594	31.3	7.8	.053	73.0	2.0	.0264	85.2	.6	.008	83.5	.8	.0026	94.0	—
.318	63.9	4.0	.10	84.6	.6	.066	93.4	—	.02	92.7	.1	.0066	97.4	—
.637	78.0	1.2	.417	92.9	—	.132	96.4	—	.04	96.2	—	.0132	98.8	—
.797	81.2	.7							.08	97.5	—	.026	99.1	—

bad conductors, we have calculated R as a function of the thickness d for $\lambda = 0.59\mu$, 25μ and 50μ. To supplement these values of R, we have also in every

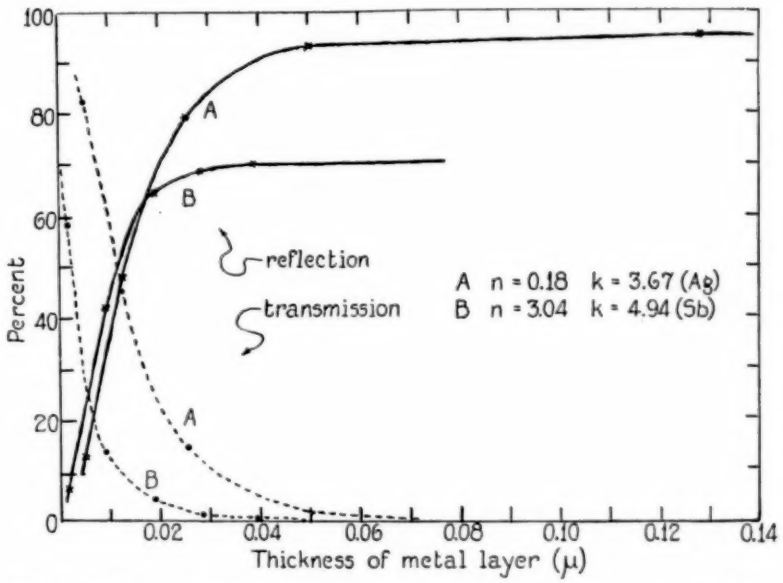

Fig. 2. Calculated reflection powers and percentage transmission for $\lambda = 0.59\mu$ as functions of the thickness of the metal layer.

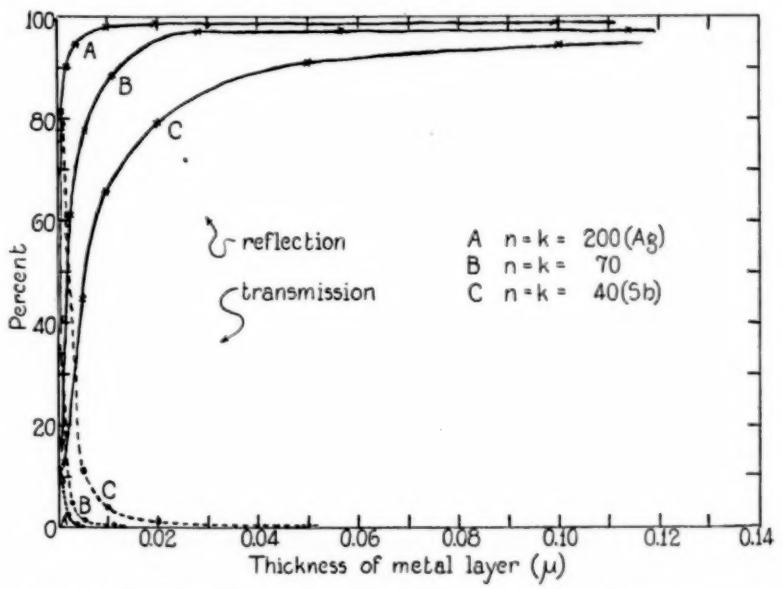

Fig. 3. Calculated reflection powers and percentage transmission for $\lambda = 25\mu$ as functions of the thickness of the metal layer.

case given the percentage transmission D, for the calculation of which an equation exactly analogous to the reflection power equation was used. This is

essentially the same as that used by Czerny[8] and by Murmann and, with the same abbreviations as are noted above, it reads

$$D = \frac{(1 - R_\infty)^2 + 4R_\infty \sin^2\psi}{(e^\beta - R_\infty e^{-\beta})^2 + 4R_\infty \sin^2(\alpha + \psi)} \tag{7}$$

In making these calculations we made use of the fact that in the region of long wave-lengths $\kappa = 1$. From this it follows that $n = k$. Further, if we neglect the effect of terms of higher orders, we can also set $n^2 = \sigma\tau$ (where σ is again the conductivity expressed in e.s.u. and τ is the period of the incident radiation).

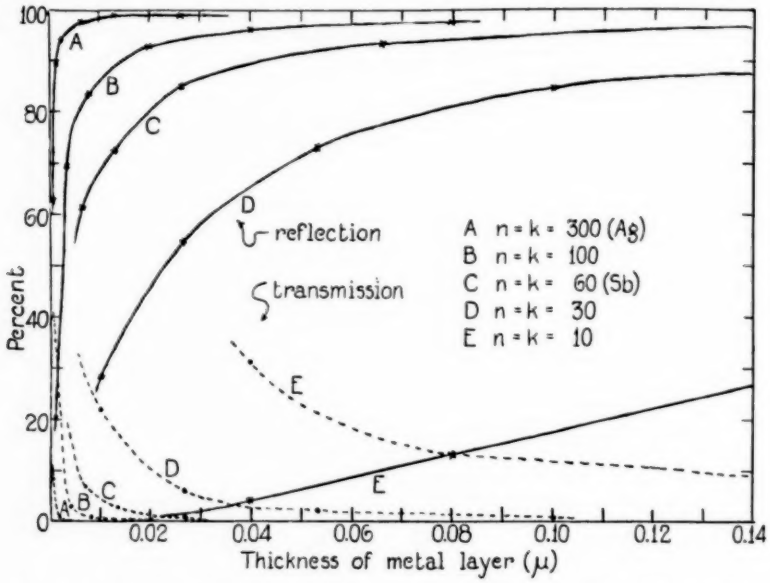

Fig. 4. Calculated reflection powers and percentage transmission for $\lambda = 50\mu$ as functions of the thickness of the metal layer.

From this latter condition we find that for $\lambda = 50\mu$ the refractive index of silver is equal to 307, while for antimony $n = 61$. For $\lambda = 25\mu$, these values are $n = 217$ and $n = 43$ respectively. Certain examples were therefore calculated and the results are given in Table I and Figs. 2, 3 and 4. The extent and manner in which the reflection power depends upon the thickness of the metal layer as is indicated by these calculations is rather surprising. For a given mirror to be "suitable" for use in any particular spectral region, we shall require that it be thick enough to have let us say, 99 percent of its R_∞ for those wave-lengths. Hence in discussing the calculations mentioned we shall center our attention only upon those thicknesses for which $R = 0.99\ R_\infty$.

From the tables and curves we find the following results for silver;

(1) For $\lambda = 0.59\mu$ $d = 0.080\mu$

(2) " $\lambda = 25\mu$ $d = 0.010\mu$

(3) " $\lambda = 50\mu$ $d = 0.012\mu$

[8] M. Czerny, Zeits. f. Physik **65**, 600 (1930).

This means that a silvered mirror 0.012μ thick, while it is for visible light still 40 percent transparent and has a reflection power of only 0.45 R_∞, is according to our above requirement perfectly suitable for use in the far infrared. For use in the visible spectrum the layer of silver must be at least 6 times as thick as that required of a silver mirror intended for infrared use.

However, when we examine the case of antimony, a poorer conductor, we find that the thickness plays a very different role and the above relations are almost exactly reversed. We see that for antimony

(1) For $\lambda = 0.59\mu$ $d = 0.032\mu$

(2) " $\lambda = 25\mu$ $d = 0.10\mu$

(3) " $\lambda = 50\mu$ $d = 0.11\mu$

Thus an antimony mirror 0.03μ thick is just opaque for visible light, and has in this region $R = 0.99\ R_\infty$. The same mirror however has for the infrared $R = 0.90\ R_\infty$ and is therefore unsuitable. The antimony layer if it is to be used in the infrared must be at least 3 times as thick as that which is suitable for use in visible light.

Comparing these two cases we see that for use in the visible spectrum the thickness required for a suitable silver mirror is about 2 times that required for an antimony mirror. On the other hand however, for use in the infrared an antimony mirror must be about 10 times as thick as a suitable silver mirror.

By weighing two of our mirrors before and after the removal of the antimony layer, we found that the thicknesses of the latter were 0.19μ and 0.18μ respectively. From our curves we should expect mirrors of these thicknesses to have their full reflection power, or in this case 96.7 percent. These two however, according to our rough measurements had reflection powers of only 77 percent and 74 percent respectively.

The reflection power for such thin metal layers is a complicated function of σ, n and k, and through them of d, the layer thickness. Low values of R, assuming that the polish of the surface is perfect, must be attributed to the influence of some one or some combination of these quantities. In all of the above discussions and calculations we have assumed that metals in these thin layers possessed normal values of σ, n and k. It is entirely possible, however, and even probable, that σ for the second modification of antimony is still lower than the normal value. The optical constants too, due to the manner in which the mirrors were prepared and to the extreme thinness of the layers may vary somewhat from the accepted values.

As the questions raised by these observations in regard to the reflection power of metals in thin layers are still unsettled it is planned that further work along this same theme shall be carried out in this institute, and it is hoped that by obtaining more exact values of R, σ, n, k, and d answers to all of these questions may be found.

STEREOPHOTOGRAPHIC MODELS OF ELECTRON MOTION IN STARK EFFECT

By R. W. Wood
Johns Hopkins University, Baltimore, Maryland

(Received June 4, 1931)

Abstract

By means of multiple exposures with a stereoscopic camera of a rotating wire frame representing the curved quadrangle formed by the intersection of the parabolic coordinates of the Epstein-Schwarzchild treatment of the Stark effect, within which quadrangle the electron is progressively advanced along a properly curved wire, the orbital motion within the anchor-ring is very clearly brought out. The pictures when viewed with a stereoscope show the anchor-ring as a wire cage within which the precessing orbit appears as a white dotted line. The change in orientation and eccentricity of the orbit, with the constancy of the distance of the electric center from the YZ plane (field parallel to X) is easily seen. Photographs are shown illustrating various assignments of the quantum numbers n_1 and n_2.

THE motion of the electron in space in the Stark effect, as brought out in the well-known treatments of Schwarzchild and Epstein, (referred to parabolic coordinates) is impossible to visualize and cannot be shown by any two-dimensional diagram. It occurred to me, in working over the subject, that a stereoscopic diagram could be built up by multiple exposures which would show the "anchor-ring" formed by the rotation of the parabolic quadrangle about the nucleus and the path of the electron within it. The quadrangle formed by the intersection of four parabolas is shown in Fig. 1, taken

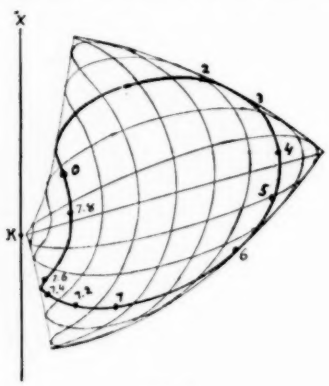

Fig. 1.

from a paper by Buchwald.[1] The electron moves within this quadrangle along the line indicated, covering eventually the entire surface. At the same time the quadrangle is rotating about the line Kx parallel to the electric field, k being the nucleus. The electron must reach the apices of the four angles of

[1] Buchwald, Ann. d. Physik **81,** 958 (1926).

the quadrangle, its motion referred to the quadrangle being along a line (straight or curved) joining opposite angles. This line then opens out into a curve which is tangent always to the four sides of the quadrangle, the curve

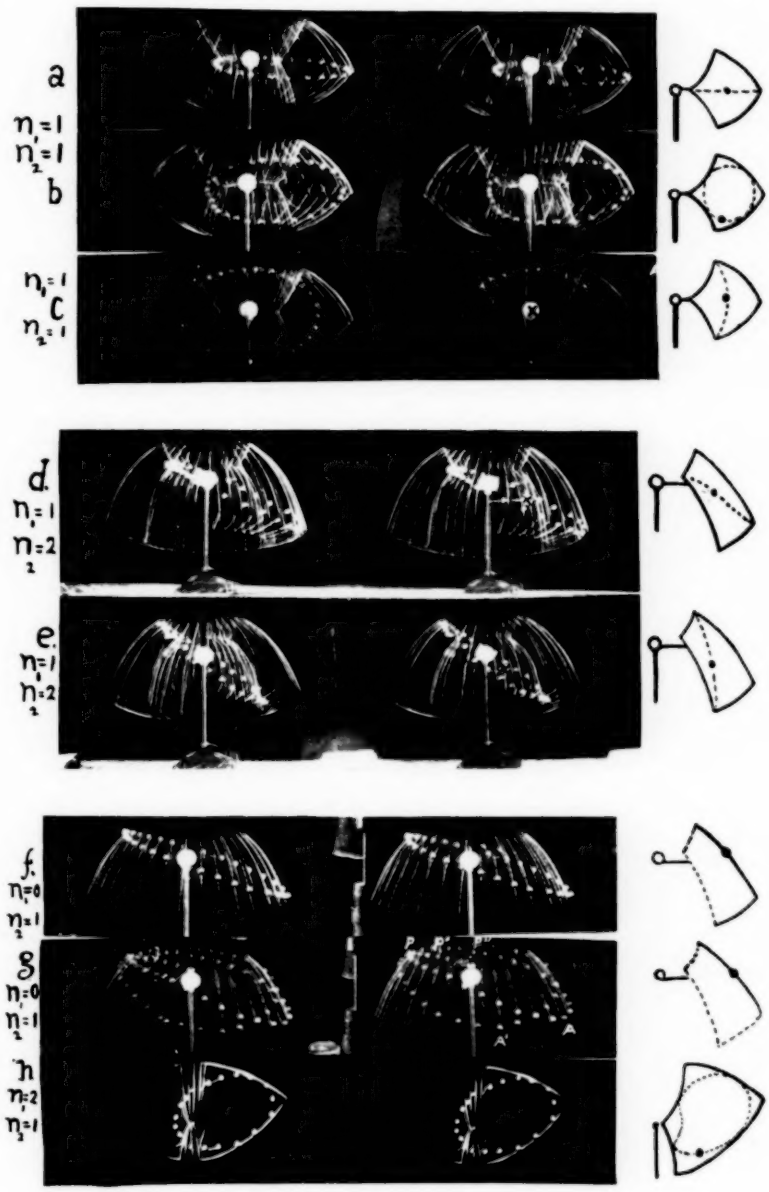

Fig. 2.

gradually changing its form until it collapses to a line joining the other two angles, as indicated in Fig. 1. During these changes the quadrangle is rotating about the x-axis, which makes the actual path of the electron in space ex-

tremely complicated for it must eventually make contact with every point on the surface of the anchor-ring. The photographs reproduced in Fig. 2 show this path very clearly if viewed with a stereoscope. Being considerably reduced in the reproduction, the two pictures are more easily brought together without a stereoscope (by viewing with eyes directed for distance view) than the usual stereoscopic photographs. They were prepared by making a wire frame of the form of one of the parabolic quadrangles arranged to rotate about a vertical axis. Within this quadrangle a curved loop, (or line) of thinner wire was mounted, on which a small ball of white wax (the electron) could be moved. A wire index and a circle graduated into 32 equal parts at the base made it possible to rotate the frame by equal jumps, the electron being advanced a suitable distance along its wire (line or loop) for each advance of the quadrangle in its circuit around the nucleus. (See Fig. 3.).

The apparatus was mounted in a strong light, in front of a black background (the open door of a large dark room) and successive exposures made with a stereoscopic camera, one for each advance of the rectangle and electron. The anchor-ring is thus built up step by step, the path of the electron within it appearing as a white dotted line within a wire cage when the picture

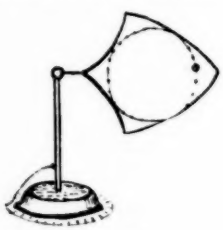

Fig. 3.

is viewed with a stereoscope. This method can doubtless be used in other ways, for example, in the preparation of stereoscopic models of crystals, a single frame on which the atoms can be suitably arranged being moved obliquely backwards.

Buchwald's paper had escaped my notice at the time the models were constructed, and was subsequently brought to my attention. As I could find no data on the form of the loops within the quadrangle or the rate of motion along different portions of the loop or line, I was obliged to space off the distances more or less by guess work. One model was, however, made from the data given in Buchwald's paper and is shown as Fig. 2h.

Two parabolic wire rectangles were constructed, representing two different quantum relations. We will take first the condition $n_2 = n_1 = 1$ which gives us $n_2 - n_1 = 0$ or no energy change, the electric center being neither up nor down field. The three photographs *a*, *b*, *c* illustrate this condition, the path along which the electron was moved, as the quadrangle was rotated being indicated by the diagram to the right. The two periods were made equal in this case, i.e. the number of divisions along the electron's path were equal to the number of steps into which the 360° rotation of the quadrangle was divided. This gives the electron a closed orbit, and corresponds to zero field. In the upper figure, in

which the electron was moved to and fro once along the horizontal wire during one complete rotation, the orbit is an ellipse lying in the yz plane with the nucleus at one focus and the electric center at x, also in the yz plane and therefore neither up nor down the field, as required for $n_2 - n_1 = 0$. The divisions on the wire were spaced as representing approximately simple harmonic motion, corrected by trial and error in the case of the horizontal wire, to take care of the more rapid motion at perihelion.

If we join the other two corners with a straight wire, and repeat the experiment, the electron path will be an ellipse (as a little calculation shows) with the nucleus at the *center* an impossible motion. In this case, Fig. 2c, the orbit must be a circle, and a little consideration shows us that the line joining the upper and lower angles must be the arc of a circle, whose center is the nucleus. As the electron is moved along this wire and the frame rotated, the electron's distance from the nucleus is constant, and its orbit is a circle inclined at an angle to the electric field. In both of these limiting cases, the electric center marked with a cross lies in a horizontal plane passing through the nucleus, that is, it is neither up field nor down field. In the transition stages (b) in which the horizontal line opens out into a loop, tangent to the parabolic rectangle at four points, for each circuit around the rectangle, the orbit in space passes gradually from the elliptical to the circular form, reaching its maximum inclination to the field when the loop has contracted to the circular arc joining the upper and lower angle. The electric center coincides with the nucleus in this case. If we make the period of revolution of the quadrangle equal to the period of the motion within the rectangle, the change in the shape and orientation of the orbit will not be progressive, i.e., there will be no precession, for if we start by moving the electron along the horizontal wire, and pass gradually to the vertical arc, and then back to the horizontal wire, our orbit is at first an ellipse with the perihelion to the left of the nucleus, changing to the inclined circle after which the motion retrogrades back to an ellipse with the perihelion placed as at the start. As a matter of fact the two periods are not equal, (except for zero electric field) and the transition from the horizontal to the vertical motion in the quadrangle occurs only as a result of the field.

In taking a photograph to show the precession of the orbit we must therefore divide our circle of rotation into, say 32 equal parts and our electron path on its wire into, say 28 properly spaced divisions. The orbit, no longer truly elliptical, precesses and at the end of a complete cycle in the quadrangle the perihelion of the ellipse will have rotated one eighth of a complete revolution. In reality the difference of period is much smaller.

For the quantum relation $n_1 = 1$, $n_2 = 2$ we have the parabolic quadrangle as shown by Fig. 2d and e.

The orbit is now very much inclined to the field, the electric center being displaced "down field." These photographs also were taken with the two periods equal (condition for zero field) and illustrate the orbital positions for one trip of the electron around or across the quadrangle. Here we notice that the electric center, marked with a cross, remains at a constant distance

down field from the nucleus in spite of the change of inclination of the orbit, for as the orbit becomes more inclined, the ellipse becomes less eccentric (shown in the photographs by the position of the nucleus) and the electric center approaches the nucleus, thus compensating the effect of the increasing inclination of the orbit, the major axis remaining unchanged.

To show the precessing orbit in space for several complete cycles in the rectangle, we must make the periods unequal and employ at least two complete revolutions of the quadrangle about the nucleus. The easiest way to accomplish this is to take the case $n_1=0$, $n_2=1$, which causes the two ξ parabolas to fuse to a single one, the electron travelling about over the surface of this *paraboloid* between the two circular sections cut by the η parabolas. In this case we have only to make our electron travel to and fro along the outer parabolic arc of the unsymmetrical rectangle just mentioned. This was divided into 28 properly spaced divisions, and two complete revolutions given to the rectangle, with two to-and-fro trips of the electron along the arc. Fig. 2g was made in this way, while 2f shows the elliptical orbit made under the same conditions, but with the two periods equal, i.e., with the wire divided into 32 divisions. The latter gives a very clear idea of the complicated form of the orbit even under this simpler condition. In Fig. 2g the path starts at the back just above the nucleus and curving to the left around the paraboloid passes just below the nucleus at the front, aphelion being at A. In its second circuit, it crosses the first part of the path at P, the perihelion point of the first loop, and reaches aphelion at A', the end of the path, in counter clockwise direction as viewed from above.

In the cases in which the motion is within the anchor-ring, the eccentricity and orientation change continuously and the electric center moves with simple harmonic motion in an elliptical orbit parallel to the zy plane.

Fig. 2h is a photograph made with a wire frame and loop made from Buchwald's figure for the quantum relation $n_1=2$ and $n_2=1$. The loop orbit in the parabolic rectangle has the shape of an artist's palette, and the positions of the electron on the loop are shown in Fig. 1. Buchwald gave the angles through which the rectangle must be rotated for each advance of the electron, and a paper circle graduated into 360° was accordingly used in this case. The wire cage is not as well defined as in the other photographs, as the angular rotations were very large at one place and very small at another as shown by Table I. Starting the electron at O, and with the pointer on the zero of the graduated scale, we have

TABLE I.

0–1	106°	6 –7	158°
1–2	121°	7 –7.2	168°
2–3	127°	7.2–7.4	203°
3–4	131°	7.4–7.6	297°
4–5	135°	7.6–7.8	307°
5–6	140°	7.8–0	360°

The elliptical orbit of the electron is very perfectly brought out.

THE CRYSTAL STRUCTURE OF ARSENIC TRIIODIDE, AsI_3

By Dorothy Heyworth
Ryerson Physical Laboratory, University of Chicago

(Received June 1, 1931)

Abstract

The crystal structure of arsenic triiodide has been investigated by means of Laue, powder, and oscillation photographs. It is shown to be a layer lattice. The underlying lattice is Γ_{Th} and the space group C_{3i}^2. The unit rhombohedron has dimensions $r = 8.25$A and $\alpha = 51°20'$; there are two molecules to the unit cell. The coordinates of the atoms are arsenic $\pm uuu$ where $u = 60°$; iodine $\pm xyz$, $\pm zxy$, $\pm yzx$ where $x = 152°$, $y = 28°$, $z = -90°$. Distances of closest approach of iodine are about 4.28A and 4.13A and of arsenic and iodine about 2.97A. The iodine ions are in hexagonal close packing; each arsenic ion is surrounded by six iodine ions.

THE majority of compounds which have a simple chemical composition have already been examined by x-rays and their structure determined. But those substances which have the general formula AX_3 are still to some extent unexamined because they are difficult to work with and prepare. They are frequently unstable, deliquescent, or occur only in the powdered state. However crystals of arsenic triiodide are easily prepared and although oxidized somewhat in air this is not sufficient to cause any real difficulty.

Material

The crystals of arsenic triiodide used in the investigation were prepared by dissolving powdered arsenic triiodide in carbon disulphide and allowing the solution to evaporate slowly in a crystallization dish. The crystals so obtained were thick tablets of a beautiful ruby red colour.

Crystallographic and Physical Properties

Arsenic triiodide belongs to the hexagonal system. Groth[1] gives $a:c = 1:2.998$ corresponding to $\alpha = 51°20'$.

The angles on the crystal faces developed were measured on a Pye gonio meter and referring to Groth two of the crystal faces were found to be 111, and 110. A stereographic projection showed a third face to lie at the intersection of two known zones and its indices were found to be 001. The crystals show good cleavage parallel to the 111 face. They are apt to twin and for this reason some of the crystals could not be used. The density of the arsenic triiodide crystals is 4.39.[2]

X-Ray Investigation

Laue photographs were taken with molybdenum radiation with the incident beam perpendicular to the basal plane. They showed a three-fold axis of symmetry. Oscillation photographs were obtained about the a axis. Because

[1] Groth, Chemische Kristallographie **1,** 226.

[2] International Critical Tables, German b table No. 269 p. 110. Vol. 1.

of the large absorption the photographs so obtained were poor and not much information was derived from them. Molybdenum radiation was used. Several powder photographs were also taken using molybdenum radiation.

The Unit Cell

A measurement of values for the layer lines of rotation photographs about the a axis gave $a_0 = 7.10$A. Using the axial ratio $1:2.998$ $c_0 = 21.30$A.

H. Braekken,[3] who has been working on the structure of arsenic, antimony, and bismuth triiodides, and who evidently had better rotation photographs gives $a_0 = 7.187 \pm 0.003$A and $c_0 = 21.394\text{A} \pm 0.010$A for arsenic triiodide. These latter values were used in assigning indices to the lines of the powder photographs and new values of a_0 and c_0 then deduced from the powder photographic data.

Sodium chloride was used as a standard, the value of the angle of reflection, θ, for each of the sodium chloride lines being known accurately. The distances between each sodium chloride line and adjacent arsenic iodide lines were then measured and the radius of the camera being known (20.39 cm) the difference between θ for each arsenic iodide line and the nearest sodium chloride line was calculated. Thus a more accurate value of θ for each arsenic iodide line was obtained than if the distance from the zero to each arsenic iodide line had been measured.

In order to index these lines, the value of $\sin^2\theta$ for each line was compared with a list of theoretical values of $\sin^2\theta$ for known planes.

For the hexagonal unit,

$$\sin^2\theta = K_1(h^2 + hk + k^2) + K_2l^2$$

where $K_1 = \lambda^2/3a_0^2$, $K_2 = \lambda^2/4c_0^2$ and h, k, l are the hexagonal indices of the plane.

Thus $\sin^2\theta$ can be calculated for any plane. In this way planes were indexed as follows:

Exptl. $\sin^2$	Th. $\sin^2$	Plane hex.	rh.	Int. (estimated by eye)
0.00986	0.00975 0.01008	1120 0006	101 222	8
0.01210	0.01227	1123	210	10
0.01975	0.01983	1126	321	$6\frac{1}{2}$
0.02908	0.02925	3030	311	$7\frac{1}{2}$
0.03227	0.03243 0.03177	1129 3033	432 300	$5\frac{1}{2}$
0.03906	0.03900 0.03933	2240 3036	202 411	6
0.04160	0.04152 0.04032	2243 00012	311 444	5
0.04909	0.04908	2246	420	2
0.06128	0.06168	2249	531	1
0.07112	0.07077	4153	401	$2\frac{1}{2}$
0.07830	0.07833	4156	510	$\frac{1}{2}$

where two theoretical values are given the line may be due to reflection from one or both planes.

[3] H. Braekken, Zeits. f. Krist. **74**, 67 (1930).

To check the cell size the experimental values of $\sin^2\theta$ for known planes were used in the above formula. With $1=0$

$$\sin^2\theta = K_1(h^2 + hk + k^2)$$

Combining results so obtained for all such planes K_1 was found to have the value 0.003267.

$$K_1 = \lambda^2/3a_0, {}^2\lambda = 0.7078A \therefore a_0 = 7.150A$$

Using other planes and knowing K_1, K_2 was found to equal 0.000276. $K_2 = \lambda^2/4c_0^2 \therefore c_0 = 21.35$A. $a_0 : c_0 = 1 : 2.986$. The Laue data check this giving $a_0 : c_0$ about 1:3.

The Lattice

The indices obtained from powder photographs are such that $2H+K=3n$ and $L=0, 3, 6, \cdots$. All the indices obtained from Laue photographs are such that h, k, l (rhombohedral indices) obtained from H, K, L (hexagonal indices) are all divisible by three. This shows that the lattice is rhombohedral, Γ_{Th} and not Γ_h.

Number of Molecules per Cell

If V is the volume of the unit cell, D the density, M the molecular weight, and H the weight of the hydrogen atom, then Z the number of molecules in the cell

$$Z = VD/MH$$

$$V = r^3 \sin^2\alpha \sin\delta'$$

where r equals the edge of the rhomb, α the rhombohedral angle, and $\sin \delta'/2 = \sin\alpha/2/\sin\alpha$.

The horizontal diagonal in the rhombohedral face is equal to the hexagonal a axis. The rhombohedral angle is 51°20′.

$$r = 7.15/2 \sin 25°40' = 8.25A$$

$$Z = (8.25)^3 \sin^2 51°20' \sin 67°23' \times 4.39/455.76 \times 1.649$$

$$= 1.86$$

i.e., there are two molecules per unit cell.

Class

The Laue photographs show that there is a three-fold axis. The possible classes to which the crystal might belong from this evidence are C_3 and C_{3i} since in Laue photographs both these appear as C_{3i}.

Space Group

The only space groups in these classes which have Γ_{rh} as the fundamental lattice are C_3^4 and C_{3i}^2.

$$C_3^4 = \left[A\left(\frac{2\pi}{3}\right), \Gamma_{rh}\right] \text{ and } C_{3i}^2 = [C_3^4 I]\Gamma_{rh}.$$

Arrangement of the Atoms

The coordinates for the general positions in the space group C_3^4 are, One equivalent position: (a) *uuu*. Three equivalent positions: (b) *xyz*, *zxy*, *yzx*. and for C_{3i}^2, One equivalent position: (a) 000; (b) $\frac{1}{2}\frac{1}{2}\frac{1}{2}$. Two equivalent positions; (c) $uuu:\bar{u}\bar{u}\bar{u}$. Three equivalent positions: (d) $00\frac{1}{2}:\frac{1}{2}00:0\frac{1}{2}0$; (e) $\frac{1}{2}\frac{1}{2}0:0\frac{1}{2}\frac{1}{2}:\frac{1}{2}0\frac{1}{2}$. Six equivalent positions: (f) $xyz:zxy:yzx:\bar{x}\bar{y}\bar{z}:\bar{z}\bar{x}\bar{y}:\bar{y}\bar{z}\bar{x}$.

All the indices of planes identified in the powder diagrams are such that $2H+K$ (hexagonal indices) is divisible by three and $L=0, 3, 6, 9, \cdots$. From this it follows that the powder films can be indexed referred to a cell with axes $a=7.150/\sqrt{3}=4.139$A and $c=21.35/3=7.12$A.

The indices referred to this small cell are

Plane	Intensity
10.0, 00.2	8
10.1	10
10.2	$6\frac{1}{2}$
11.0	$7\frac{1}{2}$
10.3, 11.1	$5\frac{1}{2}$
20.0, 11.2	6
20.1, 00.4	5
20.2	2
20.3	1
21.1	$2\frac{1}{2}$
21.2	$\frac{1}{2}$

Absent planes; 00.1:00.3:11.3.

This hexagonal cell however contains only 2/3 of a molecule of arsenic triiodide; that is 2/3 of an atom arsenic and two atoms iodine.

Consider first the two iodines alone besides which the arsenic can be neglected. Since (00.1), (00.3), and (113.) are absent the positions of the two iodines in the small cell must be (000) and (2/3, 1/3, 1/2). The Laue diagrams definitely show that the correct hexagonal cell has dimensions $a=7.15$A° and $c=21.35$A. If three of the small cells are placed on top of each other this gives the correct c axis; also if the new a axis is chosen 30° from the old one tne new hexagonal cell is obtained.

The arsenic atoms were next considered. In the old small cell there were two-thirds of an atom only. To explain all the absences in the powder photographs the arsenic atoms must be arranged in vertical rows (parallel to c) with a distance of $c/3$ between them ($c=21.35$A).

On each of these rows there can lie, however, only two arsenic atoms as there is only one arsenic per three iodine. Therefore in building up the large cell from three of the small cells two of the latter must contain each one atom

of arsenic and the third none. Braekken gives in his paper the following intensities for reflections from the basal plane.

	Large cell								
	00.3	00.6	00.9	00.12	00.15	00.18	00.21	00.24	00.27
	Small cell								
	00.1	00.2	00.3	00.4	00.5	00.6	00.7	00.8	00.9
AsI_3	0.	vs.	vw.	s.	w.	m.	0.	w.	vvw.
SbI_3	w.	s.	m.	vs.	w.	m.	vw.	w.	m.
BiI_3	m.	m.	ms.	vs.	0.	vw.	mw.	ms.	

The reflection from 00.4 (small cell) is very strong for all compounds and remains practically unchanged from arsenic to bismuth. Consequently all atoms must cooperate for 00.4. The arsenic (antimonyor bismuth) atoms must be displaced $c'/4$ with respect to iodine (c' refers to the small cell). Further, arsenic must lie on a three fold axis: therefore their position in the cell is (1/3, 2/3, 1/4).

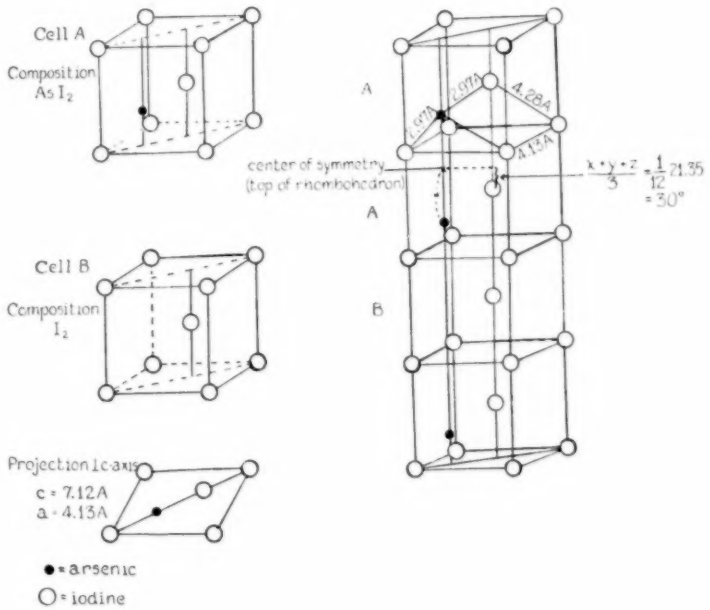

Fig. 1.

These arsenic positions are not very accurate because of the heavy iodine atoms. A somewhat different parameter, still on the three fold axis, is possible. Such a small displacement of the arsenic atoms is not incompatible with the intensities; the estimated intensities are however not accurate enough to prove whether any such displacement exists.

Fig. 1 shows the arrangement in the small and the large cells. Arsenic are separated in the vertical direction by distances 7.12A or 2×7.12A.

By placing one cell B on the top of two cells A and by choosing new a axes 30° from the old axes a cell of the correct dimensions is obtained and the atoms in the cell possess the symmetry of the space group C_{3i}^2. This arrangement explains the absent planes in the powder data and also the intensities of the different orders of reflection from the basal plane.

The coordinates of the atoms can be referred to the unit rhombohedron. The top of the rhombohedron has coordinates (000) and is the center of symmetry. The arsenic atoms have coordinates uuu $\bar{u}\bar{u}\bar{u}$ where u is their distance

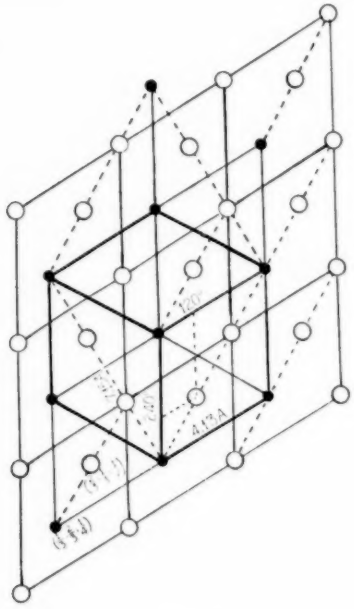

Fig. 2.

along the c axis. This distance is seen from Fig. 1 to be 1/6 the length of the c axis i.e., $u = 60°$.

The iodine atoms have coordinates $\pm xyz$: $\pm zxy$: $\pm yzx$. They are seen to lie in a plane displaced 1/12 the length of the c axis along the diagonal, i.e., $x+y+z/3 = 30°$.

Fig. 2 shows a projection of the structure perpendicular to the c axis from which it is seen that $y-z = 120°$ and $x-z = 240°$. Combining these three equations: $x = 150°$, $y = 30°$, $z = -90°$. The distance between two iodines in the same plane is the side of the small cell or 4.13°.

Two iodines in different planes are separated by a vertical distance of 60° or 3.56A. The horizontal separation is 1/3 the diagonal of the small cell or 2.38A.

Therefore the distance between two iodines in different planes

$$= ((2.38)^2 + (3.56)^2)^{1/2}$$

$$= 4.28A.$$

Arsenic and iodine are separated by a horizontal distance of 1/3 the diagonal of the small cell or 2.38A and a vertical distance of 30° or 1.78A.

Therefore the distance between arsenic and iodine

$$= ((2.38)^2 + (1.78)^2)^{1/2}$$

$$= 2.97A.$$

These are all reasonable interionic distances as arsenic is considered to have an ionic radius of about 0.9A and iodine an ionic radius of a little more than 2A. The only data, other than the general absences in the powder films, by means of which to test this structure were the Laue data.

The Laue spots were indexed in the usual way. The axial ratio obtained

TABLE I.

Plane	Observed intensity	Calculated int.	
$\{6\bar{1}1$	6	$\{2F_{As}+2.94F_I$	143
$\{61\bar{1}$	5	$\{2F_{As}+2.94F_I$	143
$\{51\bar{1}$	0	$\{F_{As}-.62F_I$	1
$\{5\bar{1}1$	4	$\{F_{As}+.62F_I$	42
$\{52\bar{2}$	3	$\{F_{As}+.26F_I$	32
$\{5\bar{2}2$	<1	$\{F_{As}-.26F_I$	12
$\{32\bar{2}$	12	$\{-2F_{As}+5.16F_I$	164
$\{3\bar{2}2$	15	$\{-2F_{As}-5.16F_I$	260
$\{40\bar{1}$	10	$\{-2F_{As}+5.16F_I$	168
$\{4\bar{1}0$	15	$\{-2F_{As}-5.16F_I$	268
$\{30\bar{1}$	9	$\{-F_{As}-.3F_I$	40
$\{3\bar{1}0$	7	$\{-F_{As}-.3F_I$	40
$\{\bar{1}02$	5	$\{F_{As}+.3F_I$	39
$\{\bar{1}20$	2	$\{F_{As}-.3F_I$	13
$\{20\bar{5}$	1	$\{-2F_{As}+5.12F_I$	158
$\{2\bar{5}0$	3	$\{-2F_{As}-5.12F_I$	252
$\{\bar{1}03$	4	$\{-F_{As}-.3F_I$	34
$\{\bar{1}30$	4	$\{-F_{As}-.3F_I$	34
$\{\bar{1}04$	10	$\{-2F_{As}-5.16F_I$	228
$\{140$	7	$\{-2F_{As}+5.16F_I$	144
$\{\bar{1}06$	0	$\{F_{As}-.58F_I$	0
$\{\bar{1}60$	4	$\{F_{As}+.58F_I$	48
$\{\bar{1}07$	3	$\{2F_{As}+2.94F_I$	172
$\{\bar{1}70$	3	$\{2F_{As}+2.94F_I$	172
$\{02\bar{1}$	8	$\{F_{As}+.3F_I$	40
$\{0\bar{1}2$	5	$\{F_{As}-.3F_I$	14
$\{05\bar{2}$	2	$\{-2F_{As}+5.12F_I$	166
$\{025$	4	$\{-2F_{As}-5.12F_I$	266
$\{03\bar{1}$	5	$\{-F_{As}-.3F_I$	35
$\{0\bar{1}3$	7	$\{-F_{As}-.3F_I$	35
$\{04\bar{1}$	13	$\{-2F_{As}-5.16F_I$	235
$\{0\bar{1}4$	9	$\{-2F_{As}+5.16F_I$	147
$\{05\bar{1}$	0	$\{-F_{As}-.26F_I$	12
$\{0\bar{1}5$	1	$\{-F_{As}-.26F_I$	12
$\{06\bar{1}$	0	$\{F_{As}-.58F_I$	0
$\{0\bar{1}6$	4	$\{F_{As}+.58F_I$	42
$\{07\bar{1}$	3	$\{2F_{As}+2.94F_I$	134
$\{0\bar{1}7$	3	$\{2F_{As}+2.94F_I$	134
$\{34\bar{3}$	2	$\{-F_{As}+.46F_I$	4
$\{3\bar{3}4$	2	$\{-F_{As}+.46F_I$	4
$\{23\bar{2}$	5	$\{-2F_{As}+5.16F_I$	141
$\{2\bar{2}3$	8	$\{-2F_{As}-5.16F_I$	221
$\{\bar{1}21$	3	$\{-F_{As}+.08F_I$	22
$\{\bar{1}12$	0	$\{-F_{As}+.84F_I$	16

from the Laue photographs was about 1:3 checking the more accurate value of the powder photographs.

Because of the high absorption of the crystal the only comparison of intensities which can be definitely relied upon are those of planes having the same sin θ and the same $n\lambda$. Pairs of spots having the same sin θ and $n\lambda$ were collected. The theoretical intensities for these planes were computed using the above structure: if the structure is correct the calculated and observed intensities for each pair of planes will be in the same proportion. This was found not to be the case. Slight variations in the orientation of iodine triangles in a plane perpendicular to the c axis were tested. These variations will not affect the general absences in the powder films or the intensities of the different orders from the basal plane which are known to check with the experimental data.

The only parameters which gave agreement with the observed Laue data were $x=152°$, $y=28°$, $z=-90°$. Many other slight variations were tested but none found to agree with observed results so well as these values of the parameters. Table I shows the calculated and observed intensities for the Laue pairs.

To obtain numerical values of the calculated intensities Thomas' method of finding atomic F values was used.[4] He has deduced that for the heavier atoms

$$F=F_0N/55$$

where F = atomic F value of the atom considered

N = atomic number of the atom considered

F_0 = atomic F value of caesium, at a point on the sin θ/λ scale given by sin θ/λ for atom N/sin θ/λ for Cs $=(N/55)^{1/3}$.

Knowing the variation of the F value of caesium with sin θ/λ, curves were plotted showing the same relation in the cases of arsenic and iodine. Using these graphs the F value for arsenic and iodine is known for any value of sin θ/λ and therefore the value to be used in calculating the intensity due to reflection from any particular plane.

Groups of plane were now collected with values of sin θ/λ and $n\lambda$ which did not differ greatly and the theoretical intensity calculated for planes in these groups. The calculated and observed intensities of planes in each group did not check nearly so well as did the pairs of planes. The only explanation seems to be that even a slight variation in sin θ/λ and $n\lambda$ must cause too large a change in absorption for such planes to be any longer comparable. The structure here proposed is a very reasonable one and it seems doubtful that any structure which is not correct would fit the Laue pairs so well.

Discussion of the Structure

The crystal structure of arsenic triiodide has been investigated by means of Laue, powder, and oscillation photographs. It is shown to be a layer lattice. The underlying lattice is Γ_{rh} and the space group C_{3i}^2. Braekken in his paper

[4] Thomas, Zeits. f. Krist. **69**, 137 (1928–9).

concluded that the lattice was hexagonal but agreed later that the lattice was rhombohedral. The incorrect fundamental lattice also led him to predict an incorrect space group although his structure is essentially the same as that given here.

The unit rhombohedron has dimensions $r=8.25$A and $\alpha=51°20'$; there are two molecules to the unit cell.

The coordinates of the atoms are: Arsenic $\pm uuu$ where $u=60°$. Iodine $\pm xyz$, $\pm zxy$, $\pm yzx$ where $x=152°$, $y=28°$, $z=-90°$. Distances of closest approach of iodine are about 4.28A and 4.13A and of arsenic and iodine about 2.97A. The iodine ions are in hexagonal close packing; each arsenic ion is surrounded by six iodine ions.

The arsenic positions are not very accurate because of the heavy iodine atoms. The arsenic atoms may be slightly displaced away from the center of the iodine octahedron in the direction of one face. Such a displacement is not only possible, but rather probable, because arsenic occurs in the form of trivalent arsenic and thus possesses two electrons more than a complete 18 shell. Such a displacement is not incompatible with the intensities though rather difficult to predict.

The writer wishes to express her appreciation to Professor W. H. Zachariasen for his assistance throughout the duration of the work and to Dr. P. M. Harris who suggested the problem.

THE MAGNETIC MOMENT OF THE PALLADIUM ATOM

By A. N. Guthrie and M. J. Copley
Laboratory of Physical Chemistry, University of Illinois

(Received June 9, 1931)

Abstract

The magnetic moment of the palladium atom has been investigated by the Stern-Gerlach method by evaporating the metal from a tungsten boat resistance furnace through beam forming slits of Pyrex glass and allowing the beam to impinge and condense on a glass plate after passing through an inhomogeneous magnetic field. It was found that images too weak to be detected could be developed satisfactorily by the method used by Stern and Gerlach for silver images. No splitting of the beam of palladium atoms was observed although the same field gave a splitting of 0.04 cm for a beam of atomic hydrogen. This indicates that the palladium atom in its normal state has zero magnetic moment in agreement with spectroscopic results giving for its ground term a ^1S.

Introduction

IT HAS been found possible correctly to predict normal states for atoms and ions containing a known number of electrons. Hund[1] worked out the rule empirically and gave a very interesting application of it in calculating the magnetic moments of ions of the rare earth elements.[2] Slater[3] has examined the validity of Hund's rule in the wave mechanics and has concluded that while not valid in its entirety its normal state predictions should be correct.

In the case of the palladium atom of atomic number (46) it can be predicted that the low energy states will arise from the structures $4d^8\ 5s^2$, $4d^9\ 5s$ and $4d^{10}$. From a consideration of the relative energies for similar structures in the nickel atom, it might be supposed that the lowest energy would be associated with the structure $4d^8\ 5s^2$. This structure gives rise to the spectral terms $^3(FPDS)$ and $^1(GFPDS)$, the multiplets being inverted. Of these terms the Hund rule gives $^3F_4$ as the ground term. Analysis of the atomic spectrum gives ^1S as the ground term.[4] This indicates that the $4d^{10}$ structure has the smallest energy since this structure gives rise to the ^1S term and the ^1S due to $4d^8\ 5s^2$ should be high in the spectrum.

The theory of the Zeeman effect gives for a $^3F_4$ term (with Russell-Saunders coupling) a magnetic moment of five Bohr magnetons and for a ^1S term zero magnetic moment. Thus, by determining the magnetic moment of the atom, its normal state may be discovered in a somewhat more direct manner than is done spectroscopically. The complete agreement of the results by

[1] F. Hund, Zeits. f. Physik **33,** 345 (1925).
[2] F. Hund, Zeits. f. Physik **33,** 855 (1925).
[3] J. C. Slater, Phys. Rev. **34,** 1293 (1929).
[4] A. G. Shenstone, Phys. Rev. **36,** 669 (1930).

the two methods for many atoms is testimony for the soundness of the theory of the Zeeman effect.[5]

This research was undertaken in order to determine the normal state of the palladium atom by measurement of its magnetic moment for comparison with the result of the analysis of its atomic spectrum.

Experimental

The experimental technique employed in this research was developed by Stern and Gerlach.[6] A ray of atoms is passed through an inhomogeneous magnetic field at right angles to the direction of the field. The deflection S_z experienced by those atoms in the ray having the most probable velocity is

$$S_z = 1/4M/RT \cdot \partial H/\partial S \cdot (L_1^2 + 2L_1L_2) \qquad (1)$$

where M is the magnetic moment in gauss-cm per mole; L_1 is the length of the pole pieces of the magnet, or the distance the atoms must travel through the magnetic field; L_2 is the distance from the end of the field to the target; $\partial H/\partial S$ is the value of the inhomogenity of the field in the path traversed by the atomic ray. In Eq. (1) $\partial H/\partial S$ is assumed constant throughout the path of the rayin the field.

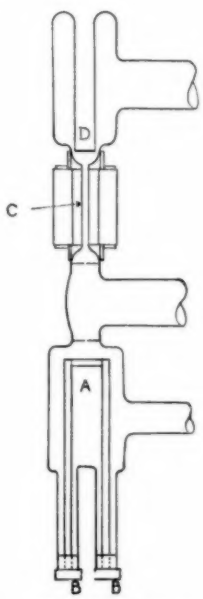

Fig. 1. Sketch of apparatus.

Furnace.

The palladium was evaporated by means of the tungsten boat furnace shown at A in Fig. 1. The tungsten boat was supported by inserting it in slots cut in the ends of two $\frac{1}{4}''$ copper rods. The copper rods also served as

[5] E. C. Stoner, Magnetism, Chap. 1, E. P. Dutton and Co., Inc., New York.

[6] Stern, Zeits. f. Physik **7,** 249 (1921); Gerlach and Stern, Zeits. f. Physik **8,** 110 (1922); **9,** 349, 353 (1922); Ann. d. Physik **74,** 673 (1924); **76,** 163 (1925).

electrodes. The rods were sealed into the apparatus by screwing on $\frac{3}{4}''$ copper lugs and soldering the lugs to copper to Pyrex seals at *BB*. The boat was heated by an electric current furnished by a low voltage transformer connected to 110 v. A.C. The primary current carried approximately 20 amperes and the secondary 100 amperes or more. It was necessary to cool the solder joints at *BB* by immersing them in a beaker of water.

The palladium used was in the powdered form and was furnished by Baker and Company. It was guaranteed to be of high purity.

The slit system and target chamber.

To produce the ray of atoms, an all Pyrex slit system was sealed to the furnace chamber as shown in Fig. 1. This consisted of two slits, 0.15 cm long and 0.005 cm wide, aligned with each other at a distance of 6 cm.[7] The space between the slits was connected through a liquid air trap to a mercury vapor pump. The second slit was connected to the target chamber by means of a small 4 mm tube *C*. The tube *C* was aligned with the two slits and traversed the magnetic field. The target chamber was also connected through a liquid air trap to a second mercury vapor pump. The target consisted of an optical Pyrex plate sealed on the end of a 1.5 cm tube as indicated at *D* in Fig. 1. It was situated a distance of 1.5 cm from the end of the pole pieces.

The magnetic field.

A large magnet constructed similarly to the Dubois magnet used by Phipps and Taylor[8] in this laboratory was used in this research. Comparison tests have shown that with an equal electric current through its coils, this

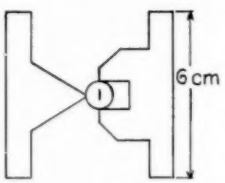

Fig. 2. Pole pieces.

magnet causes a deflection of hydrogen atoms of about the same magnitude as the Dubois magnet. The pole pieces were similar to those employed by Leu.[9] This type of pole piece produces a field with uniform inhomogeneity in the portion of the field traversed by the beam. A cross section of the pole pieces is shown in Fig. 2. They were 6 cm long and were placed 0.3 cm apart. The slot was 0.6 cm wide. The edge of the 60° wedge shaped piece was 0.1 cm wide. The position of the small Pyrex tube *C* and the path of the ray between the pole pieces are shown in Fig. 2.

Detection of the palladium.

It was found that with the type of furnace employed, a beam of sufficient intensity could not be obtained to give a visible image on the target in a

[7] Kurt and Phipps, Phys. Rev. **34,** 1357 (1929).
[8] Phipps and Taylor, Phys. Rev. **29,** 308 (1927).
[9] Leu, Zeits. f. Physik **41,** 551 (1927).

reasonable length of time. A method of developing the image was then sought. It was found that the same method used by Gerlach and Stern[10] for developing silver images was also effective for palladium. By using this method a run could be terminated in a few minutes and the target cracked-off; after immersion of the target in the developing solution for a few seconds the image of the beam would appear. Runs as long as $1\frac{1}{2}$ to 2 hours did not suffice to give a visible image without developing.

Procedure.

The assembled apparatus is shown in Fig. 1. The apparatus was pumped out for at least 2 hours before starting a run. The pressure was measured by a McLeod gauge which usually indicated a vacuum around 10^{-6} mm after this preliminary pumping. It was found necessary to attach a mercury vapor pump to the furnace chamber to take care of the gas evolved by the furnace when heated. A current of 5 amperes was then sent through the coils of the magnet to produce the field. The furnace was bought up to a temperature (M.P. 1550°C) where rapid evaporation took place. After a few minutes the current through the furnace was shut off, the vacuum broken, the target cracked off and the image developed and photographed.

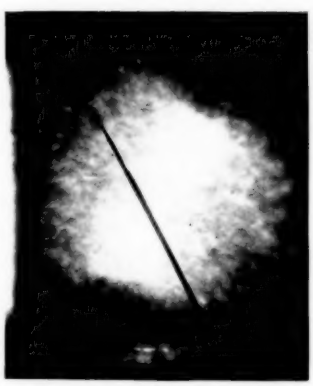

Fig. 3. Photograph of the image.

Results

No sign of a deviation of part of the beam was observed in any run. Fig. 3 is a photograph of the image, magnified ten times, obtained by a run made with the field. Photographs taken without the field are identical. It is true that if a portion of the beam was deflected it would take longer for it to build up to a point where it would reach a density that could be developed by the developing solution. However, a run was made of about 2 hours duration which should have been sufficient to bring out any sidelines but no effect was noticeable. The absence of any deflection could not have been due to weakness of the field. The same field produced a splitting of 0.04 cm on a beam of atomic hydrogen. In spite of the higher temperature of the palladium atoms

[10] Gerlach and Stern, Zeits. f. Physik **9**, 349 (1923).

an observable broadening of the trace, at least, should have been obtained if the atoms possess an appreciably magnetic moment, However, the trace, with field, as shown in Fig. 3 has exceedingly sharp boundaries and is a perfect image of the slits.

Conclusions

The most logical conclusion from these experiments is that in the normal state the palladium atom has zero magnetic moment and that the ground term of its spectrum is a ^1S. In this case it is almost certain that the most stable structure in the palladium atom is the $4d^{10}$ structure although in the nickel atom, with similar outer structures, the $3d^8\ 4s^2$ structure has proven to be the more stable.

SURFACE ENERGY OF LIQUIDS

By Henry Margenau
Sloane Physics Laboratory, Yale University

(Received June 8, 1931)

Abstract

The paper contains: (1) A brief characterization of the intermolecular forces producing surface tension and similar phenomena. (2) A review of thermodynamic relations and the development of a statistical theory of surface energy resulting in Eq. (9). (3) The results of a calculation of the surface energies of seven liquids on the basis of this formula, and their comparison with experiment. The agreement is in all cases as good as is consistent with the uncertainty of the data from which the calculation starts, and may be taken to indicate the applicability of the present theory of molecular forces to simple problems connected with the liquid state.

Introduction

Among the forces between neutral constituents of matter we may distinguish three essentially different types. The first arises from the possibility of an electron interchange which takes place when the two structures—atoms or molecules—are brought into very close proximity. If these exchange forces are attractive they produce the ordinary chemical binding; if they are repulsive they endow the individual structure with the property of "rigidity," surrounding it by a wall of potential energy which rises very steeply at a distance from its center nearly equal to its kinetic theory radius. These forces have a very short range and are imperceptible outside of this distance. Except for H and He, their variation with distance from the atomic center is not accurately known. In the case of He, in which we are primarily interested, Slater[1] has shown that the repulsive forces may be adequately represented at moderate distances by a potential energy function

$$E_r = 7.7 \times 10^{-10} e^{-2.43R/a_0} \text{ ergs}, \tag{1}$$

where a_0 is the first Bohr radius.
For all other substances we are forced at present to assume

$$E_r = \begin{cases} \infty & \text{for } R < R_0 \\ 0 & \text{for } R \geqq R_0 \end{cases}, \tag{2}$$

R_0 being the diameter of the atom or molecule given by the kinetic theory of gases.

The second type of forces is that due to the polarizing effect of one structure upon another. They may be interpreted physically as interactions between virtual multipoles associated with all possible quantum transitions of the interacting structures. Unlike the exchange forces which are very strong

[1] Slater, Phys. Rev. **32**, 349 (1928).

and appear in Schrödinger's perturbation scheme in the first approximation, the polarization forces are in general weak and appear as second order perturbations. Their nature was investigated most thoroughly by Eisenschitz and London,[2] who showed that they are, at large distances, proportional to R^{-7} and developed a general method by which the coefficient of proportionality may be determined approximately. For Helium, again, these forces are known with considerable precision,[3] and the potential energy corresponding to them is

$$E_p = -\frac{14.5}{R^6} \times 10^{-61} \text{ ergs.} \tag{3}$$

In general

$$E_p = -\frac{3}{4}\frac{\alpha^2 V}{R^6}, \tag{4}$$

where α is the polarizability and V the ionization potential, is a fair approximation. Expressions (3) and (4) take account only of dipole-dipole interactions, although there is reason to believe that in some cases virtual quadrupoles make some contribution which is appreciable in the neighborhood of R_0.[3a] The theory of polarization forces has been successfully applied in calculations of the second virial coefficients of a number of gases. Moreover, London[4] has shown that they fully account for the observed heats of adsorption of many substances and for the heats of sublimation of some molecular crystals. In this paper the theory is applied to calculate surface energies of liquids. The agreement seems quite striking and indicates that present ideas can be successfully extended to cover thermodynamic properties of liquids. It should be borne in mind that, except for He, the data to be used in this calculation are so inadequately known that one can reasonably not expect more than very rough agreement with experimental observations. But even this is significant in as much as there appears to be no other theory which allows the calculation of surface energies on the basis of entirely independent considerations.[5]

The third type of forces mentioned above is that existing between structures carrying permanent dipoles or multipoles. These forces behave in an essentially classical manner at high temperatures. At low temperatures, such as those for which the present calculations are carried out, their action may not be considered by the methods of classical physics. They play an important part in all phenomena mentioned, including surface tension. We are not interested in them at present and shall restrict our calculation to non-polar substances.

[2] Eisenschitz and London, Zeits. f. Physik **60,** 491 (1930); London, Zeits. f. Physik **63,** 245 (1930).

[3] Slater and Kirkwood, Phys. Rev. **37,** 682 (1931); Margenau, Phys. Rev. **37,** 1425 (1931).

[3a] A calculation of this effect will soon be published.

[4] London, Zeits. f. Phys. Chem. B **11,** 222 (1930).

[5] Bradley, Phil. Mag. **11,** 846 (1931), has recently calculated the surface energies of liquid He and A following the Laplace-Rayleigh theory. He assumes *ad hoc* a force law which gives correct virial coefficients. His result is in good agreement with the experimental one for A, but agrees poorly for He.

Theory of Surface Energy

The surface energy of a liquid is defined as the total energy (heat+mechanical work) required to produce unit area of fresh surface at constant volume, pressure, and temperature. We shall denote it by U. Consider an infinite body of liquid, and let it be separated into halves with plane boundary surfaces. If W is the work done by the molecular forces per unit area of boundary surface while the two halves are being carried from mutual contact to infinite separation, then clearly

$$U = -\frac{W}{2}, \tag{5}$$

since two surfaces are being produced by this process.

In creating unit area of new surface isothermally work is being done (1) against the mechanical forces of surface tension σ and of amount σ; (2) in adding to the liquid the "latent surface heat," $-T\partial\sigma/\partial T$; (3) in producing the change in density occurring in the transition of a portion of liquid from the interior to the surface of the liquid; this work may be shown to be $-p\partial\sigma/\partial p$. In general, this last term is negligible compared with the other two. It will here be disregarded. Hence

$$U = \sigma - T\frac{\partial\sigma}{\partial T}. \tag{6}$$

Since σ decreases with increasing temperature, U is larger than σ. Eq. (6) will enable us to compute U on the basis of the experimental values of σ and $\partial\sigma/\partial T$. This may then be compared with the theoretical value which is now to be calculated.

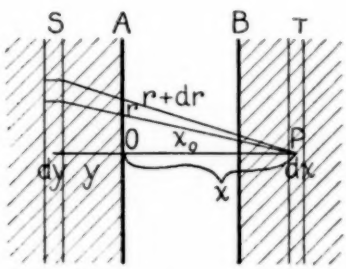

Fig. 1.

We obtain U most conveniently by way of a calculation of W as previously defined. Use will be made of an analysis given by Fowler[6] in connection with the theory of surface stresses. Let $E(r)$ be the mutual potential energy of two molecules a distance r apart. If n is the average number of molecules per unit volume, an element of volume dV at a distance r from any one molecule chosen at random will contain $ne^{-E(r)/kT}dV$ molecules. Let the two plane

[6] Fowler, Phil. Mag. **43**, 785 (1922). See also Statistical Mechanics, p. 214 ff.

boundaries A and B of the liquid in question be separated by a distance x_0 (see Fig. 1). Considering first the action of a thin film S of thickness dy on another film T of thickness dx, we observe that all molecules in an annular portion of S equidistant (between r and $r+dr$) from P, $n \cdot 2\pi\, r\, dr\, dy\, e^{-E(r)/kT}$ in number, exert a force

$$-2\pi n(x+y)drdye^{-E(r)/kT}\frac{\partial E}{\partial r}$$

along x upon one molecule at P. If this is integrated with regard to r from $(x+y)$ to ∞ we obtain the total force of the molecules in S upon one molecule at P. The result is

$$-2\pi nkT(x+y)dy\left[e^{-E(x+y)/kT}-1\right].$$

The force of S upon unit area of T is therefore

$$dF = -2\pi n^2 kT(x+y)dxdy\left[e^{-E(x+y)/kT}-1\right]. \tag{7}$$

Then the force of an infinite body of liquid to the left of A upon the molecules in unit area of T is $\int_{y=0}^{y=\infty} dF$, and finally the force of this infinite body upon a similar one to the right of B, per unit area of the latter, becomes

$$\begin{aligned} F(x_0) &= -2\pi n^2 kT \int_{y=0}^{y=\infty}\int_{x=x_0}^{\infty}(x+y)\left[e^{-E(x+y)/kT}-1\right]dxdy \\ &= -2\pi n^2 kT\left\{\int_{x_0}^{\infty}x^2(e^{-E(x)/kT}-1)dx - x_0\int_{x_0}^{\infty}x(e^{-E(x)/kT}-1)dx\right\} \end{aligned} \tag{8}$$

The last expression is the result of an integration by parts following the substitution of a single letter for $x+y$. To obtain W we merely form $\int_0^\infty F(x_0)dx_0$. Let $f(x)$ be any function of x such that $\int_0^\infty f(x)dx$ exists. Then it is easily seen that

$$\int_0^\infty x_0^n dx_0 \int_{x_0}^\infty f(x)dx = \int_0^\infty \frac{x^{n+1}}{n+1}f(x)dx.$$

Hence

$$W = -2\pi n^2 kT\left\{\int_0^\infty\left(x^3-\frac{x^3}{2}\right)(e^{-E(x)/kT}-1)dx\right\},$$

and on account of (5)

$$U = \frac{\pi}{2}n^2 kT\int_0^\infty x^3(e^{-E(x)/kT}-1)dx. \tag{9}$$

The form of (9) shows that the calculation of surface energies is highly critical, since the temperatures for which it has to be carried out are usually very low. The smallness of kT will accentuate the error in $E(x)$. It is well known that theoretical values for the second virial coefficient, which is of similar form, agree more poorly with the experimental ones for low than they do for high temperatures. This is to be remembered in judging the results

for U. For the function E we must choose, of course, E_r+E_p. In the case of He we combine (1) and (3), in all others (2) and (4). The model of a rigid wall, though incompetent to account for such phenomena as thermal expansion and compressibility of liquids, has proved serviceable *a faute de mieux* in calculations of the equation of state and will suffice here.

The calculation is very sensitive to the value assumed for R_0. Wherever possible, R_0 will be computed from the B_0-values given by Beattie and Bridgeman,[7] otherwise it will be obtained from the known critical temperature and critical pressure. n is, of course, equal to ρ/m, where ρ is the density of the liquid and m the product of the molecular weight M and 1.66×10^{-24} g. The integration in (9) is carried out graphically for the important part of the range. When we represent E by the rigid wall model, U may be conveniently decomposed into

$$\frac{\pi}{2}n^2kT\left\{-\int_0^{R_0}x^3dx+\int_{R_0}^{d}x^3(e^{-E(x)/kT}-1)dx+\int_d^{\infty}\frac{3\alpha^2V}{4kTx^3}dx\right\},$$

where d is some sufficiently large value of x. Only the second term need be evaluated graphically, while the first and third are easily computed. The results for seven gases are given in Table I.

TABLE I.

	T (°absolute)	ρ	M	$R_0\times10^8$cm	σ (dynes/cm)	$U^*_{exp.}$ (ergs/cm²)	U_{calc}
He	4	0.128	4.00		0.12	0.6	0.78
Ne	26	1.20	20.2	2.6	5.15	15.0	20
A	87	1.40	39.9	3.13	12.5	35	50
N_2	80	.808	28	3.42	8.27	25.8	26
Cl_2	223	1.60	71	3.3	29.2	73	100**
O_2	80	1.20	32.0	3.3	15.7	35	21
Hg	273	13.6	200.6	3.5	470	530	560

* Obtained using $\alpha=4.55\times10^{-24}$, $V=8.2$ volts.

** Computed from the data of σ and $\partial\sigma/\partial T$ given in I.C.T.

Discussion of Results

An examination of the table leaves no doubt as to the identity of the forces which produce surface tension. The agreement which generally prevails shows that they are the polarization forces, and that a treatment of the liquid state may be undertaken by essentially the same methods which have proved successful in the analysis of the behavior of gases. It is to be remembered that helium is the only substance for which the calculation is free from rough approximations. Here the agreement with experience is probably within the experimental error, although the simple theory here outlined may still be in need of refinement. We have not, for instance, taken account of the possible existence, at these low temperatures, of polarization molecules of the type He_2, whose contribution to the surface energy would be different from

[7] Beattie and Bridgeman, Zeits. f. Physik **62**, 95 (1930).

that of pairs of atoms in non-quantized collision states. Their presence would, indeed, make $U_{calc.}$ smaller. On the other hand, the satisfactory result obtained without considering them seems definitely to indicate that they do not play an important role in the case of He. With regard to the other substances listed, no significant conclusion is to be drawn from the circumstance that some of them agree better than others. But it is of interest to notice that the calculated values of U, with the exception of O_2, are all too large. The most inadequate feature of our model is the summary fashion of dealing with the repulsive exchange forces. Now it is known that for He these repulsive forces become appreciable at distances considerably larger than R_0, invalidating the action of the polarization forces in the region in which our formula would make them strongest. It is probable that other substances behave in a similar manner. Hence our calculation is likely to magnify the effect of the attractive forces, and the results would be too large. But it is possible at present only to ascertain the sign of this error; its elimination would require a detailed knowledge of the exchange forces. As was pointed out, Eq. (4) is definitely approximate. It is likely that the correct coefficient of R^{-6} is somewhat greater than that given by (4).[8] This would to some extent annul the effect of the first mentioned error, which, however, should be the dominant one.

A comparison of the results here obtained with those for the second virial coefficient[9] is very instructive. There appears to be a definite coordination of the following type: Deviations from experimental resulst are always in the same direction for both surface energies and second virial coefficients B, and when good agreement is found for a substance in the one instance it is also found in the other. In particular, the B for O_2 was slightly anomalous if compared with the others, and here the same anomaly appears in U. It was pointed out that a smaller value of R_0 would improve the agreement; we find the same to be true here. Although this observation may not be very significant in itself it clearly shows the essential relatedness of the two phenomena and the applicability of the theory of molecular forces. The only case for which the method of this paper failed to yield even approximate agreement is H_2. The value of $U_{calc.}$ was here vastly (about 1000 $\times$) larger than $U_{exp.}$. This discrepancy is to be ascribed to two causes: (1) Our simple assumption regarding the repulsive forces is probably much more inadequate for light substances than it is for heavier ones. (2) The possible existence of polarization molecules $(H_2)_2$. Such a molecule would, because of the small mass of its constituents, have a large vibrational zero point energy,[10] which would render the major contribution of the polarization forces ineffective. This could easily introduce an error of the above order of magnitude. Although there exists no direct evidence we feel that the existence of such loosely bound molecular structures merits serious consideration.

[8] See ref. (3).

[9] Margenau, Phys. Rev. **36,** 1782 (1930).

[10] The lowest vibrational level would fill a considerable part of the minimum of the potential energy curve.

It is of considerable interest and appears perhaps at first sight surprising that the forces producing surface energy in a liquid metal (Hg) are of the same character as those in a non-metal, and that they may be treated in the same manner. Apparently the influence of "free" electrons does not make itself felt in the interactions between the parts of the liquid, at least not in their collective description by means of a statistical theory (such as the one here presented).

In attempting to extend the present theory to other metals one encounters a natural limitation. Expression (4) or any similar one involving polarizabilities is valid only as long as $\alpha/R^3 \ll 1$, α/R^3 being essentially the perturbation parameter in the calculation by which polarization energies are determined. For Na, for instance, α/R_0^3 is nearly 1. Hg appears to be the only metal for which the procedure here outlined is legitimate. The surface energy of metals may not in general, therefore, be calculated by the method of this paper. Similar precautions apply with regard to more complex molecules which are capable of motions and interactions not considered in Eq. (4). But it seems satisfying indeed that the surface energy of substances within the range of application of the method may be calculated in a relatively simple manner. This paper presents another example exhibiting the power of the theory of molecular forces.

LETTERS TO THE EDITOR

Prompt publication of brief reports of important discoveries in physics may be secured by addressing them to this department. Closing dates for this department are, for the first issue of the month, the twenty-eighth of the preceding month; for the second issue, the thirteenth of the month. The Board of Editors does not hold itself responsible for the opinions expressed by the correspondents.

The Rotational Analysis of the First Positive Nitrogen (N_2) Bands

Two decades have passed since Fowler and Strutt (Proc. Roy. Soc. London **A85,** 377, 1911 *et seq.*) definitely showed that the greenish-yellow afterglow of active nitrogen could be ascribed to a selective excitation of a few red, yellow, and green bands belonging to the first positive system of the nitrogen molecule N_2. The vibrational analysis is given by Birge (Int. Crit. Tables **V,** 409, 1929). Previous attempts made to analyze the rotational structure of these bands have proved to be unsuccessful.

The first positive nitrogen bands lying between λ6800A and λ5900A have now been photographed in the third and second orders of the new Paschen mounting of the Rowland 21 foot grating. The dispersion thus obtained amounted to about 0.7A per mm in the third order and about 1.3A per mm in the second. The positive column of an inverted H-tube which was constructed with large aluminum electrodes capable of carrying 1.6 amps. and could be water cooled, was used as source. The current was supplied by a 5 KW transformer having a peak voltage 6600. During exposures only 0.8 amp. was sent through the tube, giving a current density of 1.6 amp. per cm^2 in the positive column of the discharge tube. The nitrogen used was prepared by heating sodium azide in vacuo. The pressure of the nitrogen in the discharge tube was about 3 mm. The time of exposure in the third order varied from 9 to 12 hours. Ilford special rapid panchromatic plates were used.

The 4–1 (λ6788A), 5–2 (λ6705A), 6–3 (λ6623A), 5–1 (λ6127A), 6–2 (λ6070A) and 7–3 (λ6013A) bands have been measured against neon standards both in the third and second orders. As the 5–2 band has its initial state in common with the final state of the 2–5 (λ3942A) band of the second positive nitrogen bands which has been analyzed by Lindau (Zeits. f. Physik **26,** 342, 1924) and Hulthén and Johansson (Zeits. f. Physik **26,** 308, 1924) an analysis of the 5–2 band was first attempted and thereafter that of the 6–3 band which is stronger than the 5–2. Nine strong branches were found in each of these bands. These nine branches could be arranged into three groups which had the following appearance starting from the red end of each band: Q, R, S; P, Q, R; and O, P, Q. A total of 26 branches was observed in each band. All the branches showed alternating intensities of consecutive lines. The quantities $\Delta_2F_i' = R_i(J) - P_i(J)$ for the 5–2 band was found to agree within experimental error with the quantities $\Delta_2F_i'' = R_i(J-1) - P_i(J+1)$ determined from Lindau's data on the 2–5 band of the second positive band system. All the strong lines and practically all the weak lines are included in the above mentioned 26 branches. The remaining weak lines may be due to the overlapping of branches of the adjoining bands and to weaker bands of higher vibrational quantum number.

The structure of the bands is exactly that predicted if one assumes a $^3\Pi \rightarrow {}^3\Sigma$ transition with the $^3\Pi$ state conforming to Hund's case *a* for the lower J values. In this case 27 branches are expected of which two for which $\Delta K = 3$, are expected to be very weak. The twenty-seventh branch which has not been observed is unfavorably situated. The three groups of three strong branches can now be identified as P_1, Q_1, R_1; P_2, Q_2, R_2; and P_3, Q_3, R_3 branches and are the main branches belonging to the transitions $^3\Pi_{low} \rightarrow {}^3\Sigma$, $^3\Pi_{med} \rightarrow {}^3\Sigma$ and $^3\Pi_{high} \rightarrow {}^3\Sigma$ where low, med, and high mean low, medium and high frequencies. In the $^3\Sigma$ state the rotational levels having odd K values have greater weight, according to which the final state must be $^3\Sigma_u^+$ or $^3\Sigma_g^-$.

As the second positive nitrogen bands are

due to a $^3\Pi \rightarrow {}^3\Pi$ transition, it is impossible to conclude anything definite from them about the Λ-type doubling in either state, as only the difference can be determined. The Λ-type doubling in the final $^3\Pi$ state which is the same as the initial $^3\Pi$ state of the first positive bands, can now be found directly from the combinations determined from the analysis of the first positive bands. It is found that the Λ-type doubling in the $^3\Pi_{low}$ decreases from $\Delta\nu_{ab}=2.0$ cm^{-1} for $J'=6\frac{1}{2}$ to $\Delta\nu_{ab}=1.05$ cm^{-1} for $J'=27\frac{1}{2}$; in the $^3\Pi_{med}$ state, it increases from $\Delta\nu_{ab}=0.20$ cm^{-1} for $J'=1\frac{1}{2}$ to $\Delta\nu_{ab}=0.80$ cm^{-1} for $J'=22\frac{1}{2}$; and in the $^3\Pi_{high}$ state it increases slowly from $\Delta\nu_{ab}=-0.06$ cm^{-1} for $J'=3\frac{1}{2}$ to $\Delta\nu_{ab}=0.33$ cm^{-1} for $J=23\frac{1}{2}$. The theory for Λ-type doubling for a $^3\Pi$ state is given by Van Vleck (Phys. Rev. **33,** 467, 1929). Comparing this theory with the above results one sees that we probably have a case where $^3\Pi_{low}$, $^3\Pi_{med}$ and $^3\Pi_{high}$ correspond to $^3\Pi_0$, $^3\Pi_1$ and $^3\Pi_2$ where the $^3\Pi$ states are Hund's case *a* and go over to case *b* for larger *J*-values. From the relative positions of $^3\Pi_0$, $^3\Pi_1$ and $^3\Pi_2$ it may be concluded that the triplet $^3\Pi$ state is normal. The separation of $^3\Pi_0$ and $^3\Pi_1$, $\Delta\nu_{12}=40$ cm^{-1} and that of $^3\Pi_1$ and $^3\Pi_2$, $\Delta\nu_{23}=35$ cm^{-1} giving 75 cm^{-1} as the total width of the triplet separation.

The lower $^3\Sigma$ state affords a new opportunity of testing Kramers' theory (Zeits. f. Physik **53,** 422, 1929) for the spin fine structure due to the interaction between the individual electrons and to the interaction of the resultant electronic spin with the rotational angular momentum. The observed fine structure can be accounted for very well by assuming the constants $\epsilon''=0.43$ and $\gamma=0.003$ (for meaning of ϵ and γ compare Naudé and Christy, Phys. Rev. **37,** 500, 1931).

The values of $B_v^{*\prime}$ and $B_v^{*\prime\prime}$ could be obtained from the quantities Δ_2F_i' and Δ_2F_i''. From B_v^* (cf. Mulliken, Rev. Mod. Physics **2,** 113, 1930) B_v can be found and thus α_e, B_e and r_e. These values are given in Table I. The

TABLE I

		B^* in cm^{-1}	B_v in cm^{-1}	B_e, α_e and r_e
$^3\Pi_0$	$v'=6$	1.481	1.515	
	$v'=5$	1.509	1.545	
	$v'=6$	1.514	1.515	
$^3\Pi_1$	$v'=5$	1.543	1.545	$\alpha_e'=0.029$ cm^{-1}
	$v'=6$	1.549	1.515	
$^3\Pi_2$	$v'=5$	1.581	1.545	
	$v''=3$	—	1.395	$\alpha_e''=0.013$ cm^{-1}
$^3\Sigma$	$v''=2$	—	1.408	$B_e''=1.440$ cm^{-1}
	$v''=0$	—	1.434	$r_e''=1.290_5\times10^{-8}$ cm

The analysis is practically complete but the above values of the constants are still liable to small changes. The detailed results will be published elsewhere in the near future.

S. MEIRING NAUDÉ

Ryerson Physical Laboratory,
University of Chicago,
June 23, 1931.

Forced Predissociation in Nitrogen

In a recent paper in this journal I have discussed the significance of the single-headedness of some of the bands of the first positive system of nitrogen, of which most of the bands possess three strong and one weak head. The significance of this phenomenon was pointed out as being an interaction between the levels from which these bands are emitted and the repulsive Heitler and London level which lies very near to the energy range in which these single-headed bands originate. That such disappearance of heads was correctly interpreted in my paper is shown by the fact that I have been able to produce the same phenomenon in bands of the system which have always been observed as four-headed. This was produced in regions of the initial vibrational states associated with this system, which should interact with other Heitler and London levels. This point will be more fully discussed in a

forthcoming report on the Auroral spectrum, in which the phenomenon of single-headedness plays a very important role.

I want to call attention in this note to another observation which I recently made on the band system which is discussed above. These bands are single-headed in ordinary discharges in nitrogen, and we may call this normal single-headedness. These are bands which correspond to the transitions from B_{13}, B_{14}, B_{15} and B_{17} in at least two sequences and possibly more than two. In the same tube in which I have produced a striking reproduction of the spectrum of the aurora, I have also obtained at higher pressures (5 mm) a normal emission of the above bands (three strong and one weak head). This observation was made in a tube containing oxygen and a small amount of nitrogen and it was characterized mainly by the fact that at pressures of 10^{-2} to 10^{-3} mm the first positive bands of nitrogen are forced to show a marked predissociation as is indicated by strong selective excitation of heads similar to the occurrence of single-headedness elsewhere in the spectrum. It is striking therefore that we have not only forced predissociation into regions of the band spectrum where it does not normally occur, but that we have now forced it out of a region in which it does occur quite readily. In the paper in which the normal predissociation was discussed, I called attention to the fact that the level on which the first positive bands arise, is one which is associated with four possible Heitler and London levels. Thus, since there is a normal combination with only one of these levels (as is indicated by the one region of single-headedness), there is a great possibility here for forced combinations with the other three levels. It is not at all surprising therefore that this level has given us such a fruitful yield of peculiar band spectrum emissions. The connection between this work and Turner's explanation of the magnetic quenching of iodine fluorescence should receive further study. These are among the first examples of forced predissociation, and, what is even more interesting, the present case is probably the first time that predissociation has been prevented from taking place.

JOSEPH KAPLAN
University of California
at Los Angeles,
June 20, 1931.

Removal of Continuous Background from Raman Spectrum of Carbon Tetrachloride

From the beginning of the study of the Raman effect writers have noted, in addition to the Raman lines, the presence of a continuous background. Attempts were early made to connect this continuous background with impurities which were either in the substance in the first place or were formed there under the action of the incident light.

Pal and Sen Gupta[1] have shown that in the case of aniline photochemical decomposition does not take place in the absence of air, therefore very little continuous spectrum is obtained from pure aniline sealed in a vacuum But in the case of benzaldehyde the decomposition takes place even in the absence of air. Hence the continuous spectrum of benzaldehyde is removed only by continuous distillation. Ganesan and Venkateswaran[2,3] have shown that in the case of glycerine the continuous spectrum is in some way connected with the viscosity of the liquid.

Carbon tetrachloride, unless it is very pure, has a strong continuous spectrum which is not removed by distillation at atmospheric pressure. It is the purpose of this note to point out that the continuous spectrum of CCl_4 may be almost totally removed by using small quantities of *m*-dinitrobenzene as a solute. There will, of course, be Raman lines due to the *m*-dinitrobenzene as well as to the CCl_4, but at the concentration used the CCl_4 lines are much the stronger.

Fig. 1 shows the Raman spectrum of CCl_4 and of a solution of *m*-dinitrobenzene in CCl_4 in the ratio of 1:25 by weight. The time of exposure in each case is 20 minutes. A longer time makes the continuous spectrum of CCl_4 too dense for measurement. The solution absorbs strongly on the short wave-length side of Hg 4358.

An Eastman 33 plate was used and calibrated by the method of neutral screens.[4] The screens were mounted on an eccentric to keep

[1] Pal and Sen Gupta, Ind. Jour. Phys. **5,** 13 (1930); Ind. Jour. Phys. **5,** 609 (1930).

[2] S. Venkateswaran, Ind. Jour. Phys. **3,** 105 (1928).

[3] Ganesan and Venkateswaran, Ind. Jour. Phys. **4,** 195 (1929).

[4] G. R. Harrison, J.O.S.A. and R.S.I. **18,** 492 (1929).

them in irregular motion. A self-recording Moll microphotometer was used to densi-

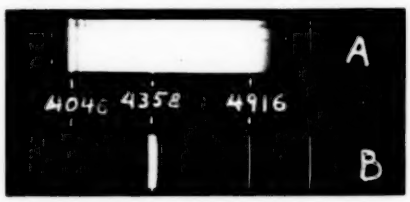

Fig. 1. (a) Raman spectrum of carbon tetrachloride. (b) Raman spectrum of carbon tetrachloride containing *m*-dinitrobenzene.

tometer the plate. The intensity measurements are given in Table I.

TABLE I. *Intensities of Raman lines and continuous spectra.*

	CCl_4	Solution	I of solution / I of CCl_4
Continuous	100	13.6	0.136
$\Delta\nu$ 216 cm^{-1}	37	42	1.13
$\Delta\nu$ 313 cm^{-1}	40	47	1.17
$\Delta\nu$ 455 cm^{-1}	41.4	48	1.16
$\Delta\nu$ 755 cm^{-1}	23.5	22.5	.96
$\Delta\nu$ 782 cm^{-1}	23.5	22.5	.95

The intensity of the continuous spectrum was measured near the point of maximum intensity, which is in the neighborhood of 4600A. The intensity of the continuous spectrum of CCl_4 was arbitrarily set at 100 and all other values are given relative to this. The second column in Table I gives the intensities of the continuous spectrum and of the Stokes lines of CCl_4 excited by Hg 4358. The third column gives these intensities when *m*-dinitrobenzene has been dissolved in the CCl_4. Referring to the last column, which gives the ratio of these intensities in the solution to those in the CCl_4, it will be seen that the continuous spectrum of the solution is only 0.136 or about 1/7 as strong as in the CCl_4 alone. As is also seen in the last column, the intensities of the Raman lines have not changed appreciably when the *m*-dinitrobenzene is added. The weakening of the continuous spectrum cannot, therefore, be due to general absorption or otherwise the lines would also be correspondingly weakened.

Impure benzene, which had a strong continuous spectrum, gave results very much like those obtained with CCl_4. Other substances besides *m*-dinitrobenzene, such as *o*, *m*, or *p*-nitrochlorobenzene or *o*, *m*, or *p*-nitrotoluene produce a similar effect. The presence of the nitro group, however, seems to be necessary as substances which do not contain it are much less effective in removing the continuous background.

M. E. HIGH
M. L. POOL

Mendenhall Laboratory of Physics,
Ohio State University,
Columbus, Ohio,
June 25, 1931.

Calculation of Effective Nuclear Magnetic Moments from Hyperfine Structure

Hyperfine structure gives a means of determining the spin of atomic nuclei. According to present available theories the interaction energy of the nucleus and the electron is supposed to be due to a nuclear magnetic moment. The numerical value of this effective magnetic moment is of interest. It may be obtained from a comparison of observed *hfs* separations with theoretical formulas.

Fermi[1] has shown that, in dealing with *s* states of single electron spectra, $\psi^2(0)$ is of main importance for the calculation of magnetic moments, $\psi(0)$ being the value of the Schroedinger function at $r=0$. Closer examination[2] showed appreciable effects of a relativity correction (e.g., in the case of x-ray levels). It is known that, in the Dirac theory, $\psi^2(0)$ should be replaced by

$$(8\pi/\Lambda)\int_0^\infty(\phi_1\phi_2/r^2)dr \Big/ \left[4\pi\int_0^\infty(\phi_1^2+\phi_2^2)dr\right],$$

where ϕ_1 and ϕ_2 are the ψ_1 and ψ_2 given by Gordon[3] and $\Lambda=(h/mc)$. $\int_0^\infty(\phi_1\phi_2/r^2)dr$ and $\int_0^\infty(\phi_1^2+\phi_2^2)dr$ were evaluated by numerical methods in the case of the 6*s* state of Cs. The difference in behavior of ϕ_2 and $(4\pi/\Lambda)\phi_1$ as compared with $r\psi$ and $r(d\psi/dr)$, respectively, is responsible for an increase in the coupling

[1] E. Fermi, Zeits. f. Physik **60,** 320 (1930).
[2] G. Breit, Phys. Rev. **35,** 1447 (1930); **37,** 1182 (1931).
[3] W. Gordon, Zeits. f. Physik **48,** 11 (1928)

of the electron to the nuclear spin by a factor of 1.46 in excess of that given by Fermi's formula. The screening effect was taken into account in these calculations to the extent of including the first two terms in the expansion of the Thomas-Fermi potential function at the nucleus. With neglect of screening effects (i.e., including only the first term in the above expansion), a solution involving Bessel's functions shows that $\psi^2(0)$ would have to be increased by a factor of 1.39.

The values of the nuclear magnetic moment obtained by Fermi's formula should be divided, therefore, by at least a factor of 1.4 for the 6*s* state of Cs.

S. W. Nile

Department of Physics,
New York University,
June 20, 1931.

A More Fundamental Thermodynamics

It has long seemed desirable to lay the foundations of a generalized thermodynamics designed: (1) to be more fundamental than classical thermodynamics in that it would comprise within its scope not only the state of equilibrium but also all possible fluctuations from that state; (2) to be more fundamental than statistical mechanics in that it would assume no mechanical laws.

The solution of this problem proves to be remarkably simple. All the laws of thermodynamics and of fluctuations may be shown to follow from a single cardinal postulate, which is essentially the following: If a given amount of some quantity such as energy or any form of matter is allowed to distribute itself between two systems, so that by one observation we find a certain fraction of the total amount in the first system, and again after a long time by a second observation we find a slightly different fraction, and so on until the statistical rules governing the observations have been ascertained—then these rules are independent of the mode of communication between the two systems.

A fuller development of this generalized thermodynamics will appear in the next number of the Journal of the American Chemical Society.

Gilbert N. Lewis

Department of Chemistry,
University of California,
June 18, 1931.

Oscillations in Discharge Tubes

Following the publication by Chow[1] and Fox[2] of their results regarding oscillations in discharge tubes carrying heavy currents, we thought it desirable to re-investigate whether oscillations were present in some cold-cathode glow discharge tubes which we have been using, in which the current densities are less than a milliampere per cm^2. For this purpose we used a discharge tube 3 cm in diameter, having electrodes of steel which could be moved up and down the tube. A collector of iron 21 mm long and 0.1 mm in diameter was let in from the side. The discharge was run in neon, but no attempt was made to obtain the gas in a pure state. To detect oscillations we used a cathode-ray oscillograph, which was connected in turn across each pair of electrodes, i.e., collector and anode, collector and cathode, and anode and cathode. A linear time-base was used to determine the waveform and frequency. Oscillations were only detected at relatively high pressures (1.4 mm to 2.1 mm) and then only when an *asymmetrical* anode glow was present. Even when a positive column was present, no oscillations were obtained so long as the discharge was symmetrical about the axis of the tube. The frequencies of the oscillations lay in the range 4 to 20×10^3 cycles per second. The amplitudes were very small, a typical variation in voltage between the floating collector and the anode being 0.7 volt on the steady potential difference of 21 volts. These results check up satisfactorily with tests made by other methods by K. G. Emeleus.[3]

W. L. Brown
H. McN. Cowan

Department of Physics,
Queens University of Belfast,
June 22, 1931.

[1] Chow, Phys. Rev. **37,** 574 (1931).

[2] Fox, Phys. Rev. **37,** 815 (1931).

[3] Emeleus, Proc. Cambridge Phil. Soc. **23,** 531 (1927).

Photoelectric and Metastable Atom Emission of Electrons from Surfaces

I. Langmuir and C. G. Found[1] concluded from experiments that resonance radiation is able to travel a considerable distance out into a tube away from the region of a discharge in Ne and cause the production of metastable atoms. They measured currents to charged electrodes which they attributed to conductivity imparted to the tube as a result of the emission of electrons from the glass walls and metal surfaces by metastable atoms. Experiments of the writer at pressures of 0.1 to 2 mm with somewhat similar apparatus confirm the conclusion of Langmuir and Found that resonance radiation travels long distances out into a tube and produces metastable atoms. These experiments indicate, however, that currents similar to those Langmuir and Found observed are made possible chiefly by the ionization of traces of impurities in the gas by metastable atoms.[2] In the case of currents to negatively charged electrodes it has been found that the emission of electrons by metastable atoms is small compared with the photoelectric effect.

In one type of experiment currents are measured between a thin nickel disk, which can be rotated so that its plane is either parallel or perpendicular to the axis of the tube (and therefore to the direction of the radiation), and a gauze cylinder symmetrically surrounding it. If the disk is made suitably negative to the cylinder approximate saturation currents are obtained which are several times greater when the disk is perpendicular to the axis of the tube than when it is parallel to this axis. For a given discharge current, these currents increase as the pressure is decreased. The ratio between the currents also increases. These facts are in accord with the view that the currents are due to a photoelectric emission from the disk, rather than to any action of metastable atoms.

Currents between disk and cylinder in the case of pure Ne are changed by only a relatively negligible extent by shining strong Ne light through the gauze from an external source. This indicates that metastable atoms are not appreciably involved in the flow of these currents. If, however, there is a trace of impurity present, say 0.005 percent A, the currents flowing are considerably larger and the external Ne light then causes a considerable decrease in them. These experiments indicate that the A is ionized by the metastable Ne atoms, and that the additional current flowing as a result of this ionization decreases as the metastable atom concentration causing it is decreased by the external Ne light. That the external Ne light used is a powerful destroyer of metastable atoms is shown also by the following experiments. Measurements of ion concentration either by a Hertz positive ion detector or by probe measurements[2] made close enough to the discharge (e.g. two tube diameters) so that the usual interpretation probably applies, show that this concentration is enormously increased by adding a trace of A to Ne. Further both types of test show that provided the argon percentage is not too great (<0.05 percent) the ion concentration is markedly decreased by shining the external source of Ne light on the tube. The effect of the Ne light is negligible in pure Ne, reaches a maximum with a few thousandths of a percent of A and again becomes negligible when the A percentage has become of the order of 0.1 percent. Meanwhile, the ion and electron concentration increases many hundred fold. These results indicate that metastable atoms are only involved in these experiments when a trace of another gas has been added which they can ionize. Further, with a sufficient amount of this other gas, the rate of destruction of metastable atoms by this ionization process becomes large compared with the rate of destruction by the external Ne light.

These experiments and conclusions are in agreement with the results of Penning[3] obtained from studies of the breakdown potential in Ne as influenced by traces of A and by irradiation with Ne light.

Experiments have been carried out in which metastable atoms have been destroyed by applying heat and also in the case of A by admitting N_2. In no case has evidence been obtained that emission of electrons by metas-

[1] I. Langmuir and C. G. Found, Phys. Rev. **36,** 604 (1930).

[2] T. E. Foulke (unpublished work) found that the conductivity of a tube such as is here considered is enormously increased by adding a trace of a gas the ionizing potential of which is lower than the metastable potential of the main gas.

[3] F. M. Penning, Zeits. f. Physik **57,** 723–38 (1929), Phil. Mag. **11,** 961–79 (1931).

table atoms under the present circumstances is comparable with the photoelectric effect.

The present experiments indicate that the emission of electrons by metastable atoms is small compared with the photoelectric effect even where the concentration of metastable atoms is high enough to give a visible beam by scattering. Hence it is believed that in much recent work[1,4] involving effects which have been ascribed to the emission of electrons from surfaces by metastable atoms too great an efficiency has been assumed for this process and too small an efficiency for the photoelectric effect.

Oliphant[5] found an apparently high efficiency for the emission of electrons from surfaces by metastable He atoms having velocities corresponding to 2000–120 volts. It would seem that for the relatively very slow (room temperature) metastable atoms of the present experiments a smaller efficiency must be assumed.

Photoelectric studies have been made in He and A as well as in Ne. Strong irradiation with light of the gas in question, as well as experiments with the disk above mentioned perpendicular and parallel to the tube show that, in these gases also, electron emission by metastable atoms is small compared with the photoelectric effect.

Rough calculations made on the basis of the experiments indicate that the photoelectric effect in this far ultraviolet region of the spectrum, (around 700A in the case of Ne) is considerably more efficient than in the nearer ultraviolet regions usually studied.

CARL KENTY

Research Laboratory,
General Electric Vapor Lamp Co.,
Hoboken, N. J.,
June 5, 1931.

[4] P. M. Morse and W. Uyterhoeven, Phys. Rev. **31,** 827 (1928); W. Uyterhoeven, Phys. Rev. **31,** 913 (1928), Proc. Nat. Acad. Sci. **15,** 32 (1929); C. G. Found, Phys. Rev. **34,** 1625 (1929); W. Uyterhoeven, and M. C. Harrington, Science **70,** 586 (1929), Phys. Rev. **35,** 438 (1930), Phys. Rev. **36,** 709 (1930).

[5] M. L. E. Oliphant, Proc. Roy. Soc. **A124,** 228 (1929).